



**Mechanistic Investigations on Lewis Acid-Catalysed Skeletal  
Rearrangement Reactions of Polysilanes and Germapolysilanes**

**- Subtle Capture of Intermediates -**

An der Fakultät für Mathematik und Naturwissenschaften  
der Carl von Ossietzky Universität Oldenburg  
zur Erlangung des Grades und Titels eines

**Doktors der Naturwissenschaften (Dr. rer. nat.)**

angenommene Dissertation

von

**Frau M.Sc. Lena Albers**

geboren am 04. November 1986 in Emden

The research for this work was performed in the institute for chemistry at the Carl von Ossietzky University Oldenburg under supervision of Prof. Dr. Thomas Müller from January 2012 until October 2015.

This work was financially supported by the ERA-chemistry program (DFG-Mu1440/8-1, FWF-I00669) “Skeletal Rearrangement Processes in Organometallic Cations of Group 14 Elements – A Powerful Concept for Assembling Complex Polysilane Frameworks”.

Referee: Prof. Dr. Thomas Müller

Second referee: Prof. Dr. Rüdiger Beckhaus

Day of Disputation: 04.12.2015



## Acknowledgments

I am indebted to Prof. Thomas Müller, not only for giving me the subject of studies and for financing this PhD thesis but also for the guidance and supervision I experienced working with him. Moreover, I would like to express my gratefulness for the generous freedom in investigating silyl cationic rearrangements. It has been a pleasure working on this project.

I thank Prof. Rüdiger Beckhaus for being the second referee. I thank Prof. Christoph Marschner for being the third referee, for the fruitful cooperation, helpful discussions and the chance to be a part of his group.

I appreciate the work of Dieter Neemeyer and Andrea Tschirne for acquiring all the NMR spectra. Especially I have to thank Andrea Tschirne for her tireless willingness to comply with special, non-regular requests. Dipl. Ing. Francesco Fabbretti is thanked for measuring the high-resolution mass spectra and Rainer Schmidt for GC/MS analyses. I thank Dr. Marc Schmidtmann for his unfailing efforts to find suitable crystals and perform X-ray single crystal analysis, structure solution and refinements. I thank Burghard Stigge for combustion analyses.

Many thanks go to the former and active members of the working group: I appreciate Maria Ahrnsen's hard work, her every-day help concerning chemicals, glassware or fresh vegetables from her garden. I thank Dr. Annemarie Schäfer for her competent, scientific and friendly ideas, whenever advice was needed. Dr. Patrick Zark, Dr. Claudia Gerdes, Dr. André Schäfer, Dr. Matti Reißmann and Dr. Natalie Kordts, M.Sc. Henning Großekappenberg and M.Sc. Zhaowen Dong, B.Sc. Katherina Rüger, B.Sc. Sandra Künzler and B.Sc. Valentin Morosow are thanked for good collegueship. Thanks to B.Sc. Jelte Nimoth for his unfailing energy and interest in polysilanes, bikes and delicious cheese. I regard B.Sc. Julian Küppers, B.Sc. Saskia Rathjen and Hanna Cramer for their work with which they contributed to this research during their theses or practical courses.

I really enjoyed working with my colleagues and friends M.Sc. Dennis Lutters and M.Sc. Crispin Reinhold and I thank them for the fun we had every day, their friendship and helpful ideas concerning chemistry, computers, bikes or other personal matters. Thank you very much for the great time.

I thank Dr. Judith Baumgartner, M.Sc. Filippo Stella, M.Sc. Mohammad Aghazadeh Meshgi, M.Sc. Malgorzata Jakacka, M.Sc. Rainer Zitz and M.Sc. Carlos Barbado from the group of Prof. Marschner who affiliated me as a member of their group during my stay in Graz.

Finally, I would like to express my gratefulness for my family's strong support and their trust.

Thank you.



I assert that I wrote this dissertation independently and used only the indicated sources. I did not submit this dissertation or parts of it to any other university for evaluation for a conferral of a doctorate.

I followed the guidelines for good scientific practice at the Carl von Ossietzky University. In connection with this dissertation project, I did not claim any commercial mentoring services.

One publication resulted from this Ph.D. project, which can be found as follows:

L. Albers, M. A. Meshgi, J. Baumgartner, C. Marschner, T. Müller, *Organometallics* **2015**, 34, 3756.

For further publications resulting from corporation with Prof. Marschner's group and conference contributions see Curriculum Vitae.



## Abstract

Several investigations of the groups of Kumada and Marschner showed that polysilanes and germapolysilanes undergo skeletal rearrangements of the silicon and germanium containing backbone into their highly branched isomers when treated with a catalytic amount of Lewis acid. These rearrangements are supposed to be the silicon analogue of the well-known Wagner-Meerwein rearrangement of carbon chemistry, and are fundamentally important reactions in organosilicon chemistry.

This work elucidated several known rearrangement reactions of polysilanes and germapolysilanes, which are predicted to proceed via cationic intermediates. These fleeting intermediates were detected in low temperature  $^{29}\text{Si}$  NMR spectroscopic studies and mechanistic proposals for these rearrangements were established. In addition, the interpretations of the  $^{29}\text{Si}$  NMR spectra and mechanistic ideas were supported by quantum mechanical calculations of  $^{29}\text{Si}$  NMR chemical shifts and ground state energies of the cationic intermediates.

Applying these techniques, it was possible to verify the presence of several silyl- and germyl cations and their solvent complexes as intermediates in the sila-Wagner-Meerwein rearrangement of tris(trimethylsilyl)trimethylgermylsilane into tetrakis(trimethylsilyl)germane. The identity of these species was verified by independent synthesis and low temperature NMR characterisation, and their interconversion was followed by NMR spectroscopy.

A new synthetic approach was established to trap highly reactive and short living cationic intermediates of these rearrangements. Well-designed hydrogen-substituted polysilanes and germapolysilanes were used to define the position of the initial positively charged atom by hydride transfer reaction to investigate the rearrangement mechanisms. The subtle formation of Si-H-Si bridges and quantum mechanical considerations illuminate reaction mechanisms of several Lewis acid-catalysed rearrangements. Previously underestimated attractive dispersion interactions were found to play a decisive role during these rearrangements.

This work provides the fundamental groundwork for mechanistic investigations on Lewis acid-catalysed rearrangement reactions in polysilanes and germapolysilanes. New synthetic methods provide the possibility to detect cationic intermediates, which have previously only been assumed.

## Kurzzusammenfassung

Die Arbeiten von Kumada und Marschner zeigen ausführlich, dass Polysilane und Germapolysilane Lewis Säure katalysierte Gerüstumlagerungen des gesamten Silicium- und Germaniumgerüsts eingehen, um dann in ihren stark verzweigten Isomeren vorliegen. Es wird angenommen, dass diese Umlagerungen in Analogie zu der, in der organischen Chemie weit bekannten, Wagner-Meerwein Umlagerung ablaufen, welche fundamental wichtige Reaktionen in der Organosilicium Chemie sind. In der vorliegenden Arbeit wurden einige bekannte Umlagerungen von Polysilanen oder Germapolysilanen beleuchtet, welche über kationische Intermediate abzulaufen scheinen. Diese kurzlebigen Intermediate wurden mittels Tieftemperatur  $^{29}\text{Si}$  NMR Spektroskopie detektiert und Mechanismen für diese Umlagerungen entwickelt. Darüber hinaus wurden die Interpretationen der  $^{29}\text{Si}$  Spektren und die mechanistischen Ideen durch quantenmechanische Berechnung der  $^{29}\text{Si}$  NMR Verschiebung und der Energien der Grundzustände der kationischen Intermediate unterstützt.

Mit Hilfe dieser Techniken war es möglich, mehrere Silyl- und Germylkationen und ihre Lösungsmittelkomplexe als Intermediate der sila-Wagner-Meerwein Umlagerung von Tris(trimethylsilyl)trimethylgermysilan in Tetrakis(trimethylsilyl)german zu detektieren. Die Identität dieser Spezies wurde durch unabhängige Synthese und Tieftemperatur NMR spektroskopischer Charakterisierung belegt. Die gegenseitige Umwandlung von einem Kation in das andere wurde mittels NMR Spektroskopie verfolgt.

Ein neuer synthetischer Ansatz zum Abfangen der hoch reaktiven und kurzlebigen kationischen Intermediate während dieser Umlagerungen wurde erarbeitet. Sorgfältig ausgearbeitete, Wasserstoff-substituierte Polysilane und Germapolysilane wurden hergestellt, um die Position der kationischen Ladung nach Hydridabstraktionsreaktion gezielt zu bestimmen. Dies ermöglichte die geschickte Ausbildung von Si-H-Si Brücken in den kationischen Intermediaten und zusammen mit quantenmechanischen Berechnungen konnten somit wiederum Reaktionsmechanismen erklärt werden. Es wurde gefunden, dass die bisher unterschätzten attraktiven Dispersionswechselwirkungen einen wichtigen Einfluss auf diese Umlagerungen besitzen.

Diese Arbeit bildet ein Fundament für mechanistische Untersuchungen an Lewis Säure katalysierten Gerüstumlagerungen in Polysilanen und Germapolysilanen. Neuartige präparative Methoden eröffneten die Möglichkeit die hochreaktiven und kurzlebigen kationischen Intermediate, welche bisher nur theoretisch vorausgesetzt wurden, zu detektieren und zu identifizieren.



# Table of Contents

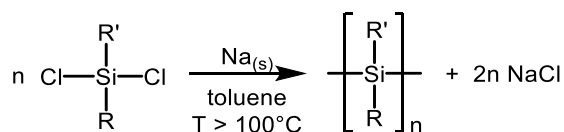
1	Introduction .....	1
1.1	Synthesis of Polysilanes.....	1
1.1.1	Nomenclature of Polysilanes and Germapolysilanes.....	1
1.2	Synthesis of Silyl Anions .....	3
1.2.1	Use of Organolithium Compounds for the Synthesis of Silyl Anions .....	4
1.2.2	Use of Alkali Alkoxide Compounds for the Synthesis of Silyl Anions .....	5
1.2.3	Transmetallation Reactions towards Silyl Magnesium Compounds.....	8
1.3	Rearrangement Reactions.....	10
1.3.1	Rearrangement Reactions of Polysilanes.....	10
1.3.2	Rearrangement Reactions of Germapolysilanes.....	14
1.4	Silyl Cations .....	17
1.4.1	Synthesis of Silylium Ions .....	19
1.4.2	Arene-Stabilised Silylium Ions .....	20
1.4.3	Silane-Stabilised Silylium Ions .....	21
1.4.4	Ferrocene-Stabilised Silylium Ions .....	25
1.4.5	Tri-Coordinated Silylium Ions .....	26
1.5	<sup>29</sup> Si NMR Chemical Shifts of Polysilanes and Germapolysilanes .....	28
2	Motivation.....	30
3	Results and Discussion .....	32
3.1	Initial Considerations on the Stability of Silyl Cations.....	32
3.2	Lewis Acid Catalysed Rearrangements in Germapolysilanes - A Stable Ion Study .....	37
3.3	Investigations on a Hydrogen-Substituted Silyl Cation .....	49
3.4	Mechanistic Investigations on Rearrangement Reactions in Polysilanes and Germapolysilanes - Subtle Trapping of Intermediates .....	57

3.4.1	Aluminium Trichloride-Catalysed Rearrangement Reactions of Linear Polysilanes and Germapolysilanes.....	57
3.4.2	Formation of Solvent-Stabilised Silylium or Germylium Ions .....	59
3.4.3	The Hydrogen Trick - Subtle Trapping of Intermediates .....	61
3.4.3.1	Mechanistic Development – Part I.....	63
3.4.3.2	Mechanistic Development – Part II.....	88
3.4.3.3	Mechanistic Development – Part III.....	97
3.5	Rearrangement Reactions in Cyclic Polysilanes .....	104
3.5.1	Rearrangement of Dodecamethylcyclohexasilane .....	105
3.5.2	The Hydrogen Trick – Trapping Intermediates in Cyclic Polysilanes.....	111
3.6	Ferrocenylsilyl Cations .....	117
3.6.1	Stabilisation of an $\alpha$ -Ferrocenylsilylium Ion.....	119
3.6.2	Stabilisation of a $\beta$ -Ferrocenylsilylium Ion.....	125
3.6.3	Computational Investigations on the 1,1-Oligosilylferrocene Cations .....	133
4	Summary and Outlook .....	136
5	Experimental .....	143
5.1	General Experimental Procedures .....	143
5.2	Synthesis of Starting Materials .....	145
5.3	Cation Preparation .....	157
6	Literature.....	178
7	Appendix .....	183
7.1	Computational Details.....	183
7.2	Index of Abbreviations .....	183
8	Curriculum Vitae .....	186

# 1 Introduction

## 1.1 Synthesis of Polysilanes

Made of silicon, one of the most important semiconductor elements, polysilanes can be seen as one-dimensional semiconductors and offer a widespread potential for so-called “smart materials”. The delocalisation of the Si-Si- $\sigma$ -bond electrons leads to interesting and technically useful properties, such as thermochromism<sup>[1-2]</sup>, piezochromism<sup>[3]</sup> and solvatochromism<sup>[4]</sup>. Unfortunately, the access to this class of compounds is mainly limited to the Wurtz-type coupling reaction (Scheme 1). In this reaction, the Si-Si chain is built up by reduction of silicon halides with alkali metals.<sup>[5]</sup> In the last ten years, alternative methods for the synthesis of polysilanes were investigated.<sup>[6]</sup> The formation of the new Si-Si bonds by electrochemical methods<sup>[7]</sup> or dehydrocoupling of hydrosilanes<sup>[8]</sup> are functional, but these methods do not reach the prominence of the Wurtz-type coupling. Moreover, they do only work well for the preparation of dialkylated linear polysilanes and small cyclosilanes but fail for substituents of enhanced complexity and the formation of defined products in moderate yields still raises difficulties.<sup>[5]</sup>



Scheme 1. Wurtz-type coupling of a dichlorosilane.

A wide variety of polysilanes and germapolysilanes can be prepared starting from commercially available methylsilyl or methylgermyl compounds. In many cases the starting material is tetrakis(trimethylsilyl)silane, which can be easily transformed into longer chains or higher branched derivatives by simple salt metathesis reactions of the silyl or germyl anions with the corresponding silyl or germyl halides or triflates.<sup>[9-15]</sup>

### 1.1.1 Nomenclature of Polysilanes and Germapolysilanes

The names of polysilanes and germapolysilanes can become very confusing if named according to IUPAC rules. In this work, the names are formed according to several publications of the group of Prof. Marschner. The understanding of the structure of the polysilanes and germapolysilanes is easier when the nomenclature is formulated as follows:

The length of the main silicon chain is counted between two silyl-substituted silicon atoms. The main chain is identified by finding the highest branched and highest silyl- or germyl-substituted silicon atom. The number of flanking trimethylsilyl or -germyl substituents and other substituents are added as prefixes to the main chain. Additionally the number of methyl groups is also indicated. If a germanium atom is included in the main chain, it is describe by the position and the prefix “germa”.

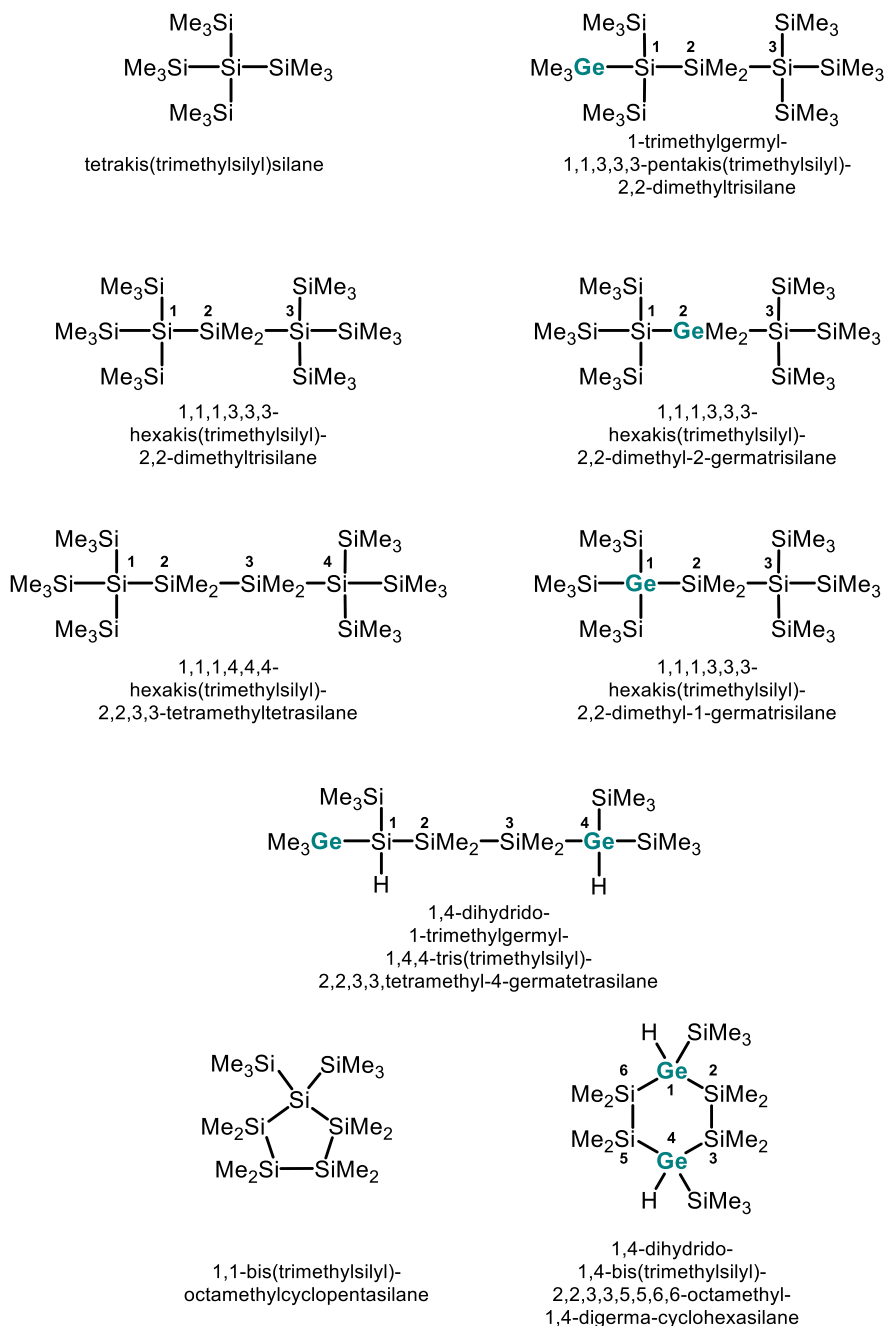
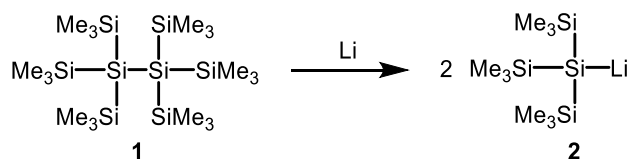


Figure 1. Examples of the used nomenclature in this work.

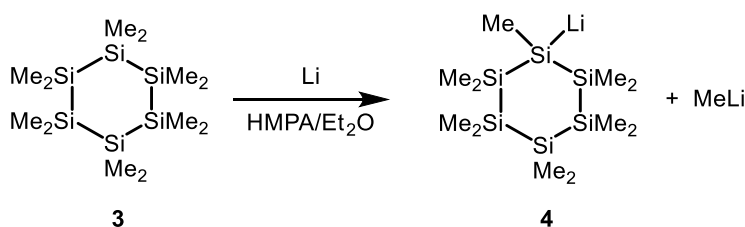
## 1.2 Synthesis of Silyl Anions

Numerous strategies<sup>[16-19]</sup> for the synthesis of silyl anions have been developed but none of them is generally applicable. For example, silyl anions can be synthesised by the cleavage of silicon-silicon or silicon-heteroelement bonds by reactive metals, alkyllithium or alkylmagnesium compounds, potassium hydride, sodium and potassium alkoxides or tetrabutylammonium fluorides. Moreover, metal-halogen exchange reactions or transmetallation reactions can lead to the formation of silyl anions. The cleavage of silicon-silicon bonds with lithium is only applicable for symmetrically substituted polysilanes, forming two equivalents of polysilanylsilyllithium compounds. Starting from unsymmetrically substituted polysilanes, this reaction leads to two different anions, which are hard to separate, and thus, decreases the synthetic applicability.



Scheme 2. Cleavage of silicon-silicon bonds with lithium yields silyllithium compounds.

The formation of silyl anions by bond breaking reactions is not only limited to silicon-silicon bonds. Lithium also cleaves silicon-carbon bonds for example in dodecamethylcyclohexasilane **3**. Its treatment with lithium in HMPA/Et<sub>2</sub>O mixtures gives undecamethylcyclohexasilyllithium **4** and methyllithium (Scheme 3).



Scheme 3. Formation of undecamethylcyclohexasilyllithium **4**.

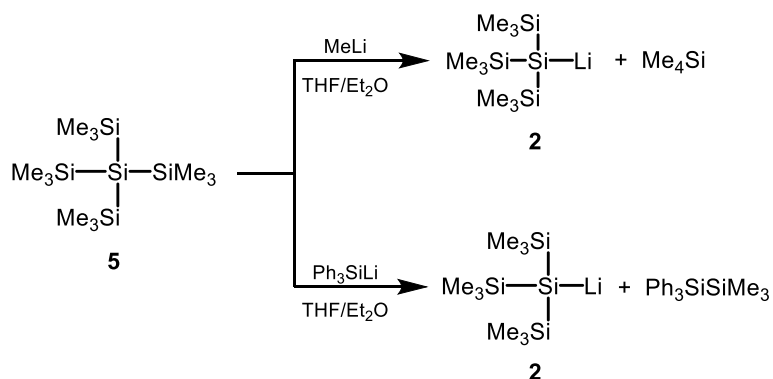
### 1.2.1 Use of Organolithium Compounds for the Synthesis of Silyl Anions

Alkylolithium reagents, especially methyllithium, cleave silicon-silicon bonds of polysilanes to give one equivalent of silyl anion together with one equivalent of alkylated silane. To synthesise sterically less hindered silyl anions, usually the presence of strongly coordinating solvents like HMPA seems to be necessary for the reaction to proceed.<sup>[20]</sup> This reaction is thermodynamically favoured by the transformation of a Si-Si bond into a stronger Si-C bond (Scheme 4).



Scheme 4. Cleavage of silicon-silicon bonds with alkylolithium reagents yields silyllithium compounds.

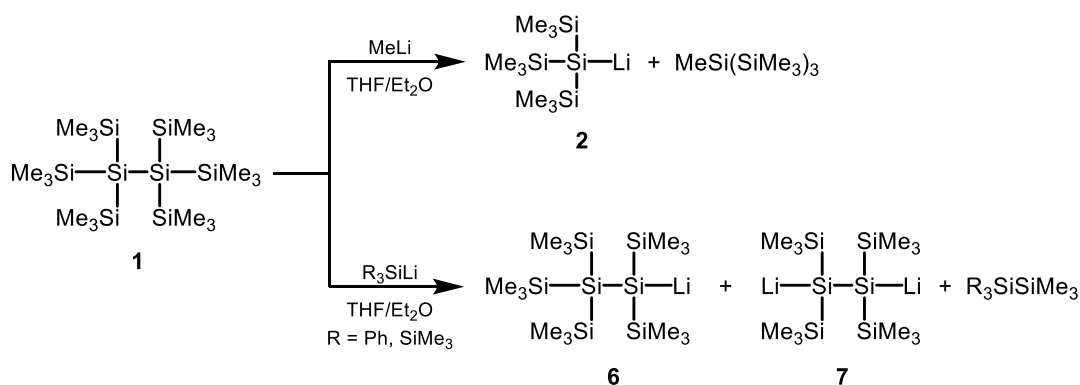
This method was established by Gilman and co-workers using methyllithium as the reagent for the synthesis of silyllithium compounds<sup>[21-23]</sup>, especially for the synthesis of the sterically hindered tris(trimethylsilyl)silyllithium **2**. Compound **2** was found to be an easily accessible precursor of the bulky nucleophilic polysilanylsilyl anion, also called “hypersilyl” group. When using triphenylsilyllithium instead of methyllithium as cleaving reagent, also tris(trimethylsilyl)silyllithium **2** was obtained (Scheme 5).



Scheme 5. Diverse reactivity of compound **5** with different lithium reagents.

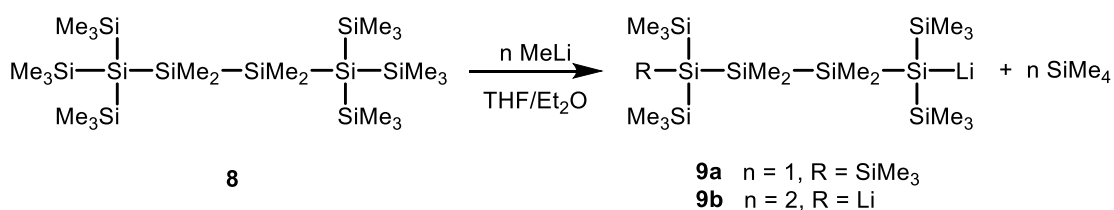
Interestingly, the attempt to cleave off one trimethylsilyl group in hexakis(trimethylsilyl)disilane **1** does not result in the formation of pentakis(trimethylsilyl)disilyllithium **6** but in the cleavage of the internal Si-Si bond and again tris(trimethylsilyl)silyllithium **2** together with one equivalent of the corresponding methylated *iso*-tetrasilane is formed (Scheme 6). On the contrary, the reaction of hexakis(trimethylsilyl)disilane **1** with more bulky reagents like Ph<sub>3</sub>SiLi or (Me<sub>3</sub>Si)<sub>3</sub>SiLi results in the

breaking of external Si-Si bonds and a mixture of mono- and dilithiated polysilanes **6** and **7** are obtained (Scheme 6).<sup>[24]</sup>



Scheme 6. Reaction of hexakis(trimethylsilyl)disilane **1** with different lithium reagents.

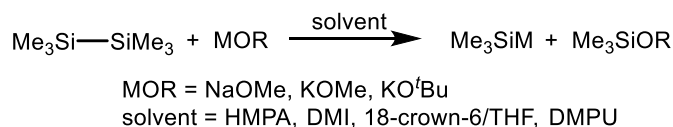
Although the different reactivity of methyllithium and triphenylsilyl- and tris(trimethylsilyl)silyllithium can be understood in terms of different steric demands, Sakurai<sup>[25]</sup> postulated an electron transfer mechanism rather than a nucleophilic attack. For the reaction of tetrasilane **8** with methyllithium, Apeloig and co-workers<sup>[26]</sup> found the cleavage of external Si-Si bonds was favoured with the formation of the corresponding monoanion **9a** and the 1,4-dianion **9b** (Scheme 7).



Scheme 7. Formation of mono- or dianions **9a** or **9b**.

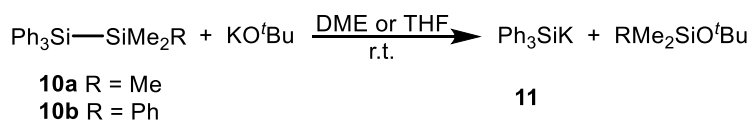
### 1.2.2 Use of Alkali Alkoxide Compounds for the Synthesis of Silyl Anions

Not only lithium reagents have the ability to cleave Si-Si bonds. Alkali alkoxides in donor solvents, e.g. NaOMe in HMPA<sup>[25]</sup> or DMI<sup>[27]</sup>, KO<sup>t</sup>Bu in 18-crown-6/THF<sup>[28]</sup> and KO<sup>t</sup>Bu in DMPU<sup>[28]</sup> are also reactive enough to cleave polysilanes (Scheme 8).



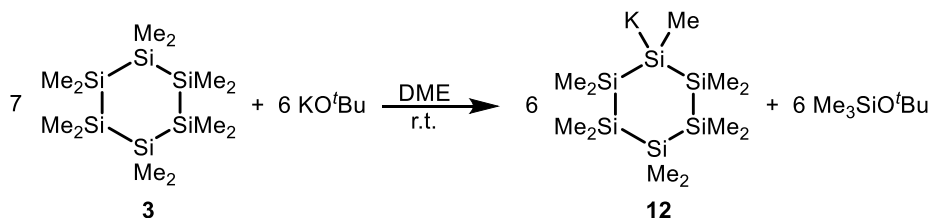
Scheme 8. Alkali alkoxides as cleaving reagents for the synthesis of silylanions.

The formation of silyl anions by the reaction of a polysilane with potassium *tert*-butoxide in ethereal solvents (e.g. Et<sub>2</sub>O, THF or DME) is very selective. Unsymmetrically substituted disilanes such as **10** give the most stable silylmetallic compound, in this case triphenylsilylpotassium **11** (Scheme 9). The reaction of cyclohexasilane **3** with potassium *tert*-butoxide gives cyclohexasilylpotassium **12** in more than 90% yield together with cyclopentasilylpotassium **14** as an impurity (Scheme 10, Scheme 11).<sup>[29]</sup>

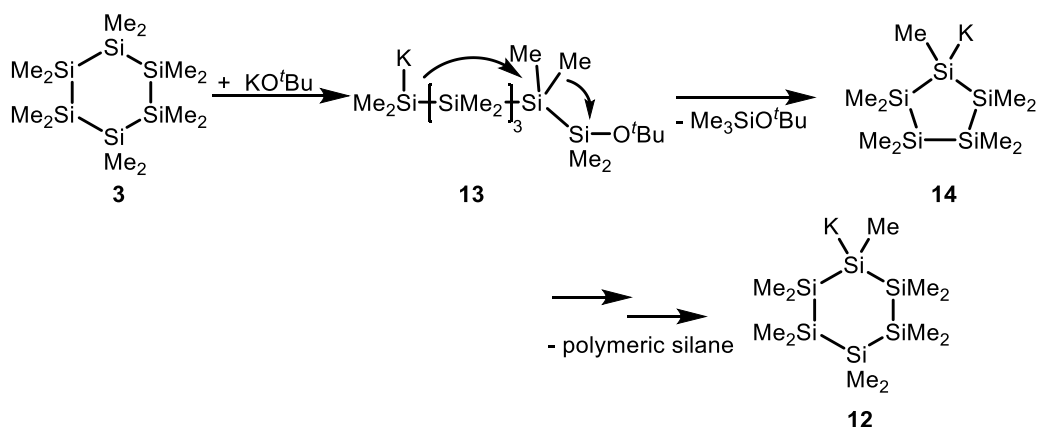


Scheme 9. Formation of the most stable silylpotassium compounds.

The latter reaction appears to be a Si-C bond cleavage; however the second by-product is not *tert*-butyl methyl ether but rather trimethylsilyl *tert*-butyl ether (Scheme 10), which can only be explained by the involvement of a more complicated rearrangement (Scheme 11).<sup>[29-30]</sup>

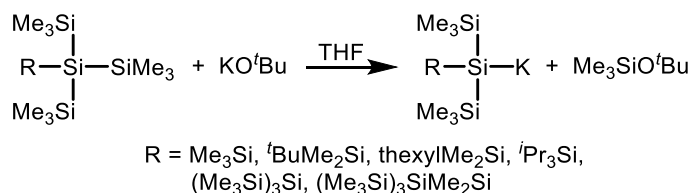
Scheme 10. Formation of undecamethylcyclohexasilylpotassium **12**.

The primary step is likely to be a Si-Si bond cleavage to give the open-chain potassium-substituted silane **13**. A methyl shift and recyclisation forms nonamethylcyclopentasilylpotassium **14**, which undergoes a second ring-opening and ring-closure reaction to lead to undecamethylcyclohexasilylpotassium **12**. An unidentified polymeric silane was found to be a reaction by-product.<sup>[29]</sup>



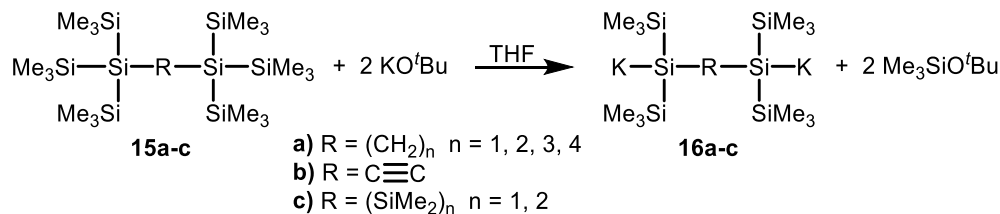
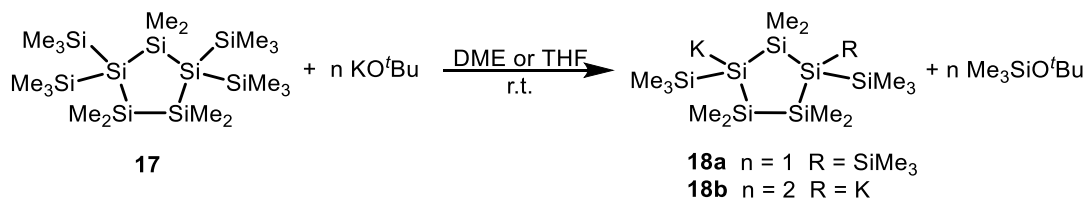
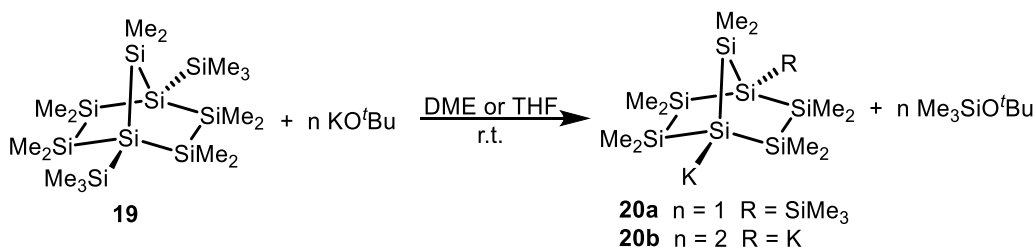
Scheme 11. Possible rearrangement of dodecamethylcyclohexasilane **3** to give undecamethylcyclohexasilylpotassium **12**.<sup>[29]</sup>

Potassium *tert*-butoxide selectively cleaves terminal trimethylsilyl groups in branched polysilanes. This selectivity contrasts to the findings of Gilman<sup>[22, 24]</sup>, Pannell<sup>[31]</sup> and Apeloig<sup>[26]</sup> in the reactions of branched polysilanes with methyllithium. Trimethylsilyl groups are selectively cleaved over bulkier silyl groups, such as *tert*-butyldimethylsilyl or tri-*iso*-propylsilyl groups (Scheme 12).



Scheme 12. Synthesis of differently substituted silylpotassium compounds.

The high selectivity of potassium *tert*-butoxide to cleave only terminal Si-Si bonds allows the formation of silyl  $\alpha,\omega$ -dianions. Both, alkylidene<sup>[32-33]</sup> as well as silylidene<sup>[9, 34]</sup> bridged  $\alpha,\omega$ -bis(tris(trimethylsilyl)silyl)silanes **15a-c** can be reacted with two equivalents of potassium *tert*-butoxide to yield the corresponding silyl  $\alpha,\omega$ -dianions **16a-c**. The reaction requires ethereal solvents and, sometimes, elevated temperatures or extended reaction times to go to completion. The selectivity is not limited to linear polysilanes. The preparation of silyl mono- and dianions is also possible in cyclic (Scheme 14) or bicyclic polysilanes (Scheme 15). In these structures, flanking trimethylsilyl groups are removed by potassium *tert*-butoxide.

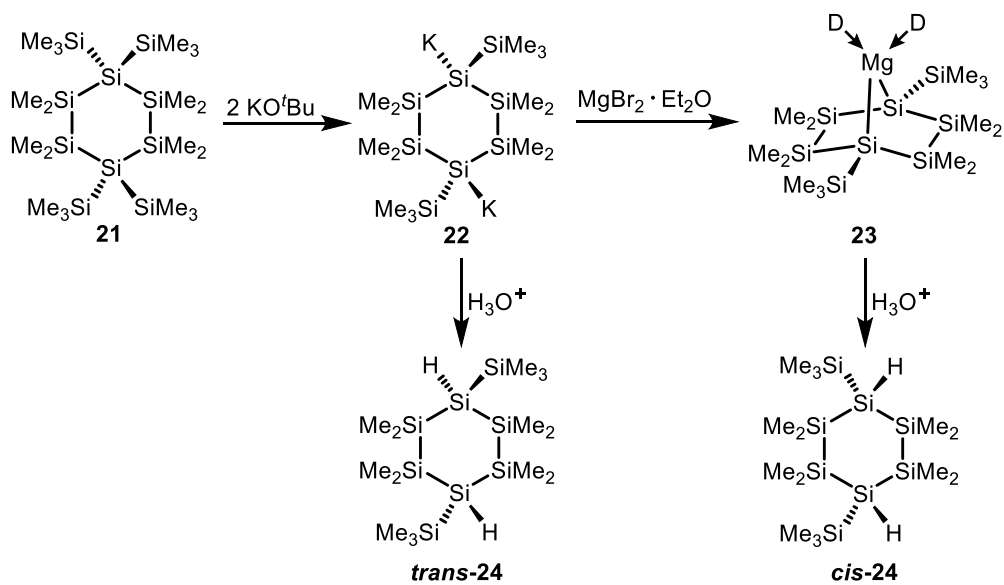
Scheme 13. Synthesis of  $\alpha,\omega$ -dianions **16a-c**.Scheme 14. Synthesis of cyclic mono- and dianions **18a-b**.Scheme 15. Synthesis of bicyclic mono- and dianions **20a-b**.

### 1.2.3 Transmetallation Reactions towards Silyl Magnesium Compounds

Reactions of silyl alkali compounds with halides of less electropositive elements such as magnesium, zinc, mercury or copper result in metal-metal exchange and the formation of a less polarised silicon-metal bond. The reduced bond polarisation leads to decreased reactivity of the silyl anion, which facilitates handling of the reagents.

Besides reduced reactivity, silyl magnesium compounds show a second difference to their potassium analogues. The transformation from potassium to magnesium has important consequences for the stereochemistry of dianions. For example the preparation of the dianion **22** of the six-membered ring **21** with potassium *tert*-butoxide gives mainly the *trans*-isomer, which can be verified after hydrolysis to give *trans*-1,4-dihydrocyclohexasilane **trans-24**. On the contrary, the hydrolysis product of the

magnesium compound **23** is the *cis*-isomer ***cis*-24**, exclusively (Scheme 16).<sup>[10]</sup> After the first hydrolysis step, the configuration of the remaining anionic silicon atom is preserved in the silyl magnesium compound because the inversion barriers of the magnesium silyls are higher than in the corresponding alkali metal derivatives.<sup>[35-36]</sup>



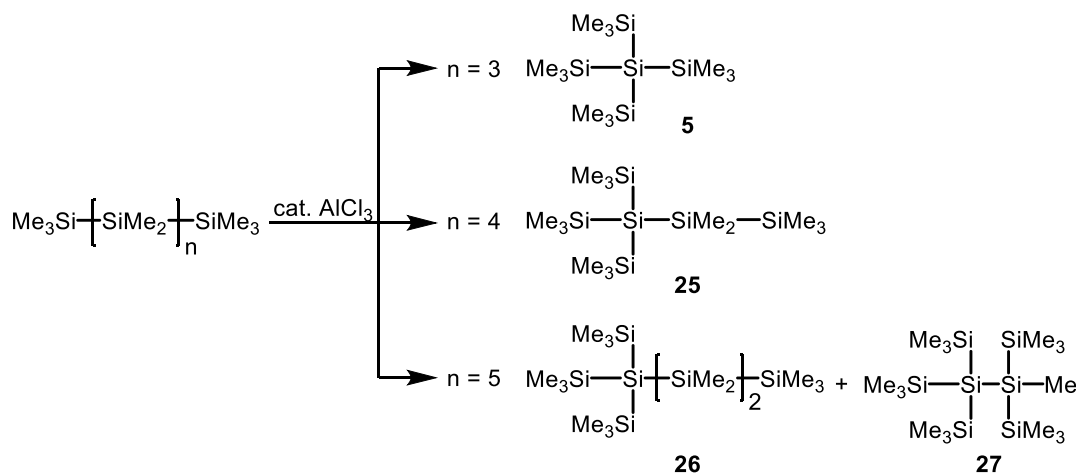
Scheme 16. Synthesis of *trans*- or *cis*-product **24** from compound **21** (D = donor molecule, e.g. Et<sub>2</sub>O).

## 1.3 Rearrangement Reactions

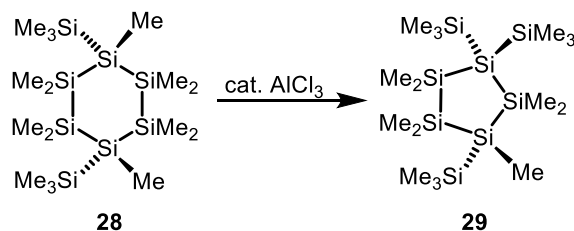
### 1.3.1 Rearrangement Reactions of Polysilanes

In the 1930s, the Lewis acid-catalysed rearrangement reactions of alkanes were studied with great interest. Nenitzescu and Drăgan<sup>[37]</sup> found aluminium trichloride was able to catalyse the isomerisation of alkanes e.g. *n*-pentane, *n*-hexane, *n*-butane and *iso*-butane.<sup>[38-40]</sup> The still famous synthesis of adamantane by Schleyer<sup>[41]</sup> was a crowning achievement in this field of research.

Almost 50 years ago, Ishikawa and Kumada discovered that Lewis acid-catalysed rearrangement chemistry also exists in the case of permethylated polysilanes.<sup>[42-43]</sup> They showed that permethylated silanes undergo skeletal rearrangements in the presence of a catalytic amount of aluminium trichloride to give their branched isomers (Scheme 17, Scheme 18).<sup>[44]</sup> Such rearrangements have been used for the synthesis of highly branched open-chain,<sup>[45]</sup> cyclic<sup>[44]</sup> and polycyclic<sup>[46]</sup> polysilanes starting from the linear isomers. Analogous to the well-known Wagner-Meerwein-rearrangement in carbon chemistry this is a fundamentally important reaction in organosilicon chemistry.

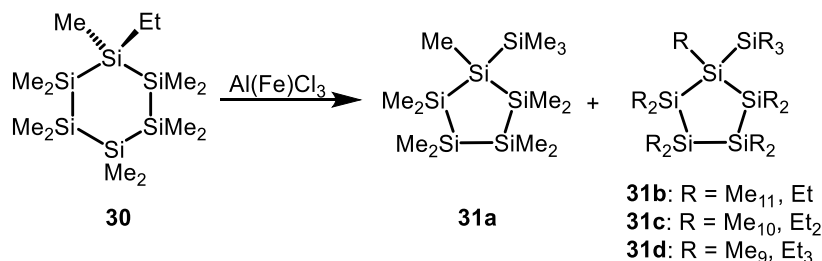


Scheme 17.  $\text{AlCl}_3$ -catalysed rearrangement of permethylated linear oligosilanes.



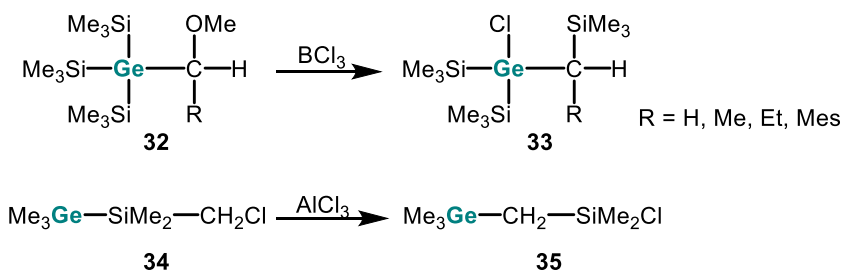
Scheme 18.  $\text{AlCl}_3$ -catalysed rearrangement of permethylated cyclic oligosilane **28**.

In 1986, Blinka and West investigated the behaviour of the ethyl substituted permethylated cyclohexasilane **30** under Lewis acid conditions.<sup>[47]</sup> Besides the formation of the five-membered ring **31a**, they found an intra- and intermolecular scrambling of the ethyl substituent to give **31ab-d** (Scheme 19).



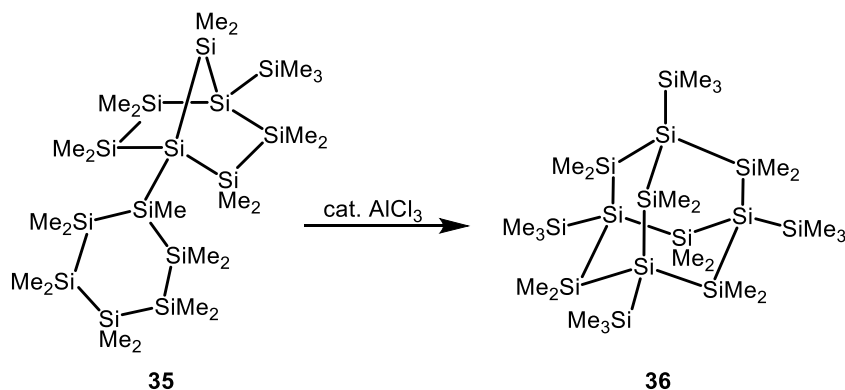
Scheme 19. AlCl<sub>3</sub>-catalysed rearrangement reaction of ethylundecamethylcyclohexasilane **30**.

Another rearrangement, a BCl<sub>3</sub>-catalysed 1,2-shift of a trimethylsilyl group in a (tris(trimethylsilyl)-germyl)methyl ether **32**, was reported in earlier studies by Märkl and Wagner.<sup>[48]</sup> Pannell and co-workers<sup>[49]</sup> investigated the chemical properties of silicon-germanium-bonds and found an AlCl<sub>3</sub>-initiated 1,2-shift of the trimethylgermyl group and a chloride in Me<sub>3</sub>GeSiMe<sub>2</sub>CH<sub>2</sub>Cl **34** (Scheme 20).

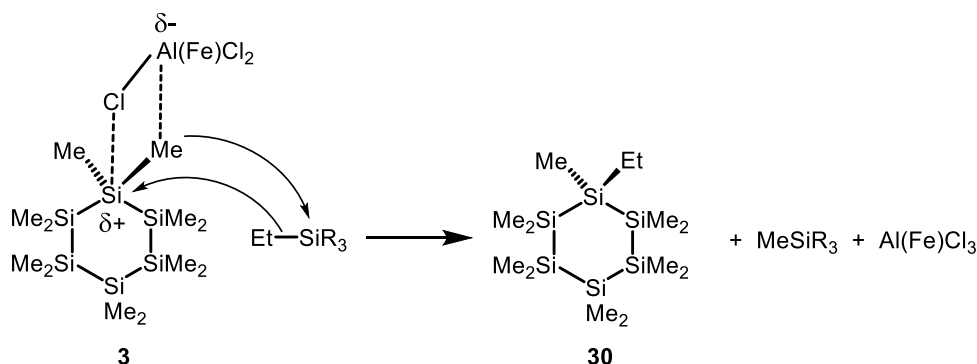


Scheme 20. Literature known 1,2-shifts in germasilanes **32**<sup>[48]</sup> and **34**<sup>[49]</sup>.

These pioneering studies revealed that the Lewis acid-catalysed Wagner-Meerwein-type rearrangement of polysilanes is an effective strategy to create structures of higher complexity. The high yield and selective synthesis of the silicon analogue of adamantane, the permethylated sila-adamantane **36**, was established by Marschner<sup>[46]</sup> and shows the great versatility of this method (Scheme 21).

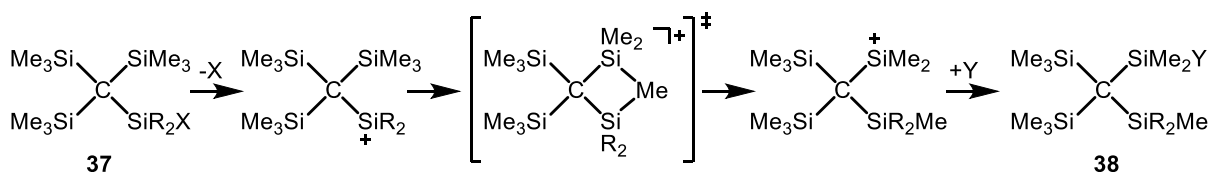
Scheme 21. Synthesis of sila-adamantane **36**.<sup>[46]</sup>

The group of Kumada<sup>[45, 50]</sup> and also Blinka and West<sup>[47]</sup> tried to clarify the mechanism of these rearrangement reactions. Due to the finding of partially chlorinated by-products, they postulated a mechanism via intermediates with partially positively charged, penta-coordinated silicon atoms with the coordination of  $\text{AlCl}_3$  to one silicon atom. This intermediate also explains the formation of ethyl-substituted polysilanes in the presence of ethylsilanes (Scheme 22).

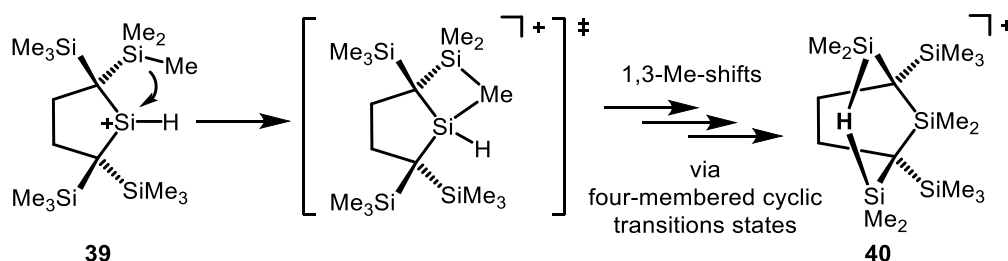
Scheme 22. Proposed mechanism for the rearrangement of cyclohexasilane **3** to ethyl-substituted cyclohexasilane **30** based on ethyl-methyl-exchange reactions.

These penta-coordinated silicon atoms formed in the course of the Wagner-Meerwein-type rearrangements may be described as silyl cationic intermediates, if the choice of Lewis acid and solvent is suitable.

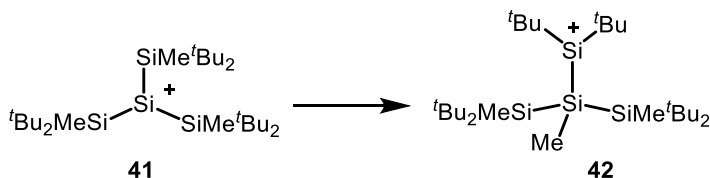
In several publications, analogous rearrangements involving 1,3-methyl group shifts have been described. The 1,3-methyl shifts are believed to pass through four-membered cyclic transition states. For example, Eaborn disclosed the occurrence of these 1,3-methylshifts via four-membered cyclic transitions states during the solvolysis of tris(trimethylsilyl)methylsilyl halides **37**.<sup>[51-54]</sup>

Scheme 23. Solvolysis of tris(trimethylsilyl)methylsilyl halides according to Eaborn.<sup>[52]</sup>

Müller and co-workers investigated the reactivity of hydrogen-substituted silylium ions and observed the surprising rearrangement of silylium ion **39** to the hydrogen-bridged cation **40**. Computationally, they located four intermediate silylium ions along the reaction path, which are interconverted by 1,3-methyl group shifts.<sup>[55]</sup>

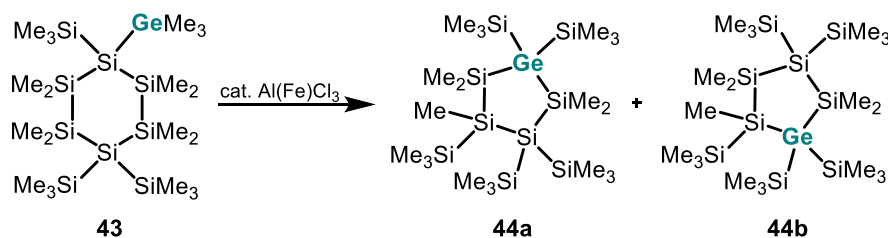
Scheme 24. Formation of the hydrogen-bridged bissilyl cation **40** starting from hydridosilylium ion **39**, the  $[\text{B}(\text{C}_6\text{F}_5)_4]^-$  anion is not shown.

The chemistry of silyl cationic species experienced immense popularity in recent years<sup>[56-58]</sup> but polysilanyl-substituted silyl cations and their role in rearrangement reactions still lack experimental evidence. One reason might be the thermolability of simple polysilanylsilyl cations, which adds to the inherent high reactivity of silyl cations. For example, Lambert and co-workers reported on the formation of tris(trimethylsilyl)silylium,  $(\text{Me}_3\text{Si})_3\text{Si}^+$ , most probably in the form of its arene complexes, but the  $^{29}\text{Si}$  NMR spectrum shows substantial decomposition of the substance.<sup>[59-62]</sup> Sekiguchi and co-workers focused on the synthesis of silylium ions with polysilyl backbones and discussed the occurrence of aromaticity and homoaromaticity in more complex, cyclic structures.<sup>[63-66]</sup> They also found evidence for 1,3-methyl shifts occurring in the dialkylpolysilanylsilyl cation **41** (Scheme 25).<sup>[67]</sup>

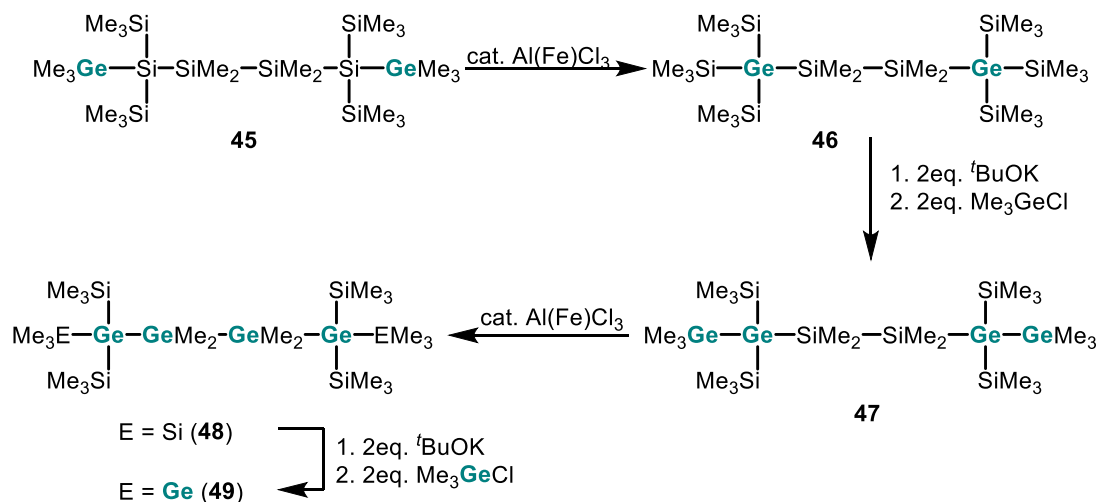
Scheme 25. Rearrangement of tris(di-*tert*-butyl(methyl)silyl)silylium ion **41** to silylium ion **42**, the  $[\text{B}(\text{C}_6\text{F}_5)_4]^-$  anion is not shown.

### 1.3.2 Rearrangement Reactions of Germapolsilanes

Based on these findings Marschner et al. investigated the fate of a germyl substituent in an otherwise methylated or silylated polysilane substrate, and illustrated that the germanium exhibits a surprising tendency to occupy central positions in the silicon framework of the products (Scheme 26).<sup>[68]</sup> The remarkable selectivity of this rearrangement, together with the polysilanylsilylpotassium chemistry of Marschner et al.,<sup>[30]</sup> offers an easy route for the synthesis of germasilanes<sup>[69]</sup> and germapolsilanes, which are difficult to synthesise by other routes (Scheme 27).<sup>[68]</sup>

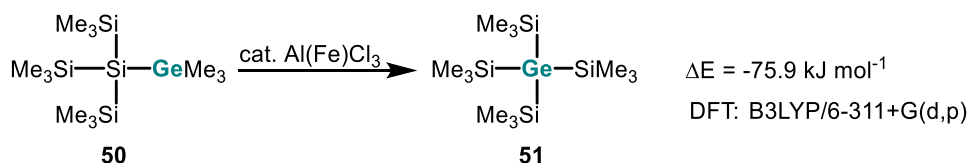


Scheme 26. Rearrangement of the germanium atom into the central positions and ring contraction of germasilane **43**.



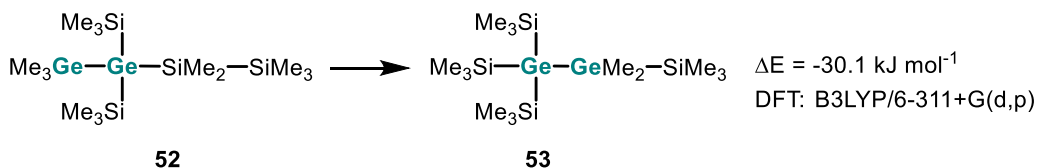
Scheme 27. Synthesis of hexagermane **49** by exploiting polysilanylsilyl anions and Wagner-Meerwein-type rearrangement reactions.

Also the treatment of the simple germysilane **50** with  $\text{AlCl}_3$  relocates the germanium atom into the central position to give tetrakis(trimethylsilyl)germane **51**. A detailed theoretical study of this intriguing rearrangement reaction was reported by Müller and Marschner<sup>[68]</sup> using the transformation of **50** to **51** as a model reaction for the calculations.



Scheme 28. Simplified rearrangement reaction, suitable for quantum mechanical calculations.

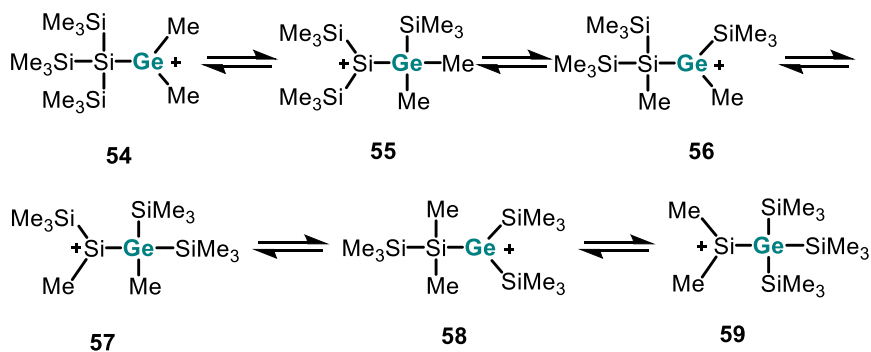
The quantum mechanical computation of the transformation **50** → **51** (Scheme 28), shows that the rearrangement is exothermic by 75.9 kJ mol<sup>-1</sup> according to density functional theory computations at the B3LYP/6-311+G(d,p) level. By analogy, the formation of tetragermane **48** from its isomer **47** (Scheme 27) can be explained by the higher stability of 2,3-digermatetrasilane (Me<sub>3</sub>Si)<sub>3</sub>Ge-GeMe<sub>2</sub>SiMe<sub>3</sub> (**53**) compared to its isomeric 1,2-digermatetrasilane (Me<sub>3</sub>Ge)(Me<sub>3</sub>Si)<sub>2</sub>GeSiMe<sub>2</sub>SiMe<sub>3</sub> (**52**) by 30.1 kJ mol<sup>-1</sup> (Scheme 29).<sup>[68]</sup>



Scheme 29. Computed rearrangement **52** → **53** is used as model reaction for the rearrangement **47** → **58**.

The authors expected the rearrangement to be analogous to Wagner-Meerwein-rearrangements, and to proceed via 1,2-methyl and 1,2-silyl shifts (Scheme 30). The rearrangement reaction is initialised by the heterolytical bond cleavage of a relatively weak Ge-C bond at the periphery of the germysilane **50** by AlCl<sub>3</sub> and to give the germyl cation **54** along with methyltrichloroaluminate, [MeAlCl<sub>3</sub>]<sup>-</sup>. The reaction cascade proceeds via subsequent 1,2-trimethylsilyl and 1,2-methyl shifts and passes through the isomeric cations **54**-**59**. The final step is methyl transfer from the aluminate to silyl cation **59** to yield the neutral tetrasilylgermane **51**.

Although several steps are endothermic, the overall isomerisation of germyl cation **54** to silyl cation **59** is an exothermic process ( $\Delta E = -44.0 \text{ kJ mol}^{-1}$ ) (Figure 2). To explain this behaviour, several factors have to be taken into account. For example the bond strengths, whereas the exchange of a Si-Si bond ( $D_E = 294 \text{ kJ mol}^{-1}$ ) by a Si-Ge bond ( $D_E = 281 \text{ kJ mol}^{-1}$ ) occurs with an energy loss of 13.0 kJ mol<sup>-1</sup>, the transfer of a methyl group from a germanium atom in **55** ( $D_E(\text{Ge-C}) = 305 \text{ kJ mol}^{-1}$ ) to a silicon atom in **56** ( $D_E(\text{Si-C}) = 347 \text{ kJ mol}^{-1}$ ) results in an energy gain of 42 kJ mol<sup>-1</sup>.

Scheme 30. Suggested isomerisation cascade of germylum ion **54** to silylium ion **59**.

Moreover, electronic effects, such as  $\alpha$ - or  $\beta$ -silyl effects, play an important role during this cascade. The calculated energies imply that silyl and germyl cations are better stabilised by  $\alpha$ -SiMe<sub>3</sub> or  $\alpha$ -GeMe<sub>3</sub> groups than by methyl groups. Even greater stabilisation is obtained by a  $\beta$ -silyl group, which occur when Si<sub>2</sub>Me<sub>5</sub> groups are present. Even though Me<sub>3</sub>Ge<sup>+</sup> is more stable than Me<sub>3</sub>Si<sup>+</sup> by 38.8 kJ mol<sup>-1</sup> at the B3LYP/6-311+G(d,p) level, the sum of these stabilising  $\beta$ -silyl groups in cation **59** dominates the thermodynamics (Figure 2).<sup>[68]</sup>

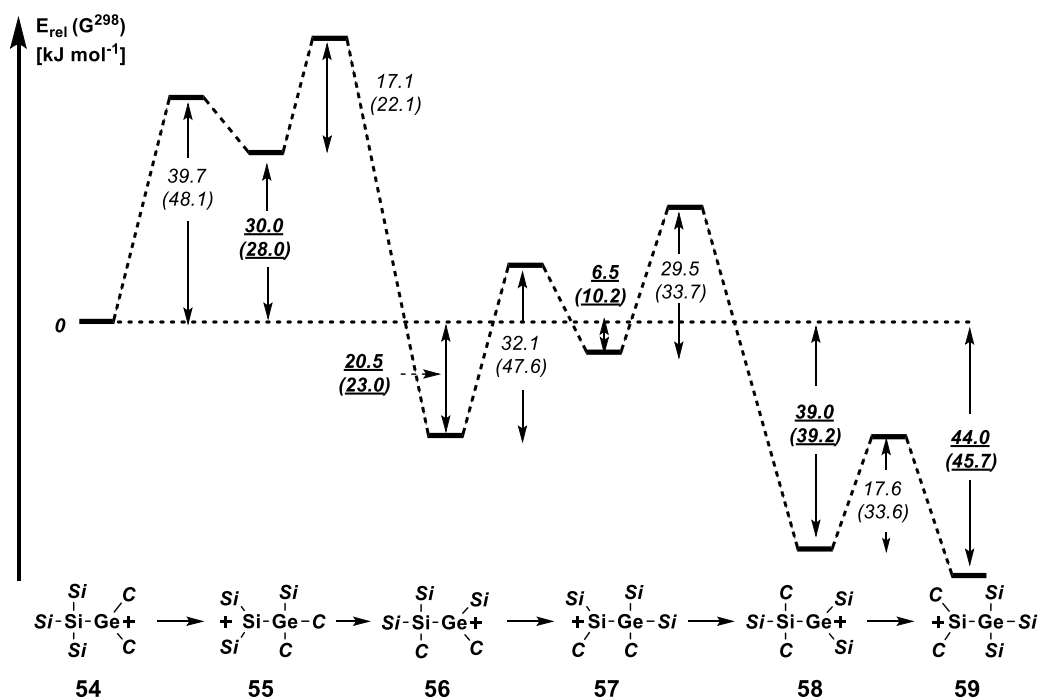


Figure 2. Reaction diagram for the isomerisation **54** → **59** computed at the B3LYP/6-311+G(d,p) level. Ground-state energies,  $E$ , and Gibbs free energies at 298.15 K,  $G^{298}$  (in parentheses), relative to cation **54** are given in bold italic print and underlined, while activation energies  $\Delta E^\ddagger$  and free energies  $\Delta G^\ddagger,^{298}$  for the forward reaction are given in italics. In the structures, Si stands for SiMe<sub>3</sub> and C for CH<sub>3</sub>.<sup>[68]</sup>

## 1.4 Silyl Cations

The silicon analogue of the well known carbenium ion, the silylium ion is a tri-coordinated silicon species with a positively charged silicon atom. Theoretically, their synthesis should be easier than the synthesis of carbenium ions, since silicon is more electropositive, easier to polarise and has a larger atomic radius than carbon. Furthermore, the stabilisation energies for  $R_3E^+$ , according to isodesmic reaction (1) (Scheme 31) is, in general, higher for  $E = Si$  than for  $E = C$ .<sup>[58]</sup>

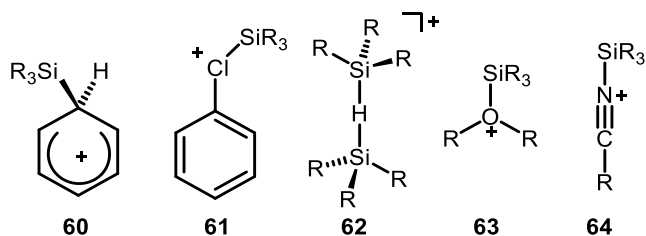


Scheme 31. Isodesmic reaction (1) used for the calculation of stabilisation energies  $\Delta E$  of  $R_3Si^+$ .

The inherent high electrophilicity and reactivity are the two major properties of silylium ions which causes these species to show interactions with solvents and counter anions in solution or even in the solid state. Unfortunately, solvents and counter anions, which are usually innocent in other areas of chemistry, are not appropriate in silylium ion chemistry. Silicon atoms are able to expand their coordination sphere and have a larger atomic radius than carbon. This facilitates nucleophilic attack, increases the requirements for anions and solvents and often leads to donor-stabilised silylium ions. Some of these interactions are shown in Scheme 32. Due to the formation of strong bonds between silicon and oxygen or silicon and halogens, especially fluorine and chlorine, the assortment of solvents is mostly limited to aromatic solvents and halogenated arenes. Depending on the substituents and on the demand of the electron deficient silicon centre, either silyl arenium ions **60**<sup>[58]</sup> or silylated arylhalonium ions **61**<sup>[70-71]</sup> are formed. To obtain non-stabilised, planar silylium ions, the substituents have to provide a sufficient steric and/or electronic stabilisation.

Another way to synthesise silylium ion-like species is by using silanes as solvent. In the case of small aliphatic moieties at the silicon atom, stabilisation by the formation of a hydrogen-bridged species of the composition  $[R^1_3Si-H-SiR^2_3]^+$  **62** can be observed.<sup>[71-72]</sup> Choosing ethers or nitriles as solvents also gives rise to solvent-stabilised silylium ion-like species, such as oxonium ions **63**<sup>[73]</sup> and nitrilium ions **64**<sup>[74]</sup>. At low temperatures, halogenated hydrocarbons, in particular dichloromethane, are suitable alternatives to arenes. At temperatures around  $T = -50\text{ }^\circ\text{C}$  the reaction of a silyl cation with the halogenated solvent is often slow enough to allow spectroscopic identification, reactivity studies or, in some cases, the isolation of silyl cation salts. At higher temperatures, the silyl cations not only form

complexes with the solvent, they react to form the corresponding chlorosilane or completely decompose.<sup>[58, 67, 75-79]</sup>



Scheme 32. Typical solvent complexes of silylium ions.

Concerning the counter anions, the choice is relatively small, because only very robust and weakly coordinating anions can be used. Fluorinated tetraaryl borates of the type  $[\text{B}(\text{C}_6\text{F}_{5-n}\text{R}_n)_4]^-$ <sup>[80]</sup> ( $\text{R} = \text{SiR}^1_3$ ,  $\text{H}$ ,  $n = 0, 1$ ), halogenated carba-*closo*-borates of the type  $[\text{RCB}_{11}\text{H}_{11-n}\text{X}_n]^-$ <sup>[80-86]</sup> and  $[\text{RCB}_{11}\text{Me}_{11-n}\text{X}_n]^-$ <sup>[87]</sup> ( $\text{R} = \text{H}$ , alkyl;  $\text{X} = \text{F}$ ,  $\text{Cl}$ ,  $\text{Br}$ ,  $\text{I}$ ,  $n = 6$ ), perhalogenated *closo*-borates  $[\text{B}_{12}\text{X}_{12}]^{2-}$ <sup>[82, 88]</sup> ( $\text{X} = \text{Cl}$ ,  $\text{Br}$ ) and  $[\text{Me}_3\text{NB}_{12}\text{Cl}_{11}]^-$ <sup>[89]</sup> and aluminates  $[\text{Al}(\text{OC}(\text{CF}_3)_3)_4]^-$ <sup>[90]</sup> fulfil all requirements.

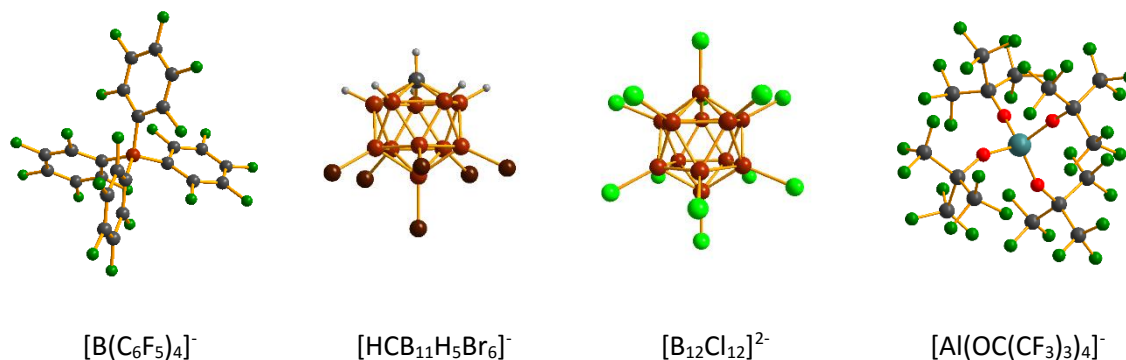
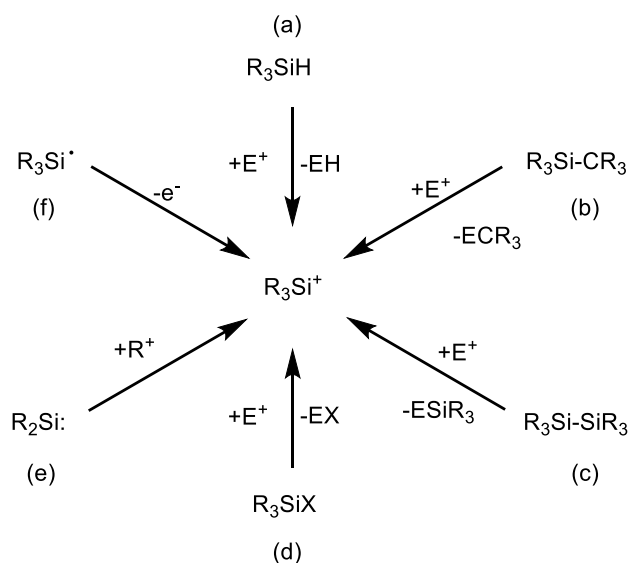


Figure 3. Weakly coordinating anions used in silylium ion chemistry.

The application of tetraaryl borates as counter anions with arene solvents gives either silyl arenium tetraaryl borates<sup>[60, 91]</sup> or, when enough steric and/or electronic stabilisation by the substituents at the silicon atom is provided, silylium borates.<sup>[92-95]</sup> On the contrary, halogenated *closo*-borate or *closo*-carborate anions with small trialkylsilylium ions form zwitterions with the silyl cation, in which the silicon atom is bonded to one of the halogen atoms of the counter anion.<sup>[80-81]</sup>

### 1.4.1 Synthesis of Silylium Ions

In the last decades, many strategies for the synthesis of silylium ions or stabilised silylium ions have been established.<sup>[56-58]</sup> The most frequently used methods are the cleavage of Si-H, Si-C and Si-Si bonds by strong electrophiles  $E^+$  (Scheme 33, path (a) - (c)). The cleavage of Si-X bonds ( $X = F, Cl, Br$ ) (Scheme 33, path (d)) is successful only in the case of strongly stabilised silyl cations. The addition reactions of cationic species  $R^+$  to silylenes (Scheme 33, path (e)) or the oxidation of silyl radicals (Scheme 33, path (f)) is rather limited, due to the small number of substrate compounds.



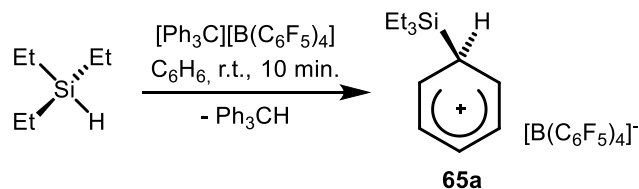
Scheme 33. Overview of the synthetic approaches to silylium ions.

The most common and established way to synthesise silylium ions in the condensed phase is a variation of the classical Bartlett-Condon-Schneider (BCS) hydride transfer reaction.<sup>[96-101]</sup> This is performed using a strong Lewis acid which leads to the formation of the silylium ion or silylium ion-like species and the hydride adduct of the Lewis acid. In most cases, triphenylcarbenium ion (trityl) is the favoured Lewis acid because in addition to its strong Lewis acidity it is available with a wide variety of weakly coordinating counter anions, such as perfluorinated tetraaryl borates<sup>[80]</sup>, carba-*closo*-borates<sup>[80-81]</sup> or *closo*-borates<sup>[82-84, 88-89]</sup> and perfluorinated aluminates<sup>[102-103]</sup>. Typically, the BCS reaction is performed in either polar solvents (sulfolane, ethers and nitriles), in chlorinated or aromatic hydrocarbons or in silanes. The nature and in particular the reactivity of the generated silyl cation depends on the substituents at the silicon atom, the solvent and the counter anion. In cases

when benzene or toluene is used as solvent, the reaction with trityl tetrakis(pentafluorophenyl)-borate  $[\text{Ph}_3\text{C}][\text{B}(\text{C}_6\text{F}_5)_4]$  at room temperature is completed within minutes and leads to the formation of a biphasic system. The upper, non-polar phase contains the Lewis acid hydride adduct, in this case triphenylmethane, and the lower, polar phase is saturated with the pure silylium borate.

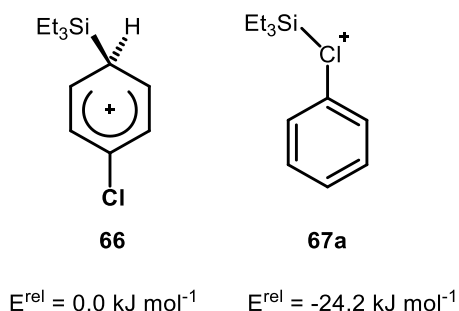
#### 1.4.2 Arene-Stabilised Silylium Ions

If the silylium ion bears only small alkyl substituents, stabilisation by the arene solvents can be observed and the formed species are best termed as silylated arenium borates **65** $[\text{B}(\text{C}_6\text{F}_5)_4]$ , e.g. triethylsilyl benzenium borate **65a** $[\text{B}(\text{C}_6\text{F}_5)_4]$ . Based on structural data obtained from X-ray diffraction analysis, it is commonly accepted that, as a consequence of  $\beta$ -silyl hyperconjugation, the structure of these silylated arenium ions should be viewed neither as a traditional  $\sigma$ -complex nor as a  $\pi$ -complex, but rather as a point along a  $\sigma$ - $\pi$ -continuum.<sup>[79]</sup>



Scheme 34. Synthesis of triethylsilyl benzenium borate **65a** $[\text{B}(\text{C}_6\text{F}_5)_4]$ .<sup>[79]</sup>

Performing the hydride abstraction reaction of silanes in chlorobenzene also yields solvent complexes. DFT calculations at the B3LYP/6-311+G(d,p) level of theory suggest that in this case the coordination of the solvent via the chlorine substituent, **67**, is favoured.<sup>[70]</sup> The formation of chloronium ion **67** is energetically preferred by 24.2 kJ mol<sup>-1</sup> at 298 K compared to the formation of the chloro-substituted arenium ion **66**. This behaviour can also be seen in the solid-state structure of  $[\text{Pr}_3\text{Si}(\text{odcb})][\text{CHB}_{11}\text{Cl}_{11}]$  (odcb = *ortho*-dichlorobenzene). The molecular structure of the cation  $[\text{Pr}_3\text{Si}(\text{odcb})]^+$  reveals a tetra-coordinated silicon atom with the fourth coordination side occupied by a chlorine atom of the coordinated *ortho*-dichlorobenzene molecule (Figure 4).<sup>[71]</sup>



Scheme 35. Stability of silyl arenium ion **66** versus silyl chloronium ion **67a** as computed according to density functional methods at the B3LYP/6-311+G(d,p) level of theory.

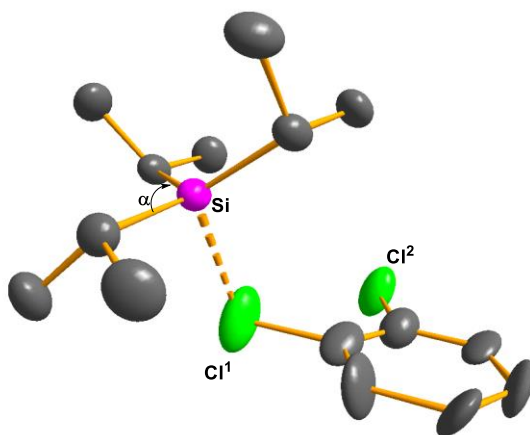
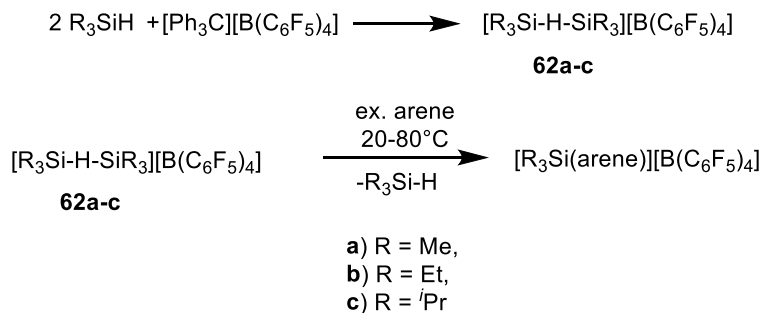


Figure 4. Molecular structure of  $[\text{iPr}_3\text{Si}(\text{odcb})]^+$  **67b** in the compound  $[\text{iPr}_3\text{Si}(\text{odcb})][\text{CHB}_{11}\text{Cl}_{11}]$ . (Ellipsoid presentation, H-atoms omitted for clarity, thermal ellipsoids at 50% probability level, only one of two disordered molecules is shown.) Important bond lengths [pm] and angles [ $^\circ$ ]: Si-Cl<sup>av</sup> = 233.2; Cl<sup>1</sup>-C = 177.4; Cl<sup>2</sup>-C = 170.9;  $\Sigma\alpha(\text{Si}) = 350.3$ <sup>[71]</sup>

### 1.4.3 Silane-Stabilised Silylium Ions

When the classical hydride transfer reaction with trityl tetrakis(pentafluorophenyl)borate is performed with alkylsilanes  $\text{R}_3\text{SiH}$  ( $\text{R} = \text{Me}, \text{Et}, \text{iPr}$ ) being both reactant and solvent, bisilyl hydronium ions  $[\text{R}_3\text{Si-H-SiR}_3]^+$  **62** can be isolated. One might regard these cations as silane-stabilised silylium ions, which are characterised by a Si-H-Si two-electron, three-centre (2e3c) bond and feature two tetra-coordinated silicon atoms.<sup>[71-72, 104]</sup> In early publications, these compounds were mistakenly described as simple silylium salts  $[\text{R}_3\text{Si}][\text{B}(\text{C}_6\text{F}_5)_4]$ . However, in 2011 it was found that redissolving  $[\text{R}_3\text{Si-H-SiR}_3][\text{B}(\text{C}_6\text{F}_5)_4]$  in a solvent that can coordinate to the  $\text{R}_3\text{Si}^+$  ion, e.g., arenes, ethers, or sulphur dioxide,

will lead to a displacement of the silane, and the formation of  $R_3Si(solvent)^+$  cations as the active silylating agents (Scheme. 36)<sup>[72, 104-105]</sup>



Scheme. 36. Preparation of hydrogen-bridged silylium ion **62** and its reaction with arenes.

In contrast to these intermolecularly stabilised silylium ions, an intramolecular Si-H-Si bridged silylium ion was reported by Müller in 2001.<sup>[106]</sup> In cases where a second Si-H functionality is present in the molecule after hydride abstraction reaction, an intramolecular 2e3c bond is formed. Several bis-silyl-, bisgermyl- or germylsilylhydronium ions **40**, and **68-73**<sup>[55, 107-110]</sup> have been prepared to date. Cations **40**, **69** and **71** are stable in aromatic solvents at room temperature and no formation of arenium ions was detected (Figure 5). The silyl cations **72** and **73** are even stable in chlorinated hydrocarbons such as  $CH_2Cl_2$  and  $CHCl_3$  at ambient conditions for several days.<sup>[108]</sup>

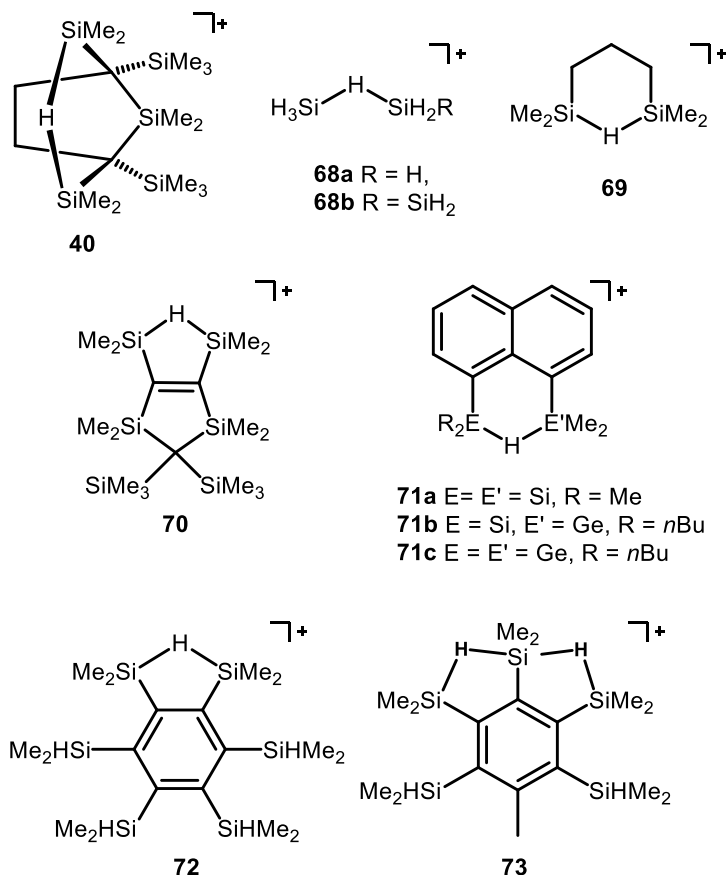
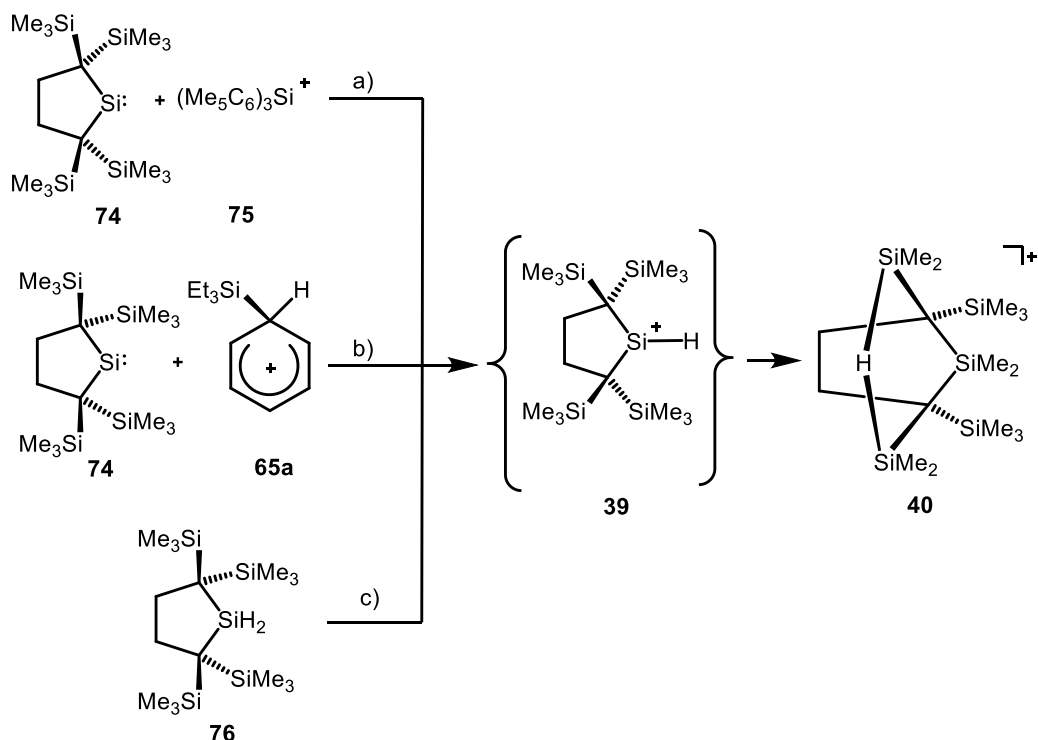


Figure 5 Bissilyl-, bisgermyl- or germysilyl ions that feature 2e3c Si-H-Si bridges.<sup>[55, 106-111]</sup>

The findings of our group<sup>[55]</sup>, summarised in Scheme 37, indicate the remarkable thermodynamic preference of silyl cations that are stabilised by a Si-H-Si multicentre bonding over classical silylium ions of the type R<sub>3</sub>Si<sup>+</sup>. Three different routes for the synthesis of silylium ion **39** were attempted but all led to the formation of the same hydrogen-bridged bissilyl cation **40**. The heterolytic cleavage of dihydrogen by the FLP formed from silylene **74** and silylium ion **75** to give the silane (Me<sub>5</sub>C<sub>6</sub>)<sub>3</sub>SiH and silylium ion **40**, or the conventional protonation of silylene **74** by using silyl arenium ion **65a** or the application of the classical hydride transfer reaction starting from dihydridosilane **76** all gave exclusively the hydrogen-bridged bissilyl cation **40**.



Scheme 37. Synthesis of hydrogen-bridged bissilyl cation **40**. The  $[\text{B}(\text{C}_6\text{F}_5)_4]^-$  anion is omitted. a)  $\text{H}_2$ , r.t., 0.103 MPa,  $\text{C}_6\text{D}_6$ ,  $-(\text{Me}_5\text{C}_6)_3\text{SiH}$ ; b)  $\text{C}_6\text{D}_6$ , r.t.,  $-\text{Et}_3\text{SiC}_6\text{H}_5$ ; c)  $[\text{Ph}_3\text{C}]^+$ ,  $\text{C}_7\text{H}_8$ ,  $T = 80^\circ\text{C}$ ,  $-\text{Ph}_3\text{CH}$ .<sup>[55]</sup>

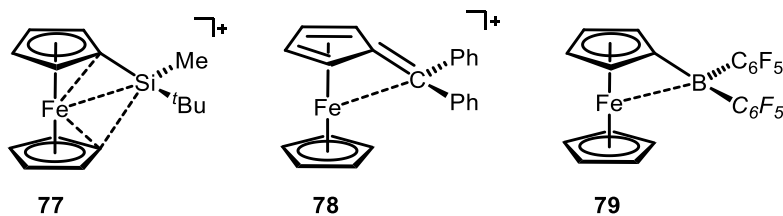
Molecular structures of the 2e3c hydrogen-bridged disilyl cations have only been obtained from XRD analysis of compounds **40** $[\text{HCB}_{11}\text{H}_5\text{Br}_6]$ , **62a** $[\text{HCB}_{11}\text{Cl}_{11}]$ , **62b** $[\text{B}(\text{C}_6\text{F}_5)_4]$  and **71a** $[\text{B}(\text{C}_6\text{F}_5)_4]$ . Kordts et al. were successful in crystallising the 2e3c hydrogen-bridged bisgermyl cationic compound **71c** $[\text{B}(\text{C}_6\text{F}_5)_4]$ .<sup>[110]</sup> Ab initio MP2 and density functional methods predict a symmetrical structure for the Si-H-Si unit, which is perfectly reflected in the solid state structures of cations **62a**, **62b** and **71a**. Calculations at B3LYP/6-311+G(d,p) predict a linear Si-H-Si linkage in cation **62a**; however experimentally a slightly bent structure (**62a**  $\alpha = 160^\circ$ <sup>[71]</sup>, **62b**  $\alpha = 172^\circ$ <sup>[104]</sup>) was found. The rather flat bending potential for the Si-H-Si unit in cations **62a** and **62b** and/or crystal lattice forces may cause the disagreement between the theoretical gas phase structures and the molecular structure of cations **62a** and **62b**.<sup>[71, 104]</sup> The cyclic structures of cations **40** and **71a** exhibit stronger bending of the Si-H-Si bridge (**40**:  $\alpha^{\text{exp.}} = 142^\circ$ ,  $\alpha^{\text{calc.}} = 139^\circ$  (M06-2X/6-311G(d,p))<sup>[55]</sup>, **71a**:  $\alpha^{\text{exp.}} = 131^\circ$ ,  $\alpha^{\text{calc.}} = 136^\circ$  (MP2/6-31G(d,p))<sup>[107]</sup>). These intramolecularly stabilised silyl cations show very characteristic  $^{29}\text{Si}$  NMR spectroscopic data. The  $^{29}\text{Si}$  resonances appear in a region of  $\delta^{29}\text{Si} = 25$ -100 and the small direct  $J$ -coupling constants of  $^1J = 39$ -58 Hz indicate a reduced bond order between the silicon and hydrogen atoms compared to regular silanes  $^1J_{\text{Si,H}} = 160 - 240$  Hz.<sup>[55, 60, 71-72, 106-110]</sup> The  $^1\text{H}$  NMR chemical shift of

the bridging hydrogen atom, which is high field shifted compared to regular Si-H functionalities, is very characteristic.

The formation of Si-H-Si bridged complexes was also found experimentally in the gas phase. In 2013, the group of Dopfer synthesised mass selected  $\text{Si}_x\text{H}_y^+\text{-Ar}$  or  $\text{Si}_x\text{H}_y^+\text{-Ne}$  clusters in a supersonic plasma expansion of silane  $\text{SiH}_4$  diluted in a rare gas mixture. They identified the silyl cation by Ne-tagging IR photodissociation (IRPD) spectroscopy. They found that the produced  $\text{Si}_x\text{H}_y^+$  with  $X > 1$  often exhibit stable Si-H-Si bridges, which exhibit characteristic bands in the  $650\text{--}2200\text{ cm}^{-1}$  range. Together with quantum mechanical calculations, these bands can be assigned to fundamentals of the bridged  $\text{H}_3\text{Si-H-SiH}_2\text{R}^+$  ( $\text{R} = \text{H}, \text{SiH}_2$ ) ions **68** (Figure 5).<sup>[111-112]</sup>

#### 1.4.4 Ferrocene-Stabilised Silylium Ions

The group of Oestreich discovered another type of intramolecular stabilisation of silylium ions.<sup>[77-78]</sup> An unprecedented structural motif is demonstrated by the intramolecularly stabilised silylium ion **77** which was synthesised by a hydride transfer reaction starting from the ferrocenyl monosilane  $\text{FcSiHMe}^t\text{Bu}$  and is characterised by a low field  $^{29}\text{Si}$  NMR chemical shift of  $\delta^{29}\text{Si} = 114.6$ . Compared to the isoelectronic carbocation **78** and the neutral boron compound **79**, the molecular structure of silyl cation **77** reveals distinctive structural details. Although an interaction of the exocyclic group with the iron centre is displayed in all three compounds **77**, **78** and **79**, the bending quantified by the dip angle  $\beta$ , in the silyl cation is most pronounced ( $\beta(\textbf{77}) = 44.8^\circ$ ,  $\beta(\textbf{78}) = 20.7^\circ$ ,  $\beta(\textbf{79}) = 16.0^\circ$ ). The extreme dip angle in **77** shifts the silicon atom closer to both cyclopentadienyl rings of the ferrocene moiety and suggests an intramolecular stabilisation of the silyl cationic centre by the ferrocene. This assumption is consistent with the results of quantum mechanical analysis of the bonding situation in **77**. Hence, two  $2e3c$  bonds involving iron, silicon and both *ipso*-carbon atoms  $\text{C}^{ipso}$  account for the unconventional molecular structure of silylium ion **77**.



Scheme 38. Ferrocene-stabilised silicon cation **77** and isoelectronic carbocation **78** and the neutral boron compound **79**.

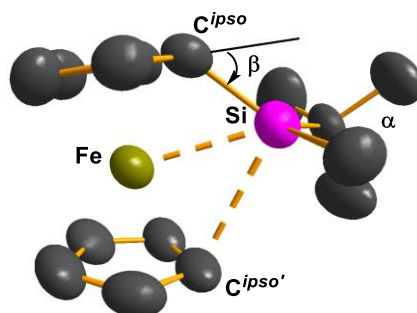
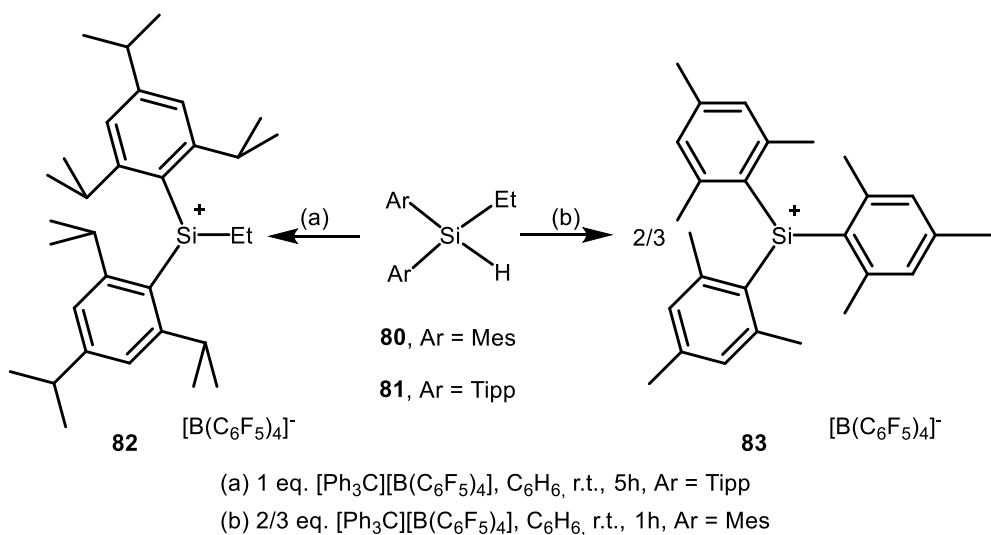


Figure 6. Molecular structure of ferrocenylsilylium ion **77**, in the crystal of **77**<sub>2</sub>[B<sub>12</sub>Cl<sub>12</sub>]. (Ellipsoid presentation, all H-atoms are omitted for clarity, thermal ellipsoids at 50% probability level) Important bond lengths [pm] and angles [°]:

Si-Fe = 249.2; Si-C<sup>ipso</sup> = 182.9; Si-C<sup>ipso'</sup> = 278.4;  $\Sigma\alpha(\text{Si}) = 353.5$ ;  $\beta = 44.8$ .<sup>[78]</sup>

#### 1.4.5 Tri-Coordinated Silylium Ions

The best approach to non-stabilised, planar, tri-coordinated silyl cations is achieved by the use of very bulky substituents at the silicon atom. Several silanes with bulky aryl substituents are very promising but due to the size of the triphenylcarbenium ion, the hydride transfer reaction with these sterically hindered silanes is very slow or even completely stopped.<sup>[92, 94, 113]</sup> Due to this steric hindrance of the reactants, the synthesis of these triarylsilylium ions from the corresponding triarylsilane is not possible. The exchange of one aromatic moiety by a smaller alkyl group enables the hydride transfer and gives the expected alkyl diarylsilylium ion **82** (Scheme 39).<sup>[113-114]</sup> However, starting from, for example, ethyldimesitylsilane **80**, the ethyl moiety is, on the one hand small enough to enable the triphenylmethyl cation to abstract the hydride but on the other hand the mesityl moieties are too small to stabilise the expected ethyldimesitylsilyl cation and to prevent any subsequent reactions.<sup>[113]</sup> In this case, the initially formed silyl cation undergoes substituent exchanges with the starting silane and trimesitylsilylium ion **83** is formed. Further results indicate a delicate balance between steric and electronic effects of the starting silane in the preparation of silylium ions.<sup>[113-114]</sup>



Scheme 39. Substituent dependency of the formation of silylium borates.

A reaction course for the formation of triarylsilylium borates utilising this substituent exchange methodology was proposed using the reaction of dimesitylmethylsilane with trityl borate to obtain trimesitylsilylium borate (**83** $[\text{B}(\text{C}_6\text{F}_5)_4]$ ).<sup>[113-114]</sup> Silylium ions **82** and **83** are two of a few recently reported silylium ions, which are stable as solids for several weeks; however during crystallisation attempts decomposition of the products was observed.<sup>[95, 113]</sup>

## 1.5 $^{29}\text{Si}$ NMR Chemical Shifts of Polysilanes and Germapolysilanes

The substitution of the silicon atoms in permethylated polysilanes and germapolysilanes can easily be identified by the  $^{29}\text{Si}$  NMR chemical shift. Different structural motifs reveal a characteristic chemical shift range of the signals in the  $^{29}\text{Si}$  NMR spectrum.<sup>[9, 14, 44-45, 115-119]</sup> The permethylated pentasilane structures shown in Figure 7 and Figure 8 act as representatives for larger molecules and demonstrate the structural motifs discussed below.

Anionic silicon atoms as in polysilanyl potassium silanides appear high field in the range of  $\delta^{29}\text{Si} = -200 - -180$  and tetrasilyl-substituted silicon atoms at  $\delta^{29}\text{Si} = -140 - -120$ . Trisilyl-substituted silicon atoms show a variance in the  $^{29}\text{Si}$  NMR chemical shift depending on the fourth moiety: a hydrogen atom leads to a shift range of  $\delta^{29}\text{Si} = -120 - -100$  and an alkyl or aryl substituent shifts the signal slightly towards low field at  $\delta^{29}\text{Si} = -90 - -70$ . A  $^{29}\text{Si}$  NMR chemical shift range of  $\delta^{29}\text{Si} = -50 - -30$  is characteristic for dimethylsilyl groups of a cyclic silane which are positioned between tetrasilyl-substituted silicon atoms. Similar shifts are found for dimethylsilyl groups of linear polysilanes also connecting tetrasilyl-substituted silicon atoms; they are slightly shifted further to low field at  $\delta^{29}\text{Si} = -50 - -20$ . Flanking dimethylsilyl groups also show a signal in the range of  $\delta^{29}\text{Si} = -35 - -15$ .

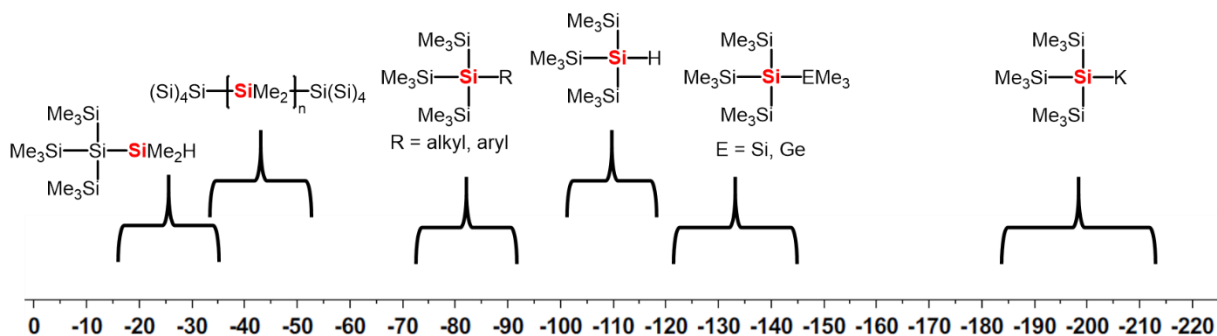


Figure 7. Characteristic  $^{29}\text{Si}$  NMR chemical shifts of structural motifs in permethylated polysilanes and germapolysilanes in the chemical shift range  $\delta^{29}\text{Si} = -220 - 0$ .

The  $^{29}\text{Si}$  NMR chemical shift of flanking trimethylsilyl groups is very characteristic and can be found at  $\delta^{29}\text{Si} = -10 - 0$ , whereas trimethylsilyl groups connected to a silicon atom usually appear around  $\delta^{29}\text{Si} = -10 - -5$  and trimethylsilyl groups connected to a germanium atom are slightly low field shifted at  $\delta^{29}\text{Si} = -7 - -0$ . The synthesis of permethylated polysilanes and germapolysilanes involves the preparation of halogen- or triflate-substituted starting materials. Due to the differences of the electron withdrawing properties of iodine, bromine, chlorine and fluorine atoms or the triflate

moiety, the substituted silicon atoms can be distinguished by their  $^{29}\text{Si}$  NMR shifts.<sup>[14, 120-127]</sup> Flanking iododimethylsilyl groups are shifted to  $\delta^{29}\text{Si} = 0 - 3$ , flanking bromodimethylsilyl groups appear at  $\delta^{29}\text{Si} = 19 - 25$ , chlorodimethylsilyl groups at  $\delta^{29}\text{Si} = 25 - 30$ , fluorodimethylsilyl groups at  $\delta^{29}\text{Si} = 35 - 40$  and triflate substitution yields a  $^{29}\text{Si}$  NMR chemical shift of  $\delta^{29}\text{Si} = 35 - 55$ .

Stabilised silylium ions can be classified by their characteristic low field shifts, which varies from  $\delta^{29}\text{Si} = 60 - 150$ , which is in significant contrast to free silylium ions at  $\delta^{29}\text{Si} = 210 - 240$ .<sup>[56]</sup>

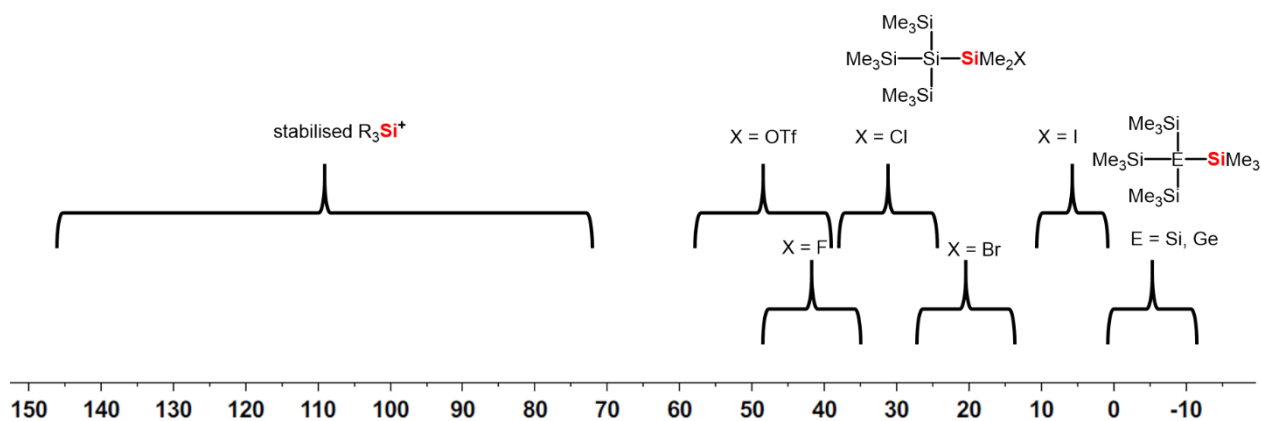
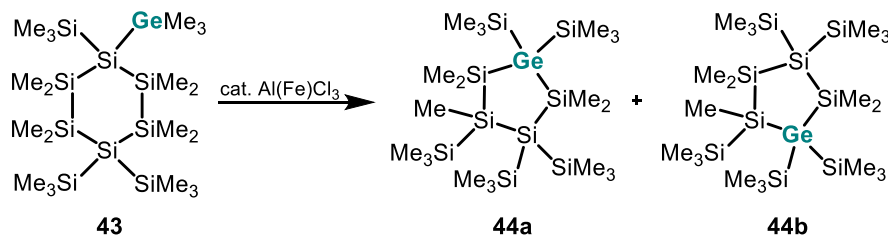


Figure 8. Characteristic  $^{29}\text{Si}$  NMR chemical shifts of structural motifs in permethylated polysilanes and germapolysilanes in the chemical shift range  $\delta^{29}\text{Si} = -10 - 150$ .

## 2 Motivation

The controlled synthesis of defined polysilanes or germapolysilanes is of great importance since they can be viewed as one-dimensional semiconductor materials and offer widespread potential for so-called “smart materials”.<sup>[1-4]</sup> Access to this class of compounds is mainly limited to the Wurtz-type coupling reaction which yields primarily linear polysilanes. Several investigations of the groups of Kumada<sup>[44-45]</sup> and Marschner<sup>[68, 119, 128-129]</sup> showed that polysilanes and germapolysilanes undergo a skeletal rearrangement of the silicon and germanium containing backbone when treated with a catalytic amount of Lewis acid, such as  $\text{AlCl}_3$ .

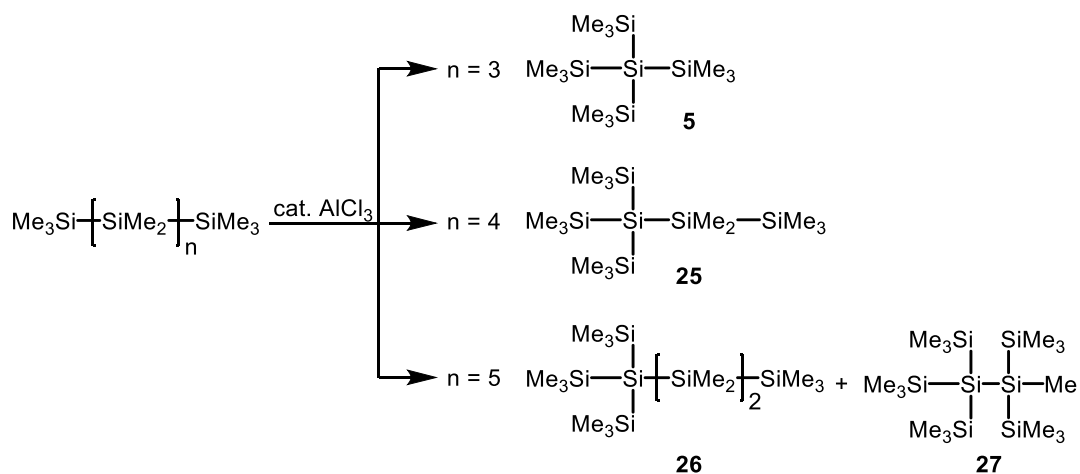
Germapolysilanes not only reorganise the silicon backbone but also shuttle the germanium atoms into the centre of the polysilane skeletal. In this reactions the germanium atoms in flanking positions show a high tendency to occupy central positions, where they are only surrounded by silicon atoms (Scheme 40).<sup>[68]</sup>



Scheme 40. Rearrangement of the germanium atom into the central position and ring contraction of germasilane **43**.<sup>[68]</sup>

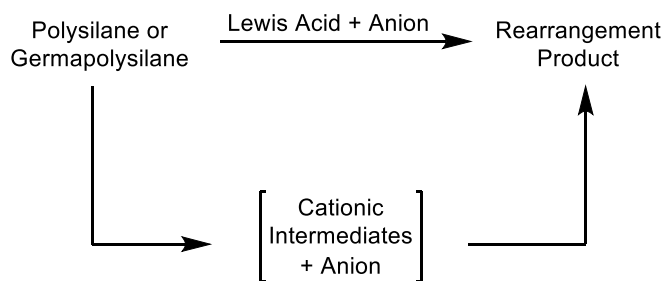
Linear and cyclic polysilanes reorganise the entire silicon backbone to give highly branched isomers (Scheme 41). These rearrangements are believed to be analogues to the well-known Wagner-Meerwein-rearrangement of carbon chemistry.<sup>[68]</sup>

Several groups have studied the Lewis acid-catalysed rearrangement of polysilyl or germapolysilyl compounds for synthetic purposes, however, very little is known about mechanistic details of these reactions. Thus, the focus of the following investigations is on the elucidation of mechanistic processes of the shuttling of the germanium atoms and other skeletal rearrangements of polysilanes.



Scheme 41.  $\text{AlCl}_3$ -catalysed rearrangement of linear polysilanes yield the branched isomers.

As mentioned in the introduction, a theoretical study of similar rearrangements in germapolysilanes predicts the rearrangement to proceed similar to the Wagner-Meerwein rearrangement in carbon chemistry via cationic intermediates. The aim of this work is to use suitable Lewis acids in combination with weakly nucleophilic anions, which should permit the stabilisation of cationic intermediates occurring during these rearrangements.



Scheme 42. General procedure for the preparation of cationic intermediates during the rearrangement reaction of polysilanes and germapolysilanes.

This research aims to find suitable ways to stabilise highly reactive silylium or germlyium ions. Not only do the nature of the Lewis acids and the counter anions play an important role during these reactions. The synthesis of well-designed starting materials is important and will be accompanied by a detailed study of substituent effects to extend the understanding of stabilisation principles in polysilanylsilyl or -germyl cation chemistry. The intriguing rearrangements in polysilanes and germapolysilanes will be clarified by mechanistic studies and the proposed cationic intermediates will be detected and characterised.

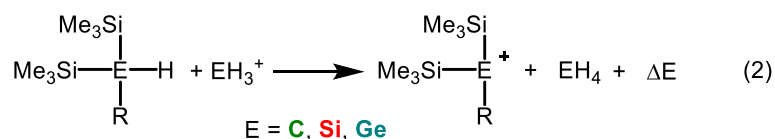
### 3 Results and Discussion

#### 3.1 Initial Considerations on the Stability of Silyl Cations

Linear and cyclic polysilanes and germapolysilanes rearrange into their highly branched isomers when treated with a Lewis acid. They are believed to proceed in a manner analogous to the well-known Wagner-Meerwein-rearrangement of carbon chemistry via silyl or germyl cationic intermediates.<sup>[45, 47, 68]</sup> Initial considerations put the properties of polysilanylsilyl or -germyl cations in focus.

In organic chemistry, the importance of substituent effects on the thermodynamic stability of carbocations is well established. It is textbook-knowledge that the stability of carbocations is influenced by inductive and mesomeric effects or hyperconjugation properties of substituents. Not only mechanistic pathways are explained by carbocation stabilities, but also selective syntheses of target molecules are possible by the correct choice of substituents of cationic intermediates.<sup>[130]</sup>

The preparation of cations of the heavier elements of group 14 is a challenging task and depends on many factors, such as the counter anion, solvent, temperature, and the steric and electronic properties of substituents at the element atom.<sup>[56]</sup> The relative thermodynamic stability of  $R_3E^+$  cations are described to increase monotonically along the series from carbon to lead for a variety of substituents  $R$ .<sup>[58]</sup> In the course of this work, the synthesis of polysilanylsilyl or polysilanylgermyl cationic compounds will be explored. As a starting point, the effect of a substituent  $R$  on the thermodynamic stability of element 14 cations will be quantified. The relative stability of polysilanyl-substituted cations of the type  $(Me_3Si)_2RE^+$  ions can be assessed by the isodesmic reaction (2) (Scheme 43). In an isodesmic reaction the number and nature of bonds remain the same, a C-H, Si-H or Ge-H bond is exchanged by a new C-H, Si-H or Ge-H bond, respectively. Variation of the substituent  $R$  allows for an estimation of the stabilisation properties of the group  $R$ .



Scheme 43. Isodesmic reaction (2) used for the calculation of the substituent effect on the thermodynamic stability of carbocations, silylium and germlyum ions.

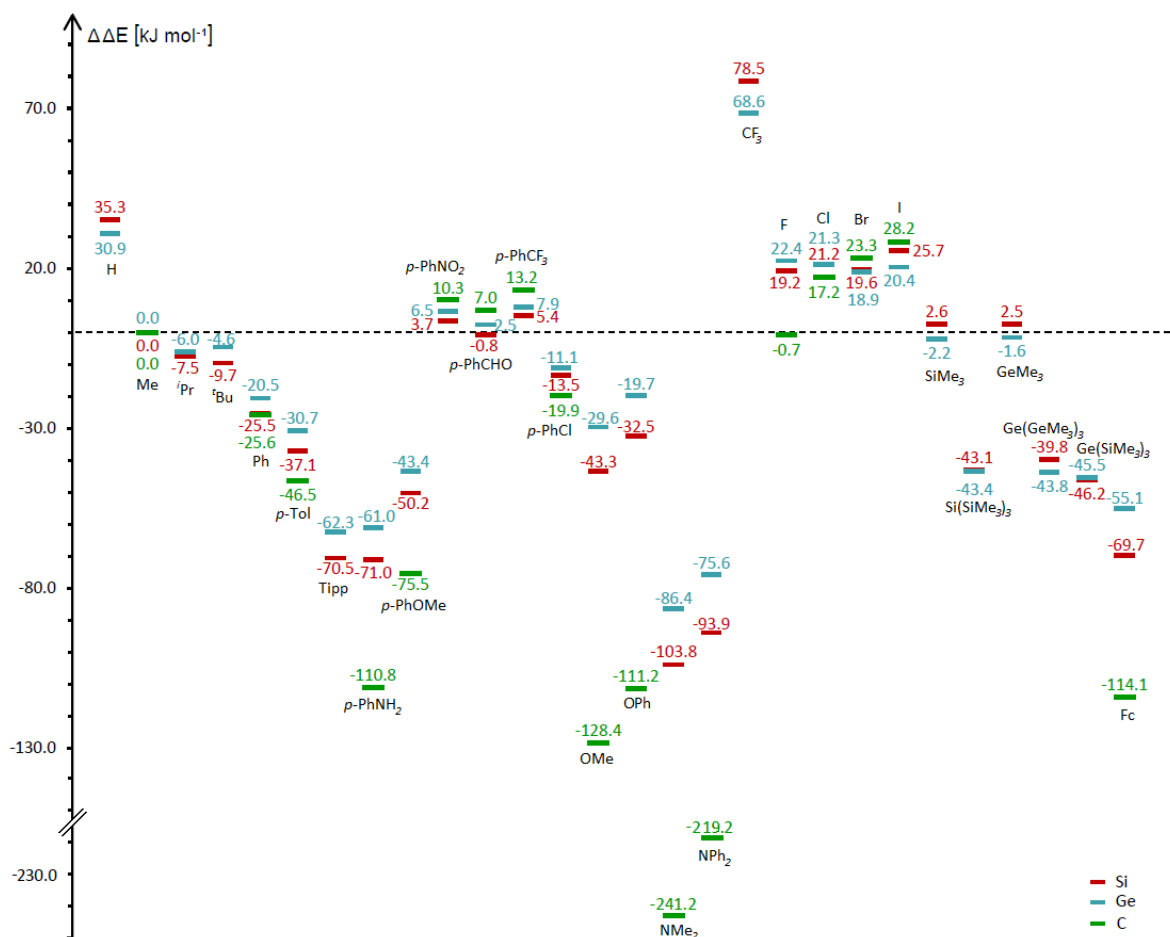


Figure 9. Relative stabilisation energies  $\Delta\Delta E$  [kJ mol<sup>-1</sup>] of  $(\text{Me}_3\text{Si})_2\text{RE}^+$  vs  $\text{R} = \text{Me}$ . Calculated according isodesmic reaction (2) at M06-2X/6-311+G(d,p) level of theory ( $\Delta\Delta E^{\text{R}} = \Delta E^{\text{R}} - \Delta E^{\text{Me}}$ ).

The diagram in Figure 9 shows the relative stabilisation energies compared to the methyl substituent for the group 14 element cations for a variety of substituents. The missing entries for carbocations are due to a lack of optimised molecular structures, as several of these species do not correspond to local minima on the potential energy surface. Some of these carbocations, e.g. those with  $\text{R} = \text{H}$ ,  $i\text{Pr}$ ,  $t\text{Bu}$ ,  $\text{CF}_3$ , Tipp (2,4,6-tri-*iso*-propylphenyl),  $\text{SiMe}_3$ ,  $\text{GeMe}_3$ ,  $\text{Si}(\text{SiMe}_3)_3$ ,  $\text{Ge}(\text{SiMe}_3)_3$  and  $\text{Ge}(\text{GeMe}_3)_3$ , either rearrange to give a secondary carbocation or undergo a trimethylsilyl or -germyl shift to give the silylium or germylium ion. This demonstrates the high preference for the formation of silyl or germylium ions compared to carbocations.

The stabilisation properties of the different substituents show a similar trend for all groups 14 element cations ( $\text{E} = \text{C}$ ,  $\text{Si}$  and  $\text{Ge}$ ). A notable feature is the pronounced substituent effect on carbocations and the general smaller effect on germylium

ions compared to silylium ions. Alkyl groups slightly stabilise silylium and germylium ions. As expected, aromatic moieties show a different effect depending on their substitution. Phenyl, *para*-toluene and Tipp stabilise the cations by delocalisation of the positive charge through the aromatic ring systems. *para*-Aminophenyl and *para*-methoxyphenyl are known for their positive mesomeric effect, which is also the reason for the high stabilisation obtained by amino moieties, such as NMe<sub>2</sub> and NPh<sub>2</sub>. In contrast, *para*-nitrophenyl and *para*-formylphenyl destabilise these cations by the negative mesomeric effect and *para*-trifluoromethylphenyl, halogens and especially trifluoromethyl groups destabilise the cations due to their strong electron withdrawing properties. As expected, carbocations are much more sensitive to mesomerism as indicated by the enormous energy differences for R = OMe, OPh, NMe<sub>2</sub>, NPh<sub>2</sub>, *para*-aminophenyl and *para*-methoxyphenyl compared to silylium or germylium ions. Interestingly, the fluorine substituent shows a higher stabilisation effect on carbocations than chlorine, bromine or iodine presumably due to its strong  $\pi$ -electron donation properties. There is almost no difference in the stabilisation effect on silylium or germylium ions by trimethylsilyl or -germyl groups. Interestingly, they have a similar influence on the stability of the silylium and germylium ions compared to alkyl groups. A significant effect is found for hypersilyl (Si(SiMe<sub>3</sub>)<sub>3</sub>) or hypergermyl (Ge(GeMe<sub>3</sub>)<sub>3</sub> or Ge(SiMe<sub>3</sub>)<sub>3</sub>) groups. They show almost an equivalent stabilisation of the silylium or germylium ions as alkoxy or aryloxy moieties (OMe or OPh) or aromatic (Ph, *p*-Tol, Tipp) substituents. Müller and Marschner have previously noted that silylium and germylium ions are markedly stabilised by  $\beta$ -silyl or  $\beta$ -germyl groups.<sup>[68]</sup> Although nitrogen- or oxygen-containing substituents were predicted to be highly stabilising substituents for silylium or germylium ions, the high affinity of the lone pairs at the nitrogen or oxygen atoms for the strong Lewis acidic silylium or germylium ions excludes them from the list of suitable substituents.

A well-established tool for quantifying the electron-donating ability of substituted aryl groups in reactions which proceed via benzylic carbocations, is Brown's substituent constants  $\sigma^+$  for a variety of *meta* and *para* substituents.<sup>[131-133]</sup> From the previous discussion of thermodynamic stabilisation, it is apparent that not only carbocations but also silylium or germylium ions are stabilised by  $\pi$ -delocalisation via aryl substituents. The similar structures of the silylium and germylium ions provides an opportunity to probe the influence of the aryl substituent on the stabilisation of the cations. A plot of the thermodynamic stability given by the isodesmic reaction (2) (Scheme 43) versus the  $\sigma^+$  constants for the eight *para* substituents<sup>[131]</sup> in carbocations and silylium and germylium ions suggests a correlation between these parameters (Figure 10). The thermodynamic stability of the cation is increased by substituents with a smaller  $\sigma^+$  constant, which translates to an increase in the

$\pi$ -donating ability of the aryl substituent. The trend lines for E = Si and Ge are very similar but have a smaller slope than the trend line for E = C. As already discussed, carbocations reveal a higher sensitivity towards a change in the  $\pi$ -donation properties of the substituents compared silylium and germlyium ions. This is also indicated by the steeper slope of the trend line for E = C, which expresses the more sensitive dependency of the stability of carbocations towards substituent variations compared to silylium and germlyium ions.

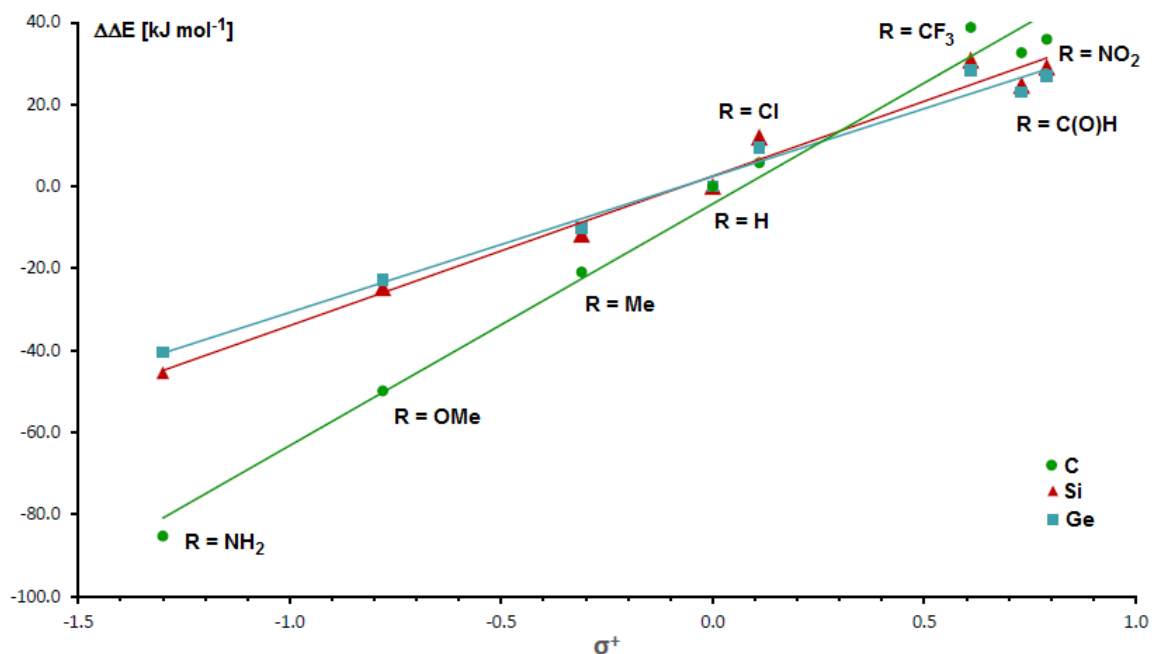
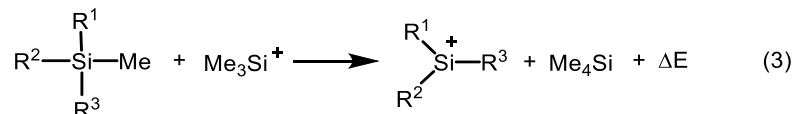


Figure 10. Plot of the thermodynamic stability  $\Delta\Delta E$  versus  $\sigma^+$ . The correlations is given by the following equations: for E = C:  $\Delta\Delta E = 58.96\sigma^+ - 4.24$ ,  $R = 0.99$ , for E = Si:  $\Delta\Delta E = 36.48\sigma^+ + 2.54$ ,  $R = 0.98$ ; for E = Ge:  $\Delta\Delta E = 33.14\sigma^+ + 2.42$ ,  $R = 0.98$ .

These results clearly demonstrate that the principles of organic chemistry for the stabilisation of carbocations are transferrable to cations of the heavier group 14 elements. A fine-tuning of the substituents is necessary to obtain the best stabilisation in these transient cationic species.

Previously, the stability of silyl cations was assessed for bis(trimethylsilyl)-substituted silyl cations with variation in the third moiety. The influence of the number of silyl groups at the cationic silicon atom was also calculated using the isodesmic reaction (3) (Scheme 44). The stabilisation energies in Table 1 clearly demonstrate the stabilising effect of three silyl substituents compared to two or only one silyl moiety.



Scheme 44. Isodesmic reaction (3) for the calculation of the stabilisation energies of silyl-substituted silylium ions.

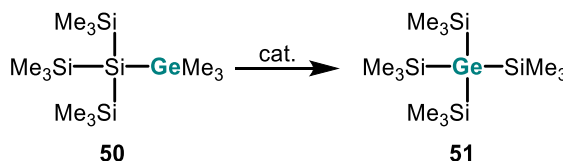
Table 1. Calculated stabilisation energies  $\Delta E$  [kJ mol<sup>-1</sup>] of silyl cations. Calculated according to isodesmic reaction (3) at M06-2X/6-311G+(d,p).

R <sup>1</sup>	R <sup>2</sup>	R <sup>3</sup>	$\Delta E$ [kJ mol <sup>-1</sup> ]
SiMe <sub>3</sub>	Me	Me	-34.5
SiMe <sub>3</sub>	SiMe <sub>3</sub>	Me	-47.7
SiMe <sub>3</sub>	SiMe <sub>3</sub>	SiMe <sub>3</sub>	-50.9

These considerations will aid in the understanding of the mechanistic investigations on Lewis acid-catalysed rearrangements of polysilanes and germapolysilanes. They demonstrate the ability of polysilanyl substituents to stabilise silylium or germylum ions, which come into play during the planned investigations on cationic intermediates in polysilanes and germapolysilanes.

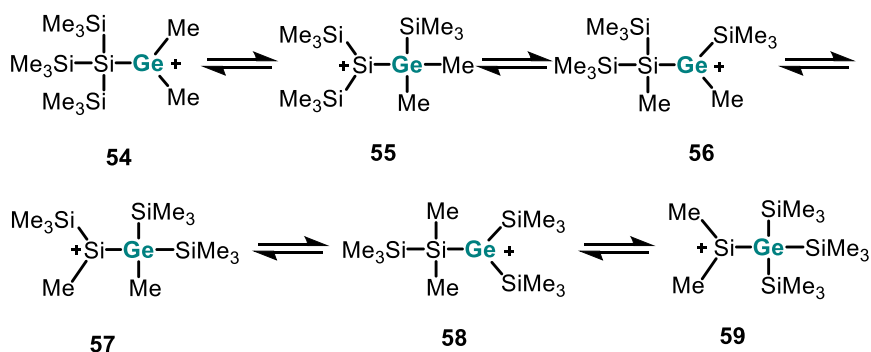
### 3.2 Lewis Acid Catalysed Rearrangements in Germapolysilanes - A Stable Ion Study

The following part of this thesis is based on the theoretical study that predicts that the shuttling of germanium atoms in a silicon backbone proceeds via cationic intermediates.<sup>[68]</sup> The goal of this work was to synthesise, detect and examine proposed intermediates, which were previously only assumed. To simplify the system, the reaction is reduced to the rearrangement of trimethylgermyltris-(trimethylsilyl)silane **50** to tetrakis(trimethylsilyl)germane **51** (Scheme 45).



Scheme 45. Rearrangement of germylsilane **50** to silylgermane **51** using Lewis acids. Method 1: cat. = 20 mol% Al(Fe)Cl<sub>3</sub>, 80°C, cyclohexane, quant.<sup>[68]</sup>, method 2: cat. = 4 mol% [Ph<sub>3</sub>C][B(C<sub>6</sub>F<sub>5</sub>)<sub>4</sub>], r.t., CH<sub>2</sub>Cl<sub>2</sub>, quant.<sup>[134]</sup>

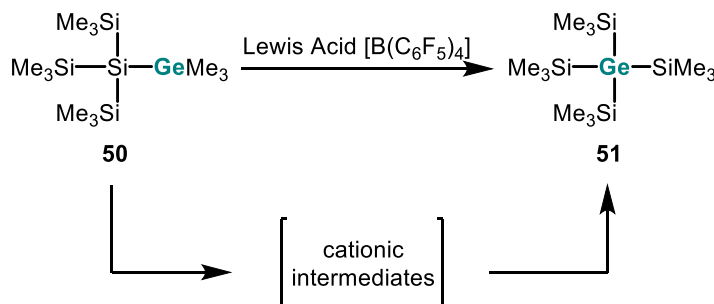
According to density functional theory computations at the B3LYP/6-311+G(d,p) level, the rearrangement of **50** to **51** was found to be exothermic by 75.9 kJ mol<sup>-1</sup>. A detailed theoretical insight was carried out by Müller who predicted on the basis the calculations a Wagner-Meerwein-type rearrangement via 1,2-methyl and 1,2-silyl shifts (Scheme 46).<sup>[68]</sup>



Scheme 46. Suggested isomerisation cascade of germylum ion **54** to silylium ion **59**.<sup>[68]</sup>

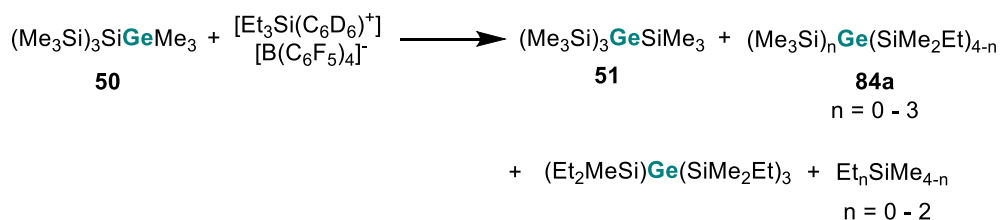
Since no cationic intermediates were detected in the reaction with catalytic amount of AlCl<sub>3</sub>, the idea was to vary the Lewis acid. The use of a Lewis acid in combination with a weakly nucleophilic anion should facilitate the stabilisation of any cationic intermediate occurring during the rearrangement. For this reason, the bulky and weakly nucleophilic tetrakis(pentafluorophenyl)borate anion was used,

which is well established in the synthesis of stable silylium ions. Strong and cationic Lewis acids, such as the trityl cation,  $\text{Ph}_3\text{C}^+$ , or silyl arenium ions,  $\text{R}_3\text{Si}(\text{arene})^+$ , were used to initiate the rearrangement and to produce a neutral by-product and, by this means, to give access to any cationic intermediate.



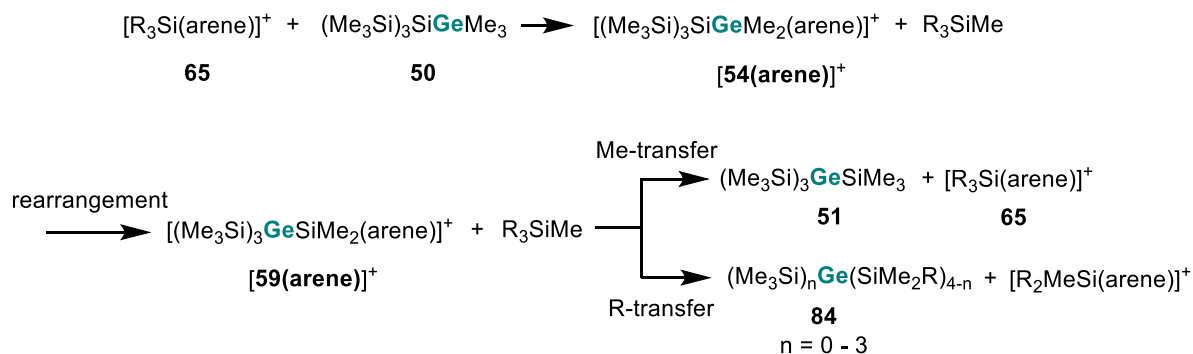
Scheme 47. General procedure for the preparation of cationic intermediates during the rearrangement reaction of germysilane **50**. (Lewis acid =  $\text{Ph}_3\text{C}^+$  or  $\text{R}_3\text{Si}(\text{arene})^+$ , R = Me, Et,  $i\text{Pr}$ , arene = benzene, toluene)

In previous studies<sup>[134]</sup>, the trityl cation was active in catalytic amounts of 4 mol% in dichloromethane and gave a clean conversion of germysilane **50** to silylgermane **51**. In order to detect the postulated cationic intermediates, stoichiometric amounts of the Lewis acids were applied, which enabled the reactions to be conducted at room temperature. When  $[\text{R}_3\text{Si}(\text{arene})][\text{B}(\text{C}_6\text{F}_5)_4]$  (a. R = Et and arene = benzene, b. R =  $i\text{Pr}$ , arene = toluene) was used at room temperature or at  $T = 6^\circ\text{C}$ , the conversion was completed in 2 h and resulted in a biphasic reaction mixture that is typical for solutions of tetrakis(pentafluorophenyl)borates in aromatic hydrocarbons.<sup>[56-58, 135]</sup>  $^{29}\text{Si}$  NMR spectra obtained of the ionic phases showed many signals, which indicated the formation of a complicated reaction mixture. The  $^{29}\text{Si}$  NMR analysis of the second, non-polar layer showed the presence of several different neutral compounds. When triethylsilyl benzenium ion **65a** was used, GC/MS and NMR analysis indicated the presence of at least nine neutral products. These nine compounds were identified as the expected silylgermane **51**, three different ethylmethysilanes and a series of silylated germanes **84a**.



Scheme 48. Stoichiometric reaction between triethylsilyl benzenium borate **65a** $[\text{B}(\text{C}_6\text{F}_5)_4]$  and germysilane **50** in benzene at  $T = 6^\circ\text{C}$ .<sup>[134]</sup>

The reaction with the tri-*iso*-propylsilyl toluenium ion **65b** only gave two side products, namely,  $(\text{Me}_3\text{Si})_3\text{GeSiMe}_2^i\text{Pr}$  and  $^i\text{Pr}_3\text{SiMe}$ . Interestingly, germanes **84**, are substituted with a different number of ethyl or *iso*-propyl groups. To result from germysilane **50**, each of these germanes must have cation **59** as a common intermediate (Scheme 49).



Scheme 49. Reaction of silylgermane **50** with different trialkylsilyl arenium borates **65** $[\text{B}(\text{C}_6\text{F}_5)_4]$  at r.t., (the  $[\text{B}(\text{C}_6\text{F}_5)_4]^-$  anion is omitted, R = Me, Et, *i*Pr, arene = benzene or toluene).<sup>[134]</sup>

At last, when trimethylsilyl toluenium borate  $[\text{Me}_3\text{Si}(\text{C}_7\text{D}_8)][\text{B}(\text{C}_6\text{F}_5)_4]$ , **65c** $[\text{B}(\text{C}_6\text{F}_5)_4]$ , was used only the expected rearrangement product **51** and tetramethylsilane were identified in the non-polar phase. These results were a clear indication that the initial step of the rearrangement reaction is cation formation by cleavage of either a Ge - C- or Si - C bond. The initial assumption that the first cationic intermediate formed should be germyl cation **54** which undergoes a rearrangement reaction to give silyl cation **59** is supported by the calculated bond strengths ( $D_e(\text{Ge} - \text{C}) = 305 \text{ kJ mol}^{-1}$ ;  $D_e(\text{Si} - \text{C}) = 347 \text{ kJ mol}^{-1}$ ). These numbers show, that the breaking of a Ge - C bond to give cation **54** is thermodynamically favoured. The terminating step in this reaction cascade is the back transfer of an alkyl group to the rearranged cation to yield either the symmetric germane **51** or the alkylated products **84**. The multiple substitution in the case of the ethyl-substituted silyl arenium ion demonstrates the ease of alkyl group exchange under the applied conditions, which is only limited by the steric requirements of the exchanging groups.

These results indicate that the rearrangement proceeds via the assumed cationic intermediates, but the reactions is too fast to detect them. Therefore, the reaction with germysilane **50** and tri-*iso*-propylsilyl toluenium ion **65b** was performed at lower temperatures to slow down the reactivity. At  $T = -20^\circ\text{C}$  in toluene, the  $^{29}\text{Si}$  NMR spectrum of the ionic phase showed four signals at  $\delta^{29}\text{Si} = -87.9, -7.9, -2.4$  and  $+98.1$  (Figure 11), wherein the signals at  $-87.9$  and  $-7.9$  dominate the spectrum (Figure 11).

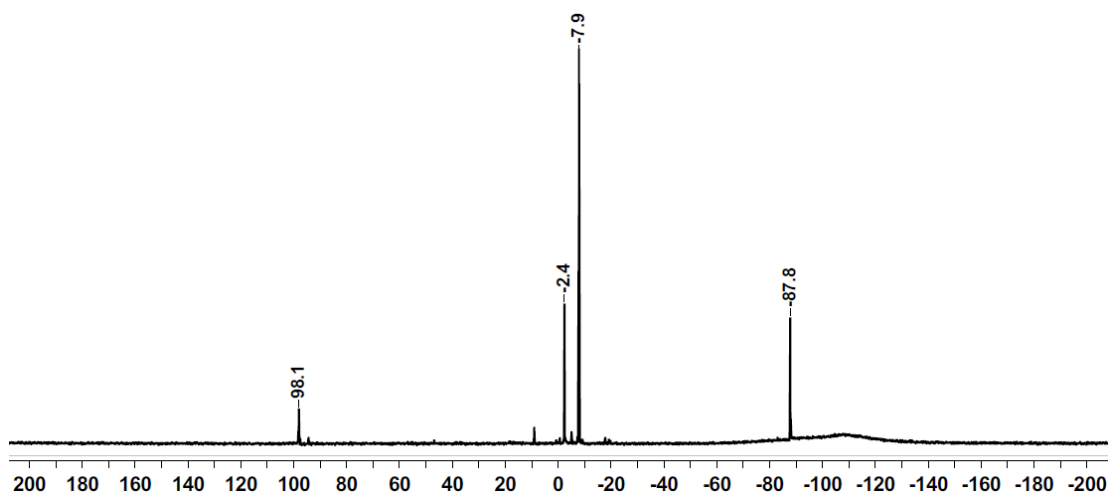


Figure 11. 99 MHz  $^{29}\text{Si}\{^1\text{H}\}$  NMR spectrum ( $\text{C}_7\text{D}_8$ ,  $T = -20^\circ\text{C}$ ) obtained from the polar phase of the reaction of germysilane **50** with tri-*iso*-propylsilyl toluenium borate (**65b** $[\text{B}(\text{C}_6\text{F}_5)_4]$ ) after 1h at  $-20^\circ\text{C}$ .

Table 2. Experimental and calculated  $^{29}\text{Si}$  NMR chemical shifts of solvent complexes of germylium ions **54** and **58** and silylium ion **59** (calculated values for the non-deuterated compounds at GIAO/M06-L/6-311G(2d,p)//M06-2X/6-311+G(d,p) in parentheses).

compound	$\delta^{29}\text{Si}$ ( $\text{Si}_4\text{Si}$ )	$\delta^{29}\text{Si}$ ( $\text{SiMe}_3$ )	$\delta^{29}\text{Si}$ ( $\text{Si}^+\text{Me}_2$ )	$\delta^{29}\text{Si}$ ( $\text{SiMe}_2$ )
[ <b>54</b> ( $\text{C}_7\text{D}_8$ )]	-87.9 (-93)	-7.9 (-7)		
[ <b>58</b> ( $\text{C}_7\text{D}_8$ )]		(8; -13)		(-13)
[ <b>59</b> ( $\text{C}_7\text{D}_8$ )]		-2.4 (0)	98.1 (108)	
[ <b>59</b> ( $\text{C}_6\text{D}_5\text{Cl}$ )] <sup>a</sup>		-1.5 (0)	154.3 (157)	

a) Calculated for the chloronium ion structure [**59**( $\text{C}_6\text{H}_5\text{Cl}$ )]. Chloronium ions are the dominating species when silyl cations are generated in chlorinated arenes, see ref.<sup>[70-71]</sup>

In the  $^{29}\text{Si}^1\text{H}$  HMBC NMR spectrum these two resonances (●) both exhibit a cross peak to the same methyl group at  $\delta^1\text{H} = 0.07$  in the  $^1\text{H}$  NMR spectrum and the signals with lower intensities at  $\delta^{29}\text{Si} = -2.4$  and  $+98.1$  (\*) correlate with two different methyl groups at  $\delta^1\text{H} = 0.12$  and  $-0.15$  (Figure 12). The resonance of the methyl group at  $\delta^1\text{H} = 0.07$  does not show any correlation to the signals at  $\delta^1\text{H} = 0.12$  and  $-0.15$  in any 2D-NMR spectrum, which indicates that they belong to two different compounds.

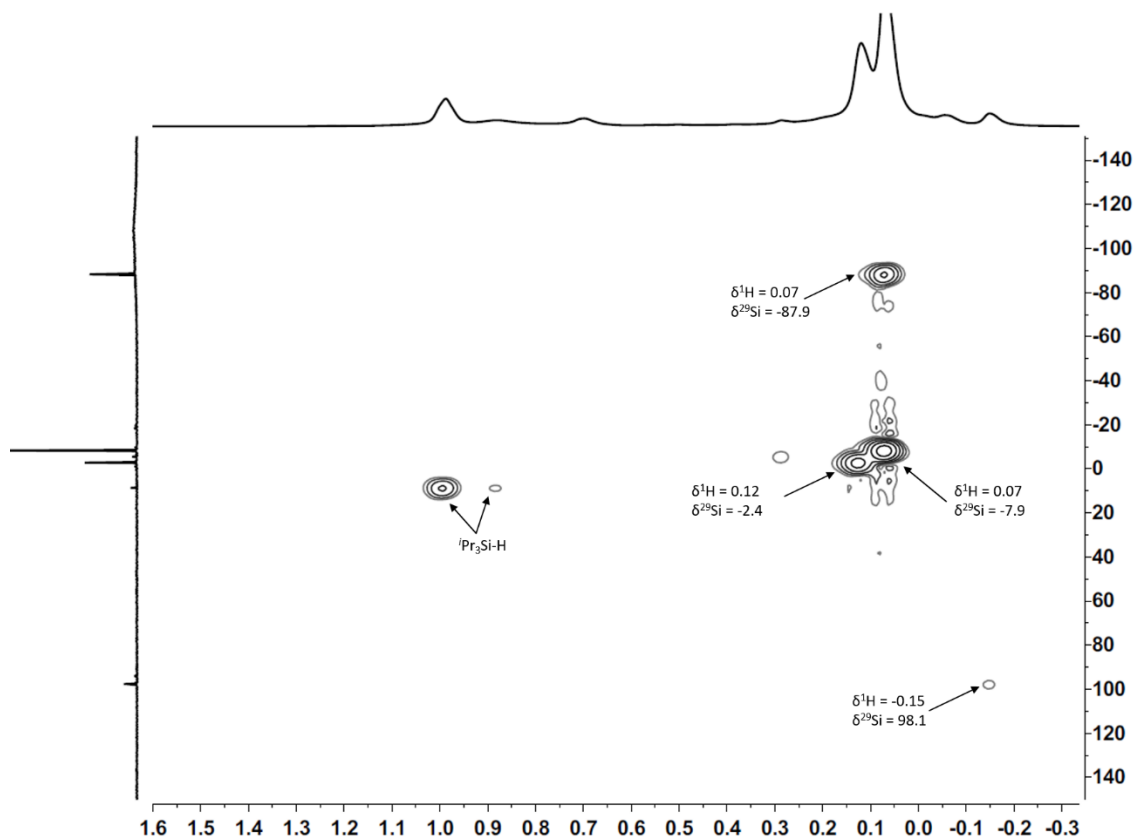


Figure 12. 500 MHz/99 MHz  $^1\text{H}/^{29}\text{Si}$  NMR spectrum ( $\text{C}_7\text{D}_8$ ,  $T = -20^\circ\text{C}$ ) obtained from the polar phase of the reaction of germysilane **50** with tri-*iso*-propylsilyl toluenium borate (**65b** $[\text{B}(\text{C}_6\text{F}_5)_4]$ ) after 1h at  $T = -20^\circ\text{C}$ .

Moreover, when measuring several  $^{29}\text{Si}$  NMR spectra successively, a change in the intensities can be observed (Figure 13). Over the course of time, the intensities of the two resonances at  $\delta^{29}\text{Si} = -87.9$  and  $-7.9$  (●) decrease and the intensities of the resonances at  $\delta^{29}\text{Si} = -2.4$  and  $+98.1$  (\*) increase, which is also an indication for the presence of two ionic compounds that are transformed into one another. After 120 days the initial compound (●) is nearly completely consumed and the ionic phase contains almost only the rearrangement product (\*).

The structural composition of the products can be assigned by the  $^{29}\text{Si}$  NMR chemical shift range. The resonance at  $-87.9$  in the  $^{29}\text{Si}$  NMR spectrum is characteristic for tetrasilyl-substituted silicon atoms ( $\text{SiSi}_4$ ) and the resonance at  $-7.9$  represents trimethylsilyl groups connected to a silicon atom. These two signals show an integral ratio in the  $^{29}\text{Si}\{^1\text{H}\}$  inverse gated experiment of 1:3. These NMR data (●) are consistent with the structure of the initially produced germyl toluenium ion **54**( $\text{C}_7\text{D}_8$ ). In addition, the results of quantum mechanical calculations of  $^{29}\text{Si}$  NMR chemical shifts for an optimised molecular structure of **54**( $\text{C}_7\text{D}_8$ ) predict values that are very close to the experiment (see Table 2).

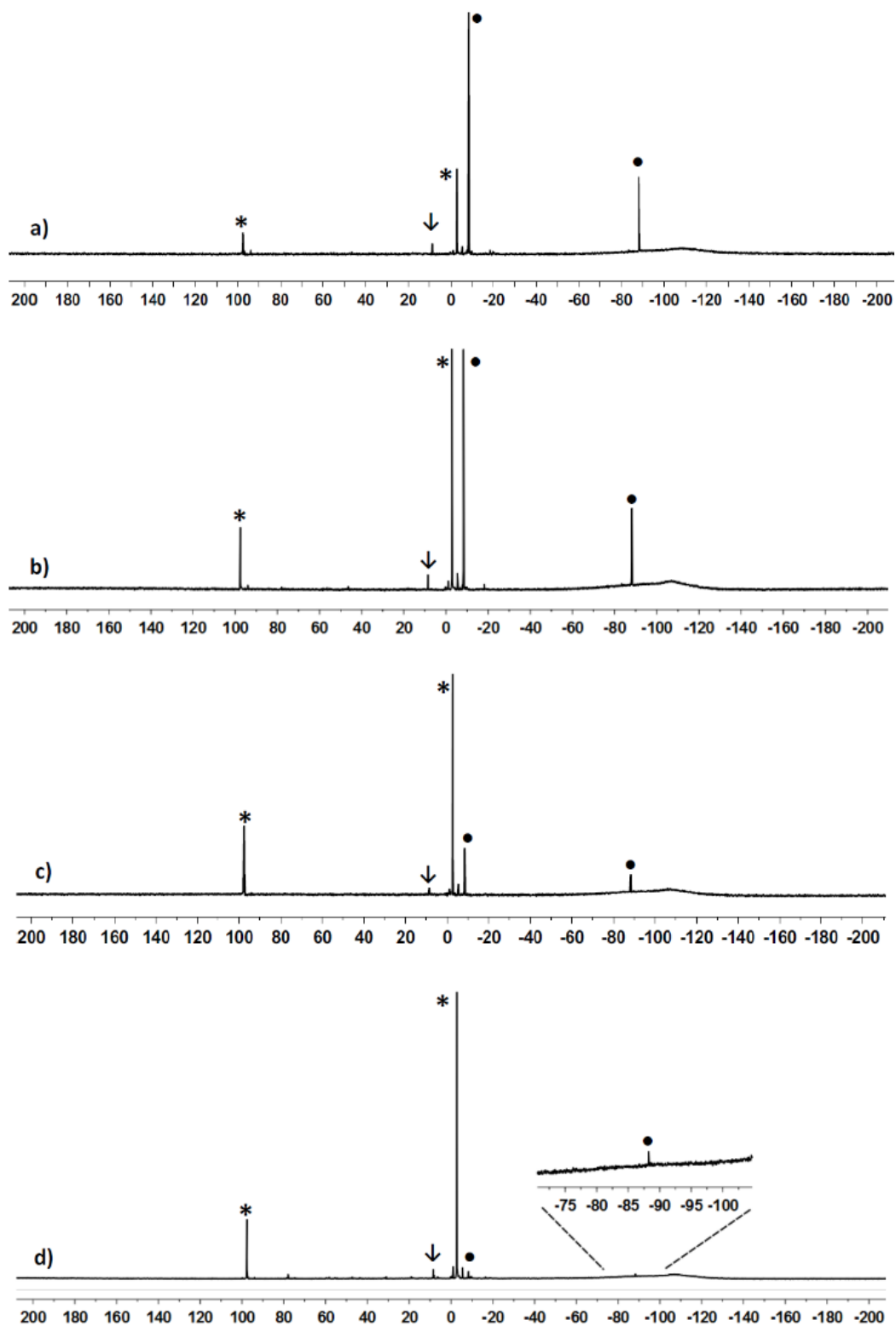
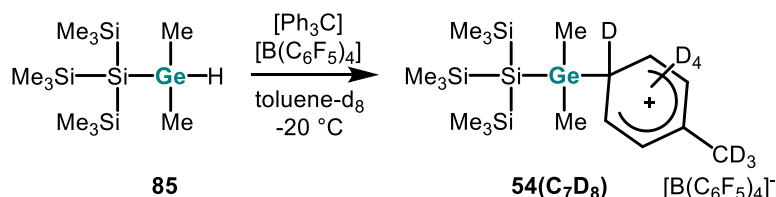


Figure 13. 99 MHz  $^{29}\text{Si}\{^1\text{H}\}$  NMR spectra ( $\text{C}_7\text{D}_8$ ,  $T = -20^\circ\text{C}$ ) of the rearrangement of germyl toluenium ion **54**( $\text{C}_7\text{D}_8$ ) (•) to silyl toluenium **59**( $\text{C}_7\text{D}_8$ ) (\*) ( $\downarrow$   $[\text{Pr}_3\text{SiMe}]$ ). a) Spectrum 2h after addition of  $[\text{Pr}_3\text{Si}(\text{C}_7\text{D}_8)][\text{B}(\text{C}_6\text{F}_5)_4]$ ; b) after 9h; c) after 25h; d) after 120 d at  $T = -20^\circ\text{C}$ .

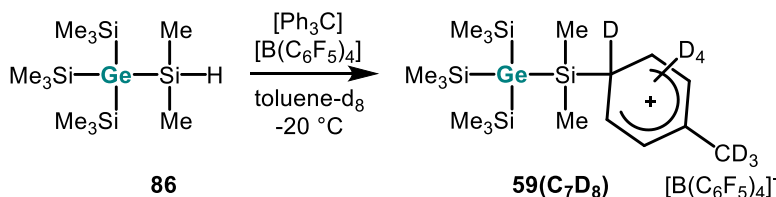
To verify this assignment of the  $^{29}\text{Si}$  NMR resonances, hydridogermane **85** was ionised by the conventional Bartlett-Condon-Schneider hydride transfer reaction with trityl borate as shown in Scheme 50. The NMR spectra of this reaction reveal the same dominating signals at  $\delta^{29}\text{Si} = -87.9$  and  $-7.9$  (•) with a similar behaviour of the signal intensities over the course of time as shown in Figure 13.



Scheme 50. Bartlett-Condon-Schneider hydride transfer reaction of hydridogermane **85** with trityl borate.

As mentioned above, the intensities of the small signals at  $\delta^{29}\text{Si} = -2.4$  and  $+98.1$  (\*) increase and a new compound is formed cleanly. The new high field signal at  $\delta^{29}\text{Si} = -2.4$  appears in the typical region for trimethylsilyl groups attached to germanium<sup>[15, 69]</sup>, but this measured chemical shift is not very diagnostic. In contrast, the low field resonance at  $\delta^{29}\text{Si} = +98.1$  is very distinctive for silyl arenium ions<sup>[56-58, 135]</sup> and these two signals reveal an integral ratio in the  $^{29}\text{Si}\{^1\text{H}\}$  inverse gated experiment of 3:1. Based on the knowledge of the characteristic  $^{29}\text{Si}$  NMR chemical shift ranges (see chapter 1.5) and the 2D-NMR spectra, these signals were tentatively assigned to silyl toluenium ion **59(C<sub>7</sub>D<sub>8</sub>)**.

The identity of the silyl toluenium ion **59(C<sub>7</sub>D<sub>8</sub>)** was verified by an alternative synthetic route via hydride transfer reaction from the appropriate hydridosilane **86**.



Scheme 51. Bartlett-Condon-Schneider hydride transfer reaction of hydridosilane **86** with trityl borate.

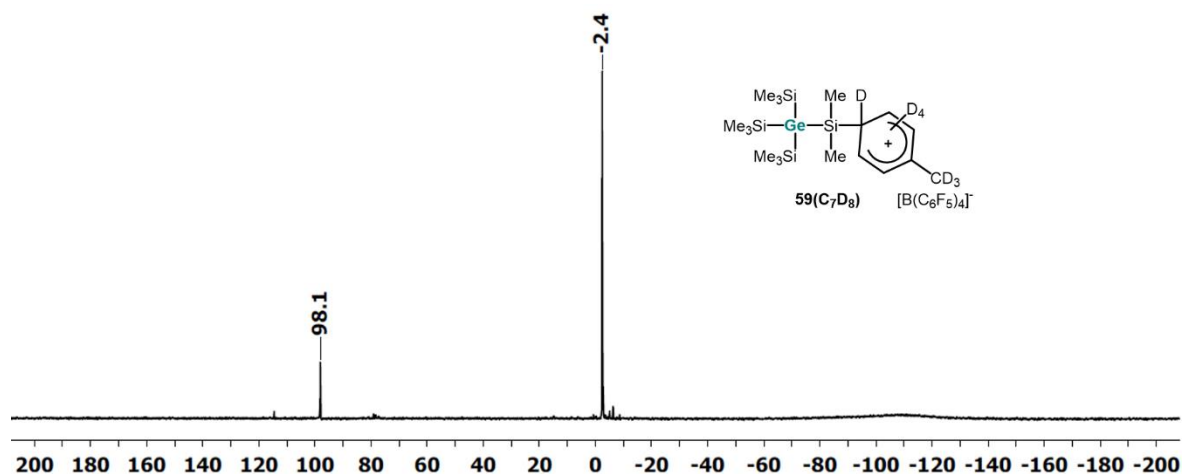


Figure 14. 99 MHz  $^{29}\text{Si}\{^1\text{H}\}$  NMR spectrum ( $\text{C}_7\text{D}_8$ ,  $T = -20^\circ\text{C}$ ) of silyl toluenium ion **59**( $\text{C}_7\text{D}_8$ ) synthesised by hydride transfer from silane **86**.

Indeed, the chemical shift of the signals in the  $^{29}\text{Si}$  NMR spectrum agree well with the low field shifted signals in  $^{29}\text{Si}\{^1\text{H}\}$  NMR spectra obtained from the first reaction (see Figure 13) and the results of the  $^{29}\text{Si}$  NMR chemical shift calculations also agree with the structure of the silyl toluenium ion **59**( $\text{C}_7\text{D}_8$ ) (Table 2). The nonpolar phase of the low temperature reactions of **50** with tri-*iso*-propylsilyl toluenium ion **65b** as the Lewis acid only contained the neutral rearrangement product **51** and methyl-tri-*iso*-propylsilane (Figure 15).

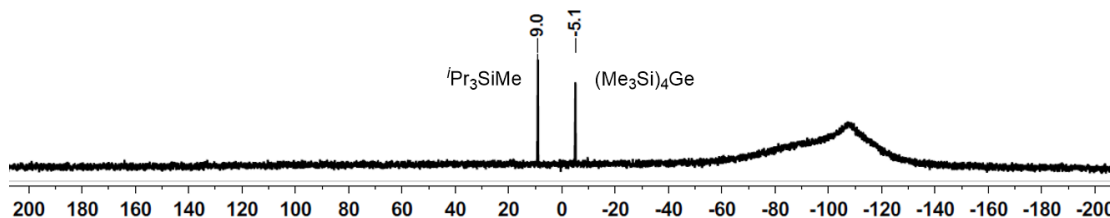


Figure 15. 99 MHz  $^{29}\text{Si}\{^1\text{H}\}$  NMR spectrum ( $\text{C}_7\text{D}_8$ , r.t.) obtained from the non-polar phase of the reaction of germysilane **50** with tri-*iso*-propylsilyl toluenium borate (**65b**) after 1h at  $T = -20^\circ\text{C}$ .

The non-polar phase of the conventional Bartlett-Condon-Schneider hydride transfer reaction of **86** with trityl borate comprises only of the neutral rearrangement product **51** and triphenylmethane as by-product (Figure 16).

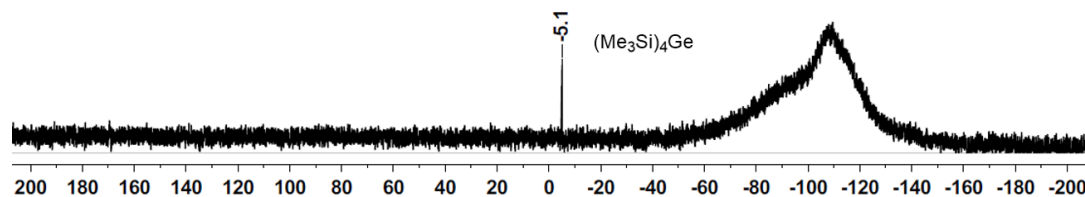


Figure 16. 99 MHz  $^{29}\text{Si}\{^1\text{H}\}$  NMR spectrum obtained ( $\text{C}_7\text{D}_8$ , r.t.) from the non-polar phase of the reaction of germane **86** with  $[\text{Ph}_3\text{C}][\text{B}(\text{C}_6\text{F}_5)_4]$  after 20h at  $T = -20^\circ\text{C}$ .

The  $^{29}\text{Si}$  NMR chemical shifts of solvent-stabilised silyl cations are reported to be very sensitive to changes of the solvent due to the replacement of the arene molecule complexed to the silicon atom. When the reaction of hydridosilane **86** and trityl borate is carried out in chlorobenzene as solvent, no separation of the polar and nonpolar phase occurs, which leads to an NMR spectrum containing more by-products, such as the neutral rearrangement product  $(\text{Me}_3\text{Si})_4\text{Ge} **51** at  $\delta^{29}\text{Si} = 5.1$  (Figure 17). The  $^{29}\text{Si}$  NMR chemical shift of the low field resonance varies significantly from that of **59(C<sub>7</sub>D<sub>8</sub>)** from  $\delta^{29}\text{Si} = 98.1$  in toluene- $\text{d}_8$  to  $\delta^{29}\text{Si} = 154.3$  in chlorobenzene- $\text{d}_5$ .$

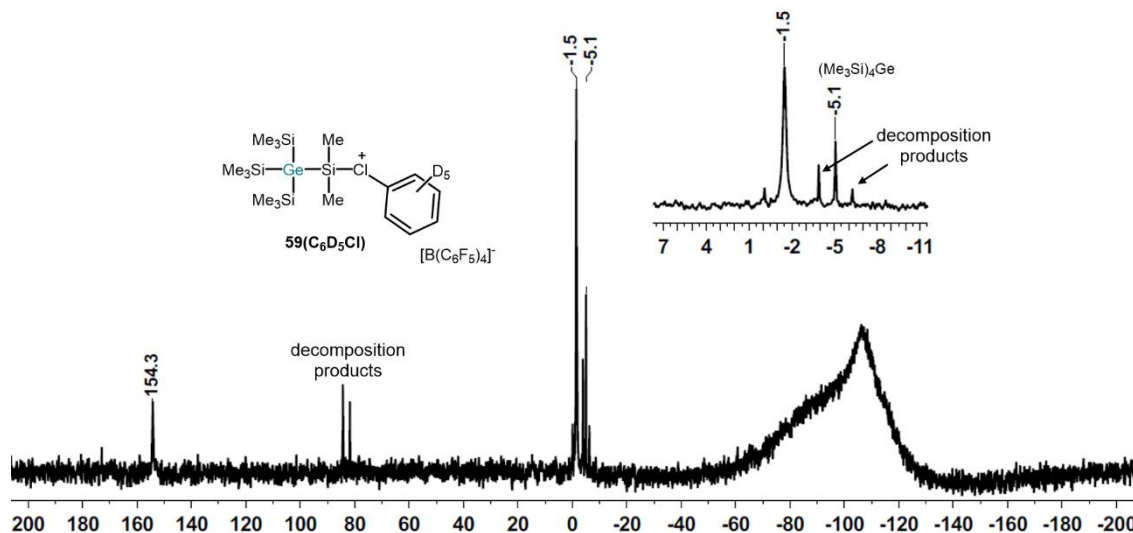


Figure 17. 99 MHz  $^{29}\text{Si}\{^1\text{H}\}$  NMR spectrum ( $\text{C}_6\text{D}_5\text{Cl}$ ,  $T = -20^\circ\text{C}$ ) of silyl chloronium ion **59(C<sub>6</sub>D<sub>5</sub>Cl)** synthesised by hydride transfer from silane **86**.

According to the NMR results, solutions of the silyl toluenium borate  $[\mathbf{59}(\text{C}_7\text{D}_8)][\text{B}(\text{C}_6\text{F}_5)_4]$  in toluene at  $T = -20^\circ\text{C}$  are stable for at least 3 days. When the temperature of the NMR probe was gradually raised in steps of  $\Delta T = 10^\circ\text{C}$ , new signals appeared in the  $^{29}\text{Si}$  NMR spectrum at  $T = -10^\circ\text{C}$ , and exposure of the NMR sample to temperatures of about  $T = 20^\circ\text{C}$  resulted in complete decomposition of cation **59(C<sub>7</sub>D<sub>8</sub>)** (see Figure 18). Moreover, NMR detection of toluenium ion **59(C<sub>7</sub>D<sub>8</sub>)** is severely

hampered at temperatures around  $T = 0\text{ }^{\circ}\text{C}$  by significant line broadening of the  $^{29}\text{Si}$  NMR resonances, most probably due to fast exchange of the toluene molecule in cation **59(C<sub>7</sub>D<sub>8</sub>)** with the solvent (for example, the line width,  $w_{1/2}$ , of the  $^{29}\text{Si}$  NMR signal at  $\delta^{29}\text{Si} = 98.1$  is  $w_{1/2} = 17\text{ Hz}$  at  $T = -20\text{ }^{\circ}\text{C}$  and  $w_{1/2} = 40\text{ Hz}$  at  $T = 10\text{ }^{\circ}\text{C}$ ). The thermal instability of arenium borate **[59(C<sub>7</sub>D<sub>8</sub>)][B(C<sub>6</sub>F<sub>5</sub>)<sub>4</sub>]** in solution essentially prevents its isolation and additional characterisation. These NMR experiments demonstrate the clean conversion of silylgermyl toluenium ion **54(C<sub>7</sub>D<sub>8</sub>)** to germylsilyl toluenium **59(C<sub>7</sub>D<sub>8</sub>)** in toluene at  $T = -20\text{ }^{\circ}\text{C}$ .

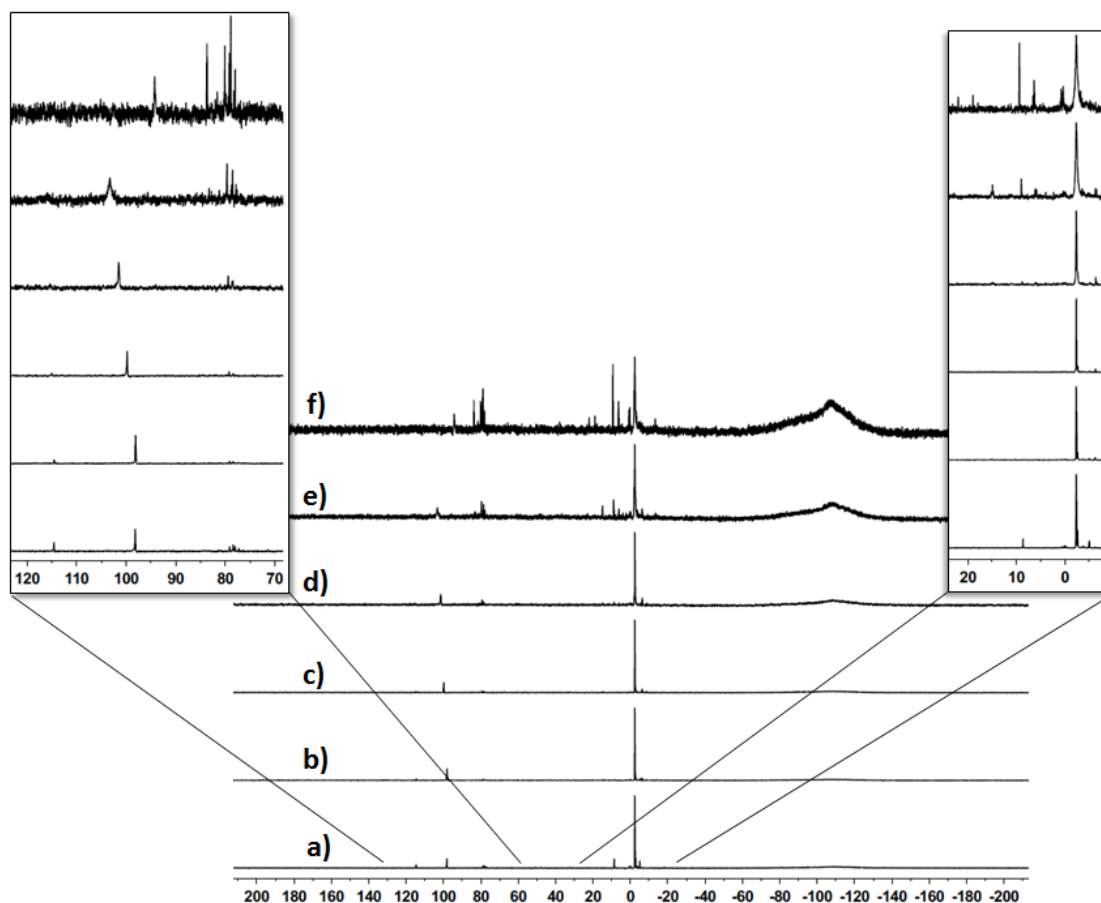
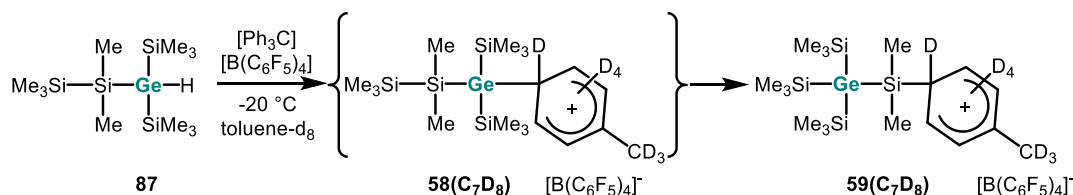


Figure 18. a) 99 MHz  $^{29}\text{Si}\{^1\text{H}\}$  NMR spectrum ( $\text{C}_7\text{D}_8$ ,  $T = -20\text{ }^{\circ}\text{C}$ ) of silyl toluenium ion **59(C<sub>7</sub>D<sub>8</sub>)** synthesised by hydride transfer from germatrisilane **87** at  $-20\text{ }^{\circ}\text{C}$ . b-f) 99 MHz  $^{29}\text{Si}\{^1\text{H}\}$  NMR spectra (toluene- $\text{d}_8$ ,  $T = -20\text{ }^{\circ}\text{C}$ ) of silyl toluenium ion **59(C<sub>7</sub>D<sub>8</sub>)** in toluene synthesised by hydride transfer from silane **86**; b) at  $T = -20\text{ }^{\circ}\text{C}$ , c) at  $T = -10\text{ }^{\circ}\text{C}$ , d) at  $T = 0\text{ }^{\circ}\text{C}$ , e) at  $T = 10\text{ }^{\circ}\text{C}$ , f) at  $T = 20\text{ }^{\circ}\text{C}$ .

The calculated relative energies for the toluene complexes of the cationic intermediates **54-59** of the reaction cascade, shown in Scheme 46, do not vary much from the previously reported energies of the free cationic intermediates (Figure 20). This shows that the complexation of the formed silyl and germyl cations with the arene solvent has no significant influence on the calculated reaction

coordinate. The formation of silyl toluenium ion **59**(**C<sub>7</sub>H<sub>8</sub>**) is predicted to be the most stable cation along the complete reaction sequence and, similar to the free cations, the overall reaction **54**(**C<sub>7</sub>H<sub>8</sub>**) → **59**(**C<sub>7</sub>H<sub>8</sub>**) is predicted to be exothermic by 44 kJ mol<sup>-1</sup>. Nevertheless, when following the rearrangement by NMR spectroscopy (Figure 13), no indications for the formation of any cationic intermediate **55** – **58** or their arenium ions are found. To prove the proposed mechanism, one specific cation along the reaction cascade was synthesised by the classical Bartlett-Condon-Schneider hydride transfer reaction with trityl borate and germatrisilane **87** (Scheme 52). By this means the cationic intermediate **58**, or more probable its toluene complex **58**(**C<sub>7</sub>D<sub>8</sub>**), should have been prepared, but the <sup>29</sup>Si NMR spectrum recorded after 15 min at T = -20 °C showed no signals expected for cation **58**(**C<sub>7</sub>D<sub>8</sub>**) (Table 2). Surprisingly, the known resonances for silyl toluenium **59**(**C<sub>7</sub>D<sub>8</sub>**) already dominated the spectrum (Figure 19). This experiment showed that the germyl toluenium ion **58**(**C<sub>7</sub>D<sub>8</sub>**) undergoes a fast 1,2-shift of the trimethylsilyl group to form the more stable cation **59**(**C<sub>7</sub>D<sub>8</sub>**). This fast rearrangement is in accord with the rather low barrier of 18 kJ mol<sup>-1</sup> that is predicted for the 1,2-trimethylsilyl shift in the free cations **58** → **59** (Figure 20)<sup>[68]</sup> and explains the absence of any signals of the intermediate **58**(**C<sub>7</sub>D<sub>8</sub>**) in the NMR spectra at T = -20 °C.



Scheme 52. Bartlett-Condon-Schneider hydride transfer reaction of hydridogermatrisilane **87** with trityl borate.

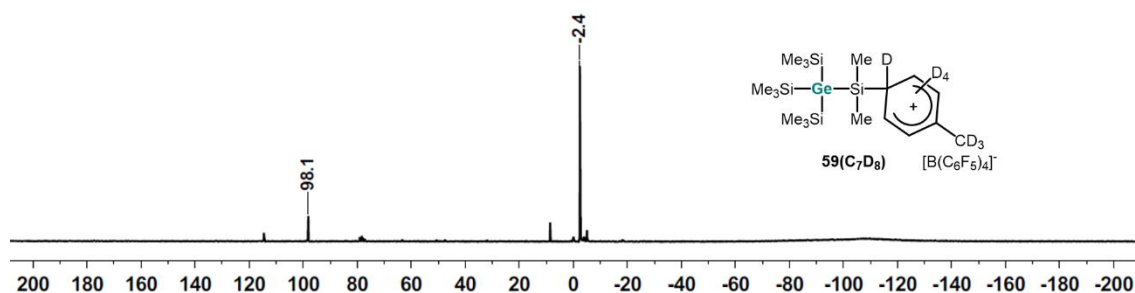


Figure 19. 99 MHz <sup>29</sup>Si{<sup>1</sup>H} NMR spectrum (C<sub>7</sub>D<sub>8</sub>, T = -20 °C) of silyl toluenium ion **59**(**C<sub>7</sub>D<sub>8</sub>**) synthesised by hydride transfer from germatrisilane **87**.

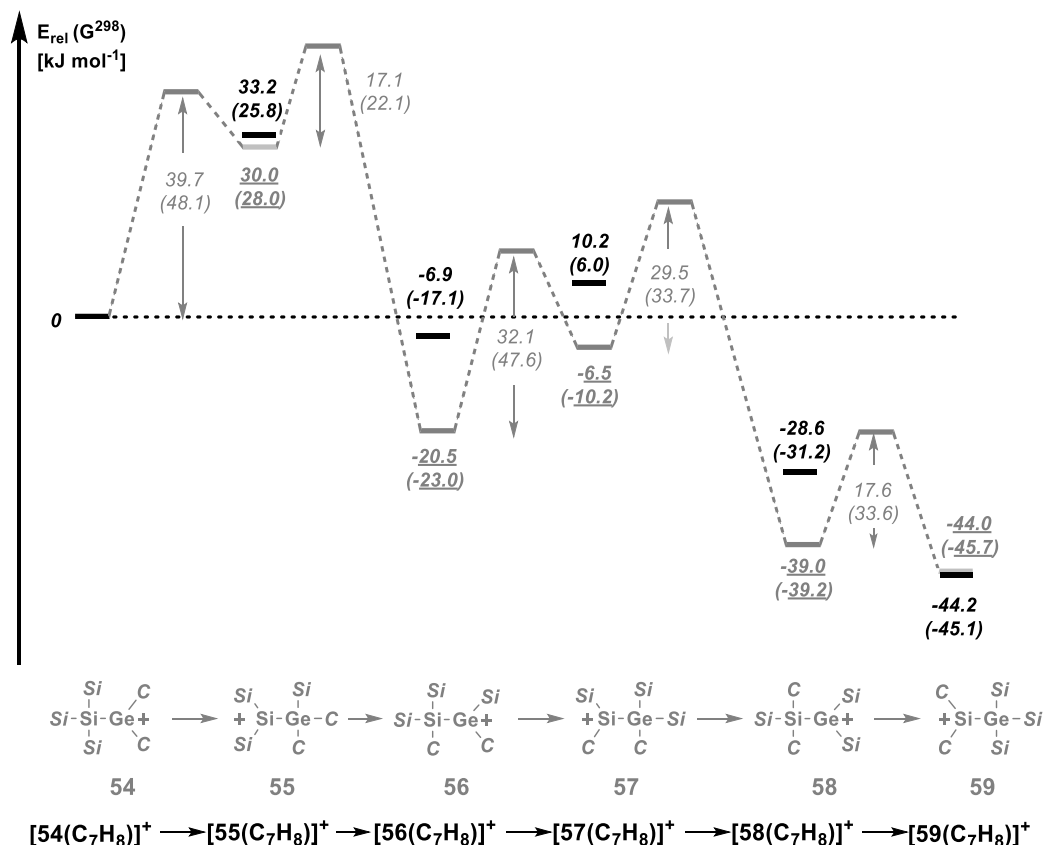
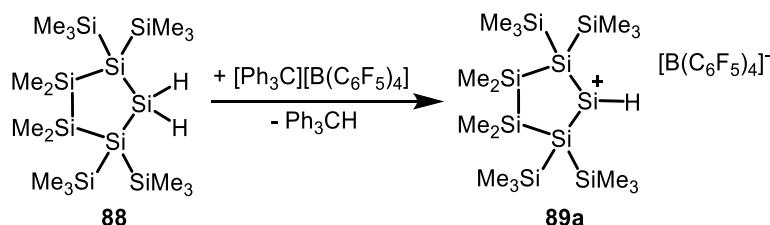


Figure 20. Diagram of relative ground state energies  $E$  and Gibbs free energies at 298.15 K,  $G^{298}$  (in parentheses), of toluene complexes of isomeric cations **54** – **59** (relative to cation **[54(C<sub>7</sub>H<sub>8</sub>)]<sup>+</sup>**, calculated at B3LYP/6-311+G(d,p), in black). The complete reaction diagram for the isomerisation of cations **54** → **59** as previously computed at B3LYP/6-311+G(d,p) is displayed in grey (from ref.<sup>[68]</sup>, Si  $\equiv$  SiMe<sub>3</sub>; C  $\equiv$  CH<sub>3</sub>).

These results show that it is possible to synthesise polysilanyl-substituted germyl and silyl cations, such as germyl cation **54** and silyl cation **59** in the form of their arene complexes at low temperatures using the weakly coordinating  $[\text{B}(\text{C}_6\text{F}_5)_4]^-$  anion. The cation synthesis was done using either the stoichiometric reaction of germapolysilanes with a cationic Lewis acid such as tri-*iso*-propylsilyl toluenium, or, in a more regio-controlled way, by the standard hydride transfer reaction between hydridosilanes and -germanes with the trityl cation. The cationic species were identified by low-temperature NMR spectroscopy supported by the results of quantum mechanical NMR chemical shift calculations. Application of these techniques allowed us to verify several silyl- and germyl cations and their solvent complexes as intermediates in the sila-Wagner–Meerwein rearrangement of germylsilane **50** (Scheme 45) and to provide strong evidence for their clean interconversion at low temperatures. This reaction is believed to be archetypical for many synthetically useful Lewis acid catalysed skeletal rearrangements of polysilanes and germapolysilanes.

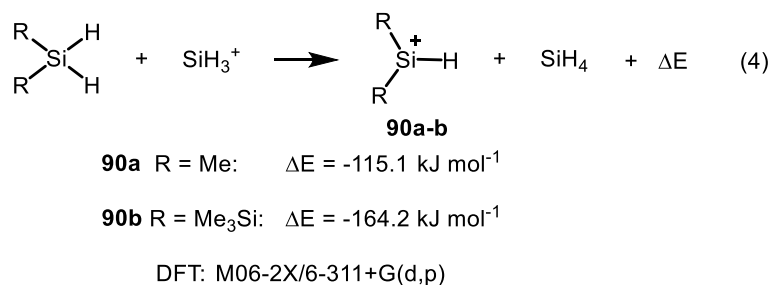
### 3.3 Investigations on a Hydrogen-Substituted Silyl Cation

The synthesis of hydrogen-substituted silylium ions is a still challenging task. The choice of suitable substituents at the silicon atom is important, as they need to stabilise the cationic centre electronically and sterically. Cyclic silane **88** was chosen for the generation of a hydridosilylium ion **89a**.



Scheme 53. Proposed synthesis of hydrogen-substituted silylium ion **89a**.

The high number of  $\alpha$ - and  $\beta$ -silyl groups is expected to stabilise the cationic centre electronically and, in addition, the flanking trimethylsilyl groups shield the cationic charge sterically from further reactions. According to isodesmic reaction (4) (Scheme 54) the stabilisation energy of the hydridobis(trimethylsilyl)-substituted silylium ion **90b** is calculated to be more stable by 49.1 kJ mol<sup>-1</sup> than the hydridodimethyl silylium ion **90a**. These numbers provide evidence that the hypothesis that silyl groups will stabilise a hydridosilylium ion is valid.



Scheme 54. Isodesmic reaction (4) for the calculation of the stabilisation energies of hydrogen-substituted silylium ions **90a-b**.

Prior to experiments, the <sup>29</sup>Si NMR spectrum of hydridosilylium ion **89a** was calculated and is shown in Figure 21. It reveals a very characteristic low field signal at  $\delta^{29}\text{Si} = 594.5$  for the hydrogen-substituted, cationic silicon atom, a signal in the typical shift range for flanking trimethylsilyl groups at  $\delta^{29}\text{Si} = 2.8$ , a signal for dimethylsilyl groups from the ring at  $\delta^{29}\text{Si} = -24.9$  and a signal for the tetrasilyl-substituted silicon atoms at  $\delta^{29}\text{Si} = -43.3$ . Compared to the resonances of tetrasilyl-

substituted silicon atoms in neutral polysilanes at  $\delta^{29}\text{Si} = -140 - -120$ , this signal appears very low field due to the neighbouring cationic silicon atom.

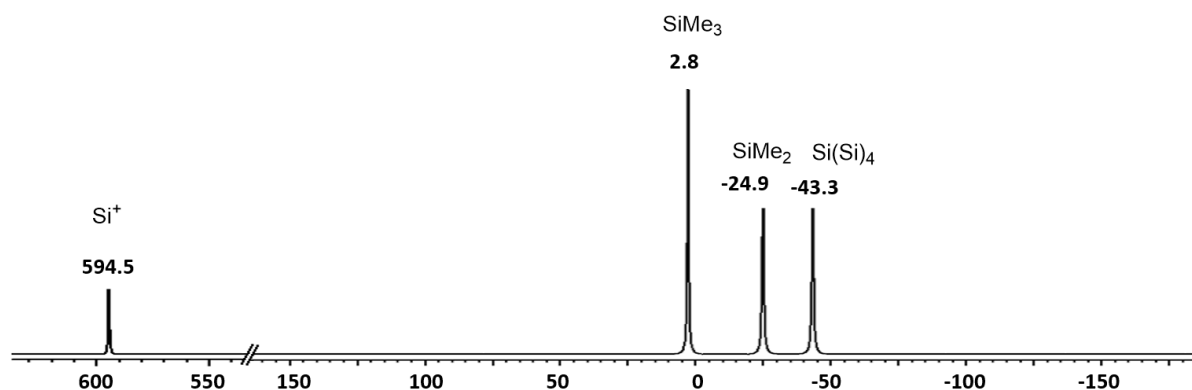


Figure 21. Calculated  $^{29}\text{Si}\{^1\text{H}\}$  NMR spectrum of hydrogen-substituted silylium ion **89a** at B3LYP/IGLOIII//M06-2X/6-311+G(d,p) level of theory.

The first attempt to synthesise hydridosilylium ion **89a** by a hydride abstraction reaction with trityl tetrakis(pentafluorophenyl)borate was performed at room temperature. In this reaction only complete decomposition occurred, therefore, the reaction was performed at  $T = -15\text{ }^\circ\text{C}$  and the NMR spectra were acquired at the same temperature (Figure 22).

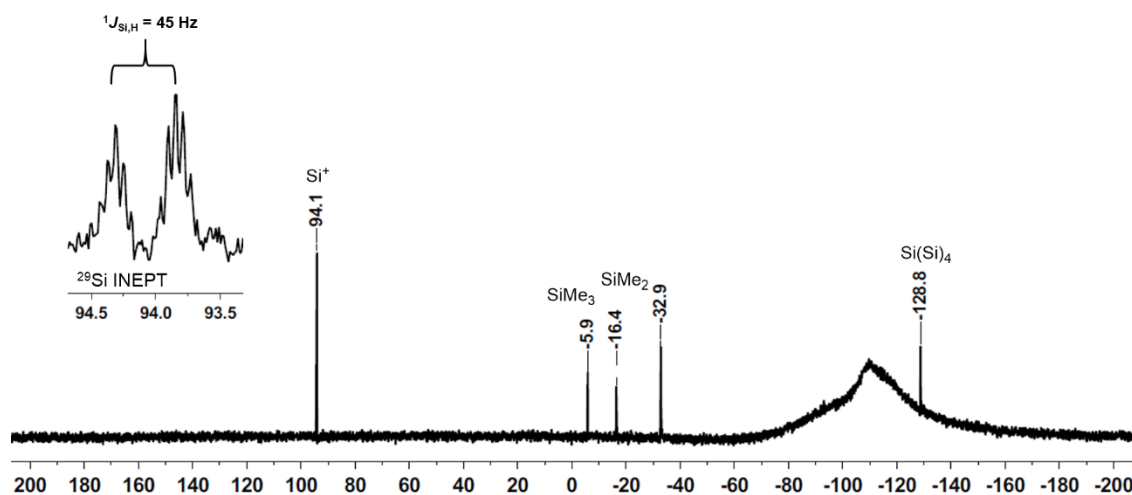


Figure 22. 99 MHz  $^{29}\text{Si}\{^1\text{H}\}$  NMR spectrum and an excerpt of the  $^{29}\text{Si}$  INEPT NMR spectrum ( $\text{C}_6\text{H}_4\text{Cl}_2$ , acetone- $d_6$  lock,  $T = -15\text{ }^\circ\text{C}$ ) obtained after hydride abstraction reaction from dihydrosilane **88**.

By comparison of the calculated  $^{29}\text{Si}$  spectrum with the experimental one, it is obvious that the hydridosilylium ion **89a** is not formed. The chemical shift ranges allow the assignment of the signals to several structural motifs as indicated in Figure 22. In the  $^1\text{H}^{29}\text{Si}$  HMQC NMR spectrum acquired

with parameters for  $^1J_{\text{Si,H}} = 45$  Hz, the tetrasilyl-substituted silicon atom can be linked to one singlet at  $\delta^1\text{H} = 0.17$  in the  $^1\text{H}$  NMR spectrum with an integral of 18 and to two smaller singlets at  $\delta^1\text{H} = 0.32$  each with integrals of 6. The silicon signals at  $\delta^{29}\text{Si} = -32.8$  features cross peaks with two singlets at  $\delta^1\text{H} = 0.19$  and  $0.20$  and the signal at  $\delta^{29}\text{Si} = -16.3$  correlates with the signal at  $\delta^1\text{H} = 0.32$ . The chemical shifts of the  $^1\text{H}$  signals at  $\delta^1\text{H} = 0.19$ ,  $0.20$  and  $0.32$  and their integrals of 6 each confirm the assignment of these signals to three dimethylsilyl groups in total, two of which represent equivalent dimethylsilyl groups and all. The signal at  $\delta^{29}\text{Si} = -5.7$  correlates with the singlet at  $\delta^1\text{H} = 0.17$  in the  $^1\text{H}$  NMR spectrum with an integral of 18, which is due to two equivalent trimethylsilyl groups. Moreover, the low field signal at  $\delta^{29}\text{Si} = 94.2$  correlates with two doublets at  $\delta^1\text{H} = 0.56$  and  $0.49$  each with an integral of 6 and with a broad singlet at  $\delta^1\text{H} = 1.10$  with an integral of 1. Together with its coupling pattern in the hydrogen-coupled  $^{29}\text{Si}$  INEPT NMR spectrum, this resonance can be related to a  $\text{Me}_2\text{Si-H-SiMe}_2$  structural motif, which is also supported by the  $^1J_{\text{H,Si}} = 45$  Hz which is typical in magnitude for the coupling between silicon and hydrogen in a 2e3c bond.<sup>[106-107, 109]</sup>

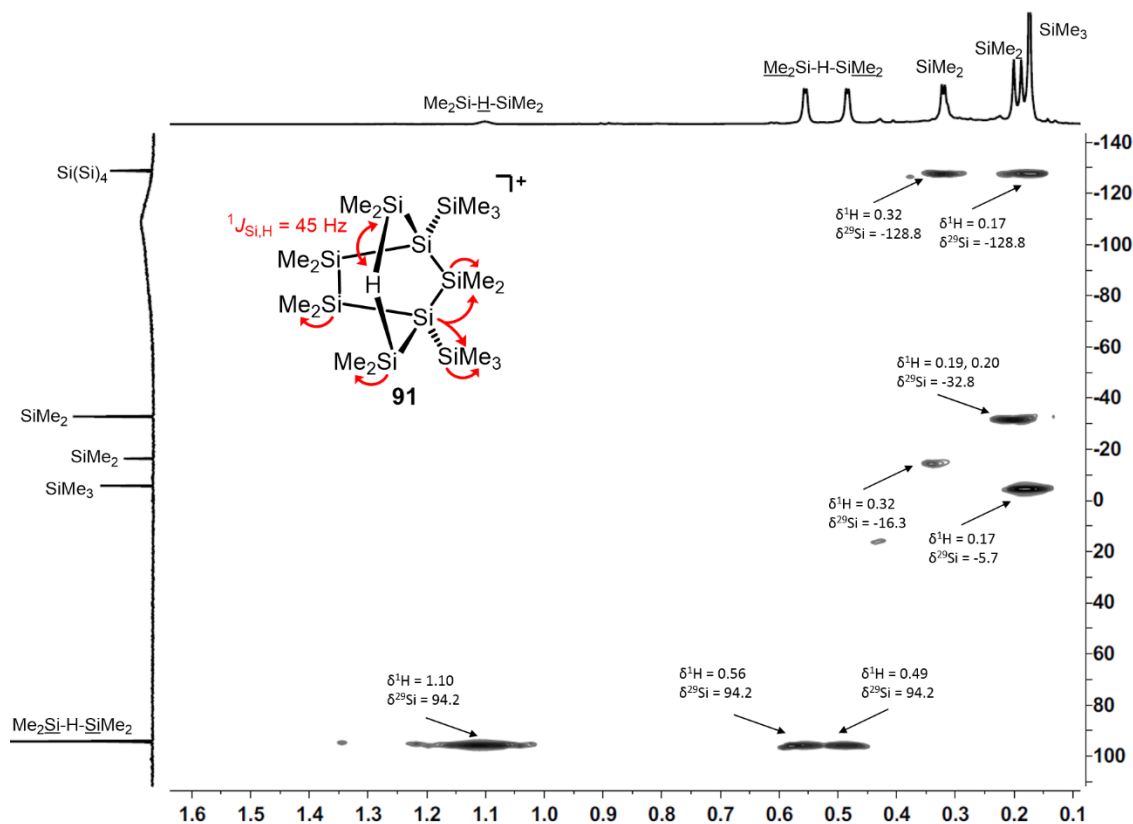
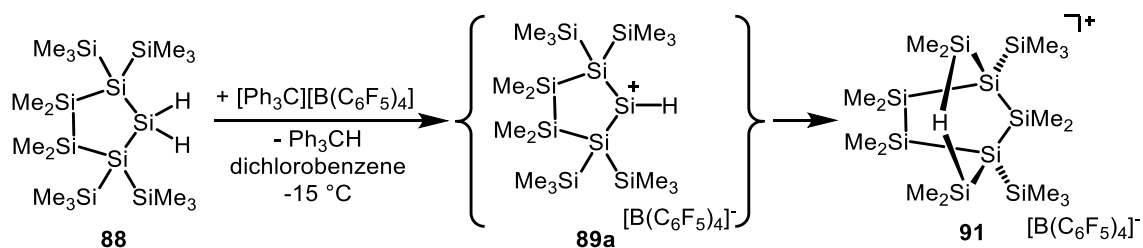


Figure 23. 500 MHz/99 MHz  $^1\text{H}/^{29}\text{Si}$  HMQC NMR spectrum ( $\text{C}_6\text{H}_4\text{Cl}_2$ , acetone- $\text{d}_6$  lock,  $T = -15^\circ\text{C}$ ) obtained after hydride abstraction reaction from dihydrosilane **88**.

Collectively, these data are consistent with the formation of the Si-H-Si bridged bissilyl cation **91** shown in Scheme 55. The calculated  $^{29}\text{Si}\{^1\text{H}\}$  NMR spectrum of cation **91** is in very good agreement with the experimental spectrum (Figure 24).



Scheme 55. Rearrangement to 2e3c Si-H-Si bridged bissilyl cation **91** after hydride abstraction from dihydrosilane **88**.

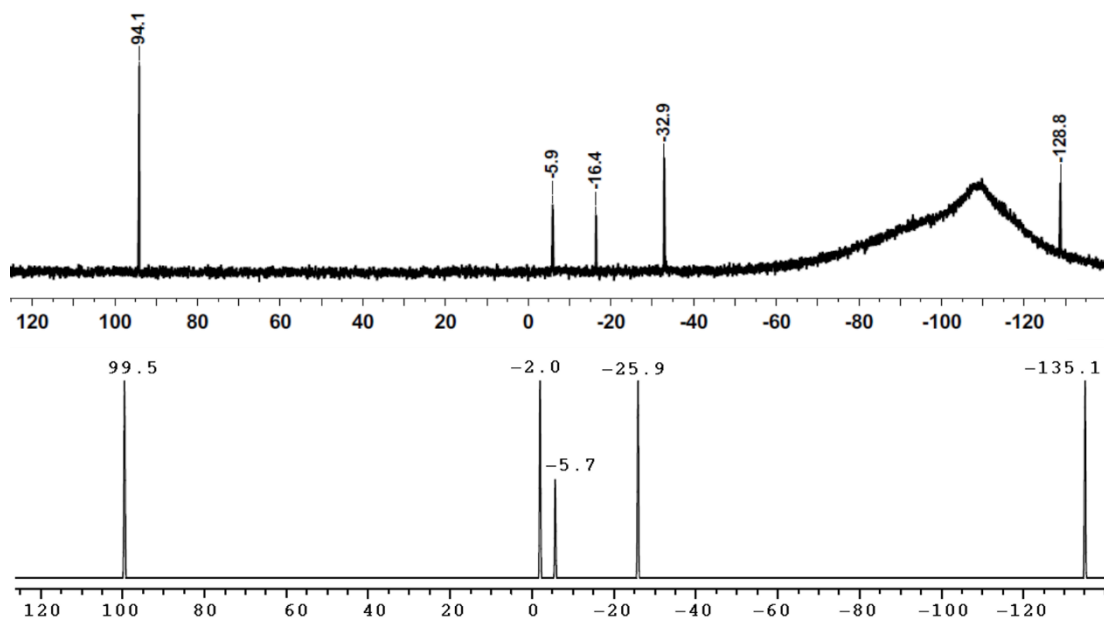
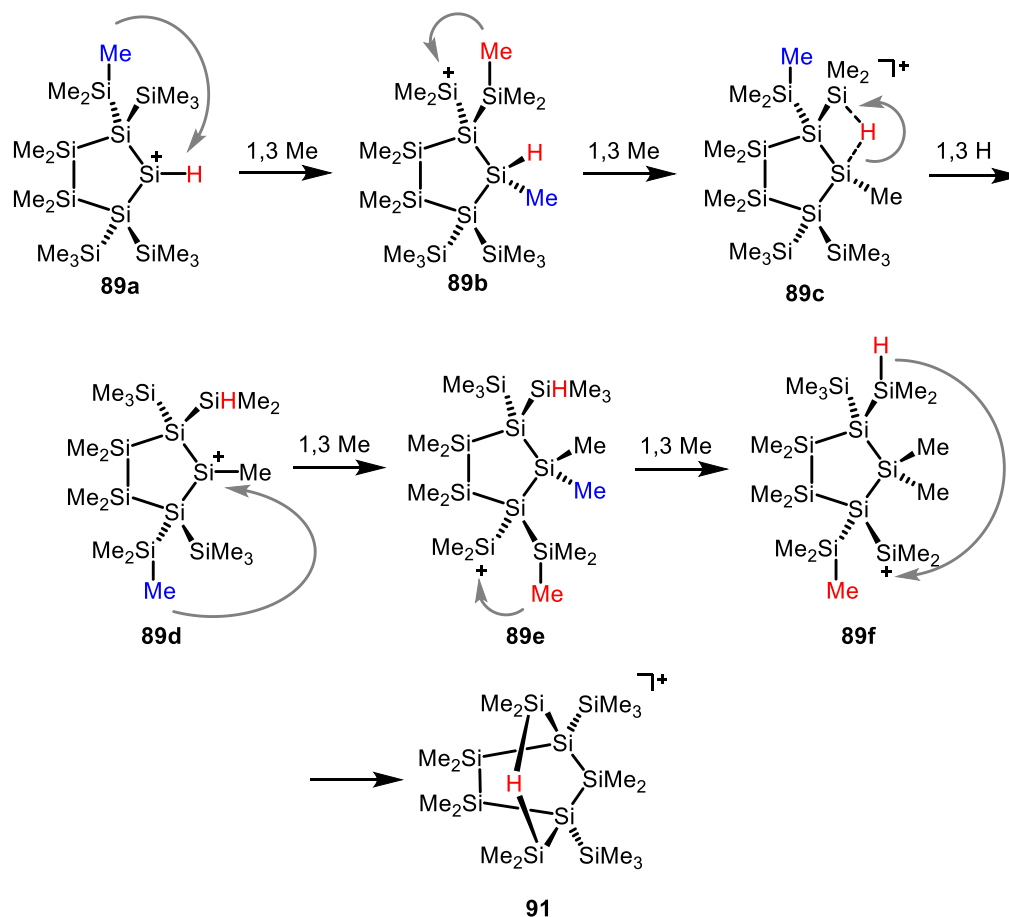


Figure 24. **top**: measured 99 MHz  $^{29}\text{Si}\{^1\text{H}\}$  NMR spectrum ( $\text{C}_6\text{H}_4\text{Cl}_2$ , acetone- $\text{d}_6$  lock,  $T = -15^\circ\text{C}$ ), **bottom**: calculated  $^{29}\text{Si}\{^1\text{H}\}$  NMR spectrum of 2e3c Si-H-Si bridge-stabilised bissilyl cation **91** at M06-L/6-311G(2d,p)//M06-2X/6-311+G(d,p) level of theory.

To study this behaviour, a rearrangement mechanism can be postulated in which the rearrangement proceeds via a series of 1,3-methyl shifts (Scheme 56).



Scheme 56. Proposed rearrangement mechanism to give the 2e3c Si-H-Si bridged bissilyl cation **91**, the  $[\text{B}(\text{C}_6\text{F}_5)_4]^-$  anion is omitted.

The initial step is a hydride abstraction to give the hydridosilylium ion **89a**. By subsequent 1,3-methyl shifts, the cationic charge is transferred to a flanking silyl group in **89c**. Interestingly, this structure is already stabilised by  $39.2 \text{ kJ mol}^{-1}$  by the formation of a 2e3c Si-H-Si bond, however it is not the global minimum. Additional 1,3-methyl shifts result the formation of isomer **89f**. The overall reaction, from the initial hydridosilylium ion **89a** to the 2e3c Si-H-Si bridged bissilyl cation **91**, is exothermic by  $67.1 \text{ kJ mol}^{-1}$ . The 1,3-methyl shifts are found to proceed by four-membered cyclic transition states. Transfer of the methyl group may occur in an antara- or suprafacial manner (Figure 25).

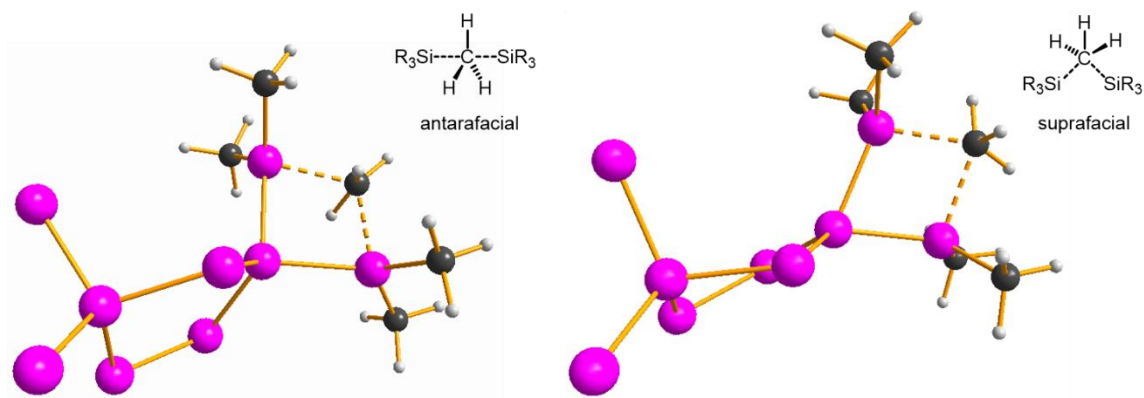


Figure 25. Computed antarafacial and suprafacial transition states of the rearrangement of cation **89e** and **89f**, calculated at M06-2X/6-311+G(d,p), selected methyl groups are omitted for clarity.

The antarafacial transition states lie very high in energy with energy barriers around 98 – 113 kJ mol<sup>-1</sup> (Figure 26). In contrast, a possible reaction channel connecting both cations, which shifts the methyl groups in a suprafacial way, reveals barriers of only 25 – 33 kJ mol<sup>-1</sup> (Figure 27). In general, the potential energy surface along the reaction coordinate is predicted by the calculations to be rather shallow with small activation barriers for the subsequent methyl shifts. Therefore, suprafacial methyl shifts are assumed to occur during the rearrangement. These small energy barriers imply that the isomerisation is fast at the applied temperature of  $T = -15\text{ }^{\circ}\text{C}$  and that none of the short-lived intermediates can be observed under the conditions using standard spectroscopic methods. Instead, the thermodynamic most stable silyl cation along this reaction cascade, the Si-H-Si bridged bisilyl cation **91** was observed and characterised.

This surprising tendency of silylium ions to undergo rearrangement reactions in which they relocate into their thermodynamically most stable isomer containing a 2e3c Si-H-Si bridge was inspiration for further investigations on the rearrangements in polysilanes. The formation of 2e3c Si-H-Si bonds was found to be an effective mean to trap highly reactive silyl cationic species, which could not be handled otherwise.

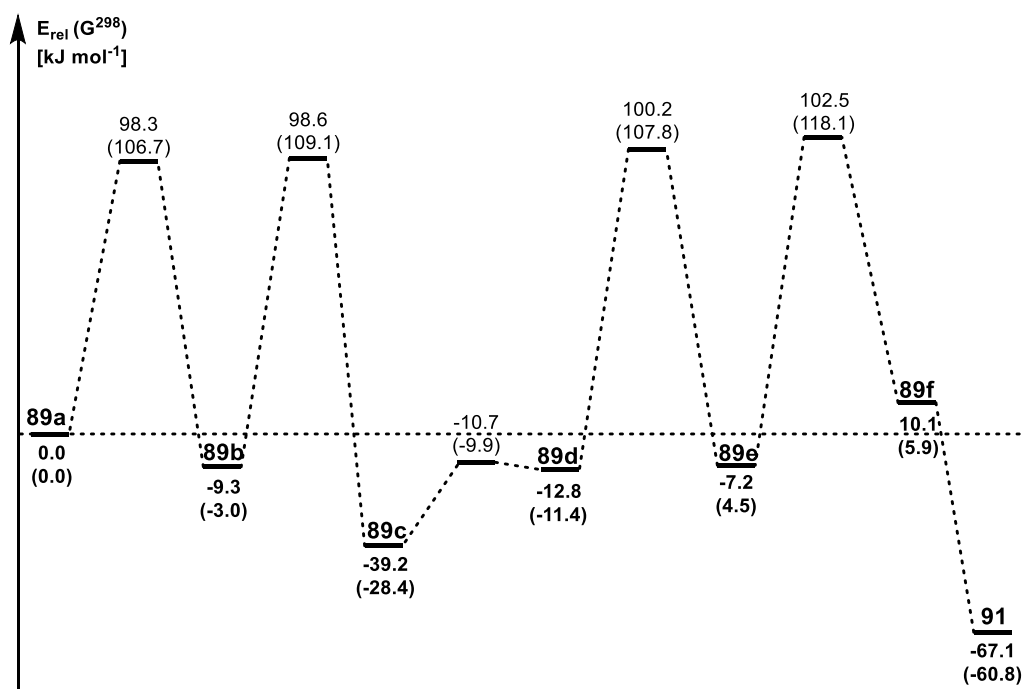


Figure 26. Diagram of relative ground state energies  $E$  and Gibbs free energies at 298.15 K,  $G^{298}$  (in parentheses) of isomeric cations **89a** – **91**, relative to cation **89a**, calculated at M06-2X/6-311+G(d,p). Rearrangement via antarafacial methyl groups shifts.

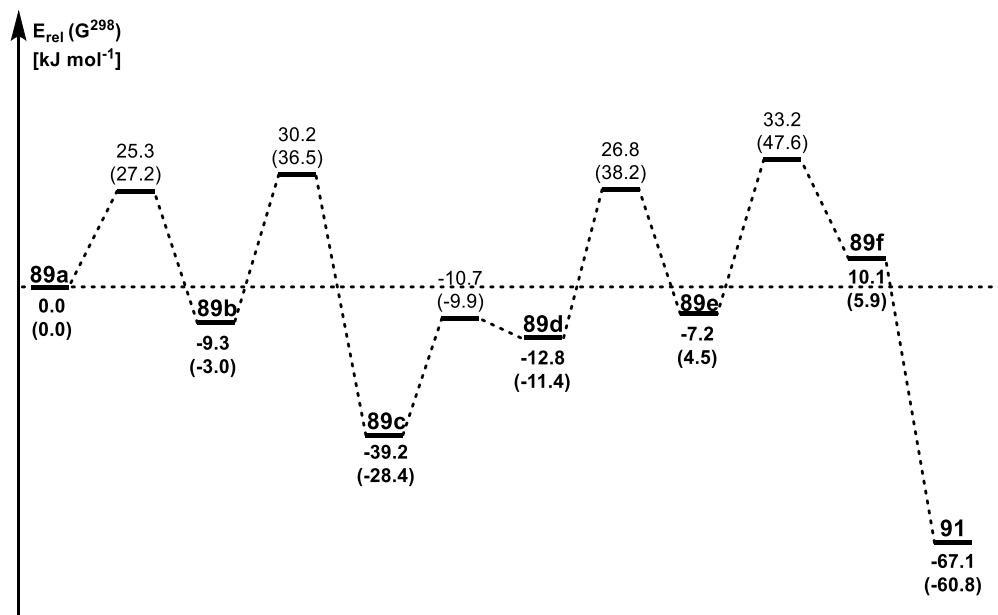
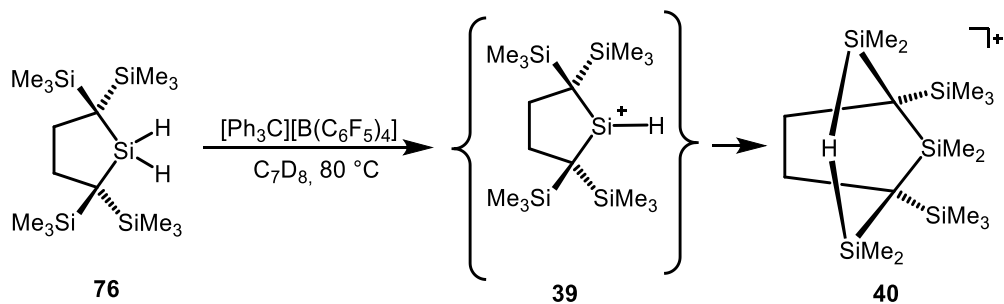


Figure 27. Diagram of relative ground state energies  $E$  and Gibbs free energies at 298.15 K,  $G^{298}$  (in parentheses) of isomeric cations **89a** – **91**, relative to cation **89a**, calculated at M06-2X/6-311+G(d,p). Rearrangement via suprafacial methyl groups shifts.

Interestingly, this behaviour of the hydridosilylium ion **88** is analogous to the rearrangement of the hydridosilylium ion **39** found by Schäfer and Müller.<sup>[55]</sup> The carbon analogue of the silane **76**, silane **76**, rearranged in a similar way to give its thermodynamically most stable isomer containing a 2e3c Si-H-Si bridge (**40**).

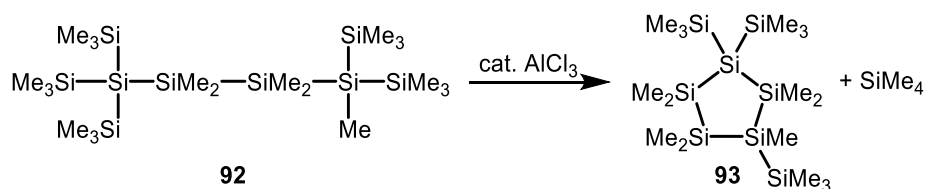


Scheme 57. Synthesis of Si-H-Si bridged bissilyl cation **40** starting from dihydridosilane **76**.<sup>[55]</sup>

### 3.4 Mechanistic Investigations on Rearrangement Reactions in Polysilanes and Germapolysilanes - Subtle Trapping of Intermediates

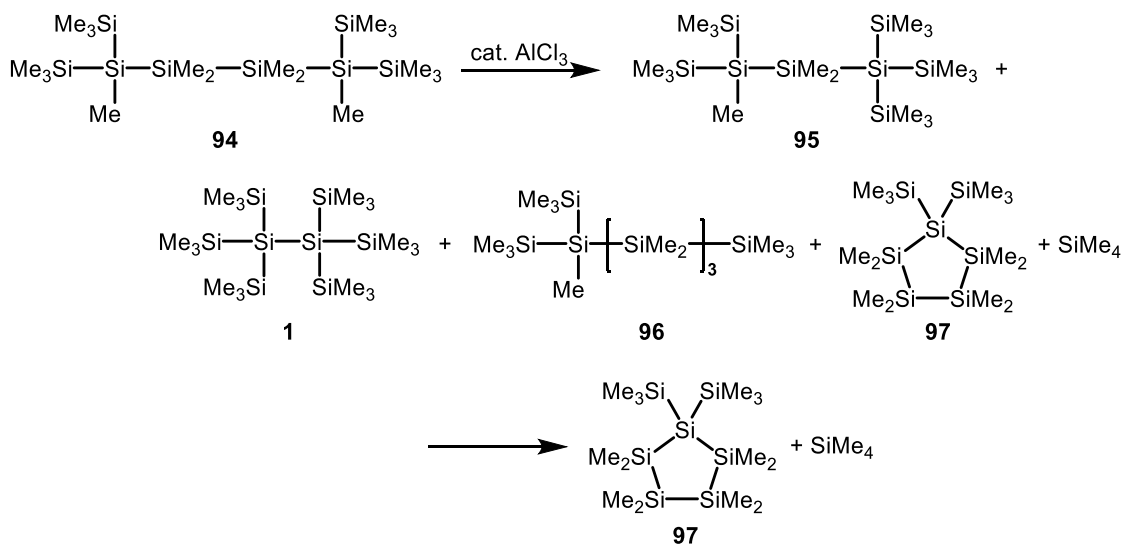
#### 3.4.1 Aluminium Trichloride-Catalysed Rearrangement Reactions of Linear Polysilanes and Germapolysilanes

Ishikawa and Kumada<sup>[43-45]</sup> and also Marschner et al.<sup>[119, 129]</sup> have investigated the Lewis acid-catalysed rearrangement reactions of polysilanes and germapolysilanes. For example, the group of Marschner treated tetrasilane **92** with a catalytic amount of aluminium trichloride and observed a cyclisation reaction to give the five-membered ring **93**.



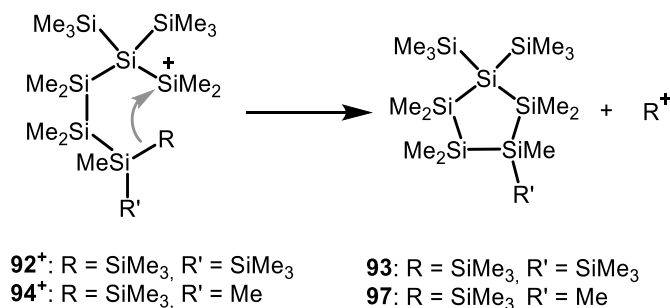
Scheme 58. Cyclisation of tetrasilane **92** to the five-membered ring **93**.

The symmetric tetrasilane **94** undergoes a similar rearrangement and cyclisation when treated with a catalytic amount of aluminium trichloride.<sup>[129]</sup> The rearrangement results in a mixture of the branched isomer trisilane **95**, disilane **1**, pentasilane **96** and cyclopentasilane **97**. After a prolonged reaction time, the cyclic compound **97** and tetramethylsilane are the major reaction products (Scheme 59)



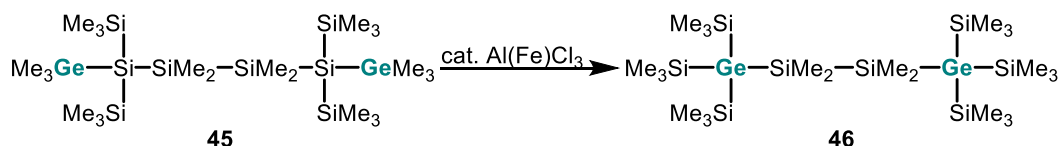
Scheme 59. Rearrangement/cyclisation reaction of branched methylated tetrasilane **94** to give branched isomers **1**, **95-97** and further to give only cyclopentasilane **97**.

Marschner et al. provided a mechanistic rationale for the cyclisation of linear silanes as shown in Scheme 60 and proposed that these rearrangements involve cationic intermediates formed through a series of 1,5-silyl migrations (Scheme 60).<sup>[129]</sup>



Scheme 60. Proposed mechanism of the cyclisation of tetrasilane **92** and **94** to give cyclopentasilanes **93** and **97**.<sup>[129]</sup>

In 2009, Marschner and Müller published a theoretical study about the rearrangement in germapolysilanes.<sup>[68]</sup> They described the shuttling of germanium atoms in an otherwise permethylated silane to proceed via cationic intermediates, which was also investigated experimentally in chapter 3.2 of this work. When treated with aluminium trichloride, the germanium atoms in germyl-substituted tetrasilane **45** move to the central positions in the silicon backbone, where they are only surrounded by silicon atoms, to give **46** (Scheme 61).<sup>[68]</sup>

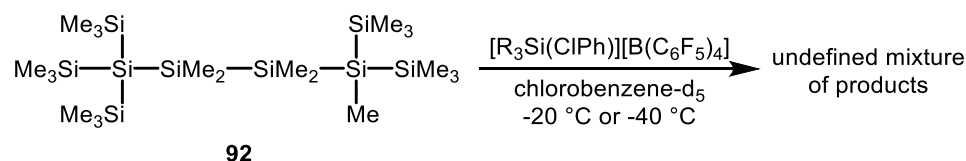


Scheme 61.  $\text{AlCl}_3$ -catalysed rearrangement of digermyl-substituted tetrasilane **45** gives digermatetrasilane **46**.<sup>[68]</sup>

### 3.4.2 Formation of Solvent-Stabilised Silylium or Germylium Ions

Since the reactions with catalytic amount of  $\text{AlCl}_3$  do not allow the detection of cationic intermediates, the idea was to use a Lewis acid in combination with a weakly nucleophilic anion, which should permit the stabilisation of any cationic intermediate occurring during the rearrangement. Again a combination of strong Lewis acidic, solvent-stabilised silyl cations ( $\text{R}_3\text{Si}(\text{toluene})^+$  or  $\text{R}_3\text{Si}(\text{chlorobenzene})^+$ ) with the bulky and weakly nucleophilic tetrakis(pentafluorophenyl)borate anion was used to initiate the rearrangement and to allow the detection of cationic intermediates.

In an attempt to observe a cationic intermediate during the cyclisation of tetrasilane **92**, the methyl group abstraction was performed at low temperatures using tri-*iso*-propylsilyl or triethylsilyl chloronium ions as the Lewis acid and tetrakis(pentafluorophenyl)borate as the weakly nucleophilic counter anion. The reaction with tri-*iso*-propylsilyl chloronium ion was conducted at  $T = -20^\circ\text{C}$  and the reaction with trimethylsilyl chloronium ion at  $T = -40^\circ\text{C}$  (Scheme 62).



Scheme 62. Methyl group abstraction reaction of tetrasilane **92** with trialkylsilyl chloronium ions. ( $\text{R} = i\text{Pr}, \text{Et}$ ).

The  $^{29}\text{Si}$  NMR spectra of both reactions (Figure 28) indicate several products, some of which are apparent in both spectra. The low field signals at  $\delta^{29}\text{Si} = 125.5, 122.3$  and  $102.5$  are a sign of the presence of silyl cationic species, but a definitive assignment is not possible. Moreover, several trimethylsilyl groups ( $\delta^{29}\text{Si} = 9.8$  to  $-12.2$ ) and tetrasilyl-substituted silicon atoms ( $\delta^{29}\text{Si} = 83.3$  to  $-137.5$ ) can be identified.

The reaction is not selective. Given that the Lewis acids are known to abstract a methyl group of a flanking trimethylsilyl group, the trialkylsilyl cations may be abstracting a methyl group from an internal silicon atom of the starting material and this might result in the complex mixture of unidentifiable products, observed.

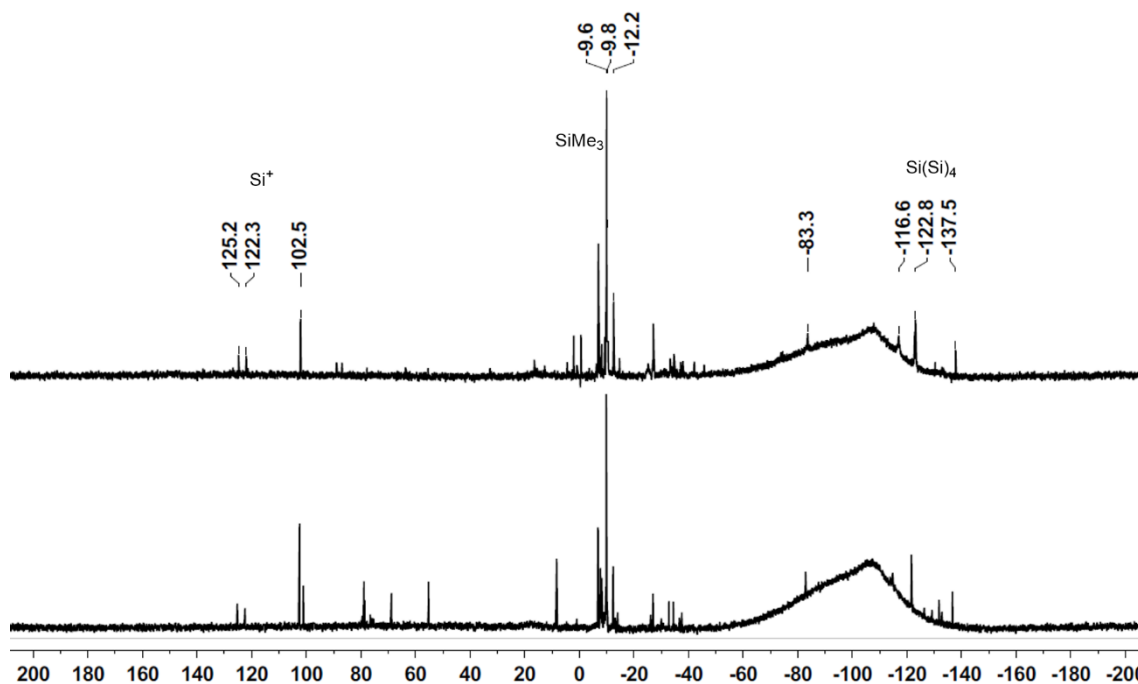
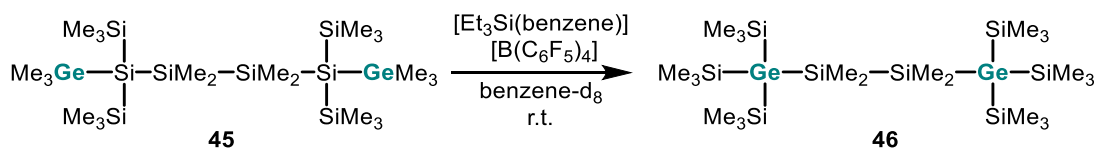


Figure 28. 99 MHz  $^{29}\text{Si}\{^1\text{H}\}$  NMR spectrum ( $\text{C}_6\text{D}_5\text{Cl}$ ,  $T = -20\text{ }^\circ\text{C}$  (**bottom**) or  $T = -40\text{ }^\circ\text{C}$  (**top**)) of the reaction mixture after methyl abstraction reaction from **92** using  $^t\text{Pr}_3\text{Si}(\text{ClC}_6\text{D}_5)^+$  (**bottom**) or  $\text{Et}_3\text{Si}(\text{ClC}_6\text{D}_5)^+$  (**top**) as Lewis acids.

In addition to this reaction, the rearrangement of digermyltetrasilane **45** was also initiated with triethylsilyl benzenium ion **65a** at room temperature and yielded digermatetrasilane **46** cleanly as the rearrangement product. The obtained  $^{29}\text{Si}\{^1\text{H}\}$  NMR spectrum of the non-polar phase is shown in Figure 29 and only reveals the signals of the literature known digermatetrasilane **46**.<sup>[68]</sup> In the polar phase, no silyl or germyl cationic compound could be identified by NMR spectroscopy.



Scheme 63. Triethylsilyl benzenium ion-catalysed rearrangement of germyl-substituted tetrasilane **45** gives digermatetrasilane **46**.

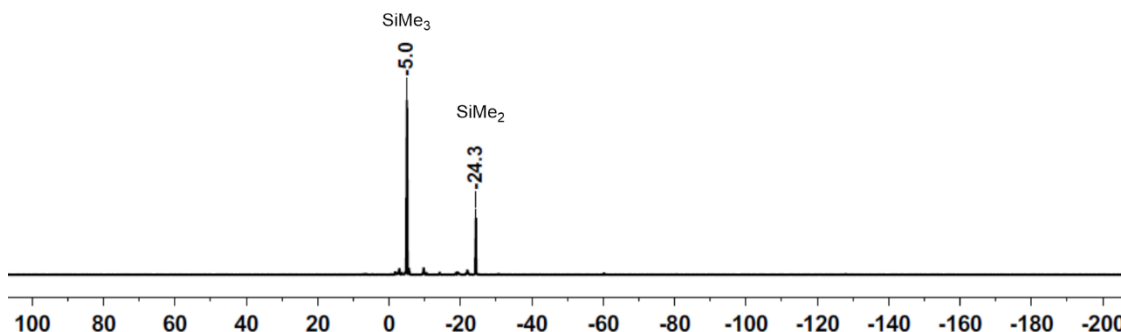
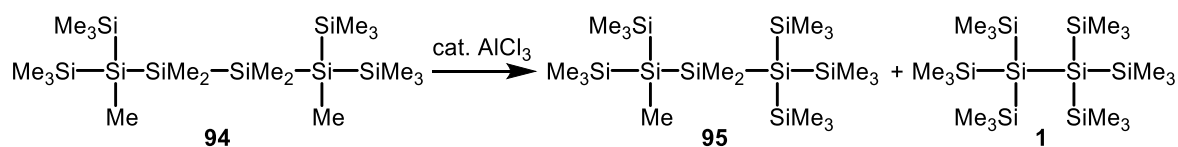


Figure 29. 99 MHz  $^{29}\text{Si}\{^1\text{H}\}$  INEPT NMR spectrum ( $\text{C}_6\text{D}_6$ , r.t.) of the non-polar phase containing digermatetrasilane **46**.

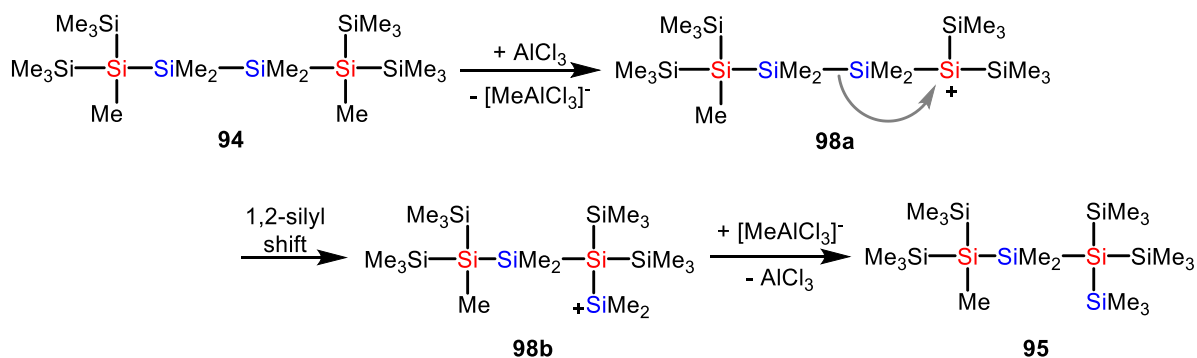
### 3.4.3 The Hydrogen Trick - Subtle Trapping of Intermediates

Marschner described that in the aluminium trichloride-catalysed rearrangement of linear tetrasilane **94**, not only was the cyclic product **97** formed but also a mixture of linear isomers (**1**, **95**, **96**, Scheme 59).<sup>[129]</sup> The focus of this part of the thesis will be on mechanistic investigations on the formation of the highly branched, linear isomers **95** and **1**.



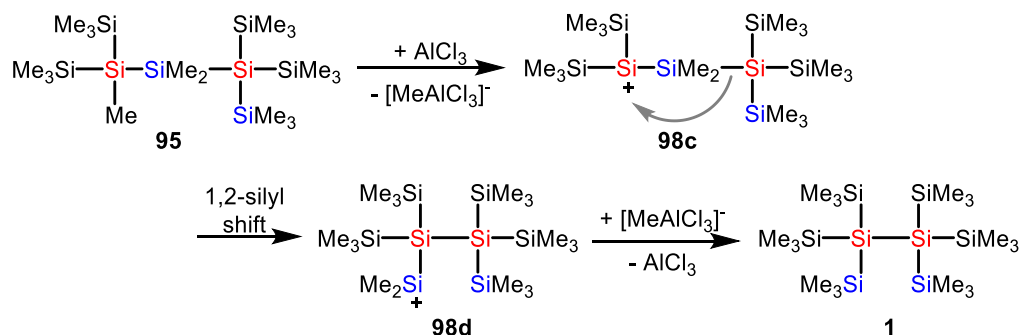
Scheme 64.  $\text{AlCl}_3$ -catalysed rearrangement of tetrasilane **94** gives the highly branched isomers **95** and **1**.

Based on the mechanistic suggestions made by Ishikawa et al. concerning the rearrangement in linear polysilanes<sup>[45]</sup>, this rearrangement is assumed to be initiated by a methyl anion abstraction from a trisilyl-substituted silicon atom with aluminium trichloride to give the silylium ion **98a**, which then undergoes a 1,2-silyl shifts to give silylium ion **98b**. The return of the methyl anion yields the rearrangement product **95** (Scheme 65).



Scheme 65. Formation of the initial silylium ion **98a**, subsequent 1,2-silyl shift and methyl anion transfer yields trisilane **95**.

The aluminium trichloride can again abstract the second methyl anion from the trisilyl-substituted silicon atom in trisilane **95** to initiate a second analogous rearrangement. Silylium ion **98c** is proposed to also rearrange via a 1,2-silyl shift to give silylium ion **98d**, which can be neutralised by the return of the methyl anion. The highly branched isomer **1** is then obtained as reaction product (Scheme 66).



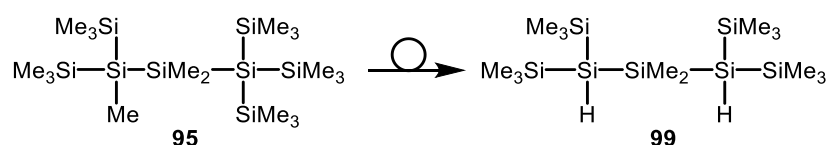
Scheme 66. Formation of the initial silylium ion **98c**, subsequent 1,2-silyl shift and methyl anion transfer yields disilane **1**.

In recent years, the formation of 2e3c Si-H-Si bonds in silyl cations have become a common method to stabilise silylium ions in the condensed phase.<sup>[106-107, 110, 136]</sup> The findings of Schäfer and Müller<sup>[55]</sup> (Scheme 37) and the previously mentioned stabilisation of the rearrangement product in the form of a Si-H-Si 2e3c bridged bissilyl cation **91** (chapter 3.3, Scheme 55) promoted the idea of a mechanistic study of hydrogen-substituted polysilanes. Therefore, the idea was to exchange the methyl groups by hydrogen atoms, which gives two advantages. First, the formation of the initial positive charge can be controlled by the use of triphenylmethyl cation or strong silyl cationic Lewis acids. Due to thermodynamics, the triphenylmethyl cation easily abstracts a hydride from a silicon atom instead of a methyl anion (Scheme 83). The replacement of a Si-H bond ( $D_E = 323 \text{ kJ mol}^{-1}$ ) by a C-H bond ( $D_E = 416 \text{ kJ mol}^{-1}$ ) in the hydride abstraction is accompanied by an energy gain of  $93 \text{ kJ mol}^{-1}$ . In

contrast, the exchange of a Si-C bond ( $D_E = 306 \text{ kJ mol}^{-1}$ ) for a C-C bond ( $D_E = 345 \text{ kJ mol}^{-1}$ ) in the methyl abstraction results in an energy gain of only  $39 \text{ kJ mol}^{-1}$  ( $D_E$  numbers taken from <sup>[137]</sup>ref.). Second, each cationic intermediate is believed to be stabilised by the formation of a 2e3c hydrogen bridge with the remaining hydrogen atom, however, only the thermodynamically most stable cation will be detected.

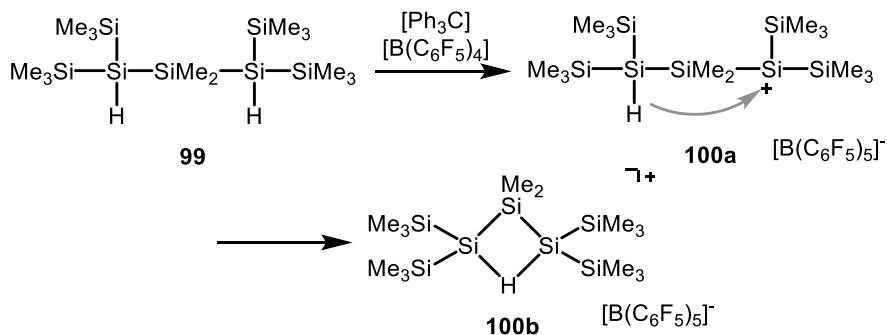
### 3.4.3.1 Mechanistic Development – Part I

The rearrangement reaction of tetrasilane **94** gives the branched isomer **95** in the first step (Scheme 65), which then rearranges to give the highly branched isomer **1** (Scheme 66). This part of this work will focus on the rearrangement from trisilane **95** to disilane **1**. A flanking methyl group and a trimethylsilyl group were replaced by hydrogen atoms (Scheme 67) to allow for selective hydride abstraction and a defined location of the initial positive charge at one of the trisilyl-substituted silicon atoms. The second hydrogen atom should be involved in the formation of a 2e3c Si-H-Si bond to stabilise the cationic intermediate.



Scheme 67. Methyl- and hydrogen-substituted tetrasilanes **95** and **99**.

The initial silylium ion **100a** was proposed to be formed by hydride abstraction with the trityl cation and was expected to be stabilised by a 2e3c Si-H-Si bond to give the bissilyl cation **100b** (Scheme 68).



Scheme 68. Probable reaction product **100b**, stabilised by a 2e3c Si-H-Si bond.

Based on our experiences with the silyl cationic rearrangements of polysilanes, the reaction was performed at low temperatures, similar to previous the hydride abstraction reactions (chapter 3.2 and 3.3). Trityl tetrakis(pentafluorophenyl)borate was evacuated in the NMR tube and then cooled to  $T = -80\text{ }^{\circ}\text{C}$ . Then a solution of silane **99** in chlorobenzene- $\text{d}_5$  was added slowly and the mixture was allowed to warm to  $T = -30\text{ }^{\circ}\text{C}$  and, as soon as the solvent melted, it was quickly shaken with a vortex mixer.

The  $^{29}\text{Si}\{^1\text{H}\}$  NMR spectrum of the solution is presented in Figure 30 and reveals seven prominent signals, which can be assigned to a tetrasilyl-substituted silicon atom ( $\delta^{29}\text{Si} = -120.6$ ), a methyltrisilyl-substituted silicon atom ( $\delta^{29}\text{Si} = -72.7$ ), three trimethylsilyl groups ( $\delta^{29}\text{Si} = -9.3, -8.1, -5.2$ ) and two cationic silicon atoms ( $\delta^{29}\text{Si} = 105.3, 110.3$ ).

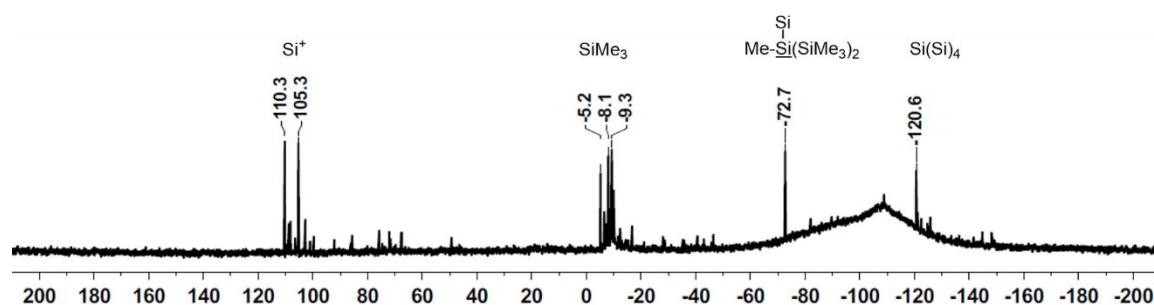


Figure 30. 99 MHz  $^{29}\text{Si}\{^1\text{H}\}$  NMR spectrum ( $\text{C}_6\text{D}_5\text{Cl}$ ,  $T = -30\text{ }^{\circ}\text{C}$ ) obtained after hydride abstraction reaction from trisilane **99**.

Due the high number of by-products, the same reaction was conducted and the NMR spectra were recorded at  $T = -40\text{ }^{\circ}\text{C}$ . The acquired  $^{29}\text{Si}\{^1\text{H}\}$  NMR spectrum (Figure 31, top) reveals the same signals as the previous one (Figure 30) but also ten additional signals. The sample was kept at  $T = -40\text{ }^{\circ}\text{C}$  in the NMR spectrometer and after 11.5 h, a second  $^{29}\text{Si}$  NMR spectrum was acquired (Figure 31, bottom), which then only contained the seven signals observed in the spectrum shown in Figure 30. Apparently, an intermediate, detected after 30 minutes, is converted into the final reaction product.

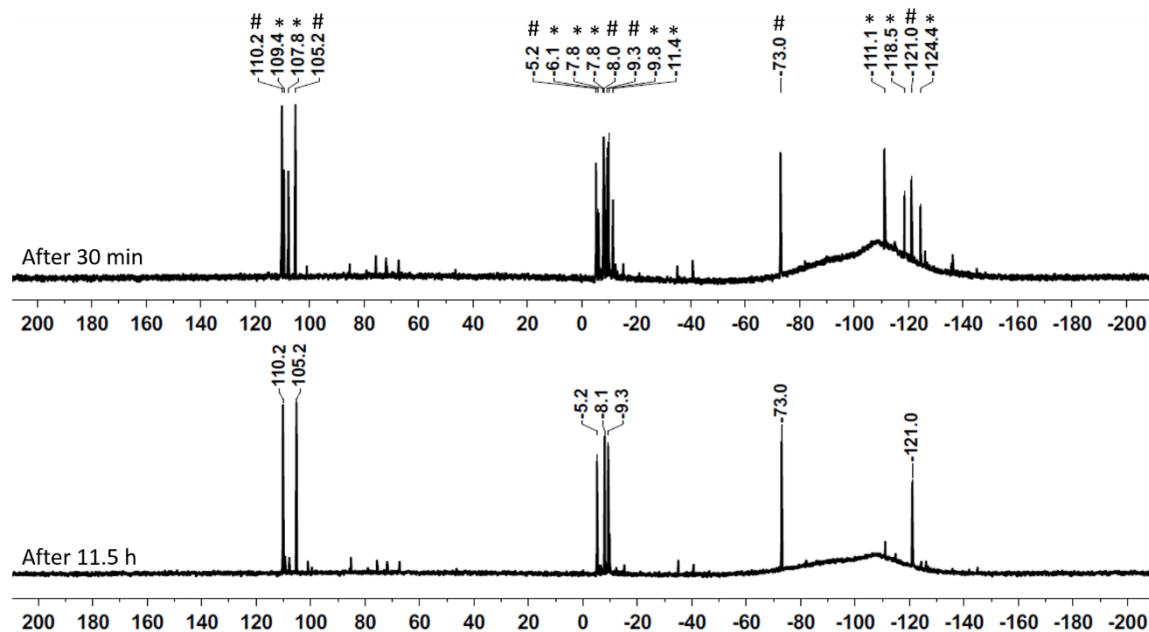


Figure 31. 99 MHz  $^{29}\text{Si}\{^1\text{H}\}$  NMR spectra ( $\text{C}_6\text{D}_5\text{Cl}$ ,  $T = -40^\circ\text{C}$ ) obtained after hydride abstraction reaction from trisilane **99**, **top**: after 30 min, **bottom**: after 11.5 h. reaction product (#), intermediate (\*).

First, to understand this transformation, the identity of the final product needs to be elucidated. Based on the chemical shifts, the structural motifs are assigned to a tetrasilyl-substituted silicon atom ( $\delta^{29}\text{Si} = -121.0$ ), a methyl- and silyl-substituted silicon atom ( $\delta^{29}\text{Si} = -73.0$ ), three trimethylsilyl groups ( $\delta^{29}\text{Si} = -9.3, -8.1, -5.2$ ) and two cationic silicon atoms ( $\delta^{29}\text{Si} = 105.2, 110.2$ ). The low field signals show a doublet of multiplets coupling pattern in the hydrogen-coupled  $^{29}\text{Si}$  INEPT NMR spectrum (Figure 32), which allows the assignment of these resonances to a  $\text{Me}_2\text{Si-H-SiMe}_2$  structural motif. This assignment is supported by the Si-H coupling constant of  $^1J_{\text{Si,H}} = 43 \text{ Hz}$ , which falls within the characteristic range for 2e3c Si-H-Si bonds and the  $^1\text{H}^{29}\text{Si}$  HMQC NMR spectrum (Figure 33) reveals all expected  $^1\text{H}^{29}\text{Si}$  correlations. Interestingly, when acquiring the data with a Si-H coupling constant of  $^1J_{\text{Si,H}} = 45 \text{ Hz}$ , cross peaks are also visible for silicon atoms, which are connected to hydrogen atoms via a  $^2J_{\text{Si,H}}$ -coupling.

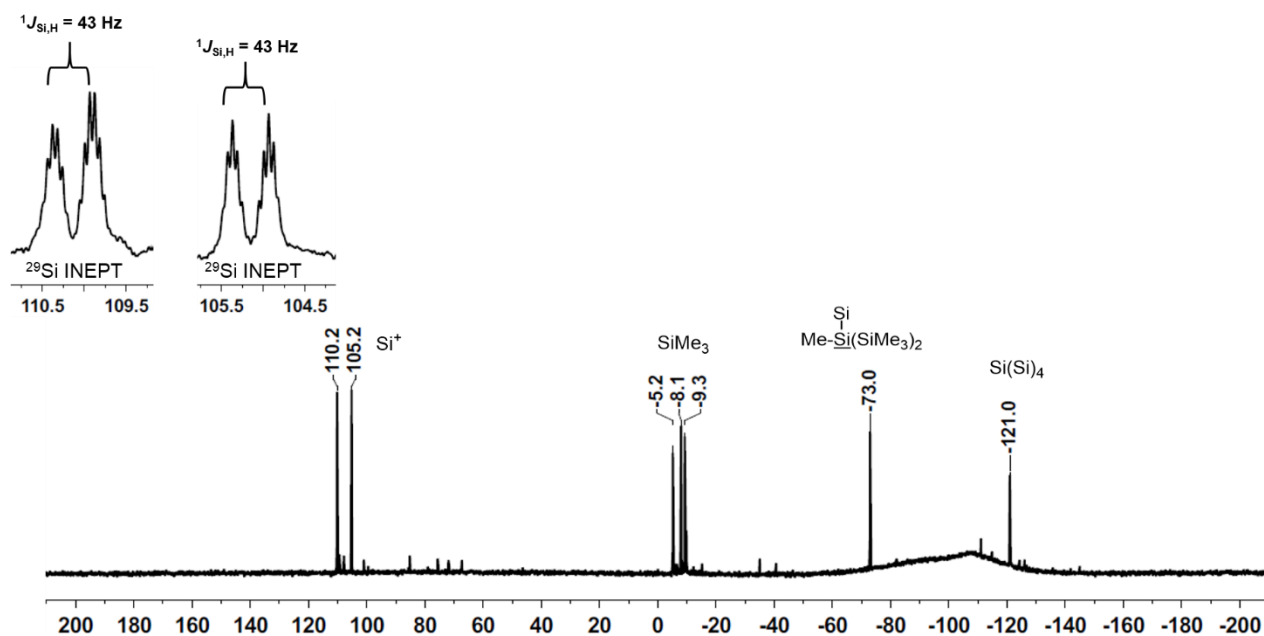


Figure 32. 99 MHz  $^{29}\text{Si}\{^1\text{H}\}$  NMR spectrum and excerpts of the  $^{29}\text{Si}$  INEPT NMR spectrum ( $\text{C}_6\text{D}_5\text{Cl}$ ,  $T = -40^\circ\text{C}$ ) obtained after hydride abstraction reaction from trisilane **99**.

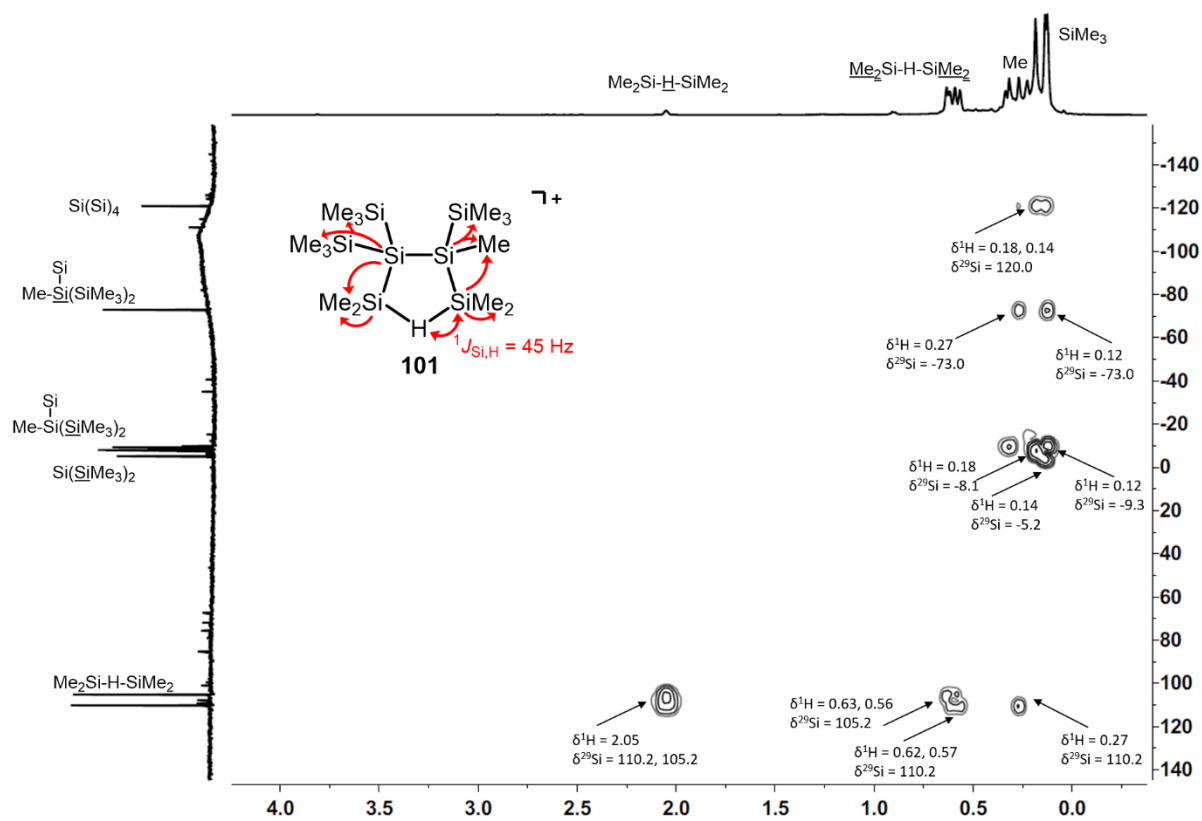


Figure 33. 500MHz/99 MHz  $^1\text{H}/^{29}\text{Si}$  HMQC NMR spectrum ( $\text{C}_6\text{D}_5\text{Cl}$ ,  $T = -40^\circ\text{C}$ ) obtained after hydride abstraction reaction from trisilane **99**.

In addition to some signals assigned to minor impurities, the  $^1\text{H}$  NMR spectrum exhibits three singlets with integrals of nine each ( $\text{SiMe}_3$ ), a singlet with an integral of three ( $\text{Me-Si}(\text{SiMe}_3)$ ), six singlets integrated to three each and a broad singlet integrated to one ( $\text{Si-H-Si}$ ) (Figure 34).

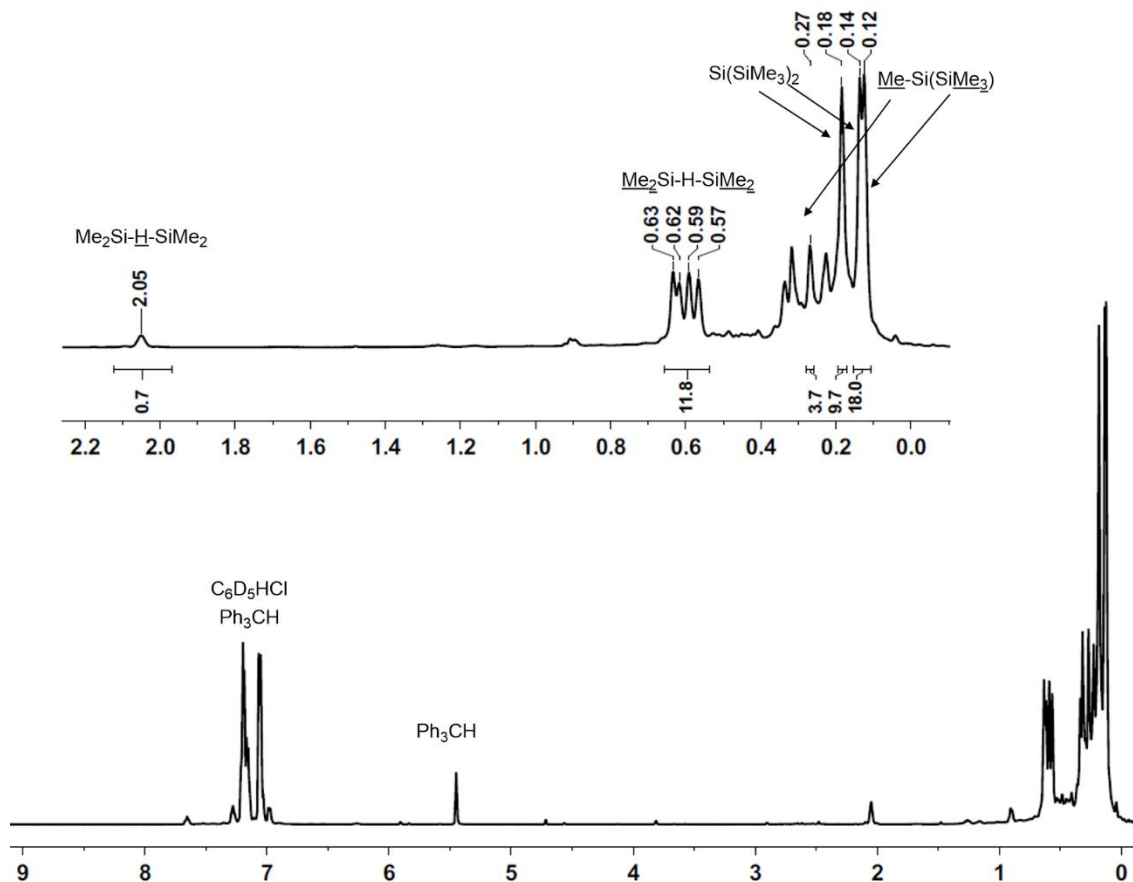
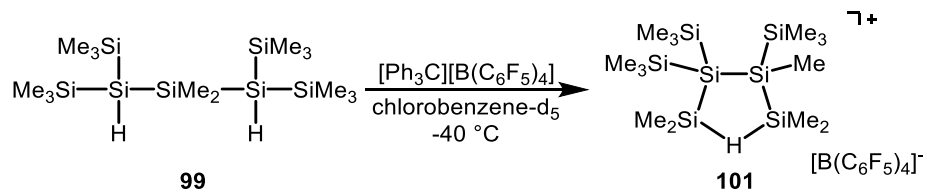


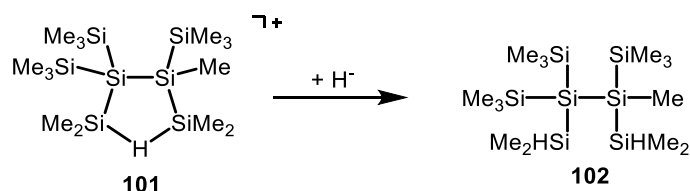
Figure 34. 500 MHz  $^1\text{H}$  NMR spectrum ( $\text{C}_6\text{D}_5\text{Cl}$ ,  $T = -40\text{ }^\circ\text{C}$ ) obtained after hydride abstraction reaction from trisilane **99**.

In summary, these spectra clearly indicate the formation of bissilyl cation **101** as the reaction product after hydride abstraction from trisilane **99**.



Scheme 69. Formation of 2e3c hydrogen-bridged bissilyl cation **101** after hydride abstraction from trisilane **99**.

Further support for this rearrangement came from a trapping reaction with  $\text{LiAl}(\text{O}^t\text{Bu})_3$ . A suspension of  $\text{LiAl}(\text{O}^t\text{Bu})_3$  in toluene was added to the NMR sample containing silyl cation **101**. The silyl cation **101** was quenched and the neutral silane **102** was expected to be formed. The solution turned from dark brown to light brown and the NMR spectra were recorded.



Scheme 70. Quenching of the bissilyl cation **101** with hydride should give neutral silane **102**.

The  $^{29}\text{Si}\{^1\text{H}\}$  NMR spectrum reveals seven intense signals, which can be assigned to typical structural fragments by their  $^{29}\text{Si}$  NMR chemical shifts (Figure 35). A tetrasilyl-substituted silicon atom ( $\delta^{29}\text{Si} = -130.1$ ), a silicon atom that is connected to three silyl groups and one methyl group ( $\delta^{29}\text{Si} = -76.5$ ) and three trimethylsilyl groups ( $\delta^{29}\text{Si} = -7.2, -5.1, -3.5$ ) are clearly identifiable. All these resonance are consistent with the structure assigned to silane **102**. However, the  $^{29}\text{Si}$  chemical shift for the expected hydrogen-substituted dimethyl groups are known to be around  $^{29}\text{Si} = -20$  to  $-30$  but unexpectedly, in the  $^{29}\text{Si}$  NMR spectra only two low field signals at  $\delta^{29}\text{Si} = 24.1$  and  $26.9$  are present. These signals fall in the characteristic range for alkoxy-substituted silicon atoms. A comparison to the ethoxy-substituted silane **103** allows a determination of the reaction product as 1,2-bis(dimethyl-*tert*-butoxysilyl)-2-methyl-1,1,2-tris(trimethylsilyl)disilane **104** (Scheme 71). It is very uncommon, that  $\text{LiAl}(\text{O}^t\text{Bu})_3$  does not act as hydride donor but a *tert*-butoxy donor instead. This reaction implies the high reactivity of this bissilyl cation **101**. The inequality of the two trimethylsilyl groups in the  $^{29}\text{Si}$  NMR spectrum bound to the same tetrasilyl-substituted silicon atom is due to the diastereotopicity of the silyl groups.

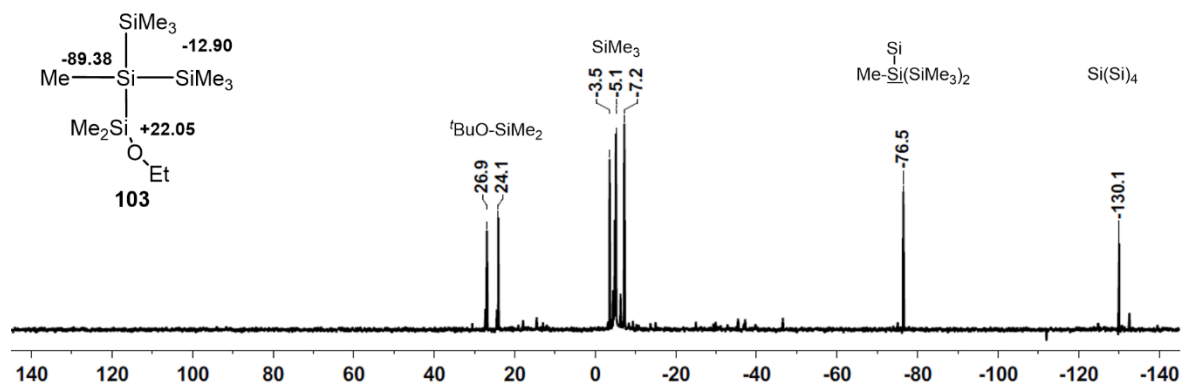
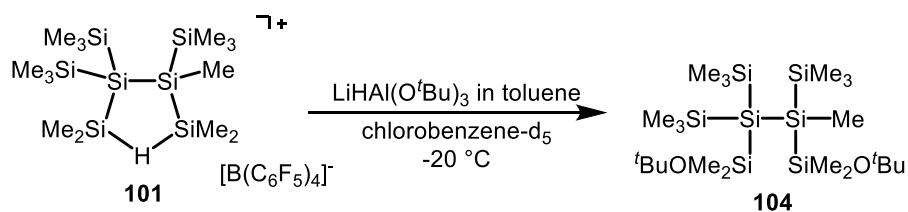


Figure 35. 99 MHz  $^{29}\text{Si}\{^1\text{H}\}$  INEPT NMR spectrum ( $\text{C}_6\text{D}_5\text{Cl}$ , r.t.) obtained after addition of tri-*tert*-butoxyaluminium hydride to bissilyl cation **101** and  $^{29}\text{Si}$  NMR chemical shifts of the known ethoxy silane **103**.<sup>[138]</sup>



Scheme 71 Formation of *tert*-butoxy-substituted silane **104**.

Quantum mechanical calculation of the  $^{29}\text{Si}$  NMR shifts of the optimised structure of **101** at the M06-L/6-311G(2d,p)//M06-2X/6-311+G(d,p) level of theory match the experimentally obtained data for the bissilyl cation **101** (Figure 36). Also the calculated doublet coupling constants on the B3LYP/IGLOIII(Si,C,H),def2TZVP(Ge)//M06-2X/6-311+G(d,p) level of theory for the Si-H-Si bond of  $^1J_{\text{Si,H}} = 40$  Hz is comparable with the experimental one of  $^1J_{\text{Si,H}} = 43$  Hz.

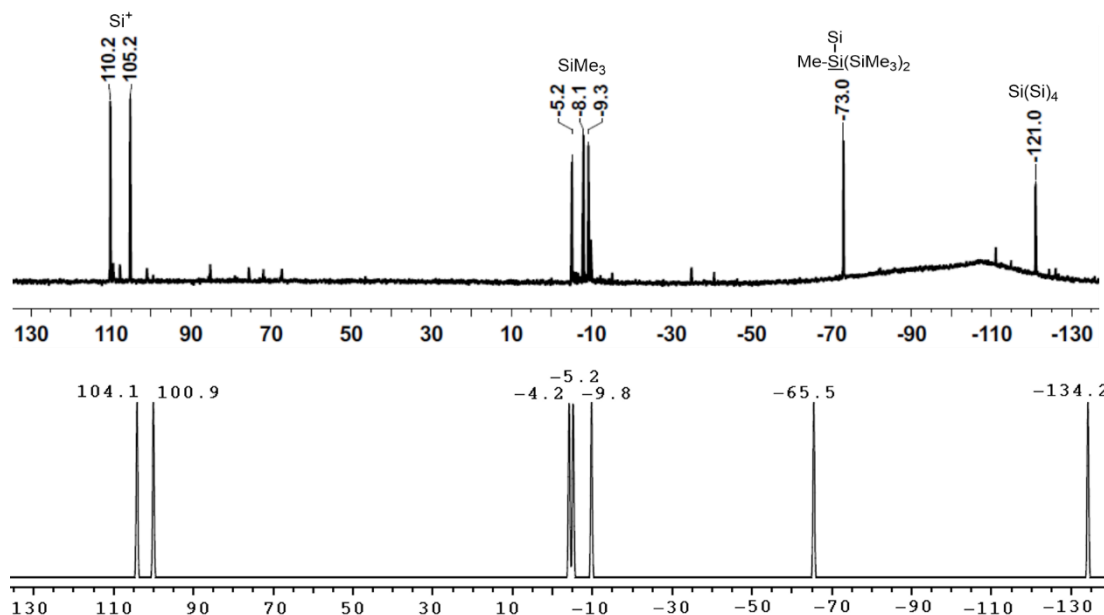
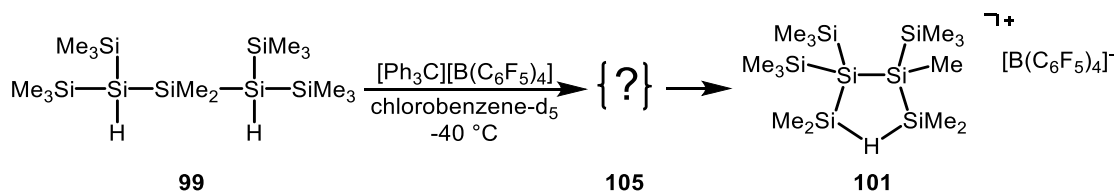


Figure 36. **top**: measured 99 MHz  $^{29}\text{Si}\{^1\text{H}\}$  NMR spectrum ( $\text{C}_6\text{D}_5\text{Cl}$ ,  $T = -40^\circ\text{C}$ ), **bottom**: calculated  $^{29}\text{Si}\{^1\text{H}\}$  NMR spectrum of 2e3c Si-H-Si bridge-stabilised bissilyl cation **101** at M06-L/6-311G(2d,p)//M06-2X/6-311+G(d,p) level of theory.

As already shown in Figure 31, the rearrangement after ionisation of trisilane **99** to 2e3c hydrogen-bridged bissilyl cation **101** proceeds via a transient cationic intermediate that was detected by NMR spectroscopy. Comparing the  $^{29}\text{Si}\{^1\text{H}\}$  NMR spectrum of cation **101** to the spectrum of the mixture, a correlation of the remaining signals to the intermediate is possible.

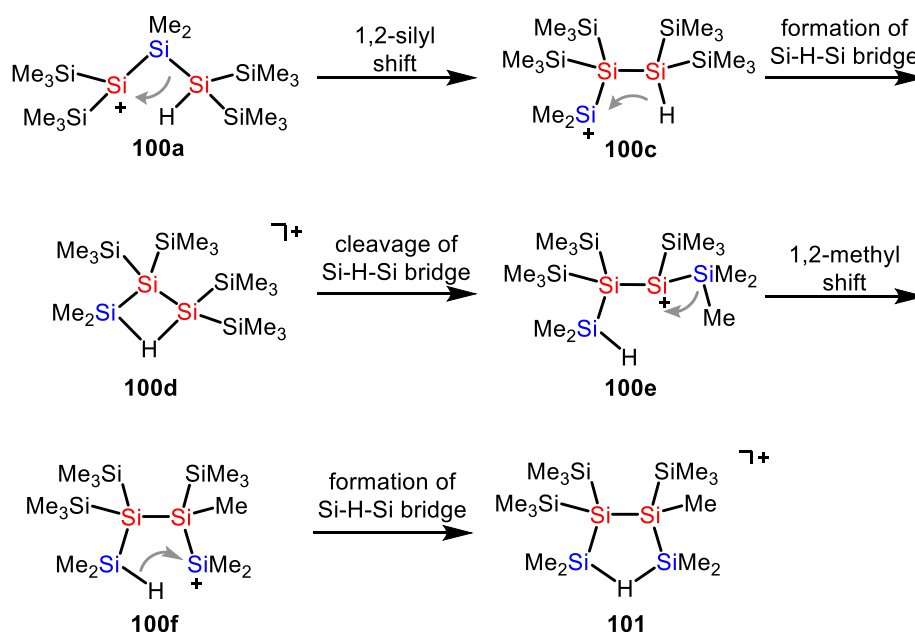


Scheme 72. Formation of 2e3c hydrogen-bridged bissilyl cation **101** after hydride abstraction from trisilane **99** via a cationic intermediate **105**.

To obtain the silyl cation **101**, several rearrangement steps must have taken place supposedly via 1,2-methyl or -silyl shifts. On the basis of quantum mechanical optimisations for the cations **100a-f** and **101**, a rearrangement mechanism can be postulated (Scheme 73). The initial step is a hydride abstraction reaction from the starting material **99** to give the trisilyl-substituted silylium ion **100a**.

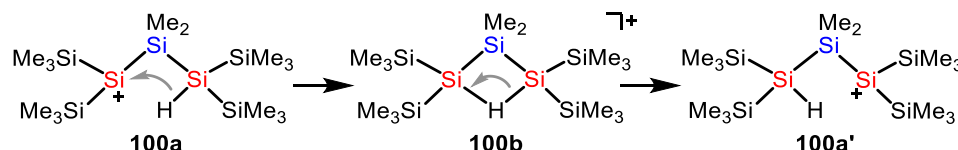
Starting from structure **100a** a 1,2-silyl shift takes place and a new bond between two silicon atoms is formed. A dimethylsilyl group moves out of the Si-Si chain and forms a new flanking dimethylsilyl

group bearing the cationic charge, see **100c**. This monosilyl-substituted silylium ions can be stabilised by the formation of a 2e3c Si-H-Si bridge to give **100d**. This hydrogen bridge can reopen again, this time giving the more stable trisilyl-substituted silylium ion **100e** (see chapter 3.1 for the stability of monosilyl- disilyl and trisilyl-substituted silylium ions). Surprisingly, this structure **100e** is not a stationary point since, during the optimisation procedure, it always rearranges to the 2e3c Si-H-Si bridged isomer **100d**. A consecutive 1,2-methyl shift yields isomer **100f**, which is a monosilyl-substituted silylium ion. The generation of a 2e3c Si-H-Si bridge leads to the reaction product **101**.



Scheme 73. Proposed mechanism for the rearrangement after hydride abstraction from trisilane **99** to give the 2e3c Si-H-Si bridged bisilyl cation **101**.

As a side-reaction it is possible that the initial silylium ion **100a** immediately forms a 2e3c Si-H-Si bond and the hydrogen-bridged bisilyl cation **100b** is generated (Scheme 74). To continue, the Si-H-Si bond must reopen again. It is irrelevant which Si-H bond is broken because both silylium ions produced are identical and can continue the rearrangement reaction.



Scheme 74. Feasible formation of a 2e3c Si-H-Si bridge starting from the initial monosilyl-substituted silylium ion **100a**.

A diagram of the relative ground state energies  $E$  and Gibbs free energies  $G^{298}$  relative to cation **100a** (Figure 37) shows that the overall postulated rearrangement is exothermic by  $74.6 \text{ kJ mol}^{-1}$ . Moreover, all hydrogen-bridged structures are much lower in energy compared to the open-chain cations but cation **101** is the thermodynamic minimum. Unfortunately, it was not possible to obtain the optimised structures of any transition state, and hence, no statement concerning the activation barriers can be made.

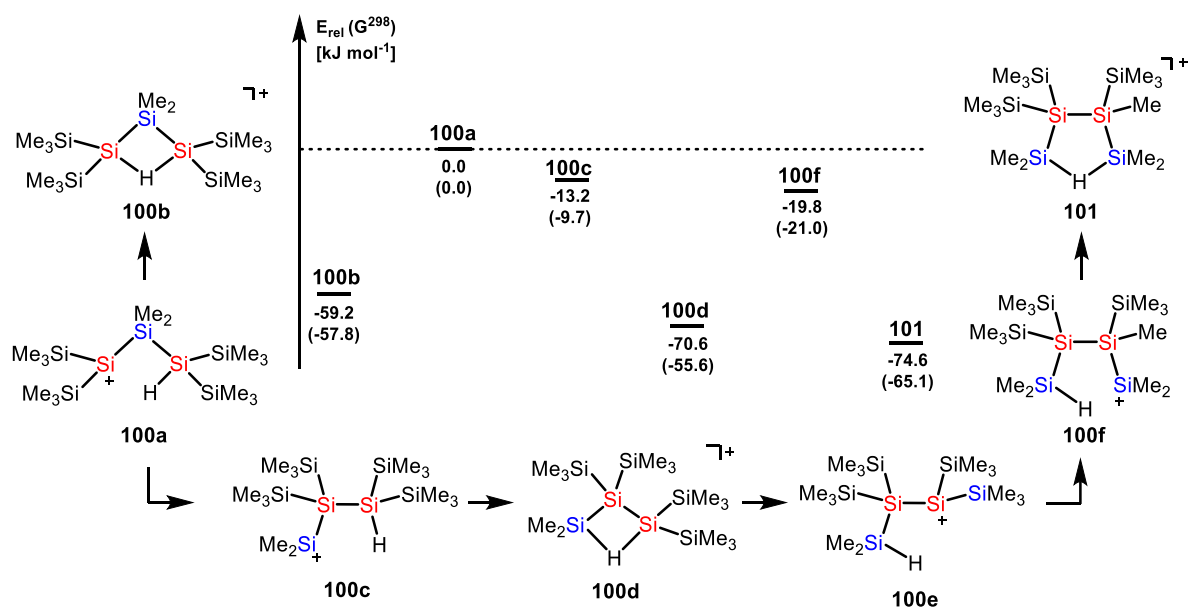


Figure 37. Diagram of relative ground state energies  $E$  and Gibbs free energies at 298.15 K,  $G^{298}$  (in parentheses) of isomeric cations **100a** – **101**, relative to cation **100a**, calculated at M06-2X/6-311+G(d,p), intermediate **100e** is not a stationary point.

The question arises, why does isomer **100a** not form the hydrogen-bridged bissilyl cation **100b** and stop the reaction in this local minimum and why is the sterically more congested isomer **101** stabilised by  $74.6 \text{ kJ mol}^{-1}$ . To answer this, the hydrogen-bridged structures were optimised with the B3LYP functional extended by the D3 version of Grimme's dispersion with the original D3 damping function<sup>[139]</sup>. This method is described in several publications and the importance of attractive dispersion interactions is reviewed by Wagner and Schreiner.<sup>[140]</sup> Dispersion likely plays a very important role in the stability of sterically much hindered systems. Grimme stated that it was, in part,

the “failure” of the implementation of DFT to not account properly for dispersion. This led to the realisation that dispersion becomes increasingly important for larger molecules.<sup>[141]</sup>

Comparing the ground state energies calculated at the B3LYP and B3LYP-D3 levels, similar values of  $\Delta E = 186 - 189 \text{ kJ mol}^{-1}$  were found for the dispersion energies for all three hydrogen-bridged structures, **100b**, **100d** and **101** (Figure 38). The negligible difference in energy between the four-membered ring **100d** and the five-membered ring **101** of  $\Delta E = 0.2 \text{ kJ mol}^{-1}$  can be understood since both cations have vicinal trimethylsilyl groups. In the four-membered ring **100b**, the trimethylsilyl groups are still relatively close to each other. The 1,3-position of the flanking trimethylsilyl groups still allows for attractive interactions which leads to an equal amount of dispersion energy and only an insignificant destabilisation in isomer **100b** ( $\Delta E = 2.4 \text{ kJ mol}^{-1}$  vs. **100d**).

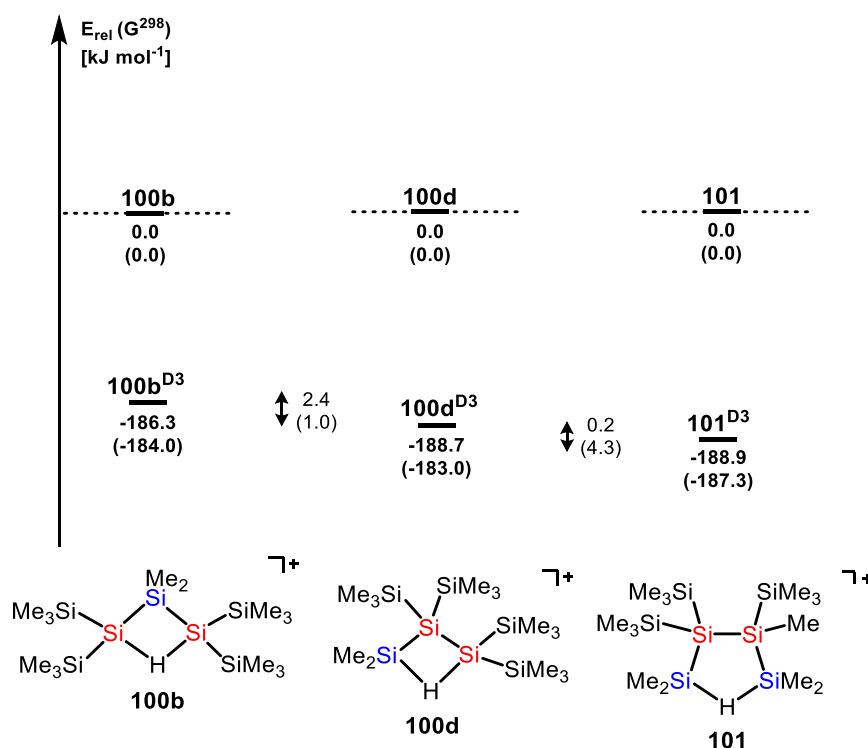


Figure 38. Diagram of relative ground state energies  $E$  and Gibbs free energies at 298.15 K,  $G^{298}$  (in parentheses) of isomeric cations **100b**, **100d** and **101**. Comparison of the energies at the the B3LYP/6-311+G(d,p) and B3LYP-D3/6-311+G(d,p) levels.

The relative energies calculated at the B3LYP and B3LYP-D3 levels show the same trend for all three isomers (Figure 39). Strikingly, both four-membered rings **100b** and **100d** are predicted to be less

stable than the five-membered ring **101**. The four-membered ring is apparently less favoured than the five-membered ring.

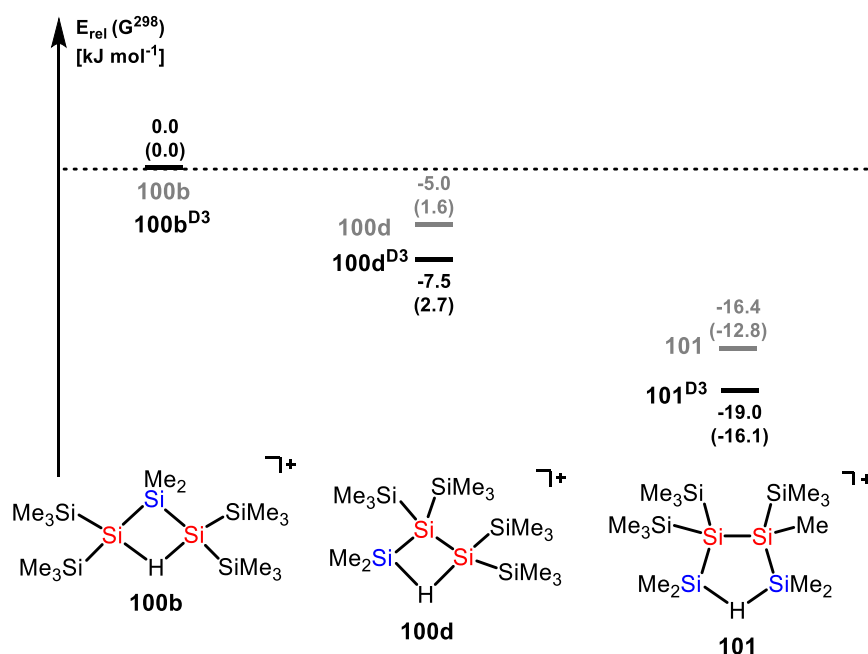
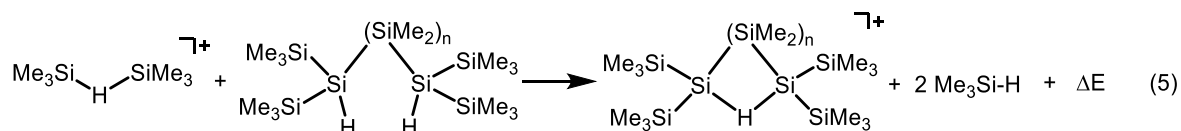


Figure 39. Diagram of relative ground state energies  $E$  and Gibbs free energies at 298.15 K,  $G^{298}$  (in parentheses) of isomeric cations **100b**, **100d** and **101**, relative to cation **100b**, calculated at B3LYP/6-311+G(d,p) (grey) and B3LYP-D3/6-311+G(d,p) (black).

Marschner and Müller calculated the free energy differences for reductive elimination reactions from metallasilacycles with the concurrent formation of cyclic, permethylated polysilanes and found similar results. They found that the cyclohexasilane is more stable than the cyclopentasilane. Further decreasing of the ring size goes along with a change of the free enthalpy differences towards endothermic situations. This means, the general preference for the formation of cyclosilanes is found as follows:  $6 > 5 > 4 > 3$ .<sup>[142]</sup> To assess whether a 2e3c Si-H-Si bridge impacts this trend, the ring strain energies in hydrogen-bridged polysilanyl cations were estimated using isodesmic reaction (5) (Scheme 75).



Scheme 75. Isodesmic reaction (5) for the estimation of ring strain effects in hydrogen-bridged polysilanyl cations.

The calculated stabilisation energies (Table 3) clearly indicate the destabilisation of the small ring sizes for  $n = 0$  and 1 and a preference for the formation of the five-, six- or seven-membered rings.

Table 3. Ring strain energies  $\Delta E$  [ $\text{kJ mol}^{-1}$ ] of Si-H-Si-bridged bissilyl cations. Calculated according to isodesmic reaction (5), at M06-2X/6-311G+(d,p).

Number of SiMe <sub>2</sub> groups (n)	Ring Size	$\Delta E$ [ $\text{kJ mol}^{-1}$ ]
0	3	133.2
1	4	52.8
2	5	12.6
3	6	-10.1
4	7	-26.1
5	8	-39.0

Even though the trimethylsilyl groups in isomer **100d** are in adjacent positions and might stabilise the molecule by attractive dispersion interactions, the small ring-size has a high destabilising effect. Even though isomer **101** has only three trimethylsilyl groups in 1,2-positions which disclose attractive dispersions interactions, this compound is found to be much more stable than the four-membered rings **100b** and **100d**. Obviously, the five-membered ring is more favoured in silicon ring systems, which leads to the high stability of cation **101**.

Still, the identity of the detected intermediate is not yet revealed. As shown in Figure 31 the hydride abstraction at  $T = -40\text{ }^{\circ}\text{C}$  gave rise to an intermediate compound that was transformed into the final rearrangement product **101** over a period of 11.5 hours. The reaction was repeated at  $T = -70\text{ }^{\circ}\text{C}$  in order to acquire the NMR spectra of the intermediate. Due to the melting point of chlorobenzene (m.p.:  $-45\text{ }^{\circ}\text{C}$ ), this time dichloromethane (m.p.:  $-97\text{ }^{\circ}\text{C}$ ) was used as solvent. Trityl tetrakis(pentafluorophenyl)borate was evacuated in the NMR tube and cooled to  $T = -80\text{ }^{\circ}\text{C}$ . Pure trisilane **99** was added to the cold trityl borate and the mixture was frozen with liquid nitrogen. Pre-cooled dichloromethane- $\text{d}_2$  was slowly added in such a way to keep it frozen. The NMR tube was slowly allowed to warm until the dichloromethane- $\text{d}_2$  melted. At that point, the NMR tube was shaken with a vortex mixer and quickly transferred to the NMR spectrometer at  $T = -70\text{ }^{\circ}\text{C}$ . The acquired  $^{29}\text{Si}\{^1\text{H}\}$  NMR spectrum reveals three high field signals at  $\delta^{29}\text{Si} = -124.4$ ,  $-119.0$  and  $-111.1$ , six signals in the

range of  $\delta^{29}\text{Si} = -11.1 - -5.6$  and two low field signals at  $\delta^{29}\text{Si} = 107.4$  and  $110.5$  (Figure 40, bottom). Comparison of this  $^{29}\text{Si}\{^1\text{H}\}$  NMR spectrum and the  $^{29}\text{Si}\{^1\text{H}\}$  NMR spectrum obtained at  $T = -40^\circ\text{C}$  in chlorobenzene- $d_5$  indicates that the spectrum at  $T = -70^\circ\text{C}$  only shows the signals of the previously detected intermediate **105** (Figure 40). This may help to identify the composition of this intermediate.

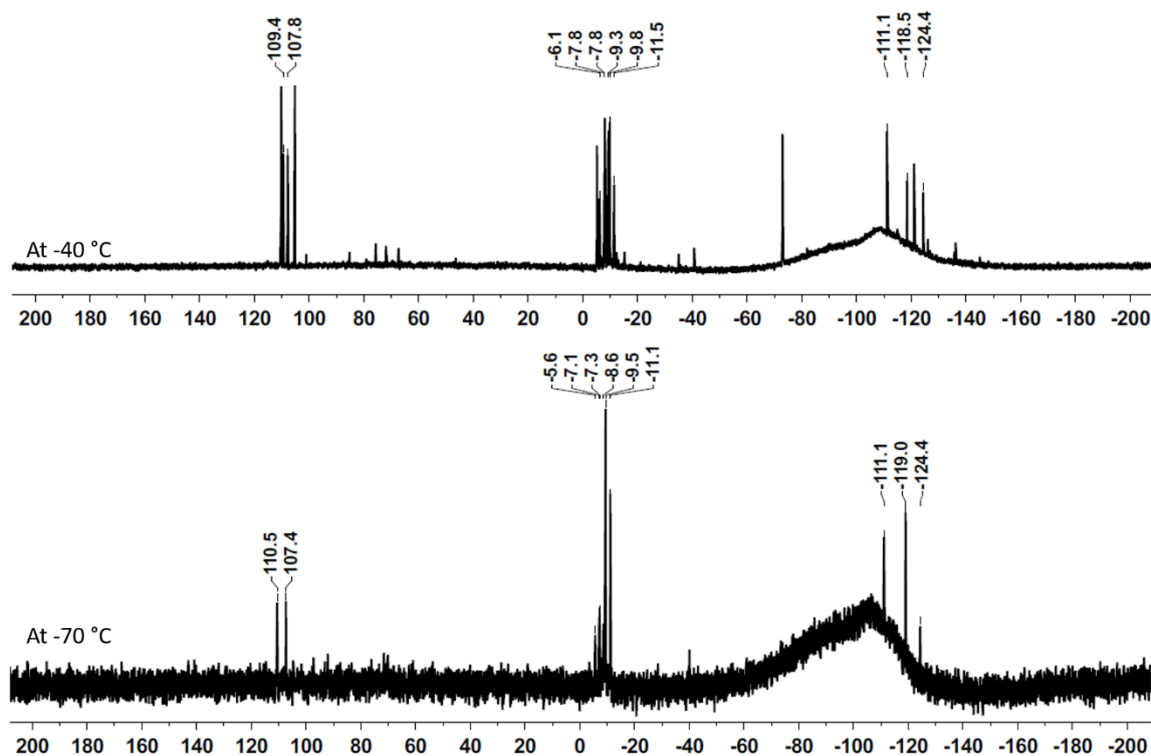


Figure 40. 99 MHz  $^{29}\text{Si}\{^1\text{H}\}$  NMR spectra obtained after hydride abstraction reaction from trisilane **99**, **top**: at  $T = -40^\circ\text{C}$  in  $\text{C}_6\text{D}_5\text{Cl}$ , **bottom**: at  $T = -70^\circ\text{C}$  in  $\text{CD}_2\text{Cl}_2$ . Only the chemical shifts of the intermediate **105** are indicated.

The coupled  $^{29}\text{Si}$  INEPT NMR spectrum discloses additional information. Interestingly, in this spectrum not only three, but four high field signals in the range of  $\delta^{29}\text{Si} = -111 - -138$  are visible. The absence of the fourth signal at  $\delta^{29}\text{Si} = -137.3$  in the  $^{29}\text{Si}\{^1\text{H}\}$  inverse gated spectrum is rationalised to be a result of its low intensity and of the poor signal to noise ratio in that spectrum. Two of the four high field signals are doublets with a Si-H coupling constant of  $^1J_{\text{Si,H}} = 171$  Hz and 154 Hz which are characteristic of a trisilyl-substituted  $(\text{Si})_3\text{Si-H}$  building block, the other two resonances appear as singlets. The low field signals represent two silicon atoms being part of a 2e3c Si-H-Si bond as indicated by the doublet of multiplets coupling pattern with  $^1J_{\text{Si,H}} = 44$  Hz and 42 Hz (Figure 41).

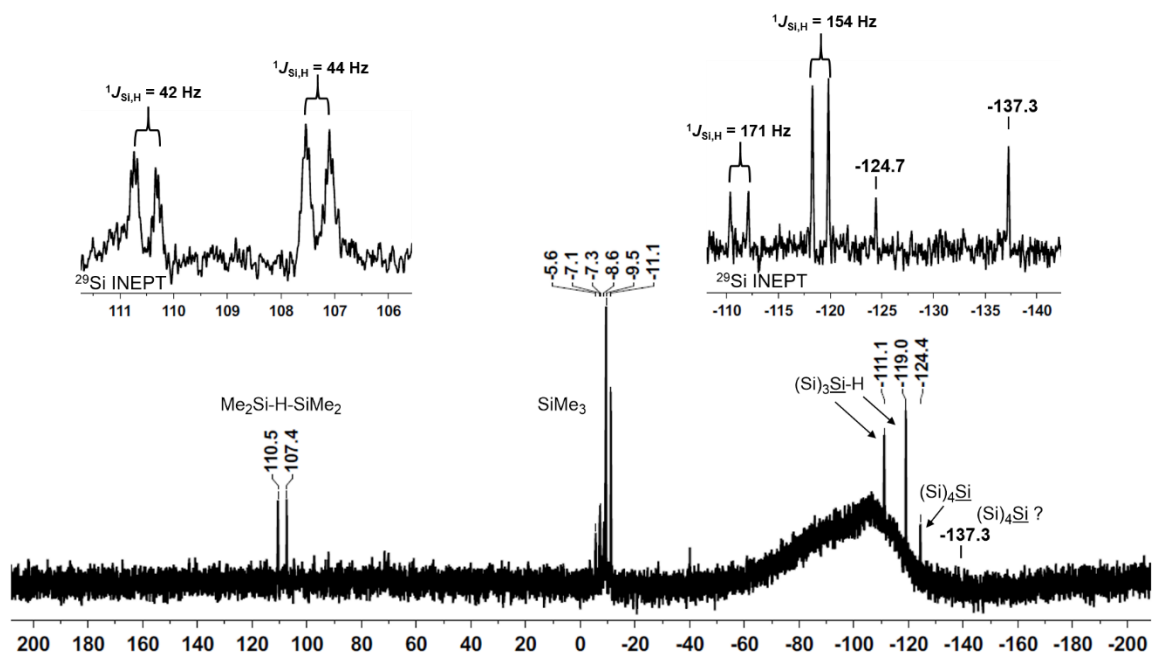


Figure 41. 99 MHz  $^{29}\text{Si}\{^1\text{H}\}$  NMR spectrum and excerpts of the hydrogen coupled  $^{29}\text{Si}$  INEPT NMR spectrum ( $\text{CD}_2\text{Cl}_2$ ,  $T = -70^\circ\text{C}$ ) of the intermediate **105**, obtained after hydride abstraction reaction from trisilane **99**.

The  $^1\text{H}$  NMR spectrum is in accordance with the structural motifs found in the  $^{29}\text{Si}$  NMR spectra. Two resonances for Si-H hydrogen atoms appear at  $\delta^1\text{H} = 2.36$  and  $3.18$  and a broad signal for the bridging hydrogen atom is found at  $\delta^1\text{H} = 2.30$  (Figure 42). Moreover, the signals for the methyl groups connected to the cationic silicon atoms resonate at  $\delta^1\text{H} = 0.97$  and several methyl groups of trimethylsilyl groups appear in a range of  $\delta^1\text{H} = 0.36 - 0.13$ .

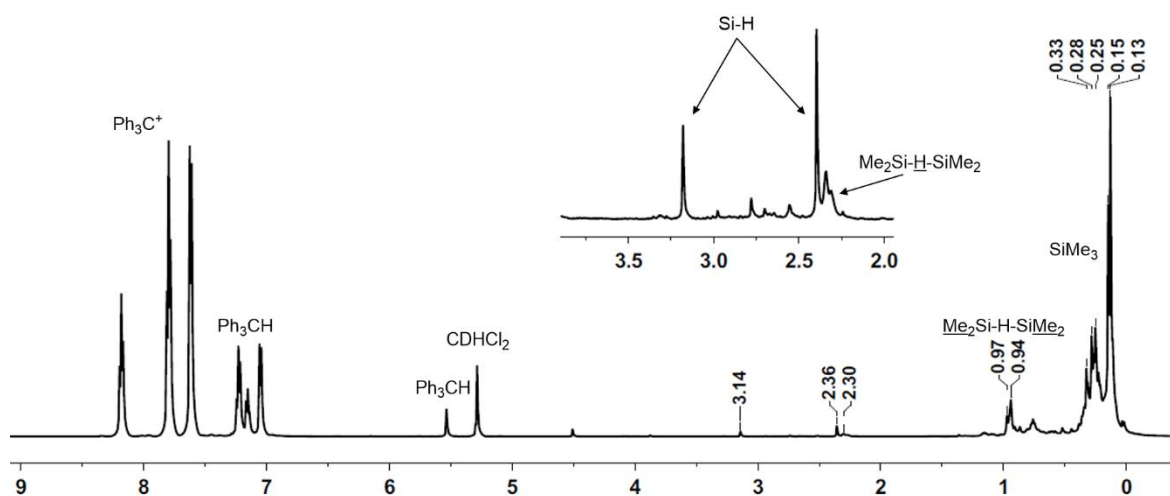


Figure 42. 500 MHz  $^1\text{H}$  NMR spectrum ( $\text{CD}_2\text{Cl}_2$ ,  $T = -70^\circ\text{C}$ ) of the intermediate **105**, obtained after hydride abstraction reaction from trisilane **99**.

On the basis of the moieties already identified, the appropriate cross peaks were observed in the  $^1\text{H}^{29}\text{Si}$  HMBC and HMQC NMR spectra (Figure 43 and Figure 44).

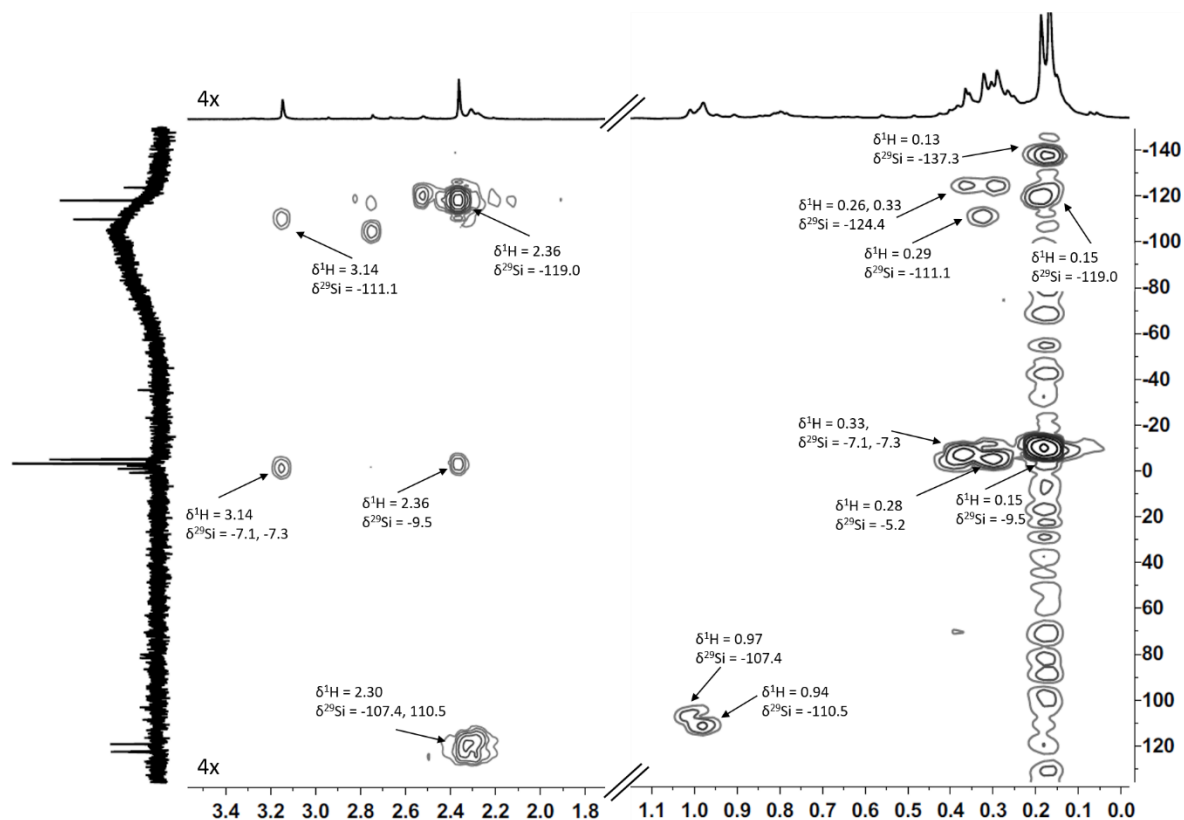


Figure 43. 500 MHz/99 MHz  $^1\text{H}^{29}\text{Si}$  HMQC NMR spectrum ( $\text{CD}_2\text{Cl}_2$ ,  $T = -70^\circ\text{C}$ ) of the intermediate **105**, obtained after hydride abstraction reaction from trisilane **99**.

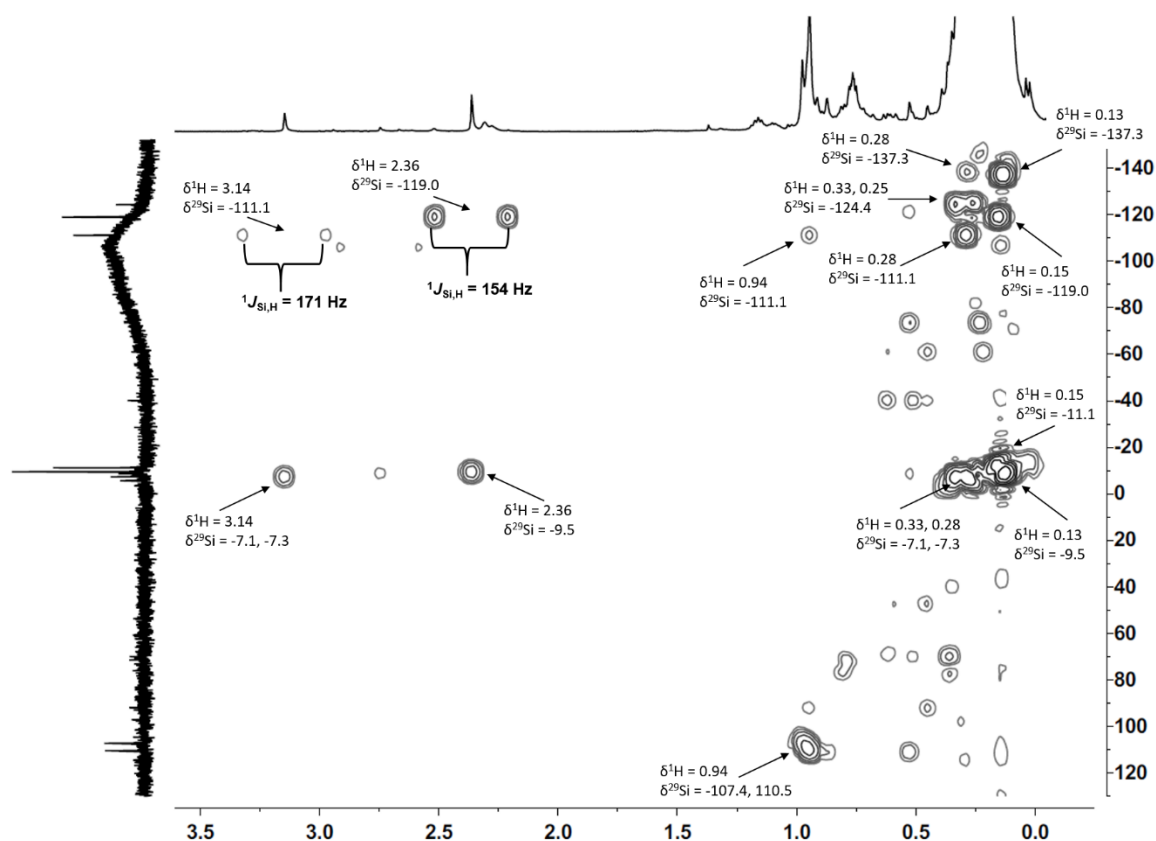


Figure 44. 500 MHz/99 MHz  $^1\text{H}/^{29}\text{Si}$  HMBC NMR spectrum ( $\text{CD}_2\text{Cl}_2$ ,  $T = -70^\circ\text{C}$ ) of the intermediate **105**, obtained after hydride abstraction reaction from trisilane **99**.

The sample was kept at  $T = -70^\circ\text{C}$  in the NMR machine and NMR spectra were acquired over a long period of time. Selected  $^{29}\text{Si}\{^1\text{H}\}$  NMR spectra recorded after 45 minutes, 11.5 hours and 15 hours are shown in Figure 45. An interesting behaviour is noted. After 11.5 hours, a set of new signals (#) appeared. Besides the already assigned signals of the intermediate **105** (\*), these new signals are assigned to the rearrangement product **101** as verified by comparison to the spectrum obtained in chlorobenzene- $d_5$  at  $T = -40^\circ\text{C}$  (Figure 36). The slightly different  $^{29}\text{Si}$  NMR chemical shifts are justified by the change in solvent and temperature.

Although the composition of the previously formed silylium ion **105** is still unclear, it is believed that this compound is an intermediate during the rearrangement after hydride abstraction from trisilane **99**. To see whether this intermediate completely rearranges to give silylium ion **101**, the sample was stored at  $T = -70^\circ\text{C}$  for additional 6 hours and then investigated by NMR spectroscopy.

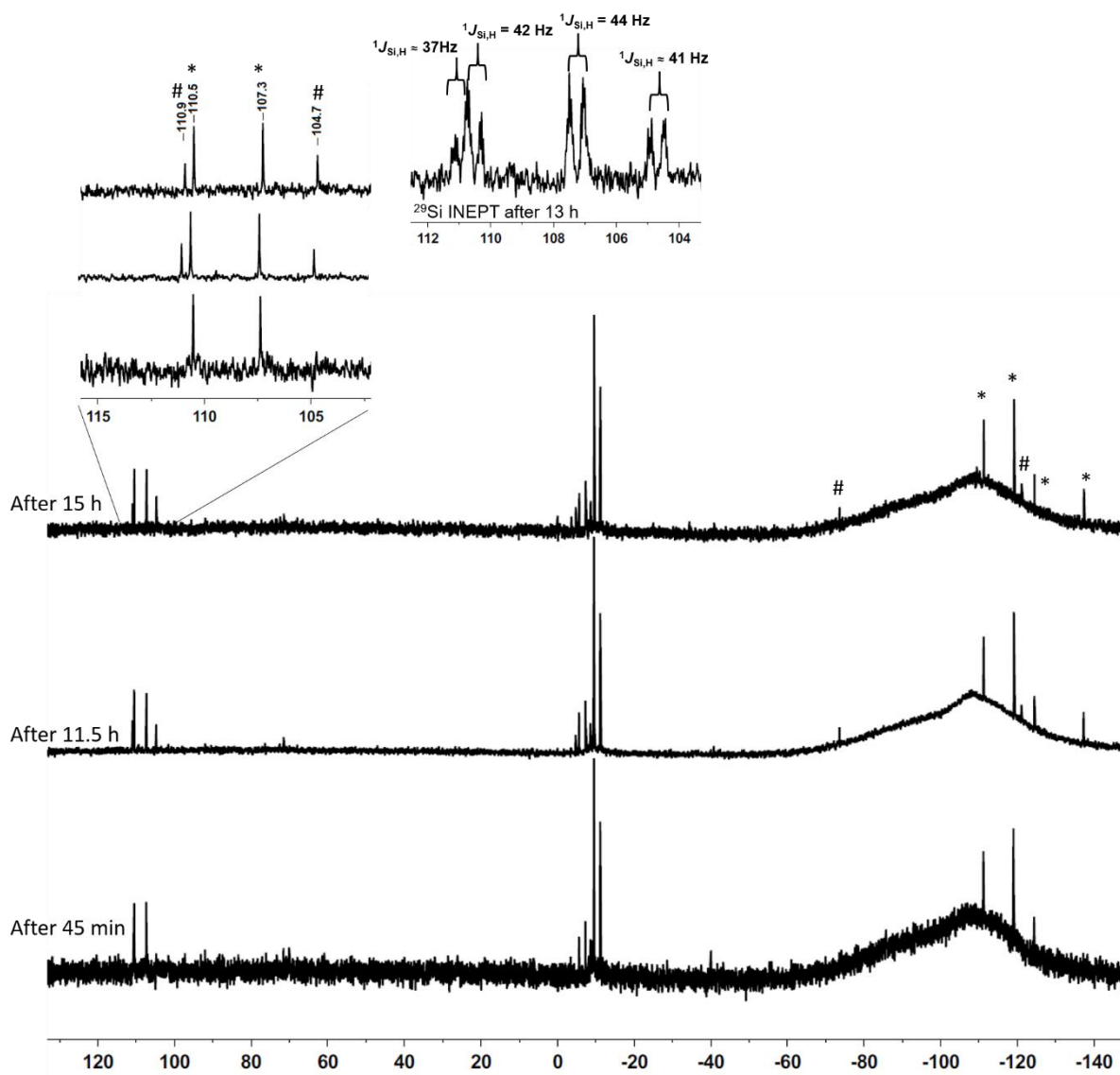


Figure 45. 99 MHz  $^{29}\text{Si}\{^1\text{H}\}$  NMR spectra after 45 min, 11.5 h and 15 h; and excerpts of the hydrogen coupled  $^{29}\text{Si}$  INEPT NMR spectrum after 13 h ( $\text{CD}_2\text{Cl}_2$ ,  $T = -70^\circ\text{C}$ ) obtained after hydride abstraction reaction from trisilane **99**. Intermediate **105** (\*), hydrogen-bridged bisilyl cation **101** (#).

After additional 6 hours at  $T = -70^\circ\text{C}$ , the  $^{29}\text{Si}\{^1\text{H}\}$  NMR spectrum showed a third set of signals (o) whose intensities increase over the time (Figure 46). Interestingly, the two new low field signals are not doublets in the hydrogen coupled  $^{29}\text{Si}$  INEPT NMR spectrum. This means, these new silicon atoms are no longer connected to a hydrogen atom neither directly nor by a 2e3c bond. The new signal at  $\delta^{29}\text{Si} = -125.5$  represents a new tetrasilyl-substituted silicon atom. Due to the high number of signals, the new signals in the chemical shift range for trimethylsilyl groups are not analysed in detail.

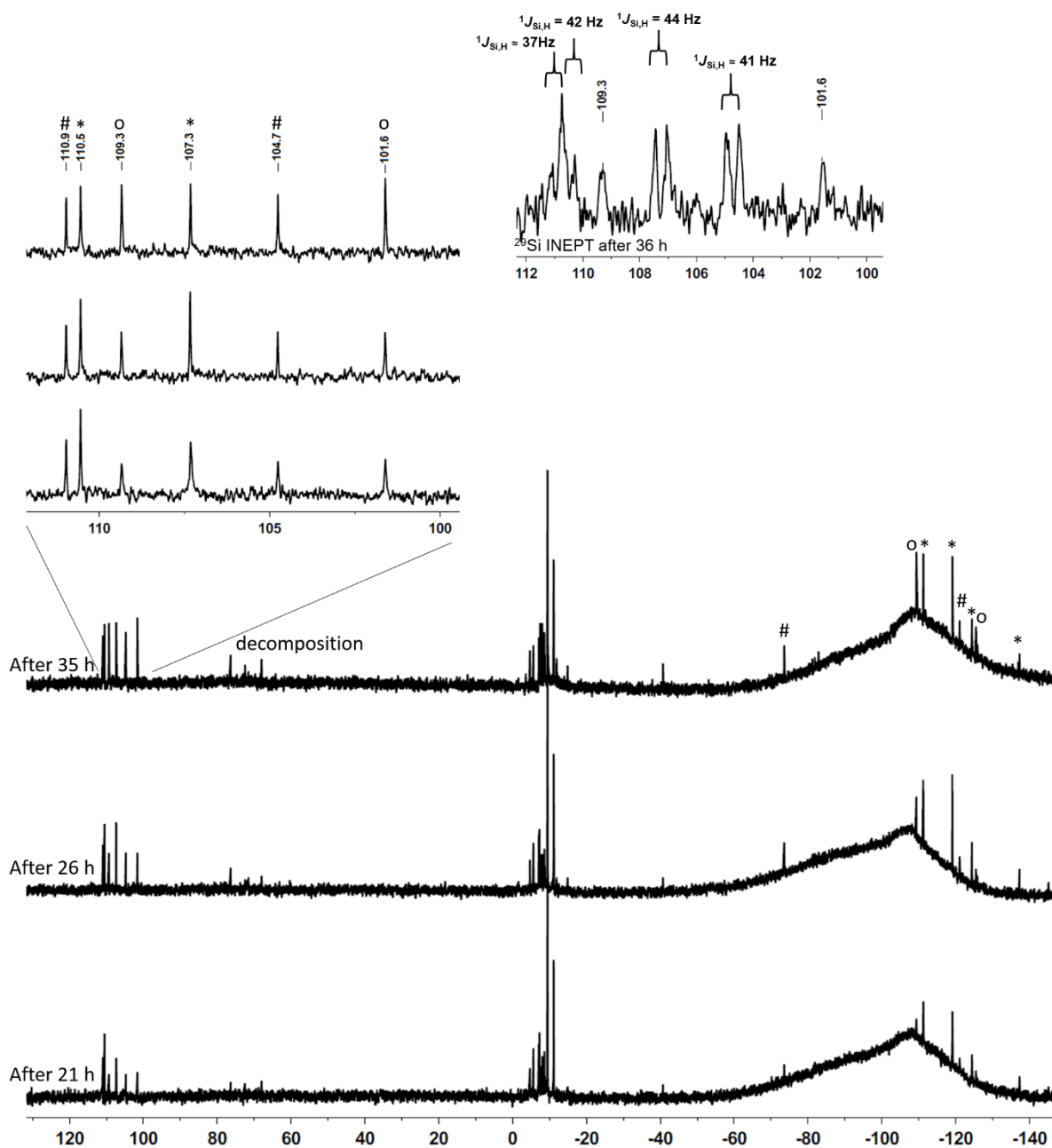


Figure 46. 99 MHz  $^{29}\text{Si}\{^1\text{H}\}$  NMR spectra acquired after 21 h, 26 h and 35 h; and excerpts of the hydrogen coupled  $^{29}\text{Si}$  INEPT NMR spectrum after 36 h ( $\text{CD}_2\text{Cl}_2$ ,  $T = -70^\circ\text{C}$ ) after hydride abstraction reaction from trisilane **99**. Intermediate (\*), hydrogen-bridged silyl cation **101** (#) and silyl chloronium ion **106** (o).

A similar trend was observed in the  $^1\text{H}$  NMR spectra (Figure 47). As already discussed with the help of the hydrogen-coupled  $^{29}\text{Si}$  INEPT NMR spectrum, the initially formed compound (\*) exhibits a  $\text{Me}_2\text{Si-H-SiMe}_2$  group ( $\delta^1\text{H} = 2.30$ ) and two Si-H groups ( $\delta^1\text{H} = 2.36$  and  $3.16$ ). After 15 hours the bisilyl cation **101** (#) appeared with a broad signal at  $\delta^1\text{H} = 2.27$ . In accordance with the  $^{29}\text{Si}\{^1\text{H}\}$  NMR spectrum after 21 hours, a third compound **106** (o) was detectable with a Si-H group that resonates in the  $^1\text{H}$  NMR spectrum at  $\delta^1\text{H} = 2.94$ .

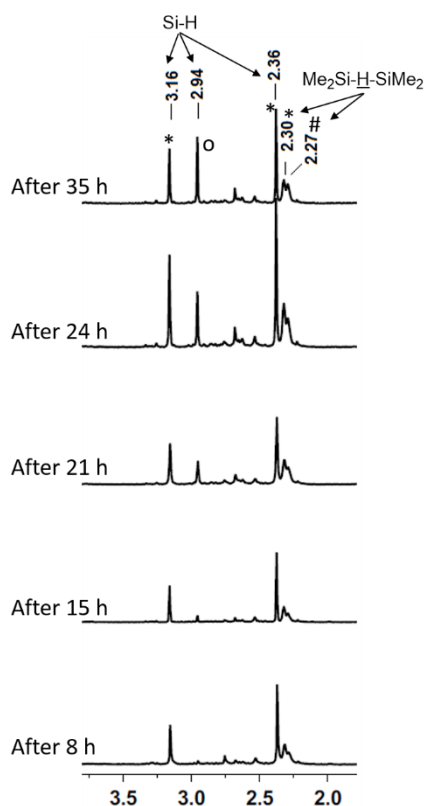


Figure 47. Excerpts of the 500 MHz  $^1\text{H}$  NMR spectra acquired after 8 h, 15 h, 21 h, 24 h and 35 h ( $\text{CD}_2\text{Cl}_2$ ,  $T = -70^\circ\text{C}$ ) after hydride abstraction reaction from trisilane **99**. Intermediate **105** (\*), hydrogen-bridged silyl cation **101** (#) and by-product **106** (o).

In order to promote the rearrangement towards the complete transformation of these intermediates, the sample was warmed by  $\Delta T = 10^\circ\text{C}$  and stored at  $T = -60^\circ\text{C}$  for 8 h. Only four signals are visible in the low field area of the  $^{29}\text{Si}\{^1\text{H}\}$  NMR spectrum and only two in the high field range. On the basis of the NMR chemical shifts it is obvious that one set of signals, marked with (o), is the same as previously observed in the  $^{29}\text{Si}\{^1\text{H}\}$  NMR spectrum recorded at  $T = -70^\circ\text{C}$  after 35 h. The other set of signals ( $\Delta$ ) represents a newly formed compound **107** (Figure 48).

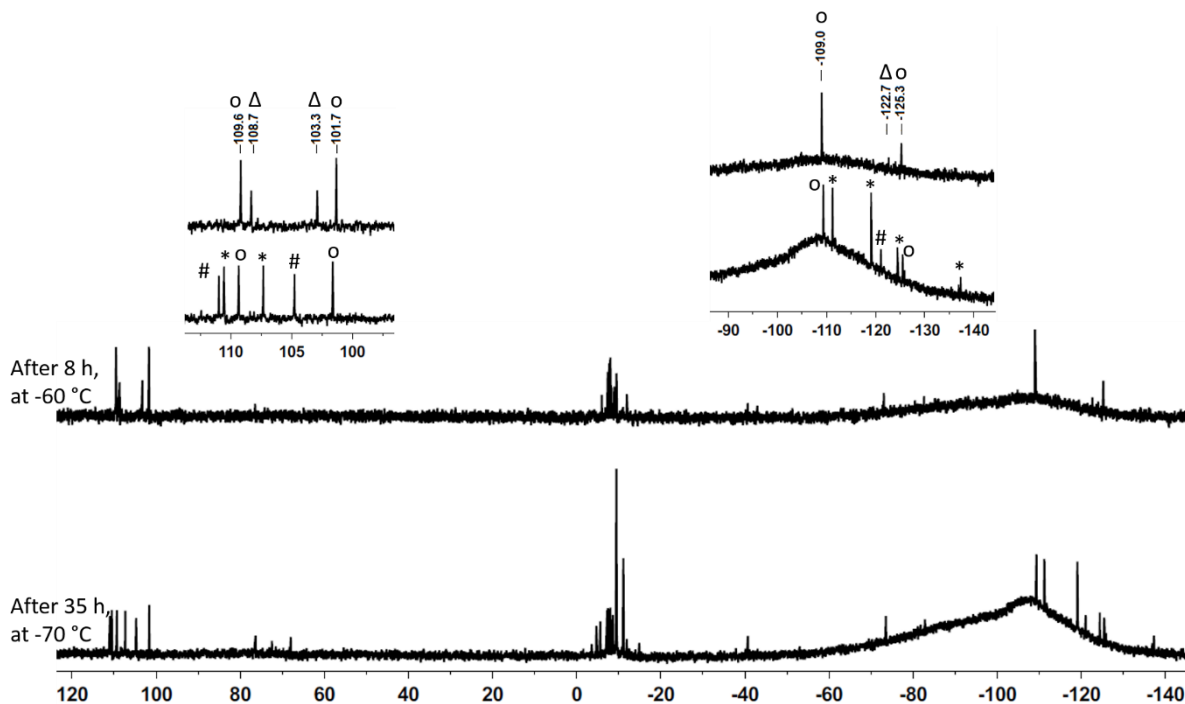


Figure 48. 99 MHz  $^{29}\text{Si}\{^1\text{H}\}$  NMR spectra acquired after 35 h at  $T = -70^\circ\text{C}$  and after 8 h at  $T = -60^\circ\text{C}$  ( $\text{CD}_2\text{Cl}_2$ ) after hydride abstraction reaction from trisilane **99**. Hydrogen-bridged silyl cation (#) and by-products **106** (o) and **107** ( $\Delta$ ).

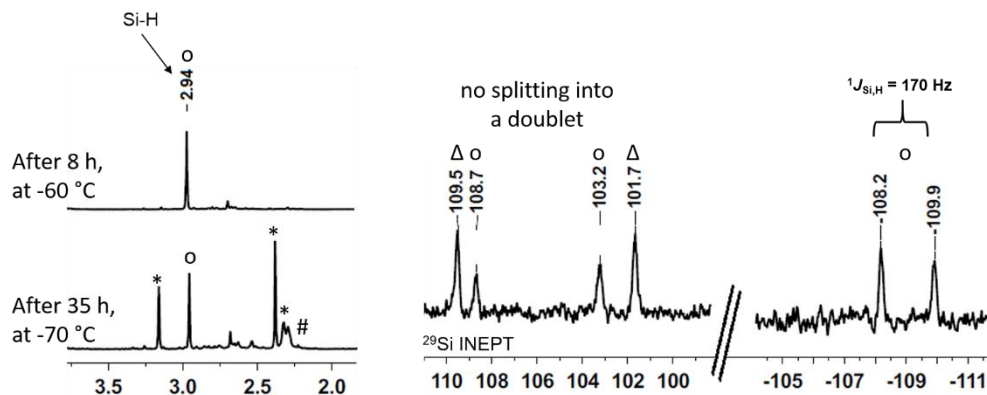


Figure 49. **left**: Excerpts of the 500 MHz  $^1\text{H}$  NMR spectra acquired after 35 h at  $T = -70^\circ\text{C}$  and after 8 h at  $T = -60^\circ\text{C}$  ( $\text{CD}_2\text{Cl}_2$ ), **right**: excerpt of the hydrogen-coupled 99 MHz  $^{29}\text{Si}$  INEPT NMR spectrum after 8 h at  $T = -60^\circ\text{C}$  ( $\text{CD}_2\text{Cl}_2$ ) after hydride abstraction reaction from trisilane **99**. Intermediate (\*), hydrogen-bridged silyl cation **101** (#) and by-products **106** (o) and **107** ( $\Delta$ ).

It is known that silylium ions are only stable in chlorinated alkanes at very low temperatures and cleave the C-Cl bond of chlorinated alkanes at higher temperatures. Given that the low field signals in the hydrogen coupled  $^{29}\text{Si}$  INEPT NMR spectrum are singlets, it is assumed that these signals belong to cationic silicon atoms bridged by a chlorine atom analogues to 4e3c bonded chloronium ions quoted in literature.<sup>[107, 109, 143]</sup>

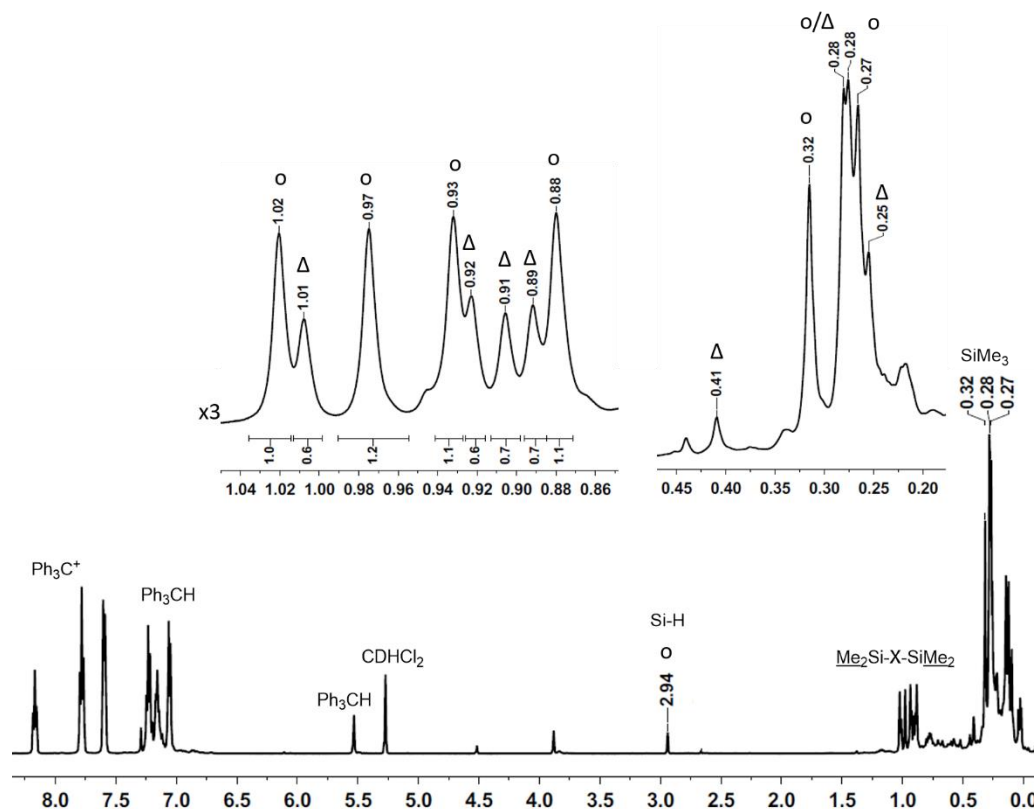


Figure 50. 500 MHz  $^1\text{H}$  NMR spectrum ( $\text{CD}_2\text{Cl}_2$ ,  $T = -60\text{ }^\circ\text{C}$ ) obtained after hydride abstraction reaction from trisilane **99**. Silyl chloronium ions **106** (o) and **107** ( $\Delta$ ).

The  $^1\text{H}$  and  $^{29}\text{Si}$  spectra (Figure 48 top, Figure 50) reveal the resonances of two compounds. The signals of the dominant species were identified in the  $^1\text{H}^{29}\text{Si}$  HMBC NMR spectrum and are visualised in Figure 51 as unframed numbers. The low field signals at  $\delta^{29}\text{Si} = 109.6$  and  $101.7$  are again characteristic for cationic silicon atoms and correlate with methyl groups at  $\delta^1\text{H} = 1.02$ ,  $0.97$ ,  $0.93$  and  $0.88$ . These singlets have equal integrals and their  $^1\text{H}$  NMR chemical shifts identify them as methyl groups connected to cationic silicon atoms. The signals at  $\delta^{29}\text{Si} = -8.0$ ,  $-7.8$  and  $-1.4$  show a cross peak with the large singlets in the  $^1\text{H}$  NMR spectrum at  $\delta^1\text{H} = 0.32$ ,  $0.28$  and  $0.27$ , thus, they are assigned to be the resonances of three different trimethylsilyl groups. These singlets in the  $^1\text{H}$  NMR spectrum also correlate to two signals in the high field region of the spectrum. The resonance at  $\delta^{29}\text{Si} = -125.3$  represents a tetrasilyl-substituted silicon atom. More interesting is the signal at  $\delta^{29}\text{Si} = -109.0$  as it correlates to a singlet in the  $^1\text{H}$  NMR spectrum at  $\delta^1\text{H} = 2.94$  and is a doublet with  $^1J_{\text{Si,H}} = 170\text{ Hz}$  which is a typical size for a direct Si-H bond. The hydrogen resonance also correlates to the trimethylsilyl silicon atoms.

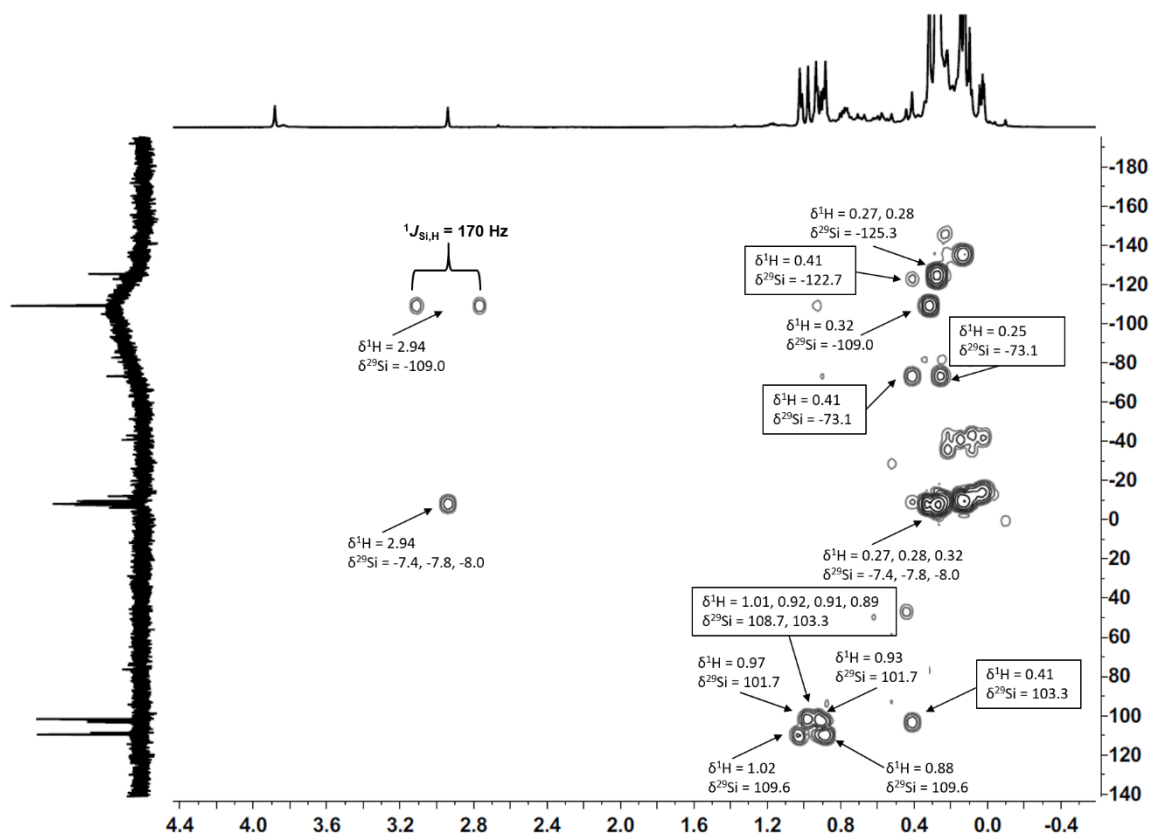
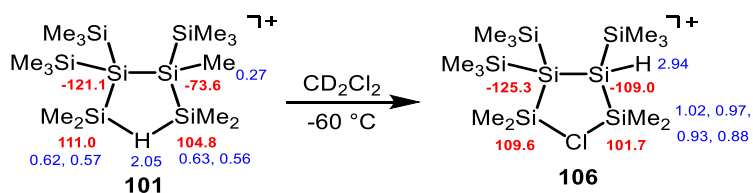


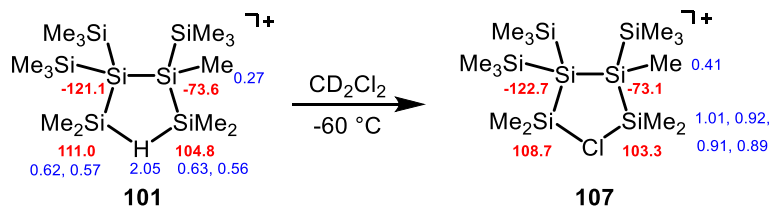
Figure 51. 500 MHz/99 MHz  $^1\text{H}/^{29}\text{Si}$  HMBC NMR spectrum ( $\text{CD}_2\text{Cl}_2$ ,  $T = -60^\circ\text{C}$ ) obtained after hydride abstraction reaction from trisilane **99**.

The data suggest the formation of a silyl chloronium ion shown in Scheme 76. Up to now, a reasonable mechanism for the formation of this silyl chloronium ion **106** is not possible to suggest because the spectra do not provide enough information.



Scheme 76. Formation of silyl chloronium ion **106** starting from hydrogen-bridged bisilyl cation **101**.  $\delta^{29}\text{Si}$  in red,  $\delta^1\text{H}$  in blue ( $\delta^1\text{H}$  for **101** were measured in  $\text{C}_6\text{D}_5\text{Cl}$  because the spectrum in  $\text{CD}_2\text{Cl}_2$  is not significant enough), the  $[\text{B}(\text{C}_6\text{F}_5)_4]^-$  anion is omitted.

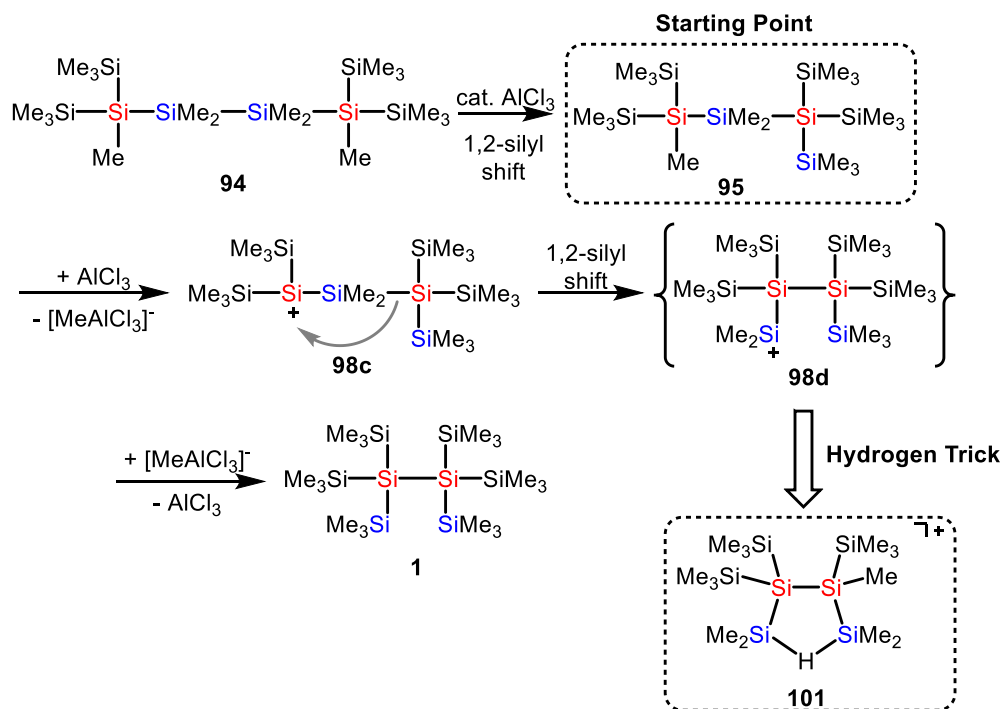
Now, the less intensive set of signals is discussed (framed in Figure 51). The connections in the  $^1\text{H}^{29}\text{Si}$  HMBC NMR spectrum clearly indicate the presence of a silyl cation composed of several known structural building blocks. The two different signals at  $\delta^{29}\text{Si} = 108.7$  and  $103.3$  correlate to four singlets in the  $^1\text{H}$  NMR spectrum at  $\delta^1\text{H} = 1.01, 0.92, 0.91$  and  $0.89$  which all have similar integrals. Based on previous results, the  $^1\text{H}$  chemical shifts are characteristic of methyl groups connected to a cationic silicon atom. A very significant fact is the chemical shift of  $\delta^{29}\text{Si} = -73.1$  since it represents a methyltrisilyl-substituted silicon atom and correlates in the  $^1\text{H}^{29}\text{Si}$  HMBC NMR spectrum to a singlet at  $\delta^1\text{H} = 0.41$ . If the methylsilyl signals are each set to integrals of 3, then, this singlet also integrates to 3, which assigns it to a methyl group. A tetrasilyl-substituted silicon atom, detected as a very small signal at  $\delta^{29}\text{Si} = -122.7$ , shows a weak cross-peak with the methyl group at  $\delta^1\text{H} = 0.41$ . Although an exact assignment of the signals in a range of  $\delta^1\text{H} = 0.32 - 0.27$  in the  $^1\text{H}$  NMR spectrum to signals at  $\delta^{29}\text{Si} = -6 - -11.9$  and assigned to trimethylsilyl groups is not possible, these facts indicate the presence of the chlorine-bridged silyl cation **107**, shown in Scheme 77, as a decomposition product of the hydrogen-bridged silyl cation **101** with dichloromethane.



Scheme 77. Formation of chlorine-bridged silyl cation **107** starting from hydrogen-bridged silyl cation **101**.  $\delta^{29}\text{Si}$  in red,  $\delta^1\text{H}$  in blue ( $\delta^1\text{H}$  for **101** were measured in  $\text{C}_6\text{D}_5\text{Cl}$  because the spectrum in  $\text{CD}_2\text{Cl}_2$  is not significant enough), the  $[\text{B}(\text{C}_6\text{F}_5)_4]^-$  anion is omitted.

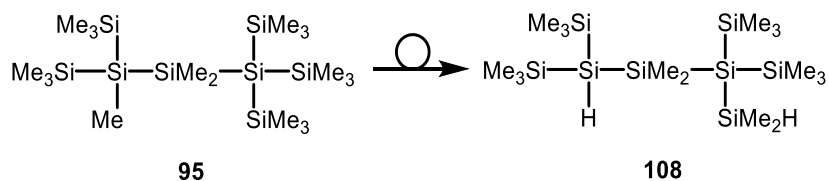
In summary, several conclusions can be drawn based on the NMR investigations. On the one hand, the same intermediate **105** (marked with an asterisk (\*) in the spectra) present during the rearrangement of trisilane **99** to bisilyl cation **101** (marked with a hash (#) in the spectra) was detected in chlorobenzene- $\text{d}_5$  at  $T = -40^\circ\text{C}$  and dichloromethane- $\text{d}_2$  at  $T = -70^\circ\text{C}$ . In both solvents, this intermediate **105** rearranges over time to silyl cation **101**. On the other hand, in dichloromethane- $\text{d}_2$  this intermediate **105** decomposes already at  $T = -70^\circ\text{C}$  to give hydrogen-substituted silyl chloronium ion **106** (o). At slightly elevated temperatures of  $T = -60^\circ\text{C}$ , the hydrogen-bridged silyl cation **101** also reacts with the solvent and forms silyl chloronium ion **107** ( $\Delta$ ). These results clearly demonstrate the high reactivity of these silyl cations and their instability even at very low temperatures.

Although it was not possible to identify the fleeting intermediate **105**, the detection of hydrogen-bridged silyl cation **101** and the quantum mechanical investigations provide enough pieces of evidence to postulate the mechanism of the rearrangement of trisilane **95** to give disilane **1** as shown in Scheme 78.



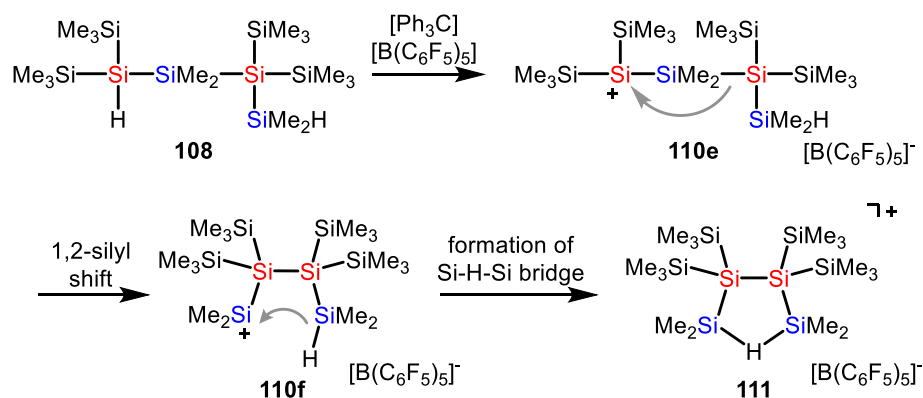
Scheme 78. Abbreviated mechanism of the rearrangement of tetrasilane **94** to give isomer **1** via trisilane **95**. Cationic intermediate **98d** was identified in the form of its Si-H-Si bridged analogue **101**.

For further work, the silane **108** should be prepared because it is a more suitable precursor for mechanistic investigations on this rearrangement.



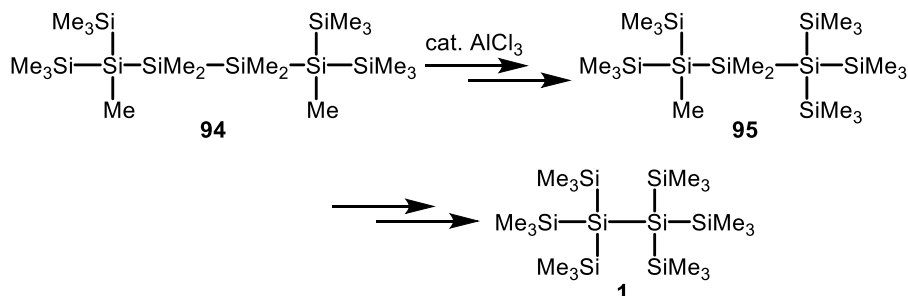
Scheme 79. Methyl- and hydrogen-substituted silanes **95** and **108**.

After hydride abstraction and formation of trisilyl-substituted silylium ion **110e** and only one 1,2-silyl shift, the exact Si-H-Si bridged analogue **111** of the rearrangement intermediate **98d** towards product **1** would be obtained (Scheme 80).

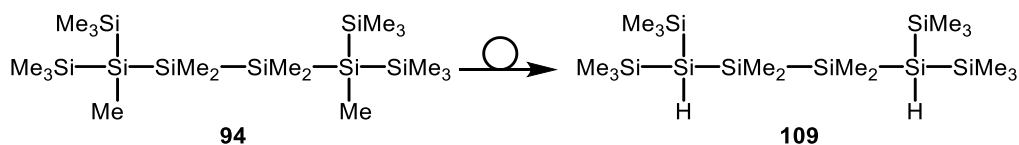
Scheme 80. Proposed mechanism of the rearrangement of trisilane **108**.

### 3.4.3.2 Mechanistic Development – Part II

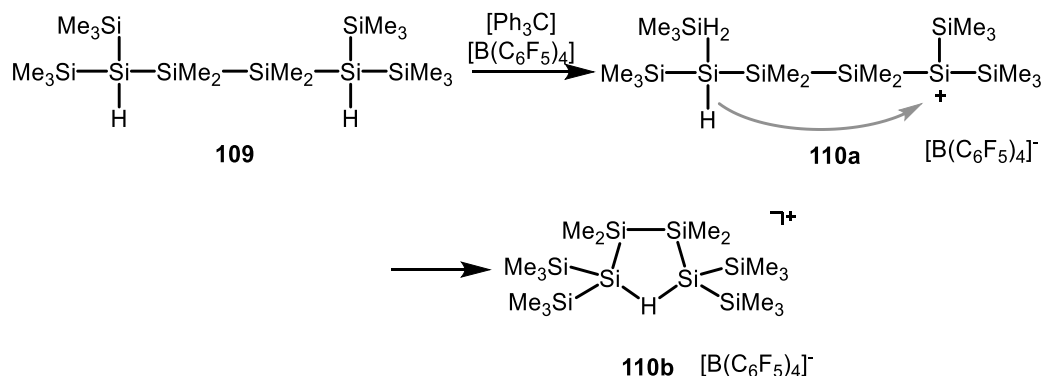
The previous results concentrated on the rearrangement starting from trisilane **95** to give the final rearrangement product **1**. The following part will illuminate the overall rearrangement from tetrasilane **94** via trisilane **95** en route to disilane **1**.

Scheme 81. Rearrangement of tetrasilane **94** via trisilane **95** gives disilane **1**.

A dihydrido analogue of tetrasilane **94** was prepared, namely the methyl groups at the trisilyl-substituted silicon atom were exchanged by hydrogen atoms to result in tetrasilane **109** (Scheme 82).

Scheme 82. Methyl- and hydrogen-substituted tetrasilanes **94** and **109**.

Again, in this compound the dihydrido-substitution permits the controlled positioning of the cationic charge by the hydride abstraction reaction with triphenylmethyl cation and yields the trisilyl-substituted silylium ion **110a**. It was expected that the remaining hydrogen atom is expected to form the 2e3c Si-H-Si bond for stabilisation reasons, to give the hydrogen-bridged bissilyl cation **110b** (Scheme 83).



Scheme 83. Specific hydride abstraction reaction of hydrogen-substituted tetrasilane **109** and stabilisation of the silylium ion **110a** by Si-H-Si 2e3c bond gives bissilyl cation **110b**.

The hydride abstraction reaction was conducted in chlorobenzene at  $T = -30\text{ }^{\circ}\text{C}$ . The obtained  $^{29}\text{Si}\{^1\text{H}\}$  NMR spectrum shown in Figure 52 does not accord with the hydrogen-bridged silyl cation **110b**. Three main signals appear at  $\delta^{29}\text{Si} = -120.9$ ,  $-6.4$  and  $108.9$ , which are characteristic chemical shifts for tetrasilyl-substituted silicon atoms ( $\delta^{29}\text{Si} = -120.9$ ), trimethylsilyl groups ( $\delta^{29}\text{Si} = -6.4$ ) and cationic silicon atoms ( $\delta^{29}\text{Si}\{^1\text{H}\} = -108.9$ ). The presence of only three signals indicate the formation of a highly symmetric structure. In the hydrogen-coupled  $^{29}\text{Si}$  INEPT NMR spectrum, the low field signal is a doublet of multiplets with a coupling constant of  $^1J_{\text{Si,H}} = 43\text{ Hz}$ , the signal at  $\delta^{29}\text{Si} = -6.4$  is a decet and the high field signal is only a broad singlet. These multiplicities are in accordance with the assignment of the different structural motifs mentioned above and displayed in the  $^{29}\text{Si}\{^1\text{H}\}$  NMR spectrum (Figure 52).

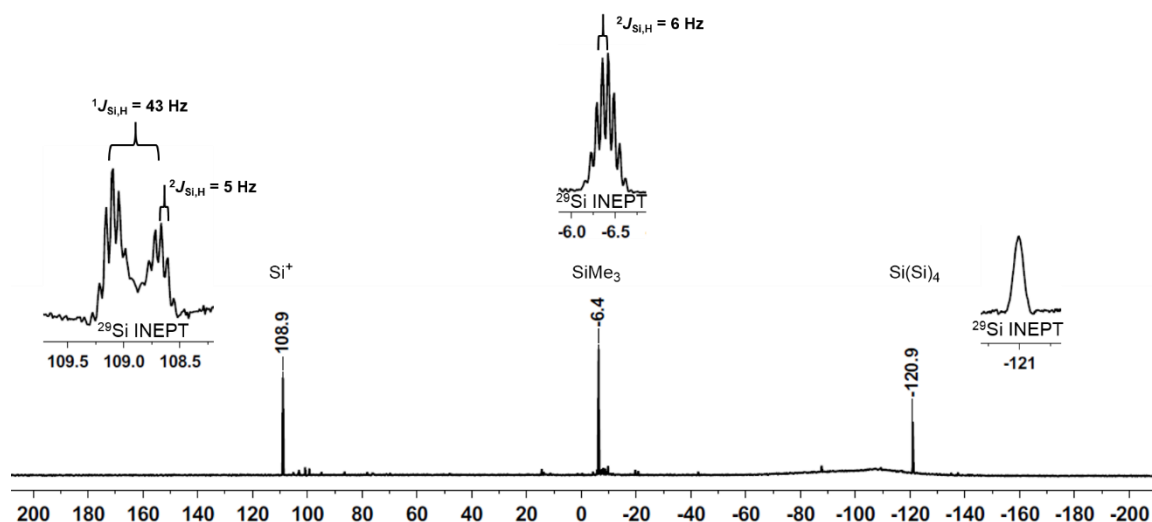
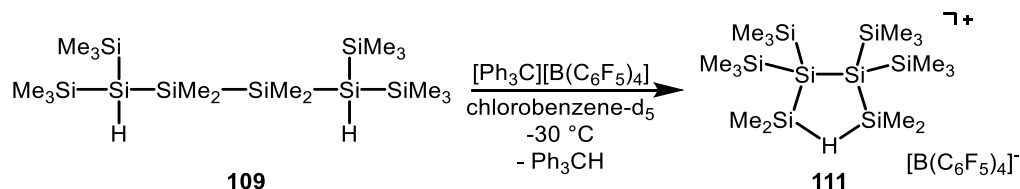


Figure 52. 99 MHz  $^{29}\text{Si}\{^1\text{H}\}$  NMR spectrum ( $\text{C}_6\text{D}_5\text{Cl}$ ,  $T = -30^\circ\text{C}$ ) and excerpts of the  $^{29}\text{Si}$  INEPT NMR spectrum obtained after hydride abstraction reaction from tetrasilane **109**.

As observed in the  $^1\text{H}^{29}\text{Si}$  HMBC NMR spectrum, the tetrasilyl-substituted silicon atom correlates to a singlet in the  $^1\text{H}$  NMR spectrum at  $\delta^1\text{H} = 0.21$  with an integral of 36 and another singlet at  $\delta^1\text{H} = 0.67$  with an integral of 12. As expected, the silicon signal at  $\delta^{29}\text{Si} = -6.4$  exhibits a cross peak with the singlet at  $\delta^1\text{H} = 0.21$  which confirms the assignment to four trimethylsilyl groups. Moreover, the low field signal at  $\delta^{29}\text{Si} = 108.9$  correlates to the singlet at  $\delta^1\text{H} = 0.67$  and in the  $^1\text{H}^{29}\text{Si}$  HMQC NMR spectrum with a broad singlet at  $\delta^1\text{H} = 2.15$ . Together, with the coupling pattern seen in the hydrogen coupled  $^{29}\text{Si}$  INEPT NMR spectrum, these resonances can be assigned to a  $\text{Me}_2\text{Si-H-SiMe}_2$  structural motif. Additionally, this is supported by the  $^1J_{\text{Si,H}} = 43$  Hz which is a typical size of the coupling between silicon and hydrogen in a 2e3c bond.<sup>[106-107]</sup>

These facts clearly indicate not the formation of the assumed hydrogen-bridged bissilyl cation **110b** (Scheme 83) but the formation of hydrogen-bridged bissilyl cation **111** as the reaction product after hydride abstraction from tetrasilane **109** (Scheme 84).



Scheme 84. Formation of 2e3c hydrogen-bridged bissilyl cation **111** after hydride abstraction from tetrasilane **109**.

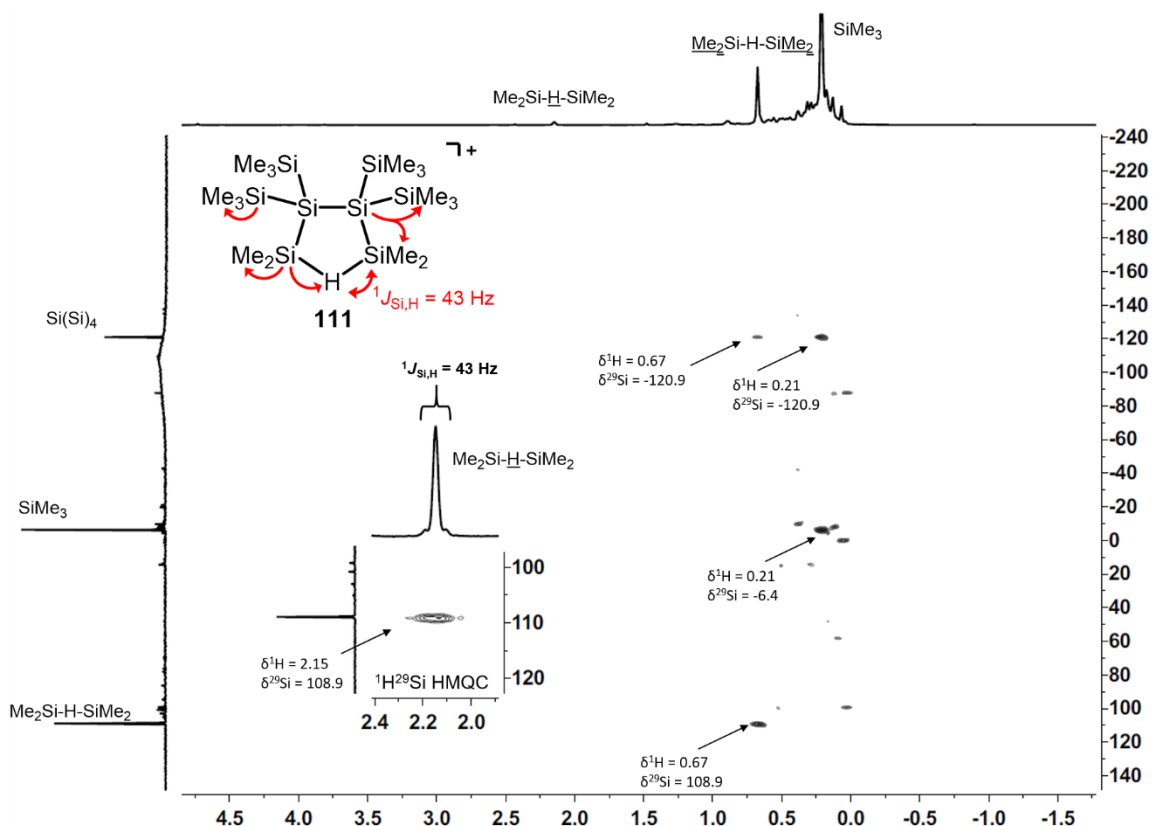


Figure 53. 500 MHz/99 MHz  $^1\text{H}/^{29}\text{Si}$  HMBC NMR spectrum ( $\text{C}_6\text{D}_5\text{Cl}$ ,  $T = -30^\circ\text{C}$ ) and an excerpt of the  $^1\text{H}/^{29}\text{Si}$  HMQC NMR spectrum obtained after hydride abstraction reaction from tetrasilane **109**.

The  $^{29}\text{Si}\{^1\text{H}\}$  INEPT NMR spectrum also verifies the composition of the silyl cation **111** (Figure 54). Surprisingly, it reveals the  $J_{\text{Si,Si}}$  coupling constants which are rarely visible in  $^{29}\text{Si}$  NMR spectra due to the low abundance of  $^{29}\text{Si}$  nuclei. The silicon-silicon coupling provides information about the connection between the silicon atoms. The signal at  $\delta^{29}\text{Si} = 108.9$  reveals satellites with  $J_{\text{Si,Si}} = 36\text{ Hz}$  and the signal at  $\delta^{29}\text{Si} = -6.4$  with  $J_{\text{Si,Si}} = 48\text{ Hz}$ . The signal of the tetrasilyl-substituted silicon atom at  $\delta^{29}\text{Si} = -120.9$  features two pairs of satellites, with the same magnitudes of  $J_{\text{Si,Si}} = 36\text{ Hz}$  and  $48\text{ Hz}$ . This means unambiguously that the high field signal is bound to both flanking silyl groups but the dimethylsilyl and trimethylsilyl groups are not linked to each other.

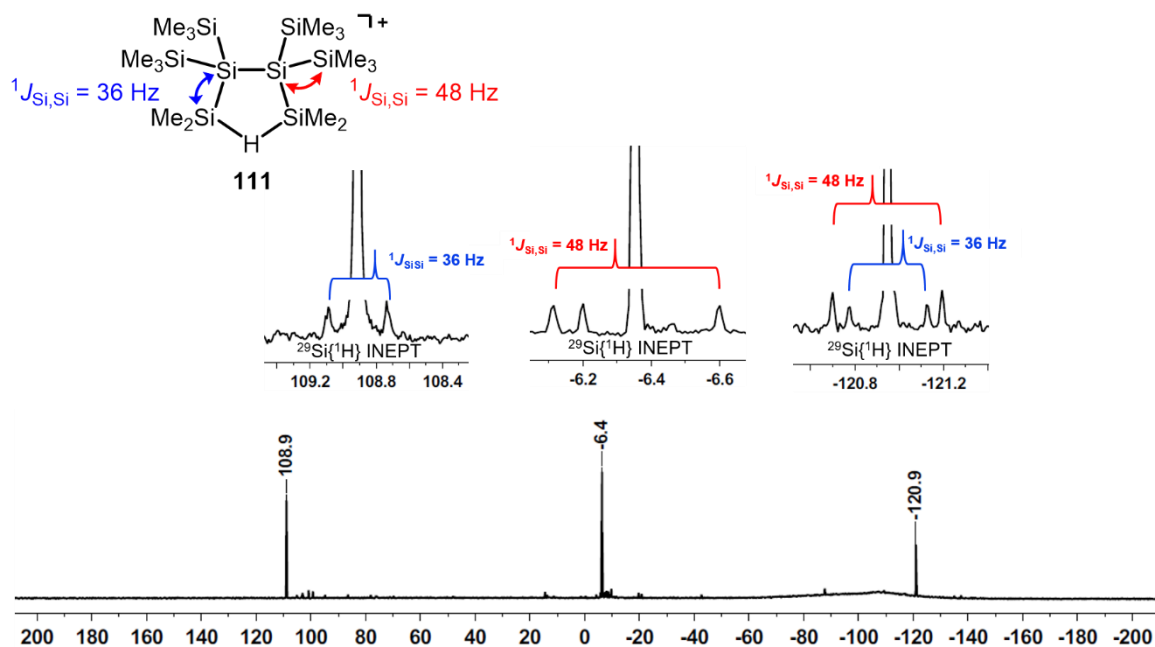
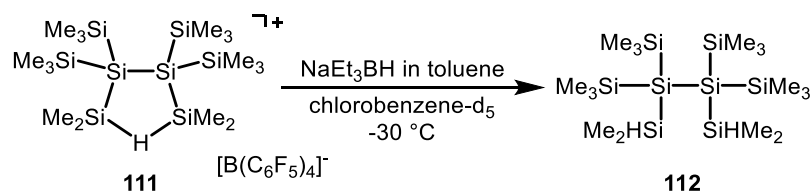


Figure 54. 99 MHz  $^{29}\text{Si}\{^1\text{H}\}$  NMR spectrum ( $\text{C}_6\text{D}_5\text{Cl}$ ,  $T = -30^\circ\text{C}$ ) and excerpts of the  $^{29}\text{Si}\{^1\text{H}\}$  INEPT NMR spectrum of 2e3c hydrogen-bridged bissilyl cation **111**.

Further support for this rearrangement came from a trapping reaction. A solution of sodium triethylborohydride was added to the NMR sample of this reaction at  $T = -30^\circ\text{C}$ . This reagent is a good hydride donor and allows quenching of the bissilyl cation **111**, which results in the formation of neutral silane **112** (Scheme 85). The group of Marschner synthesised the silane **112** according to a different synthetic protocol and comparison of the  $^{29}\text{Si}$  chemical shifts allows the unambiguous identification of the reaction product as silane **112**.



Scheme 85. Quenching of the bissilyl cation **111** with sodium triethylborohydride.

Moreover, quantum mechanical calculation of the  $^{29}\text{Si}$  NMR chemical shifts of the optimised structure of the 2e3c hydrogen-bridged bissilyl cation **111** at the M06-L/6-311G(2d,p)//M06-2X/6-311+G(d,p) level of theory provide satisfactory results compared to the experimental  $^{29}\text{Si}$  shifts (Figure 55). In addition, the calculated coupling constant for the Si-H-Si bond of  $^1J_{\text{Si,H}} = 40\text{ Hz}$  at the

B3LYP/IGLOIII//M06-2X/6-311+G(d,p) level of theory agrees well with the experimental value of  $^1J_{\text{Si,H}} = 43$  Hz which is typical in magnitude for coupling constants of 2e3c Si-H-Si bonds.

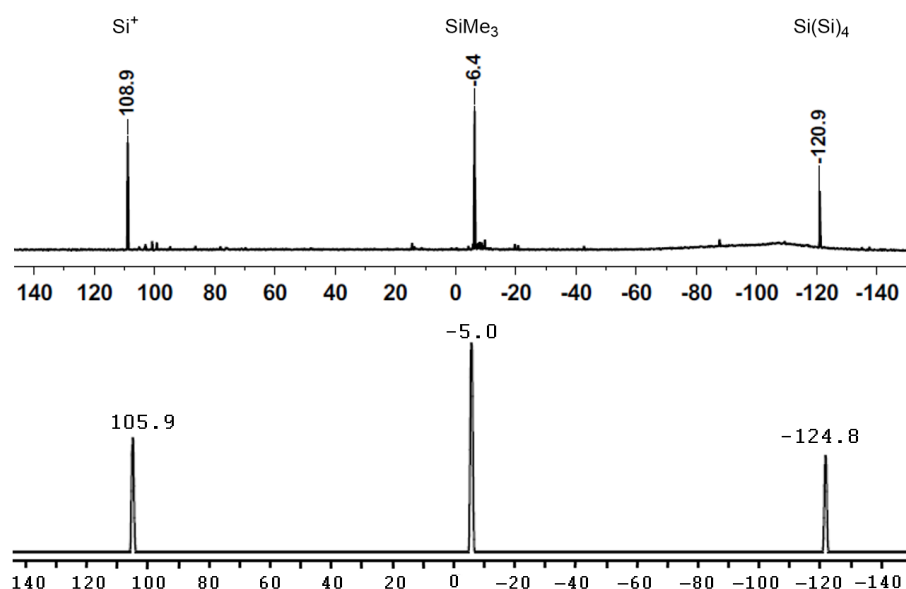
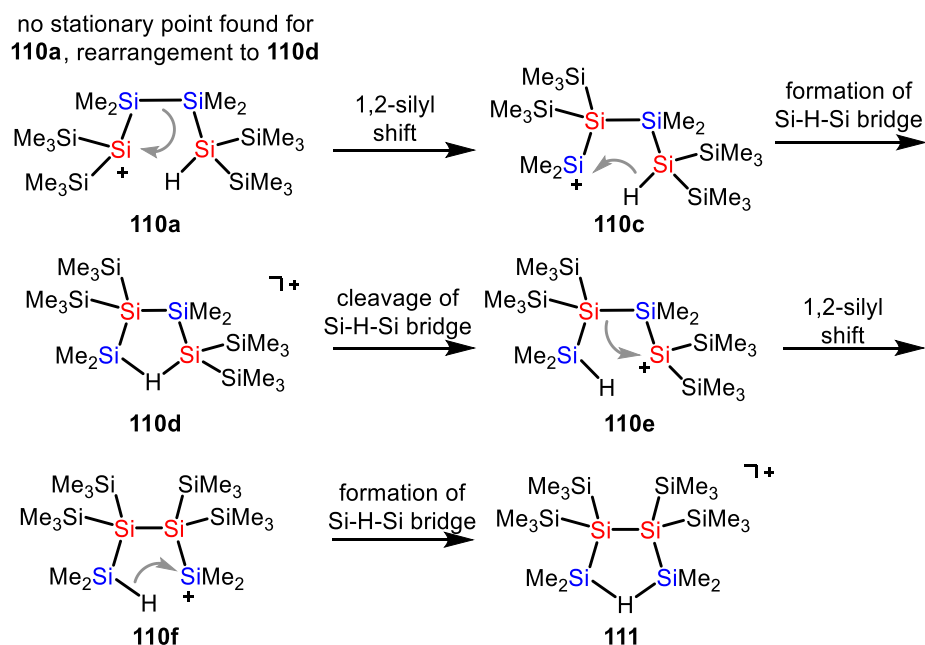


Figure 55. **top**: measured 99 MHz  $^{29}\text{Si}\{^1\text{H}\}$  NMR spectrum ( $\text{C}_6\text{D}_5\text{Cl}$ ,  $T = -30$  °C). **bottom**: calculated  $^{29}\text{Si}\{^1\text{H}\}$  NMR spectrum of 2e3c Si-H-Si bridge-stabilised bissilyl cation **111** at M06-L/6-311G(2d,p)//M06-2X/6-311+G(d,p) level of theory.

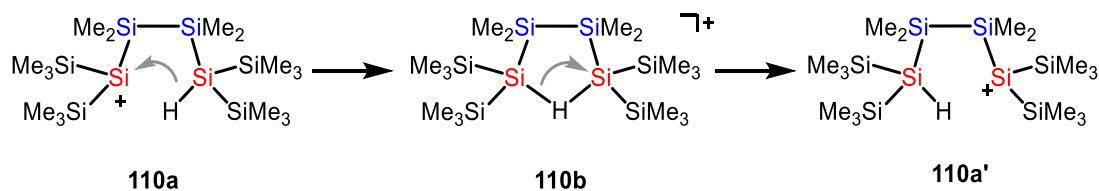
Several rearrangement steps must have taken place to obtain the rearranged bissilyl cation **111**, which are presumed to involve 1,2-methyl or -silyl shifts. Based on quantum mechanical optimisations for the cations **110a** and **111** and several isomers **110c-f**, a rearrangement mechanism can be postulated (Scheme 86). The initial step is a hydride abstraction reaction from the starting material **109** to give trisilyl-substituted silylium ion **110a**. Surprisingly, this structure **110a** is not a stationary point since during the optimisation procedure it rearranges to the 2e3c Si-H-Si bridged isomer **110d**. This indicates the high tendency of polysilanyl silyl cation to undergo a rearrangement reaction. Starting from structure **110a**, a 1,2-silyl shift takes place and a new bond between two silicon atoms is formed. A dimethylsilyl group moves out of the Si-Si chain and forms a new flanking dimethylsilyl group bearing the cationic charge, see **110c**. This monosilyl-substituted silylium ion can be stabilised by the formation of a 2e3c Si-H-Si bridge to give **110d**. This hydrogen bridge can reopen again, this time giving, compared to **110c**, the more stable trisilyl-substituted silylium ion **110e** (see chapter 3.1 for the stability of monosilyl-, disilyl- and trisilyl-substituted silylium ions). A second 1,2-silyl shift gives isomer **110f**, which contains a monosilyl-substituted silylium ion. The generation of a 2e3c Si-H-Si bridge leads to the reaction product **111**.



Scheme 86. Proposed mechanism for the rearrangement after hydride abstraction from tetrasilane **109** to give 2e3c Si-H-Si bridged bisilyl cation **111**.

It is noteworthy that intermediate **110e** is the initial silylium ion in the mechanistic proposal shown in Scheme 80, in which silane **108** is considered to be an even better starting material for the mechanistic investigations on the rearrangement of **95** to give **1**. This means, the proposed mechanism in Scheme 86 is an extended version of the previous one (Scheme 73), and provides solid evidence for the proposed mechanism for the aluminium trichloride-catalysed transformation of linear tetrasilane **94** into the branched disilane **1** via trisilane **95** (Scheme 65 and Scheme 66).

The initial silylium ion **110a** may also form a 2e3c Si-H-Si bond to give the hydrogen-bridged bisilyl cation **110b** (Scheme 87). To continue along the reaction path, the Si-H-Si bond must reopen again. It is irrelevant which Si-H bond is broken because both resulting silylium ions **110a** and **110a'** are identical and can continue in the rearrangement reaction.



Scheme 87. Feasible formation of a 2e3c Si-H-Si bridge starting from initial trisilyl-substituted silylium ion **110a**.

A diagram of relative ground state energies  $E$  and Gibbs free energies  $G^{298}$  of cation **110b-f** and **111** relative to cation **110c** (Figure 56) shows that the overall postulated rearrangement is exothermic by  $82.4 \text{ kJ mol}^{-1}$ . Moreover, all hydrogen-bridged structures are very low in energy compared to the open-chain cations. Cation **111** is the thermodynamic minimum. Unfortunately, it was not possible to optimise the structures of the transition states, and hence, no statement concerning the activation barriers can be made.

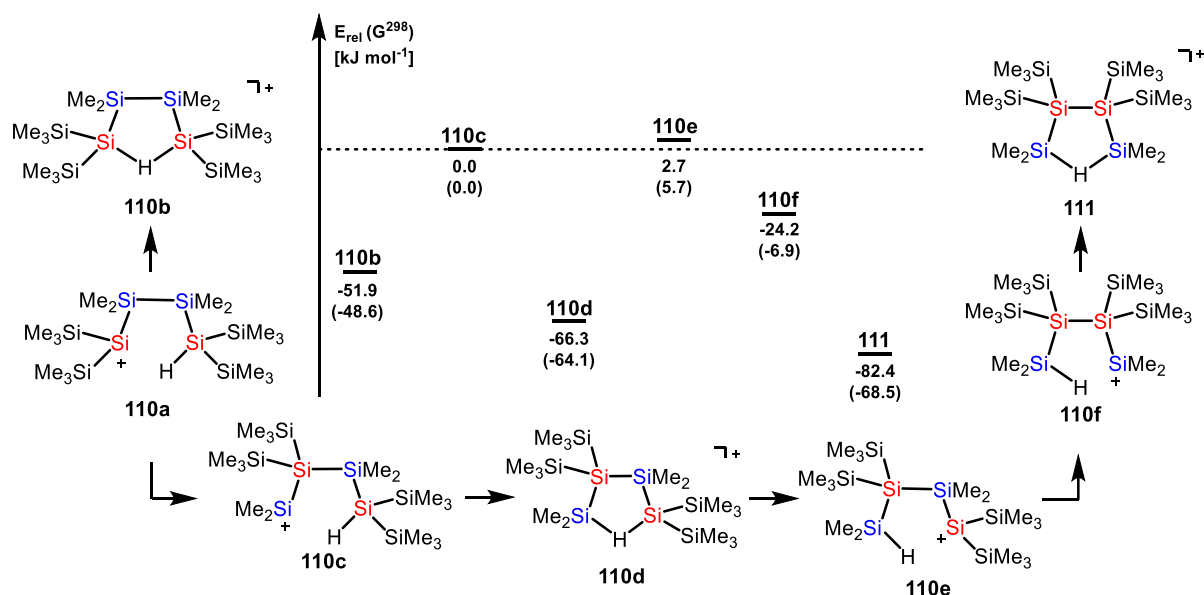


Figure 56. Diagram of relative ground state energies  $E$  and Gibbs free energies at 298.15 K,  $G^{298}$  (in parentheses) of isomeric cations **110b** – **111**, relative to cation **110c**, calculated at M06-2X/6-311+G(d,p), **110a** is no stationary point.

The question arises, why does isomer **110a** not form the hydrogen-bridged bisilyl cation **110b** and why does the reaction not stop in this local minimum. Furthermore, why is the obviously sterically more congested isomer **111** stabilised by  $82.4 \text{ kJ mol}^{-1}$ ? To investigate the hydrogen-bridged structures in more detail, the B3LYP functional extended by the D3 version of Grimme's dispersion with the original D3 damping function<sup>[139]</sup> was used for the structure optimisations, which adds a dispersion correction to the density functional. Plotting the relative energies calculated at the B3LYP level shows a higher stability of isomer **110d** compared to **110b** and **111** (Figure 57). This is expected since in isomer **110d**, the bulky trimethylsilyl groups are separated from each other and in structure **110b** and **111** there are relatively close. These neighbouring trimethylsilyl groups might destabilise the molecule due to steric hindrance on the B3LYP level. In contrast, at the B3LYP-D3 level, isomer **111** is calculated to be the most stable one. This is explained by attractive dispersion interactions, which are expected to stabilise the molecule.<sup>[140, 144]</sup>

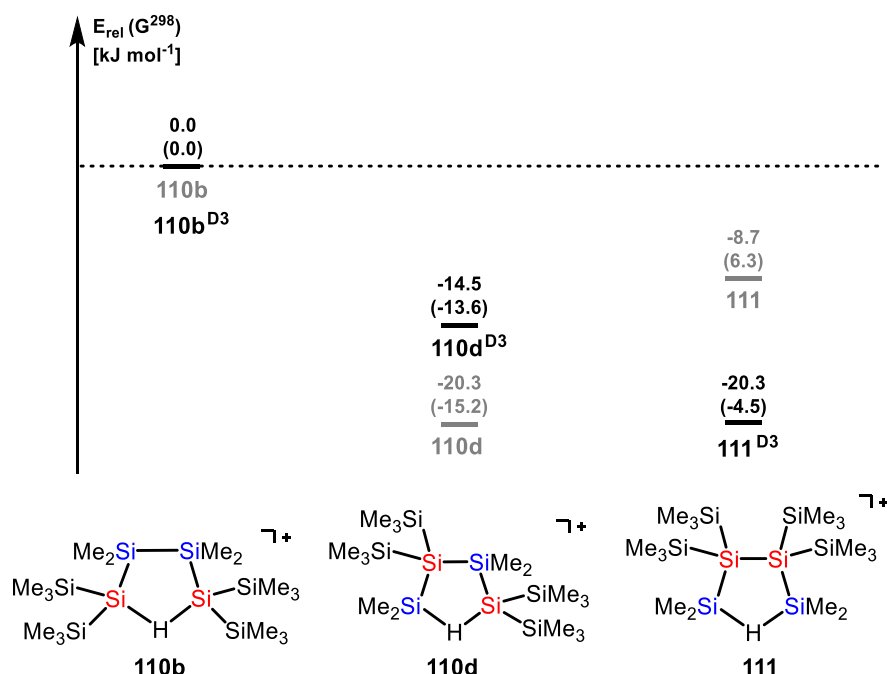


Figure 57. Diagram of relative ground state energies  $E$  and Gibbs free energies at 298.15 K,  $G^{298}$  (in parentheses) of isomeric cations **110b**, **110d** and **111**, relative to cation **110b**, calculated at the B3LYP/6-311+G(d,p) (grey) and B3LYP-D3/6-311+G(d,p) levels (black).

Figure 58 shows the differences in energy calculated with the B3LYP functional and with the B3LYP functional extended by the D3 version of Grimme's dispersion with the original D3 damping function<sup>[139]</sup>. The difference is relatively high for all isomeric cations **110b** ( $\Delta E = -226.2 \text{ kJ mol}^{-1}$ ), **110d** ( $\Delta E = -188.9 \text{ kJ mol}^{-1}$ ) and **111** ( $\Delta E = -237.9 \text{ kJ mol}^{-1}$ ) and represents the absolute contribution of the dispersion interactions. More interestingly are the differences between these values, which reflect the relative amount of dispersion in these isomers. As mentioned before, in contrast to isomer **110d** the trimethylsilyl groups in **110b** and **111** are close together and stabilise the cation by attractive dispersion interactions. Compared to the intermediate structure **110d**, the stabilisation energy for the actual reaction product **111** was determined to be  $49.0 \text{ kJ mol}^{-1}$  and for the initial structure **110b**, only  $37.4 \text{ kJ mol}^{-1}$ . These numbers justify the formation of the rearrangement product **111** instead of the initial hydrogen bridged structure **110b** or the intermediate isomer **110d**.

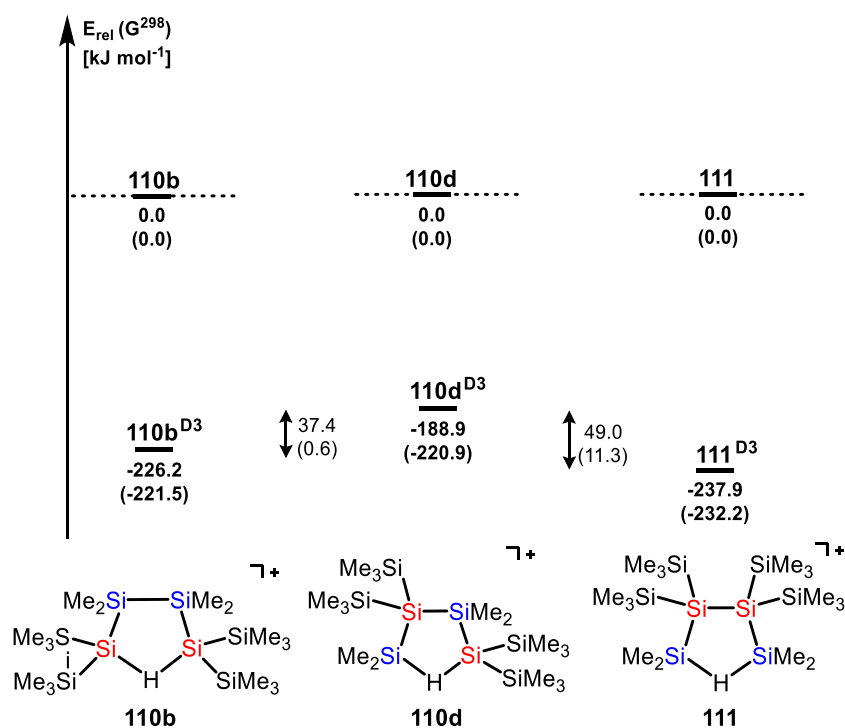
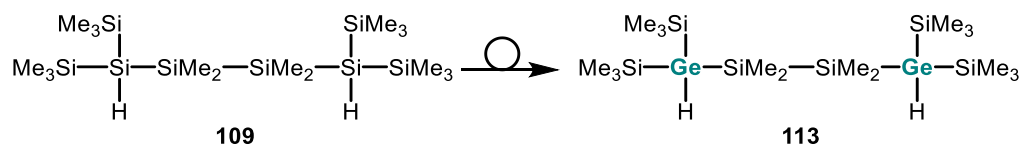


Figure 58. Diagram of relative ground state energies  $E$  and Gibbs free energies at 298.15 K,  $G^{298}$  (in parentheses) of isomeric cations **110b**, **110d** and **111**. Comparison of the energies at the B3LYP/6-311+G(d,p) and B3LYP-D3/6-311+G(d,p) levels.

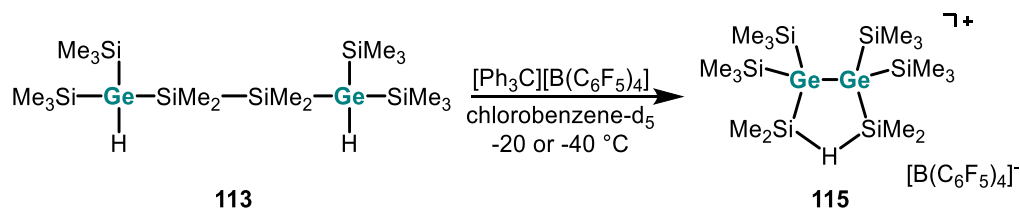
### 3.4.3.3 Mechanistic Development – Part III

The actual fate of the silicon atoms in the pure polysilanes was not yet illuminated experimentally because labelling of each silicon atom was not possible. Hence, to study this reaction in more detail, two germanium atoms were introduced into the starting molecule (Scheme 88). These germanium atoms can act as a label to enable the monitoring of the movement of the atoms. In analogy to tetrasilane **109**, the same mechanistic pathway via 1,2-silyl shifts was expected for the rearrangement of 1,4-digermatetrasilane **113** to give the 2e3c Si-H-Si bridged compound **115** (Scheme 89).



Scheme 88. Hydrogen-substituted tetrasilane **109** and 1,4-digermatetrasilane **113**.

The hydride abstraction was performed similarly to the reaction of silane **109**: in chlorobenzene- $d_5$  at  $T = -20\text{ }^{\circ}\text{C}$  (Scheme 89). The  $^{29}\text{Si}\{^1\text{H}\}$  NMR spectra reveal many signals in the chemical shift range for trimethylsilyl groups and several signals in the area where typical decomposition products of silyl cations appear ( $\delta^{29}\text{Si} = 40$  to  $80$ ). Interestingly, a low field signal is detected at  $\delta^{29}\text{Si} = 117.5$ , which is a doublet of multiplets with a coupling constant of  $^1J_{\text{Si,H}} = 45\text{ Hz}$  in the hydrogen-coupled  $^{29}\text{Si}$  INEPT NMR spectrum (Figure 59 top).



Scheme 89. Proposed formation of 2e3c hydrogen-bridged bissilyl cation **115** after hydride abstraction from 1,4-digermatetrasilane **113**.

This experiment indicated the possibility that bissilyl cation **115**, analogous to the all-sila bissilyl cation **111**, was formed. The reaction was reacted at  $T = -40\text{ }^{\circ}\text{C}$  to minimise side reactions and decomposition. The resulting  $^{29}\text{Si}\{^1\text{H}\}$  NMR spectrum is shown in Figure 59, bottom.

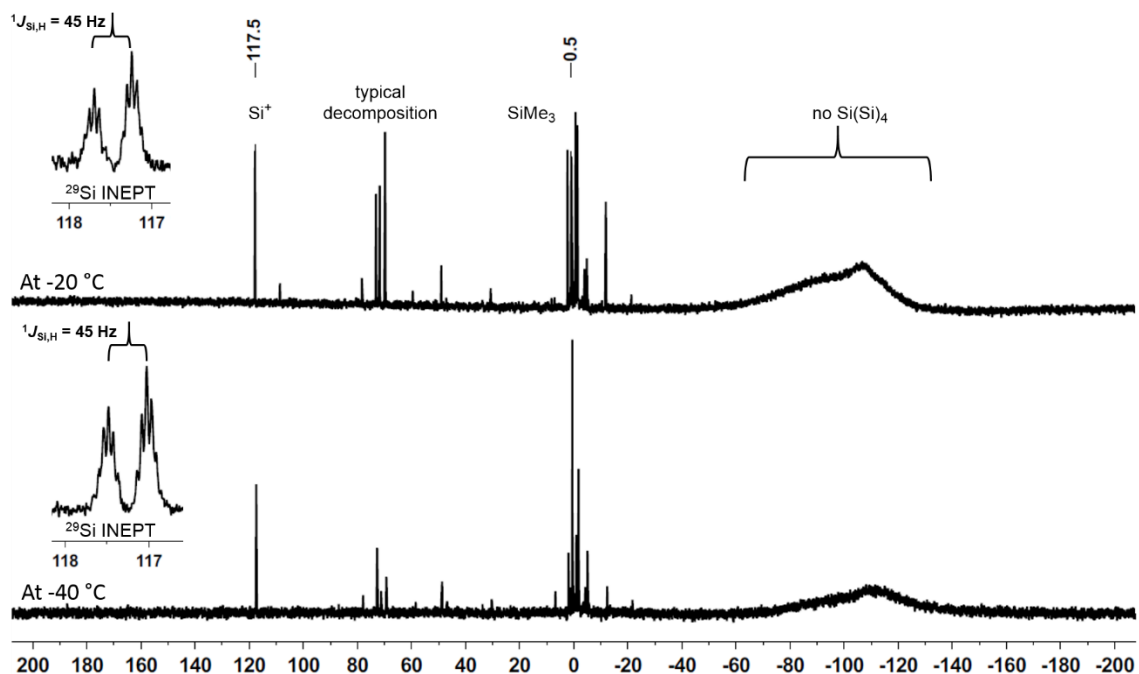


Figure 59. 99 MHz  $^{29}\text{Si}\{^1\text{H}\}$  NMR spectra ( $\text{C}_6\text{D}_5\text{Cl}$ , **top**:  $T = -20\text{ }^{\circ}\text{C}$ , **bottom**:  $T = -40\text{ }^{\circ}\text{C}$ ) and excerpts of the  $^{29}\text{Si}$  INEPT NMR spectra obtained after hydride abstraction reaction from 1,4-digermatetrasilane **113**.

Similar to the all-sila version of this reaction, the characteristic low field signal at  $\delta^{29}\text{Si} = 117.5$  correlates in the  $^1\text{H}^{29}\text{Si}$  HMBC NMR spectrum to the singlet at  $\delta^1\text{H} = 0.71$  with an integral of 12 and in the  $^1\text{H}^{29}\text{Si}$  HMQC NMR spectrum with a broad singlet at  $\delta^1\text{H} = 2.47$ . Together with its coupling pattern in the hydrogen- coupled  $^{29}\text{Si}$  INEPT NMR spectrum, these resonances can again be assigned to a  $\text{Me}_2\text{Si-H-SiMe}_2$  structural motif, supported by the  $^1J_{\text{H,Si}} = 43 \text{ Hz}$  which is typical for the coupling constant between silicon and hydrogen in a 2e3c bond.<sup>[106-107]</sup> The silicon signal at  $\delta^{29}\text{Si} = 0.5$  features a cross peak with the singlet at  $\delta^1\text{H} = 0.25$  with an integral of 36, which confirms the presence of four trimethylsilyl groups. In contrast to the bissilyl cation **111**, no signal in the chemical shift range of tetrasilyl-substituted silicon atom ( $\Delta^{29}\text{Si} = -140 - -120$ ) is present. This can be understood if the germanium atoms have migrated to a tetrasilyl-substituted position, where they are only surrounded by silicon atoms. In general, trimethylsilyl groups connected to tetrasilyl-substituted germanium atoms show a low field shift compared to trimethylsilyl groups connected to tetrasilyl-substituted silicon atoms. Accordingly, the chemical shifts of the trimethylsilyl groups in cation **115** ( $\delta^{29}\text{Si} = 0.5$ ) are downfield compared to the ones in the bissilyl cation **111** ( $\delta^{29}\text{Si} = -6.4$ ).

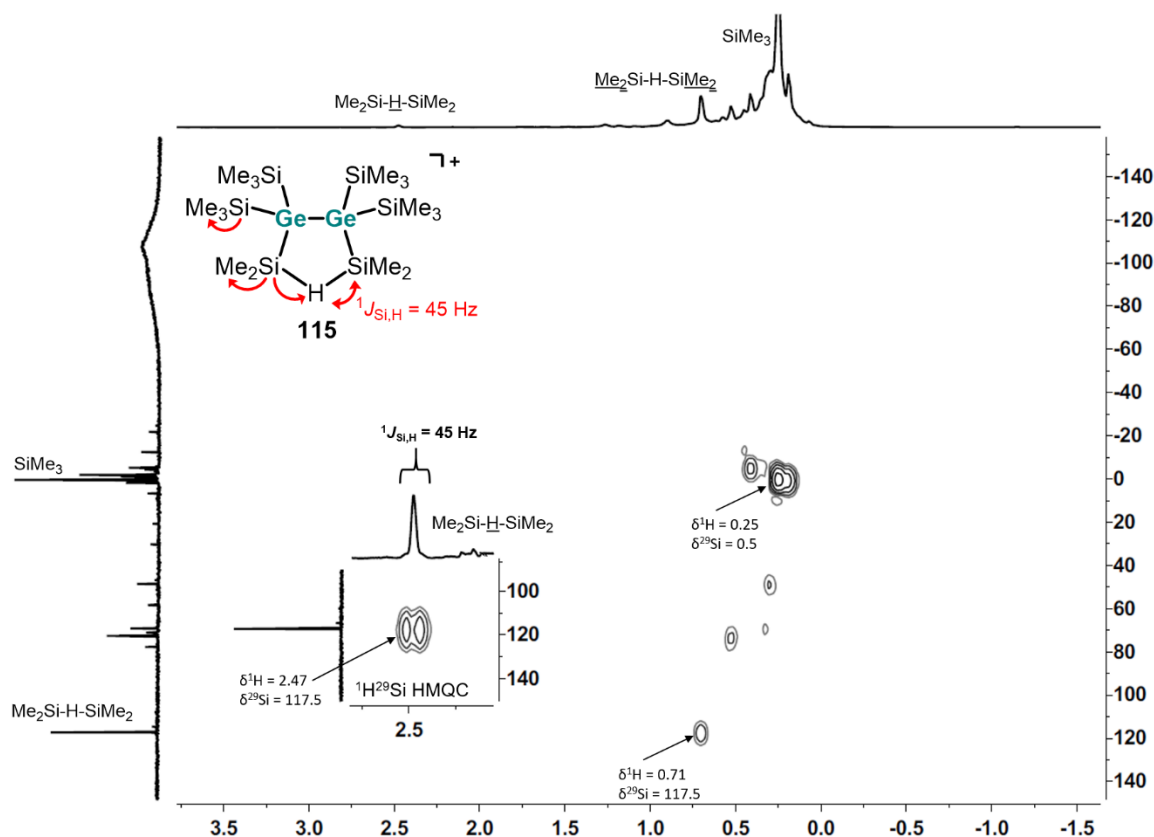


Figure 60. 500 MHz/99 MHz  $^1\text{H}^{29}\text{Si}$  HMBC NMR spectrum ( $\text{C}_6\text{D}_5\text{Cl}$ ,  $T = -40^\circ\text{C}$ ) and an excerpt of the  $^1\text{H}^{29}\text{Si}$  HMQC NMR spectrum obtained after hydride abstraction reaction from 1,4-digermatetrasilane **113**.

In this reaction, the germanium atoms have, evidently, moved to central positions, where they are surrounded by silicon atoms. This behaviour is already known for the aluminium catalysed rearrangement reaction of germasilanes<sup>[68]</sup> and was the subject in chapter 3.2 of this work.

Quantum mechanical calculations of the  $^{29}\text{Si}$  NMR chemical shifts of the optimised structure **115** at the M06-L/6-311G(2d,p)//M06-2X/6-311+G(d,p) level of theory supports the assignment of the 2e3c Si-H-Si bridged bissilyl cation. The computed  $^{29}\text{Si}$  shifts are in good agreement with the experimental data (Figure 61). The calculated coupling constant for the Si-H-Si bond of  $^1J_{\text{Si,H}} = 42$  Hz at the B3LYP/IGLOIII(Si,C,H),6-311+G(d,p)(Ge)//M06-2X/6-311+G(d,p) level of theory agrees well with the experimental value of  $^1J_{\text{Si,H}} = 45$  Hz.

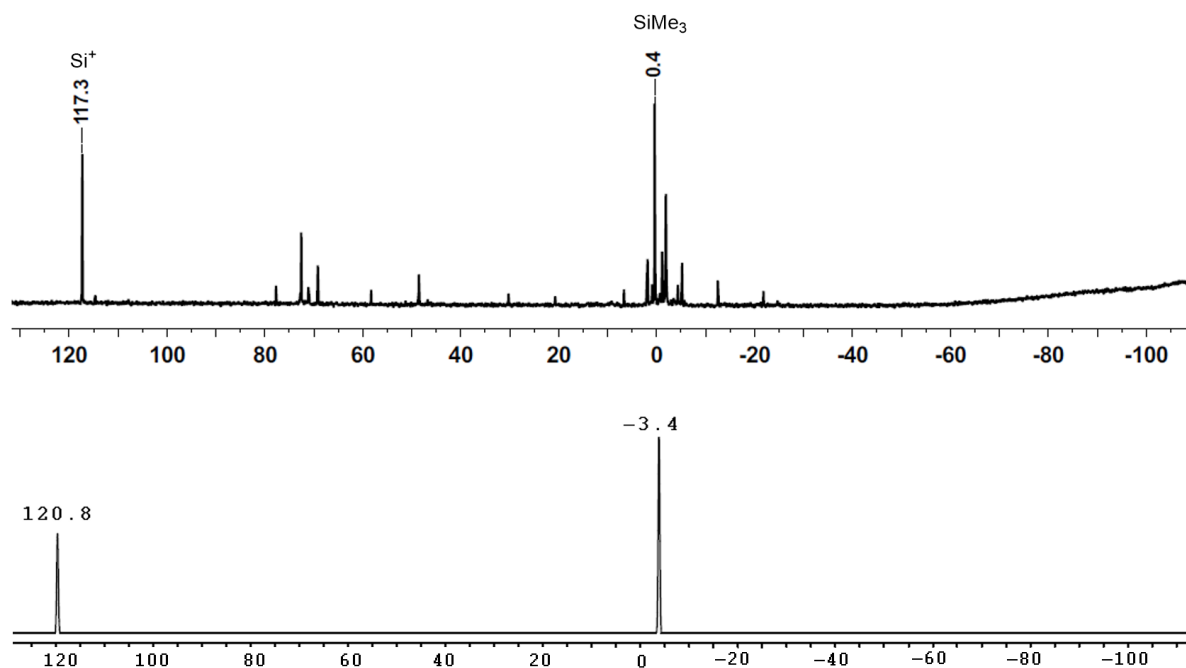
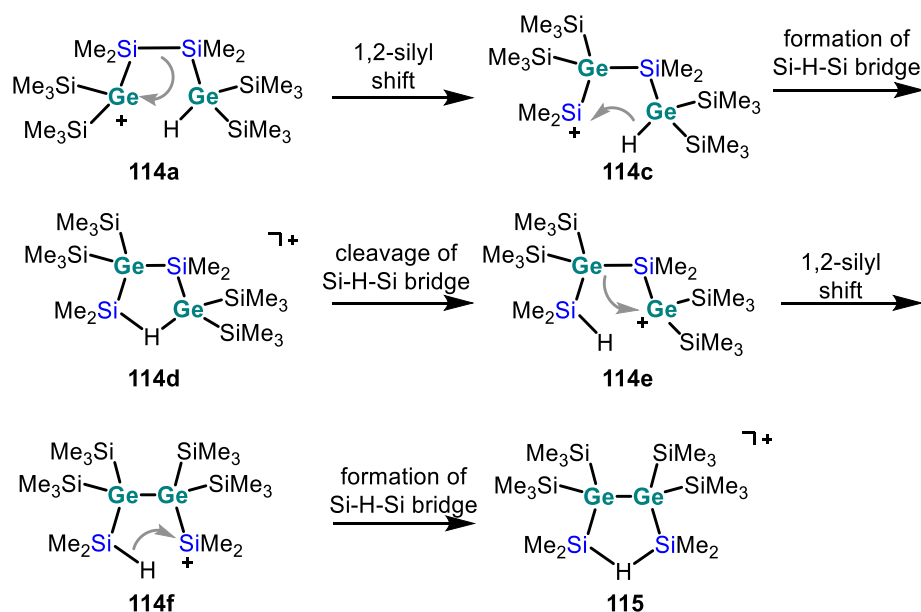


Figure 61. **top**: measured 99 MHz  $^{29}\text{Si}\{^1\text{H}\}$  NMR spectrum ( $\text{C}_6\text{D}_5\text{Cl}$ ,  $T = -40^\circ\text{C}$ ), **bottom**: calculated  $^{29}\text{Si}\{^1\text{H}\}$  NMR spectrum of 2e3c Si-H-Si bridge-stabilised bissilyl cation **115** at M06-L/6-311G(2d,p)//M06-2X/6-311+G(d,p) level of theory.

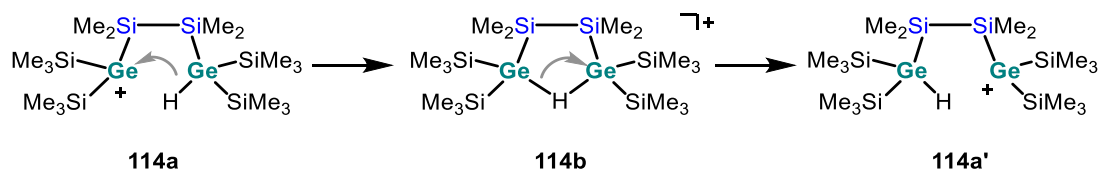
The presence of the germanium atoms in the starting material helps to support the proposed mechanism. The rearrangement starts with hydride abstraction from the 1,4-digermatetrasilane to give the initial germylium ion **114a**. A 1,2-silyl shift places a dimethylsilyl group out of the main chain into a flanking position where it bears a cationic charge (**114c**). This monosilyl-substituted silylium ion can be stabilised by the formation of a 2e3c Si-H-Si bond as shown in isomer **114d**. This bond can reopen again to give a Si-H bond and a new trisilyl-substituted germylium ion **114e**, which can then undergo another 1,2-silyl shift. This step creates a new Ge-Ge bond and the cationic charge is now

located at the new flanking dimethylsilyl group **114f**. Final formation of a 2e3c Si-H-Si bond produces the reaction product **115**.



Scheme 90. Proposed mechanism for the rearrangement after hydride abstraction from the 1,4-digermatetrasilane **113** to give the 2e3c Si-H-Si bridged bisilyl cation **115**.

Not only can the cations **114c** and **114f** be stabilised by the formation of 2e3c Ge-H-Si (**114d**) or Si-H-Si (**115**) bonds, but also the initial cation **114a** can be written as a Ge-H-Ge bridged structure **114b** (Scheme 91). When this bridge opens again, the rearrangement proceeds as shown in Scheme 90.



Scheme 91. Feasible formation of a 2e3c Si-H-Si bridge **114b** starting from initial monosilyl-substituted germylium ion **114a**.

Quantum mechanical structure optimisations of all cationic intermediates and a diagram of their relative energies (Figure 62) support the proposed mechanism. From Figure 62 it is evident that the formation of the E-H-E' bridge (**114b**: E = E' = Ge, **114d**: E = Si, E' = Ge, **115**: E = E' = Si) stabilises the cations by 70 – 97 kJ mol<sup>-1</sup> compared to initial cation **114a**. Unfortunately, the optimised structures of any transition state have not been determined and hence, no statement concerning the activation barriers can be made.

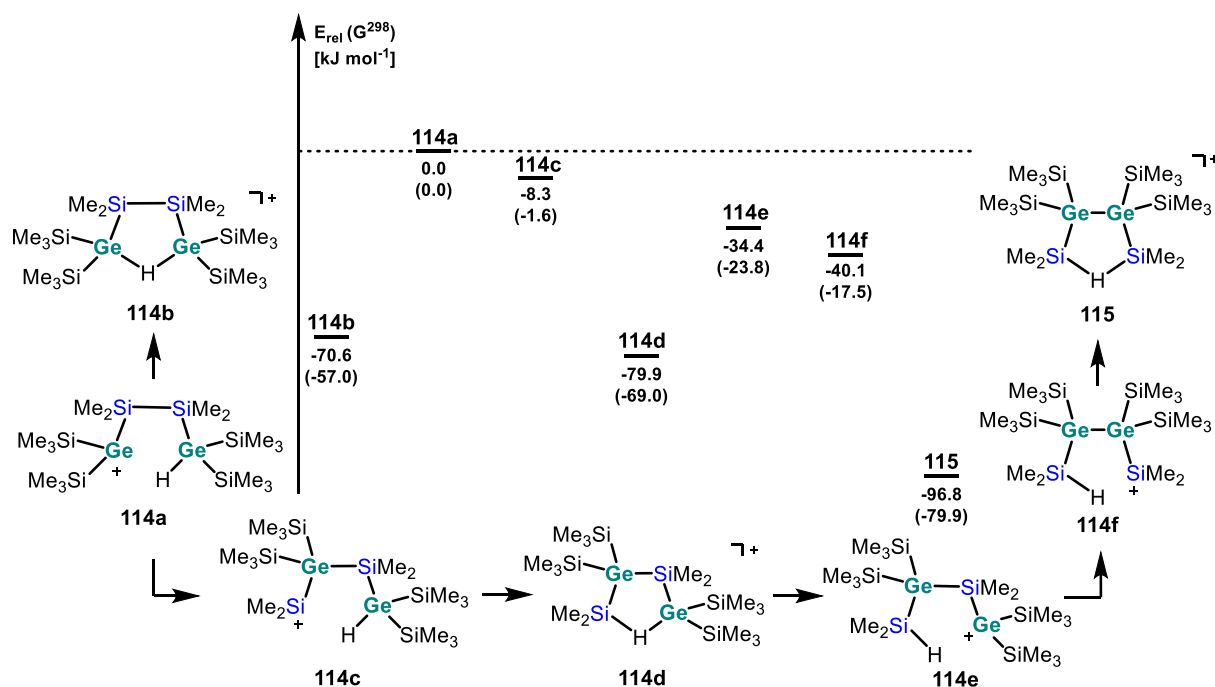
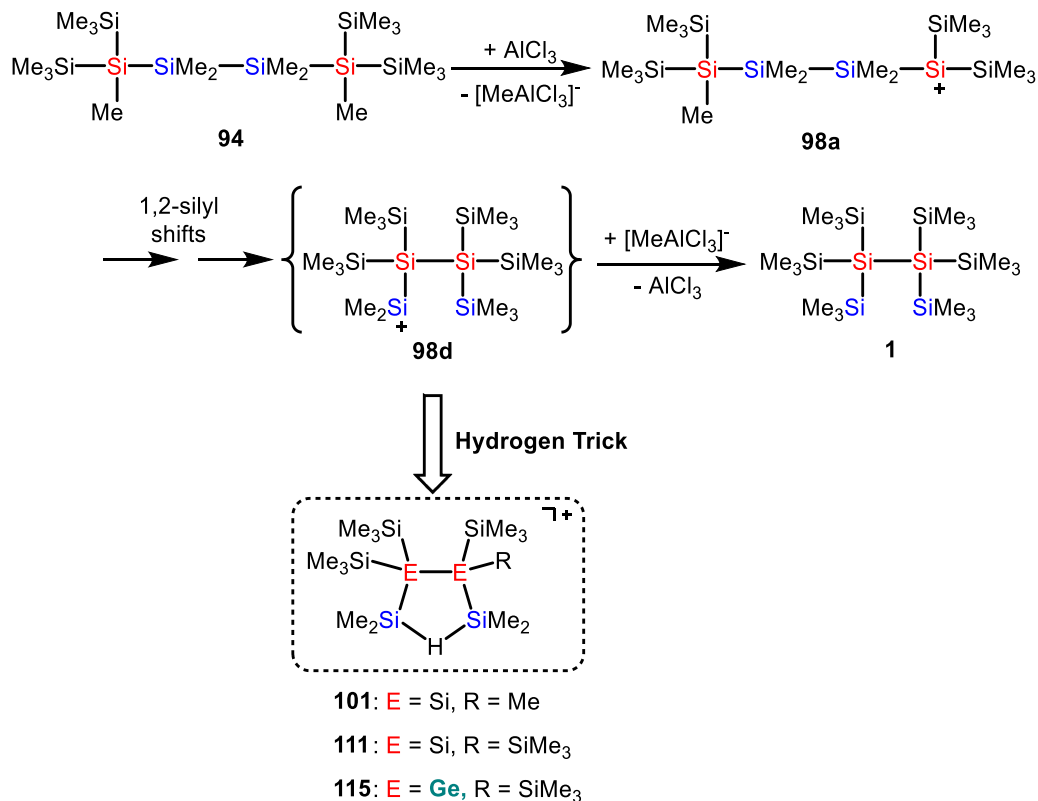


Figure 62. Diagram of relative ground state energies  $E$  and Gibbs free energies at 298.15 K,  $G^{298}$  (in parentheses) of isomeric cations **114a** – **115**, relative to cation **114a**, calculated at M06-2X/6-311+G(d,p).

These results show that it is possible to detect and trap the last cationic intermediate during the rearrangement of tetrasilane **94** to the highly branched isomer **1** (Scheme 65 and Scheme 66). By introducing an available hydrogen atom, the cationic, flanking dimethyl-substituted silicon atom is able to form a 2e3c Si-H-Si bond and, by this means, the germabissilyl cation **115** is stabilised and detectable (Scheme 92). These mechanistic investigations on the rearrangement of tetrasilane **94** to its highly branched isomer **1** support the supposed reaction channel, which proceeds via silyl cationic

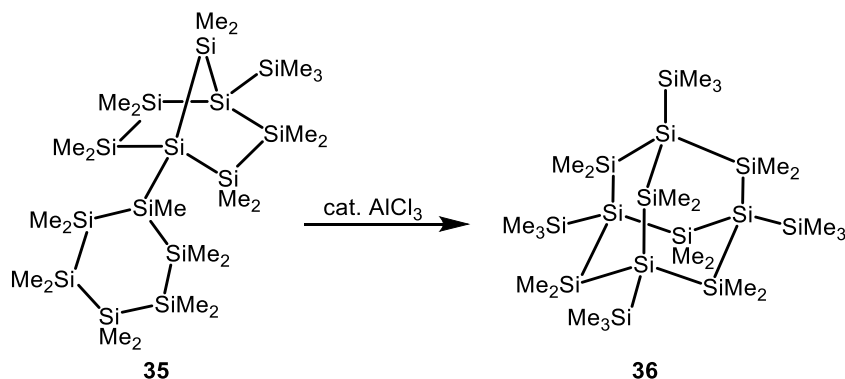
intermediates. The formation of the all-sila bissilyl cations **101** and **111** and the germabissilyl cation **115** has provided enough pieces of evidence to validate the mechanistic path of this rearrangement.



Scheme 92. Abbreviated mechanism of the rearrangement of tetrasilane **94** to give isomer **1**. Cationic intermediate **98d** was identified in the form of its Si-H-Si bridged analogues **101**, **111** and **115**.

### 3.5 Rearrangement Reactions in Cyclic Polysilanes

Not only linear, but also cyclic polysilanes rearrange when reacted with a Lewis acid such as  $\text{AlCl}_3$ . The most famous reaction of this type is the synthesis of the permethylated sila-adamantane<sup>[46]</sup>, starting from a tricyclic precursor, published by Marschner et al. (Scheme 93). This raised the question, whether the rearrangement reactions of cyclic polysilanes also proceed via cationic intermediates and whether or not they can be detected.



Scheme 93. Synthesis of sila-adamantane **36**.

As shown before, the triphenylmethyl cation is able to initiate the rearrangement reactions in polysilanes. Thus, the rearrangement of bicyclo[2.2.1]heptasilane **35** was performed in chlorobenzene using the triphenylmethyl cation as a Lewis acid along with tetrakis(pentafluorophenyl)borate as the counter anion in order to detect any cationic intermediates during the rearrangement. After 24 h at room temperature, no reaction had taken place as evidenced by the presence of the signals assigned to the starting material in the  $^{29}\text{Si}$  NMR spectrum. The mixture was stored at room temperature for an additional 35 days and the  $^{29}\text{Si}$  NMR spectrum, shown in Figure 63, was acquired.

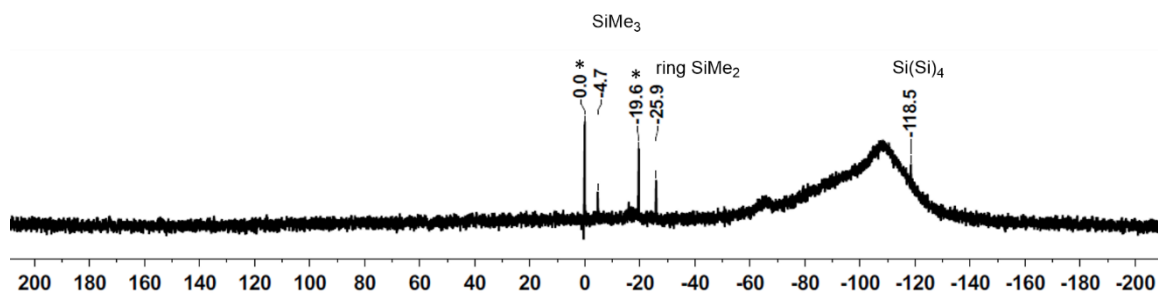
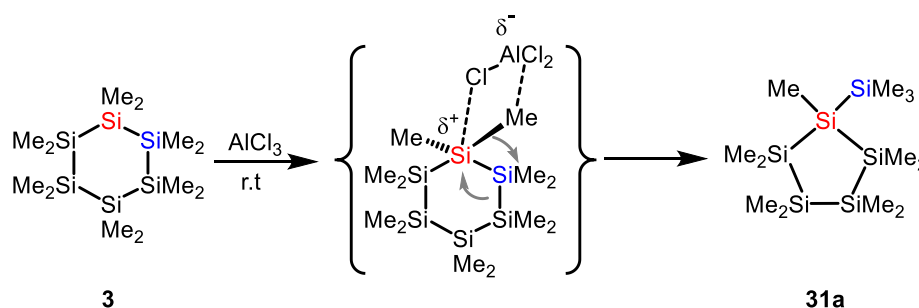


Figure 63. 99 MHz  $^{29}\text{Si}\{^1\text{H}\}$  NMR spectrum ( $\text{C}_6\text{D}_5\text{Cl}$ , r.t.) of the mixture of sila-adamantane **36** and by-products (\*).

This spectrum indicates the formation of sila-adamantane starting from tricyclic silane **35** initialised by the triphenylmethyl cation. Besides the three signals assigned to sila-adamantane at  $\delta^{29}\text{Si} = -118.5, -25.9$  and  $-4.7$ , two additional signals are visible at  $\delta^{29}\text{Si} = -19.6$  and  $0.0$ , which can be assigned to the formation of  $(\text{Me}_2\text{SiO})_3$  and tetramethylsilane. From previous work, it is known that  $(\text{Me}_2\text{SiO})_3$  forms when silyl cations or the trityl cation react with silicon grease. Tetramethylsilane appears to be a decomposition product.

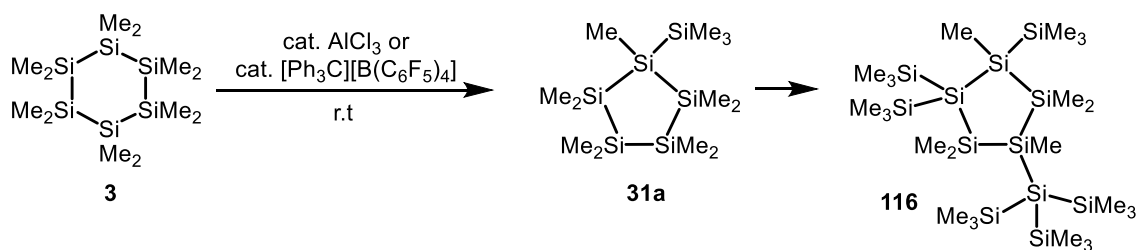
### 3.5.1 Rearrangement of Dodecamethylcyclohexasilane

The elucidation of the rearrangement pathway to sila-adamantane **36** is a challenging task. The synthesis of bicyclo[2.2.1]heptasilane is very complex and this makes it a very precious compound. Therefore, the rearrangement of cyclic compounds will firstly be elucidated using the six-membered ring **3**. Dodecamethylcyclohexasilane rearranges to give the five-membered ring **31a** when reacted with a catalytic amount of aluminium chloride. This rearrangement is proposed to proceed via cationic intermediates.<sup>[47]</sup>



Scheme 94. Proposed mechanism of the rearrangement of cyclohexasilane **3** to give cyclopentasilane **31a**.<sup>[47]</sup>

To test the Lewis acids which have bulky, weakly nucleophilic counter anions, 1 mol% of trityl tetrakis(pentafluorophenyl)borate was used at room temperature in benzene- $d_6$  and in dichloromethane- $d_2$  to initiate the rearrangement. The mixture was stirred overnight and the  $^{29}\text{Si}$  NMR spectra of the mixture reveal the signals of the known five-membered ring **31a**<sup>[44]</sup> and signals assigned to the minor amounts of the branched by-product **116**<sup>[119]</sup>.



Scheme 95. Ring contraction reaction of cyclohexasilane **3** to give cyclopentasilane **31a** and subsequent reaction gives the branched cyclopentasilane **116**.

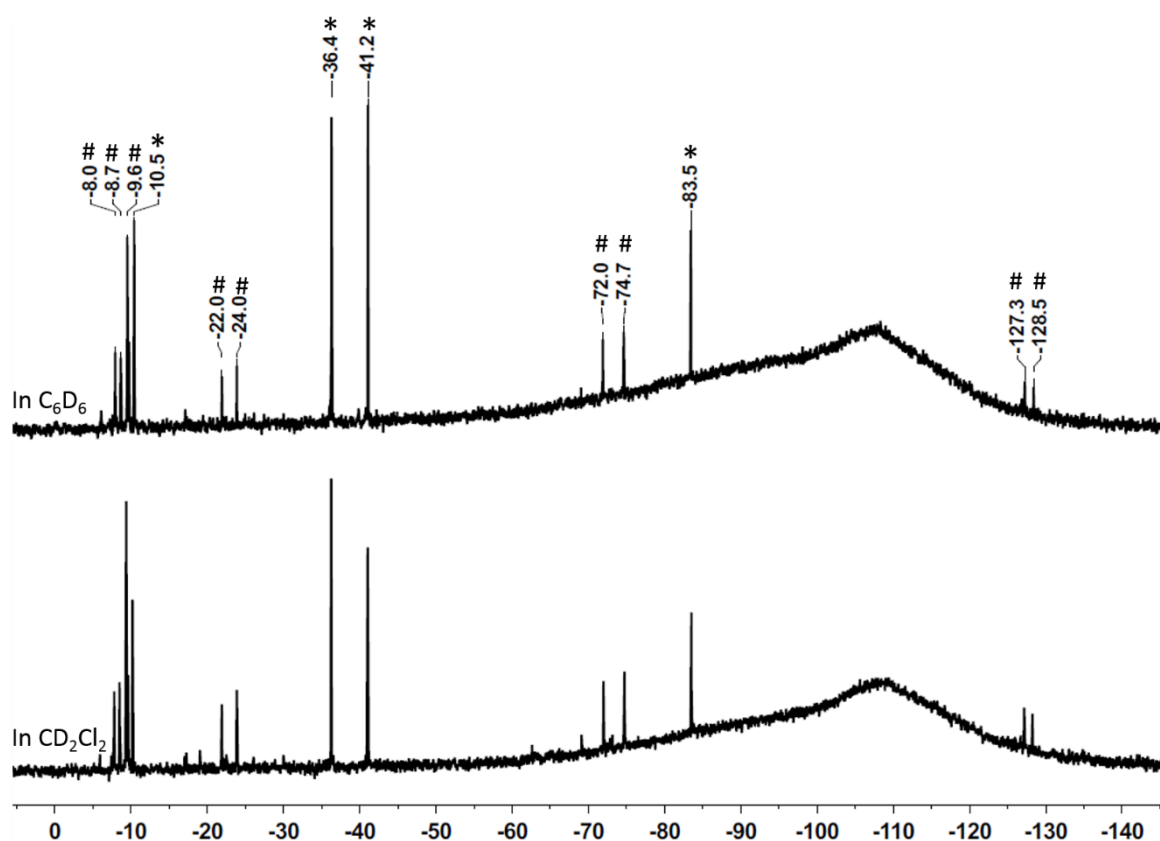


Figure 64. 99 MHz  $^{29}\text{Si}\{^1\text{H}\}$  NMR spectrum (**top**:  $\text{C}_6\text{D}_6$ , r.t., **bottom**:  $\text{CD}_2\text{Cl}_2$ , r.t.) of the mixture of cyclopentasilane **31a** (\*) and by-product **116** (#).

This experiment demonstrates that the trityl cation is able to catalyse the rearrangement. Thus, based on these findings, the stoichiometric reaction was performed at room temperature in benzene- $\text{d}_6$  and the  $^{29}\text{Si}\{^1\text{H}\}$  NMR spectrum was recorded after one hour and it shows only the presence of the starting material **3** and the rearrangement product **31a**.

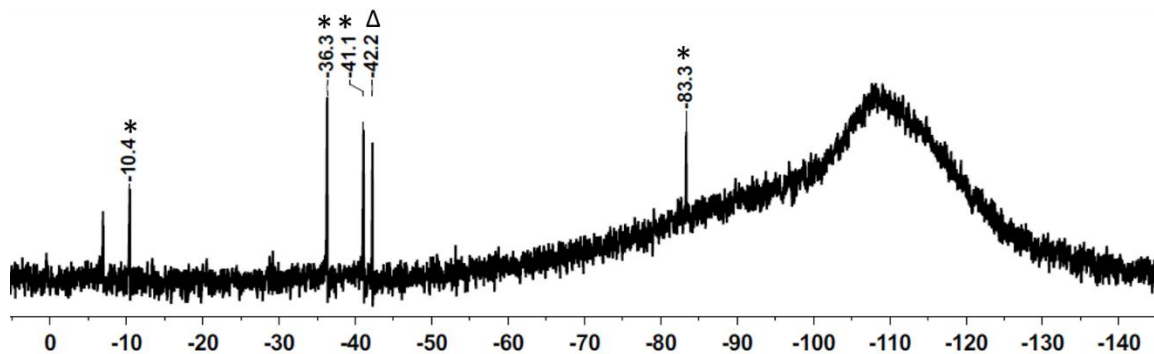
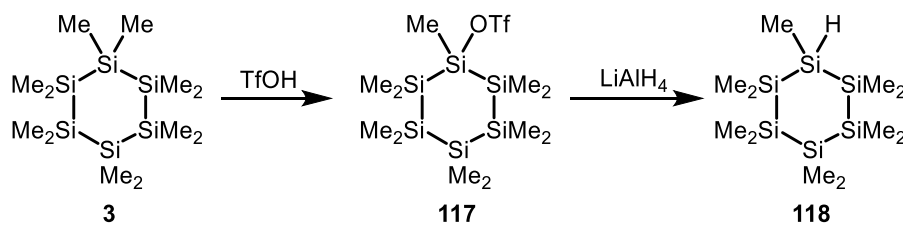


Figure 65. 99 MHz  $^{29}\text{Si}\{^1\text{H}\}$  NMR spectrum ( $\text{C}_6\text{D}_6$ , r.t.) of the mixture of cyclohexasilane **3** ( $\Delta$ ) and cyclopentasilane **31a** (\*).

Although the bulky counter anion was present in a stoichiometric amount, no cationic compound was detected at room temperature. Therefore, the reaction was repeated with a stoichiometric amount of trityl borate at  $T = -20\text{ }^\circ\text{C}$  in toluene- $\text{d}_8$ , but no reaction took place at this temperature.

A hydrogen-substituted precursor was prepared to facilitate the silyl cation formation at low temperatures by hydride abstraction instead of methyl anion abstraction from the starting material.



Scheme 96. Synthesis of undecamethylcyclohexasilane **118**.

The hydride abstraction reaction was performed with trityl tetrakis(pentafluorophenyl)borate at  $T = -20\text{ }^\circ\text{C}$  and, due to many by-products formed in this reaction, was repeated a second time at  $T = -40\text{ }^\circ\text{C}$ . In addition to several by-products, six main signals are present in both  $^{29}\text{Si}\{^1\text{H}\}$  NMR spectra (Figure 66).

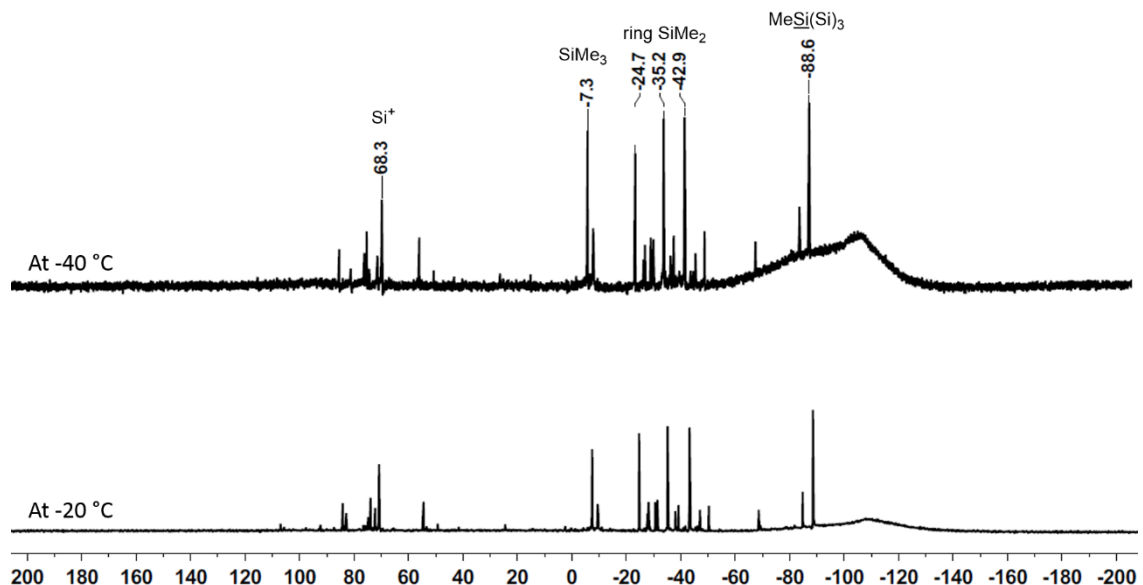
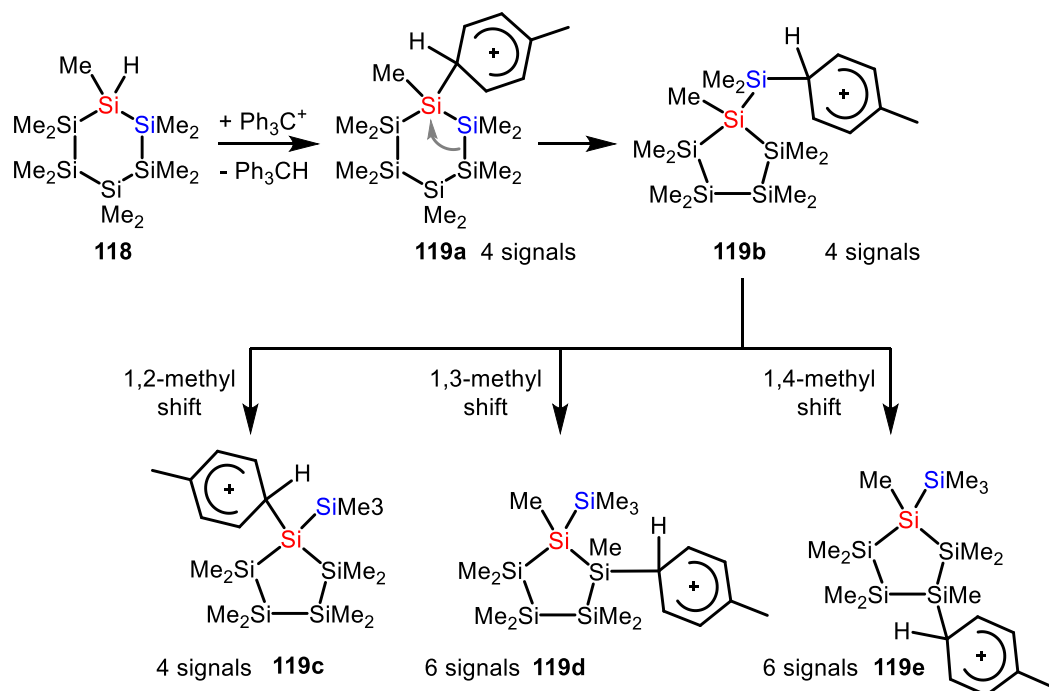


Figure 66. 99 MHz  $^{29}\text{Si}\{^1\text{H}\}$  NMR spectrum ( $\text{C}_7\text{D}_8$ , **top**:  $T = -40\text{ }^\circ\text{C}$ ., **bottom**:  $T = -20\text{ }^\circ\text{C}$ .) of the reaction mixture after hydride abstraction from cyclohexasilane **118**.

The presence of six signals indicates that the reaction product must be unsymmetrical so that every silicon atom of the molecule gives a signal in the  $^{29}\text{Si}\{^1\text{H}\}$  spectrum. The proposed rearrangement mechanism may proceed via cationic intermediates **119a** and **119b** as shown in Scheme 97. However, on the basis of the quantum mechanical structure optimisations of the toluene-stabilised analogues and predictions of the  $^{29}\text{Si}$  NMR chemical shifts, none of these structures are supported (Figure 67). The most reasonable structures, according to the predicted  $^{29}\text{Si}$  chemical shifts, are the toluene-stabilised silylium ions **119d** or **119e**, which result from rearrangement of the six-membered ring and a subsequent 1,2- or 1,4-methyl shift (Scheme 97).



Scheme 97. Formation of silyl arenium ions **119a-e** after hydride abstraction from cyclohexasilane **118** and the expected number of signals in the  $^{29}\text{Si}$  spectra.

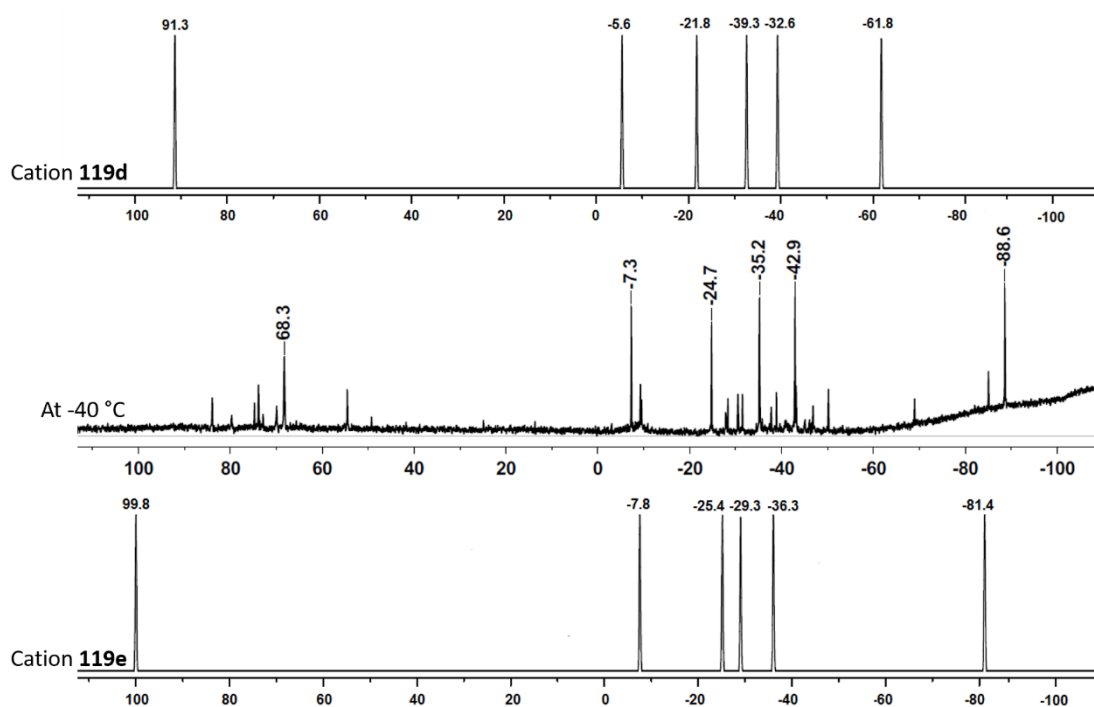


Figure 67. **middle**: measured 99 MHz  $^{29}\text{Si}\{^1\text{H}\}$  NMR ( $\text{C}_6\text{D}_5\text{Cl}$ ,  $T = -40^\circ\text{C}$ ) spectrum, **top** and **bottom**: calculated  $^{29}\text{Si}\{^1\text{H}\}$  NMR spectrum of toluene-stabilised silyl cations **119d** and **119e** at M06-L/6-311G(2d,p)//M06-2X/6-311+G(d,p) level of theory.

The NMR results and the comparison with the predicted  $^{29}\text{Si}$  NMR chemical shifts did not permit a clear confirmation of the proposed mechanism of the experimental chemical shifts. A diagram of the relative ground state energies of isomeric compounds **119a-e** shows that isomer **119e** is the most stable, however, only by  $-3.7\text{ kJ mol}^{-1}$ . Such small difference may just result from changes in the conformations (Figure 68).

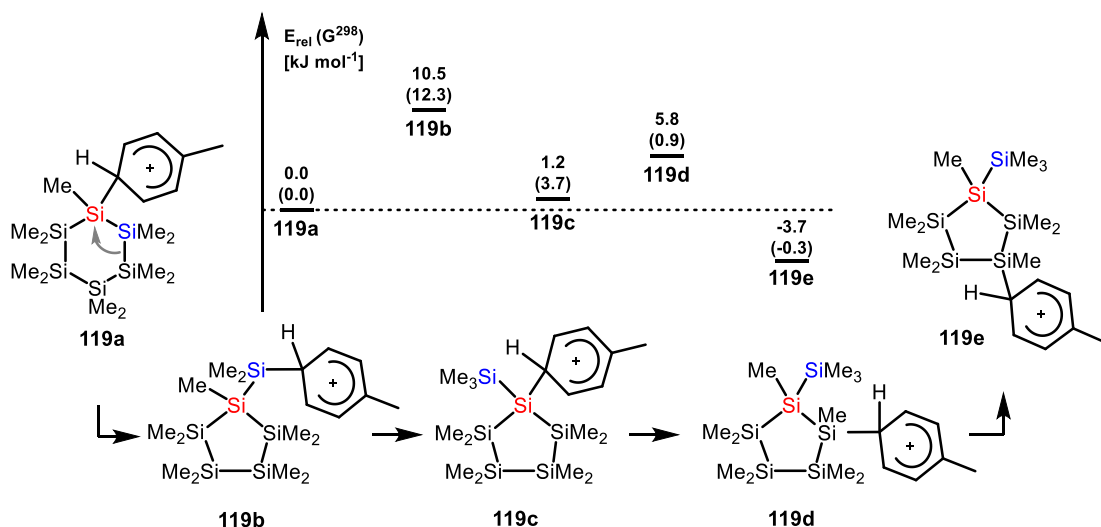
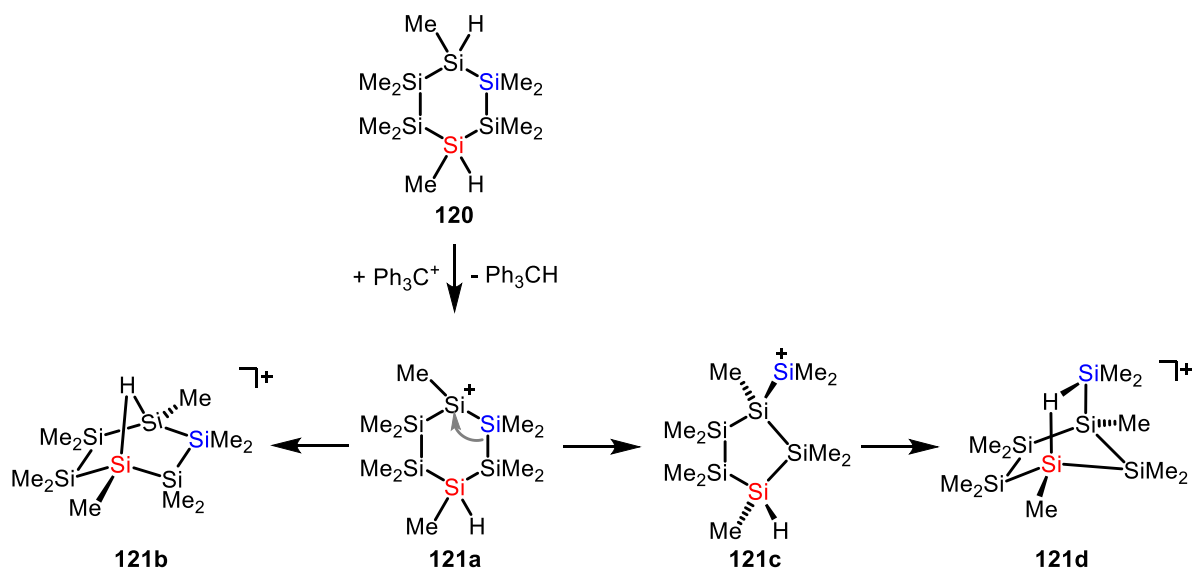


Figure 68. Diagram of relative ground state energies  $E$  and Gibbs free energies at 298.15 K,  $G^{298}$  (in parentheses) of isomeric cations **119a-e**, relative to cation **119a**, calculated at M06-2X/6-311+G(d,p).

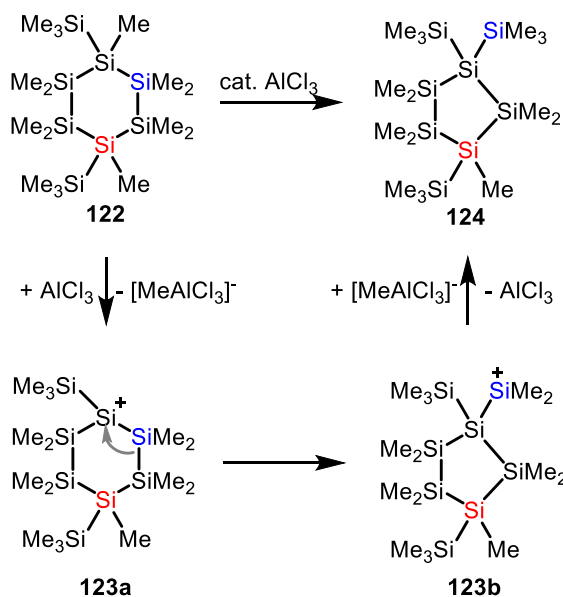
In summary, it was not possible to obtain clean conversion of the hydrogen-substituted six-membered ring to a single cation or to trap any intermediate. Probably, this reaction has to be performed at even lower temperatures or another way to stabilise the cationic intermediates has to be found. One possibility may be given by the formation of 2e3c Si-H-Si bond. Therefore, a 1,4-dihydrogen-substituted cyclohexasilane **120** should be prepared and hydride abstraction reactions at low temperatures might allow for the trapping of cationic intermediates **121b** or **121d** as shown in Scheme 98. Unfortunately, the synthesis of the above mentioned 1,4-dihydridodecamethylcyclohexasilane **120** is quite challenging, especially placing the hydrogen atoms in the right positions.



Scheme 98. Proposed formation of 2e3c Si-H-Si bridged bissilyl cation **121b** and **121d** after hydride abstraction reaction of the 1,4-dihydrogen-substituted cyclohexasilane **120**.

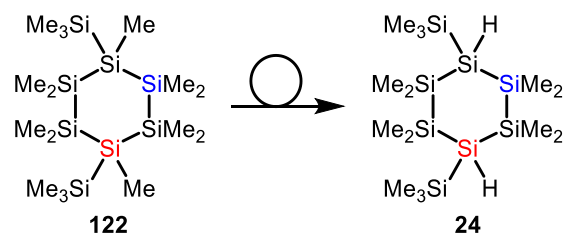
### 3.5.2 The Hydrogen Trick – Trapping Intermediates in Cyclic Polysilanes

Rearrangement of the related 1,4-bis(trimethylsilyl)decamethylcyclohexasilane **122** to the five-membered ring **124** was found by Marschner (Scheme 99).<sup>[119]</sup> By analogy to the above-mentioned ring contraction reaction, it is assumed that  $\text{AlCl}_3$  abstracts a methyl anion from the trisilyl-substituted silicon atom and the first silyl cation **123a** is formed. After a 1,2-silyl shift, a new Si-Si bond is formed. The ring contracts to a five-membered ring and the dimethylsilyl group moves out of the ring and becomes an additional flanking silyl group bearing a positive charge (**123b**). The return of the methyl anion from the aluminate neutralises the silyl cation and the neutral rearrangement product **124** is formed (Scheme 99).<sup>[47]</sup>



Scheme 99. Proposed mechanism of the rearrangement of cyclohexasilane **122** to give cyclopentasilane **124**.

In the previous experiments, it was shown that the polysilanyl cations can be stabilised by intramolecular 2e3c Si-H-Si bonds. Hence, the idea was to exchange the methyl groups by hydrogen atoms (Scheme 100), in order to possibly stabilise cationic intermediates occurring during the rearrangement. Moreover, hydrogen substitution allows the preparation of a defined initial cation by a hydride abstraction reaction with triphenylmethyl cation. In contrast,  $\text{AlCl}_3$  does not specifically abstract the methyl group as indicated in Scheme 99; in fact, it can abstract a methyl group from any silicon atom.



Scheme 100. Exchange of methyl groups in **122** by hydrogen atoms to give **24**.

Figure 69 displays the formation of two possible bissilyl cations trapped by 2e3c Si-H-Si bonds. Either the initially formed six-membered ring silyl cation **125a** just forms the Si-H-Si bridge to give **125b**, or rearrangement takes place to give the five-membered ring **125c**. The cationic charge at the flanking silyl group can be trapped by the Si-H-Si bridge to give **126**. These structures **125b** and **126** are

calculated to be an energy minimum, but the five-membered ring structure **126** is, compared to the six-membered ring structure **125b**, more stable by approx. 20 kJ mol<sup>-1</sup> (Figure 69).

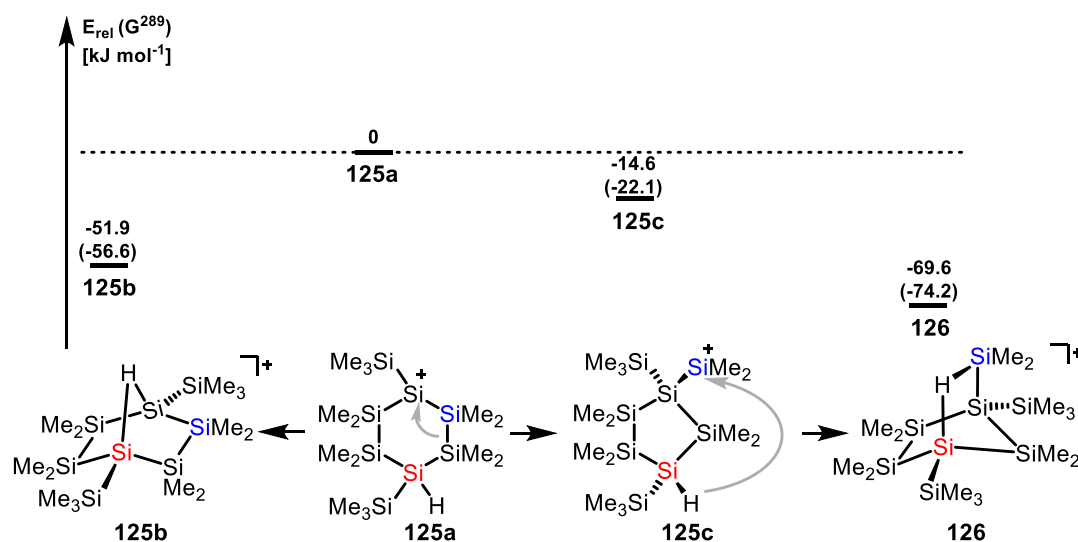


Figure 69. Diagram of relative ground state energies  $E$  and Gibbs free energies at 298.15 K,  $G^{298}$  (in parentheses) of isomeric cations **125a-c** and **126**, relative to cation **125a**, calculated at M06-2X/6-311+G(d,p).

The reaction of the hydrogen-substituted analogue **24** was performed at  $T = -40^\circ\text{C}$  in chlorobenzene- $d_5$  and the acquired  $^{29}\text{Si}\{^1\text{H}\}$  NMR spectrum is shown in Figure 70. This spectrum reveals eight signals. Compared to the number of silicon atoms in the molecule, which is also eight, it is obvious that an unsymmetrical product must be present. On the basis of the  $^{29}\text{Si}$  chemical shifts, an assignment to several structural motifs is possible. The signal at  $\delta^{29}\text{Si} = -107.5$  represents a tetrasilyl-substituted silicon atom, the three signals at  $\delta^{29}\text{Si} = -35.3$ ,  $-33.4$  and  $-33.0$  result of dimethylsilyl groups from the ring system, flanking trimethylsilyl groups appear at  $\delta^{29}\text{Si} = -4.3$  and  $-0.7$  and two different cationic silicon atoms are present in the molecule as indicated by two different low field signals at  $\delta^{29}\text{Si} = 64.1$  and  $78.1$ .

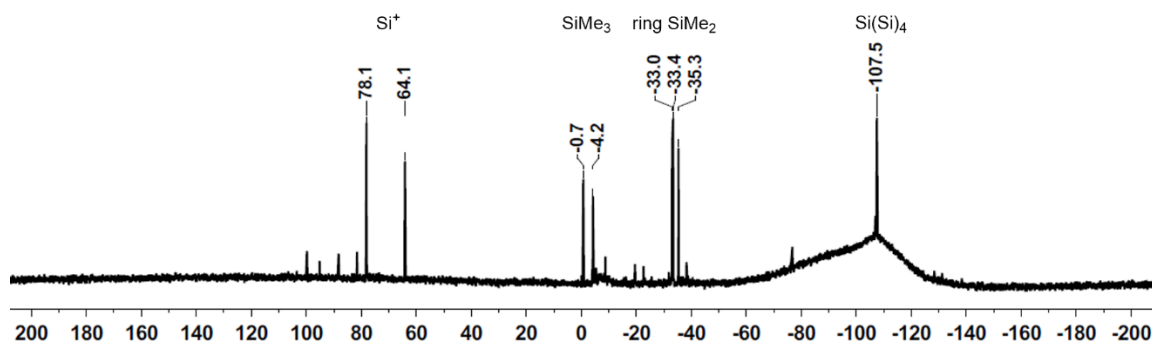


Figure 70. 99 MHz  $^{29}\text{Si}\{^1\text{H}\}$  NMR spectrum ( $\text{C}_6\text{D}_5\text{Cl}$ ,  $T = -40^\circ\text{C}$ ) obtained after hydride abstraction of cyclohexasilane **24**.

In the hydrogen-coupled  $^{29}\text{Si}$  INEPT NMR spectrum (Figure 71) the two low field signals are doublets with coupling constants of  $^1J_{\text{Si,H}} = 46$  Hz and 39 Hz, which are characteristic of a Si-H-coupling in 2e3c Si-H-Si bonds. The signal at  $\delta^{29}\text{Si} = 64.1$  is only a doublet with no fine structure, which means, this silicon atom is only connected to one hydrogen atom and there are no methyl groups bound to it. In contrast, the signal at  $\delta^{29}\text{Si} = 78.1$  reveals a doublet of septets pattern, which is due to coupling to a directly attached hydrogen atom and to six equivalent hydrogen atoms, meaning two methyl groups. Consequently, the reaction product must contain a  $(\text{Si}_3)\text{Si-H-SiMe}_2$  building block. Interestingly when acquiring the  $^{29}\text{Si}$  INEPT NMR spectrum with delays fitted for one hydrogen atom ( $n = 1$ ) and a silicon-hydrogen coupling constant of  $^1J_{\text{Si,H}} = 41$  Hz, which was extracted from the Si-H coupling in the  $^1\text{H}$  NMR spectrum, almost all by-products seen in the  $^{29}\text{Si}\{^1\text{H}\}$  spectrum are suppressed and only the signals of the reaction product can be visualised. This also implies that the by-products do not possess a 2e3c Si-H-Si bridge, which would otherwise be amplified in this hydrogen-coupled Si INEPT NMR spectrum.

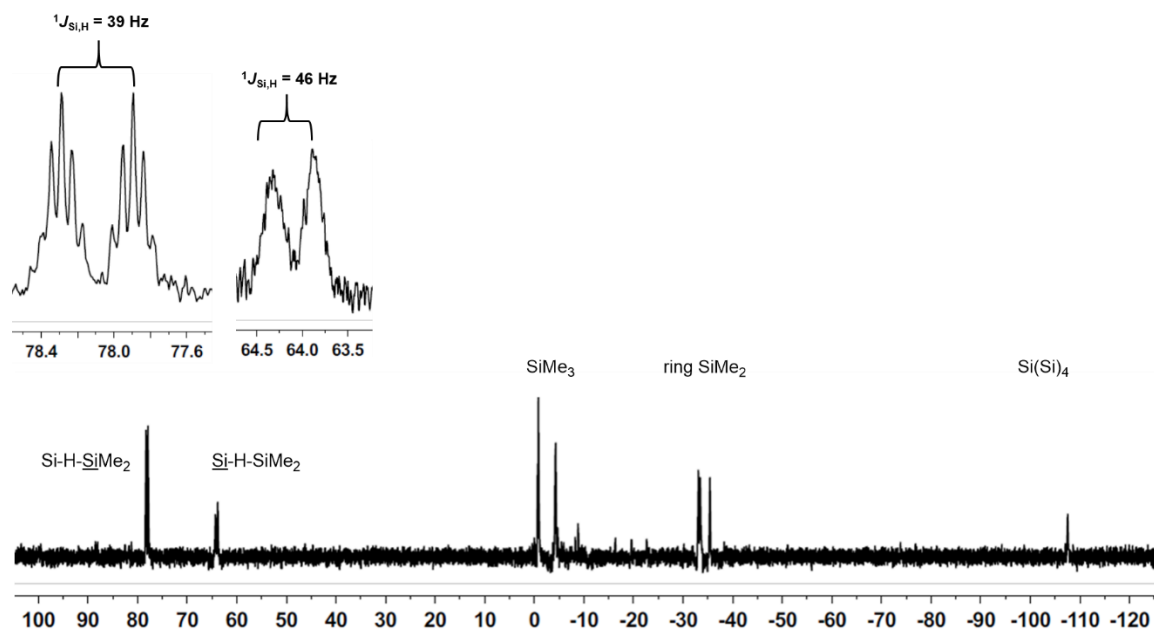


Figure 71. 99 MHz  $^{29}\text{Si}$  INEPT NMR spectrum ( $\text{C}_6\text{D}_5\text{Cl}$ ,  $T = -40^\circ\text{C}$ ) obtained after hydride abstraction of cyclohexasilane **24**.

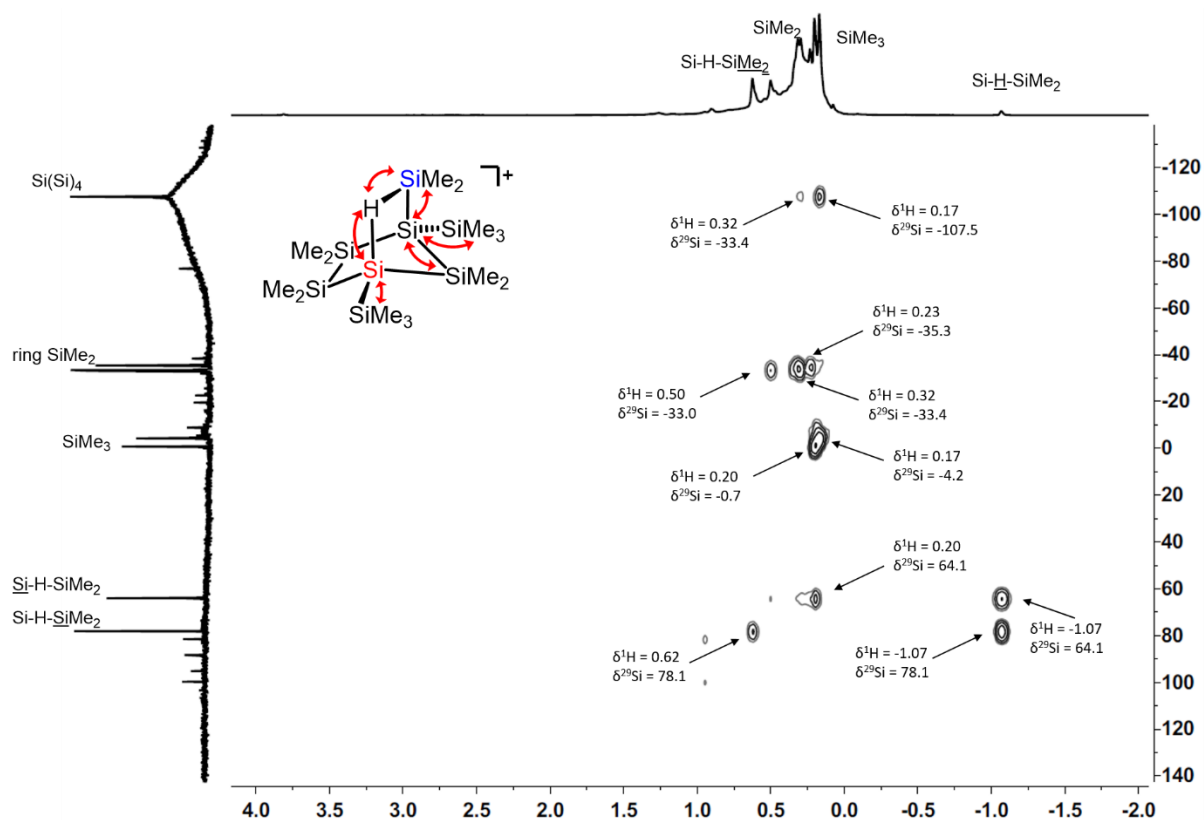
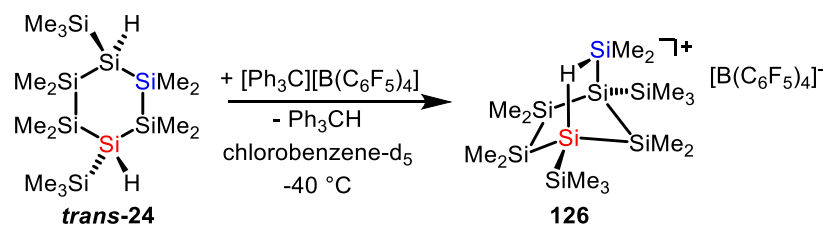


Figure 72. 500 MHz/99 MHz  $^1\text{H}/^{29}\text{Si}$  HMQC NMR spectrum ( $\text{C}_6\text{D}_5\text{Cl}$ ,  $T = -40^\circ\text{C}$ ) of 2e3c hydrogen-bridged bissilyl cation **126**.

Moreover, the  $^1\text{H}/^{29}\text{Si}$  HMQC and HMBC NMR spectra show all relevant cross peaks to support the formation of the Si-H-Si bridged five-membered ring **126** as demonstrated in Scheme 101.



Scheme 101. Formation of 2e3c hydrogen-bridged bissilyl cation **126**.

Quantum mechanical calculations of the  $^{29}\text{Si}$  NMR chemical shifts of the optimised structure at the M06-L/6-311G(2d,p)//M06-2X/6-311+G(d,p) level of theory provide satisfactory results in comparison to the experimental  $^{29}\text{Si}$  shifts (Figure 73). In addition, the calculated coupling constants  $^1J_{\text{Si,H}}((\text{Si})_3\text{Si-H}) = 37\text{ Hz}$  and  $^1J_{\text{Si,H}}(\text{Me}_2\text{Si-H}) = 39\text{ Hz}$  at the B3LYP/IGLOIII//M06-2X/6-311+G(d,p) level of theory agree well with the experimental values of  $^1J_{\text{Si,H}}((\text{Si})_3\text{Si-H}) = 46\text{ Hz}$  and  $^1J_{\text{Si,H}}(\text{Me}_2\text{Si-H}) = 39\text{ Hz}$ .

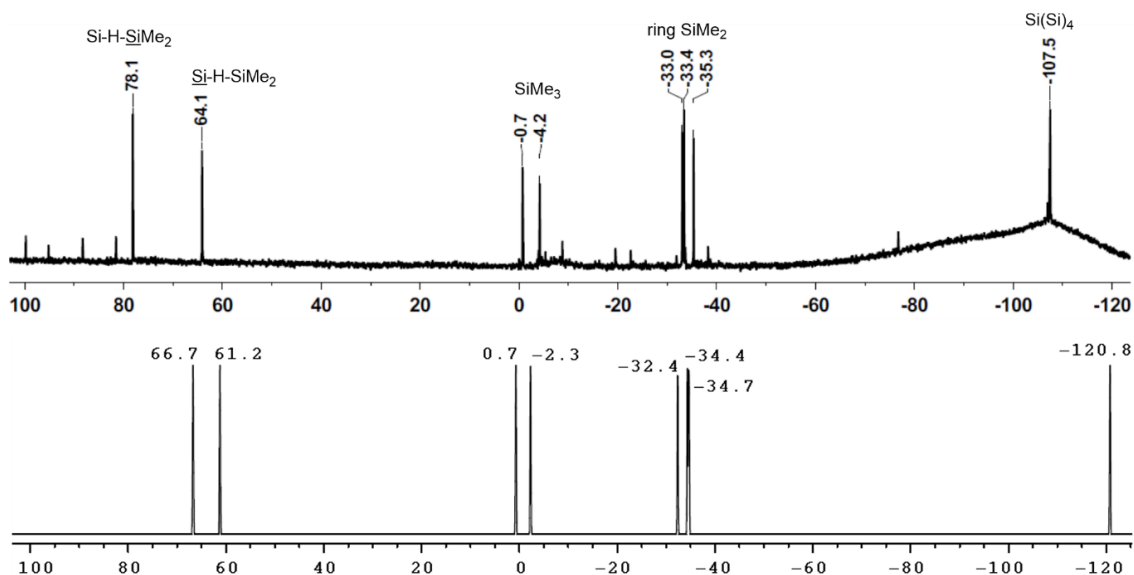
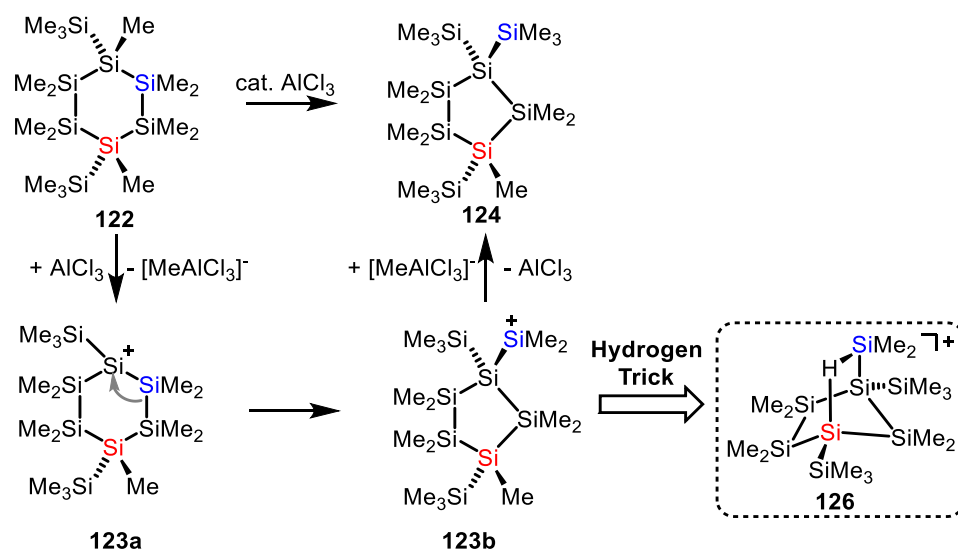


Figure 73. **top**: measured 99 MHz  $^{29}\text{Si}\{^1\text{H}\}$  NMR spectrum ( $\text{C}_6\text{D}_5\text{Cl}$ ,  $T = -40\text{ }^\circ\text{C}$ ), **bottom**: calculated  $^{29}\text{Si}\{^1\text{H}\}$  NMR spectrum of 2e3c Si-H-Si bridge-stabilised bissilyl cation **126** at M06-L/6-311G(2d,p)//M06-2X/6-311+G(d,p) level of theory.

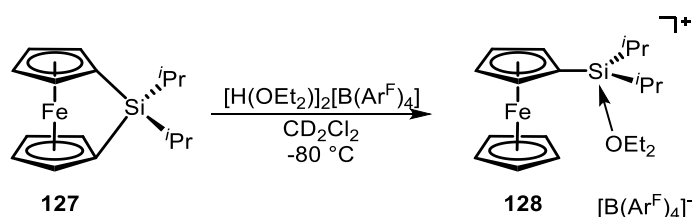
These results demonstrate that the proposed initial cation, the six-membered ring **123a**, is either not an intermediate or its lifetime is very short and it immediately gives five-membered ring **123b**. The existence of intermediate **123b** was verified by the formation and detection of the hydrogen-bridged bissilyl cation **126**. The evidence supports the proposed mechanism for the rearrangement of cyclohexasilane **122** to cyclopentasilane **124**, which involves cationic intermediates **123a** and **123b** (Scheme 102).



Scheme 102. Proposed mechanism for the rearrangement of cyclohexasilane **122** to give cyclopentasilane **124**. Cationic intermediate **123b** was identified in the form of its Si-H-Si bridged analogue **126**.

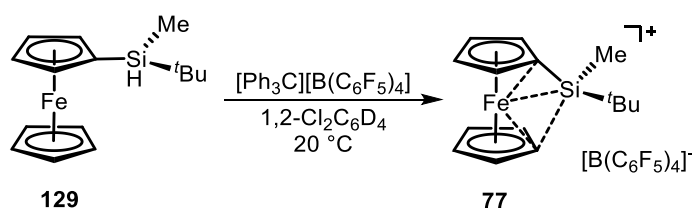
### 3.6 Ferrocenylsilyl Cations

The first attempts to prepare ferrocene-stabilised silylium ions were made by Corey's group.<sup>[145]</sup> They provided evidence for the generation of ferrocenyldiphenylsilylium ion in solution at low temperatures by trapping reactions with NaBD<sub>4</sub>. The Manners group found that strained sila[1]ferrocenophanes undergo ring-opening protonolysis producing cationic silicon compounds. For example, the treatment of **127** with [H(OEt<sub>2</sub>)<sub>2</sub>][B(C<sub>6</sub>F<sub>5</sub>)<sub>4</sub>] generates a ferrocenyl-substituted cation.<sup>[146-147]</sup> Diethyl ether, which is brought in by the proton source, immediately quenches the silylium ion, forming Et<sub>2</sub>O-solvated silylium ion **128**, a siloxonium ion.<sup>[148]</sup>



Scheme 103. Ring-opening protonolysis of sila[1]ferrocenophane **127**.  
[B(Ar<sup>F</sup>)<sub>4</sub>]<sup>-</sup> = tetrakis(3,5-bis(trifluoromethyl)phenyl)borate<sup>[146-147]</sup>

Oestreich et al. have successfully synthesised ferrocene-stabilised silylium ions. These compounds consist of ferrocene, which is substituted with alkylsilyl groups at only one cyclopentadienyl ring. Using the classical Bartlett-Condon-Schneider hydride abstraction reaction the cationic charge was formed at the silicon atom and stabilised by the iron atom and the cyclopentadienyl rings.<sup>[77-78]</sup>

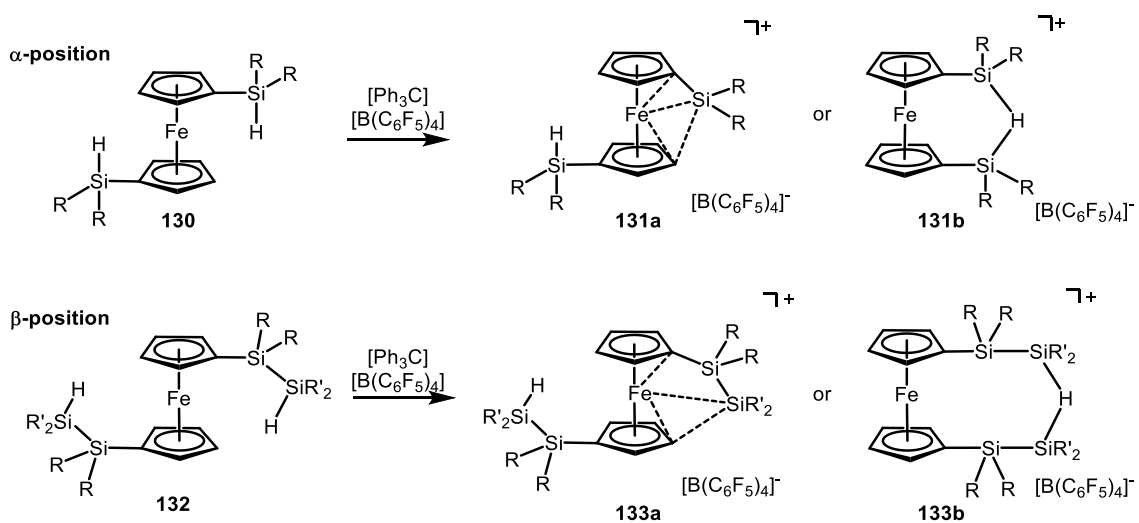


Scheme 104. Synthesis of ferrocene-stabilised silylium ion **77** by Oestreich.<sup>[78]</sup>

These previous works only designed monosilyl-substituted precursors in which a hydride abstraction led to the formation of silylium ions  $\alpha$  to the ferrocene backbone and stabilised by the ferrocene moiety. Based on the known rearrangement reactions of cationic polysilanes and their stabilisation via 2e3c hydrogen bridges, the question arises, over how many bonds will the ferrocene influence

the rearrangement or stabilisation of polysilanylsilyl cationic compounds and how do 1,1'-bissilyl-substituted ferrocenes react after hydride abstraction.

Well-designed silane precursors **130** and **132** were synthesised in which the initial positive charge will be generated either  $\alpha$  or  $\beta$  to the ferrocene backbone. In both cases, two possible stabilisation models are expected for the silylium ions. On the one hand, the silylium ion may coordinate to the iron to receive electron density for stabilisation of the cationic charge i.e. **131a** and **133a**. On the other hand, the presence of a Si-H unit allows for the formation of a 2e3c Si-H-Si bridge which may facilitate the preparation of these silyl cationic compounds (**131b** and **133b**).

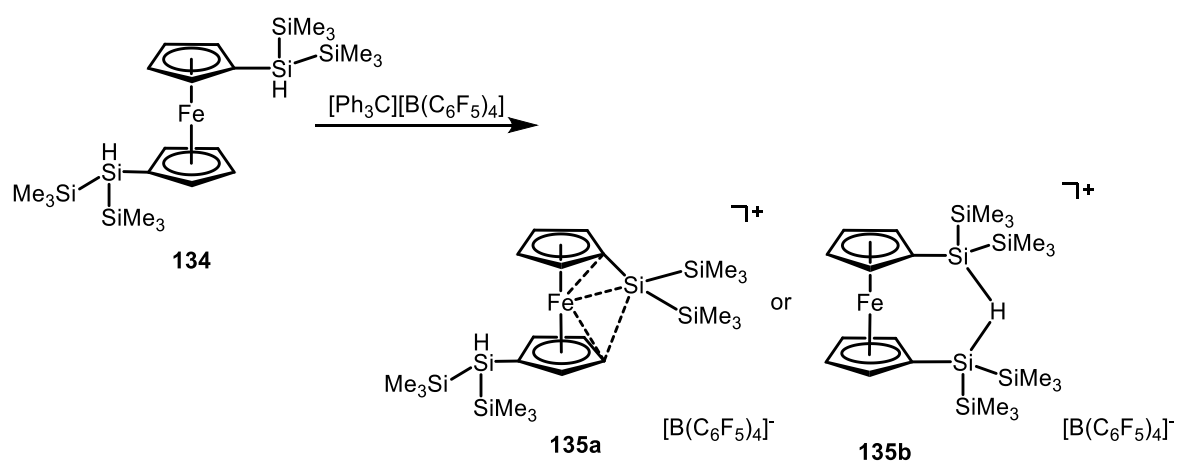


Scheme 105. Possible stabilisation of the cationic silicon atom, either by the ferrocene backbone in **131a** and **133a** or by formation of a Si-H-Si bridge in **131b** and **133b**.

In contrast to  $\alpha$ -ferrocenylsilyl cation **131**, the distance between the initial cationic silicon atom and the ferrocene backbone is increased, when the initial cationic charge is produced at the  $\beta$ -position to the Cp-ring in **133**. By this means, an interaction between the ferrocene and the silyl cation might be hampered and the possibility to form a 2e3c hydrogen bridge may increase.

### 3.6.1 Stabilisation of an $\alpha$ -Ferrocenylsilylium Ion

The first reaction of interest was the hydride abstraction reaction from 1,1'-bissilylferrocene **134** with trityl tetrakis(pentafluorophenyl)borate. As mentioned above, two cations are thought to be possible. First, in analogy to Oestreich's cations, after abstraction of the hydride from one silyl group, the positive charge may be stabilised by the ferrocene backbone (**135a**) and the second silyl moiety does not interact. Secondly, the cation may adopt a conformation that allows for the formation of an intermolecular Si-H-Si bridge as shown in cation **135b**. In both cases, the borate anion acts as weakly nucleophilic anion and allows the detection of any free silyl cationic compound.



Experiments at room temperature or  $T = -20\text{ }^{\circ}\text{C}$  resulted in decomposition of the starting material. A successful cation preparation was observed at  $T = -40\text{ }^{\circ}\text{C}$ . The  $^{29}\text{Si}\{^1\text{H}\}$  NMR spectrum obtained at  $T = -40\text{ }^{\circ}\text{C}$  in chlorobenzene- $d_5$  (Figure 74) reveals five signals. On the basis of the  $^{29}\text{Si}$  NMR chemical shifts, together with the hydrogen-coupled  $^{29}\text{Si}$  INEPT NMR spectrum and 2D NMR experiments, these resonances can be assigned to typical silyl fragments.

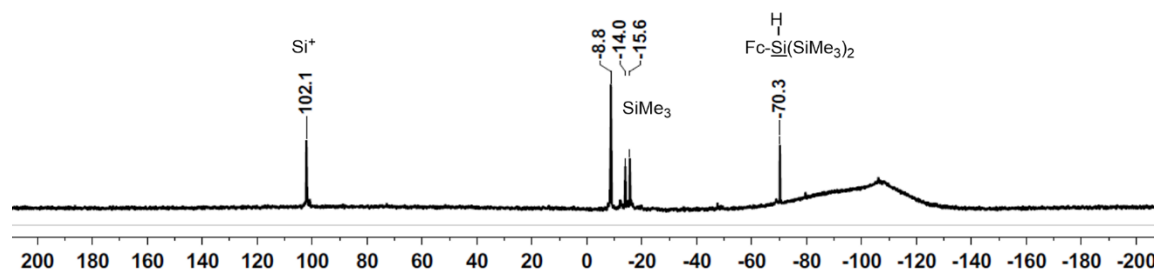


Figure 74. 99 MHz  $^{29}\text{Si}\{^1\text{H}\}$  NMR spectrum ( $\text{C}_6\text{D}_5\text{Cl}$ ,  $T = -40\text{ }^{\circ}\text{C}$ ) after hydride abstraction from 1,1'-bissilylferrocene **134**.

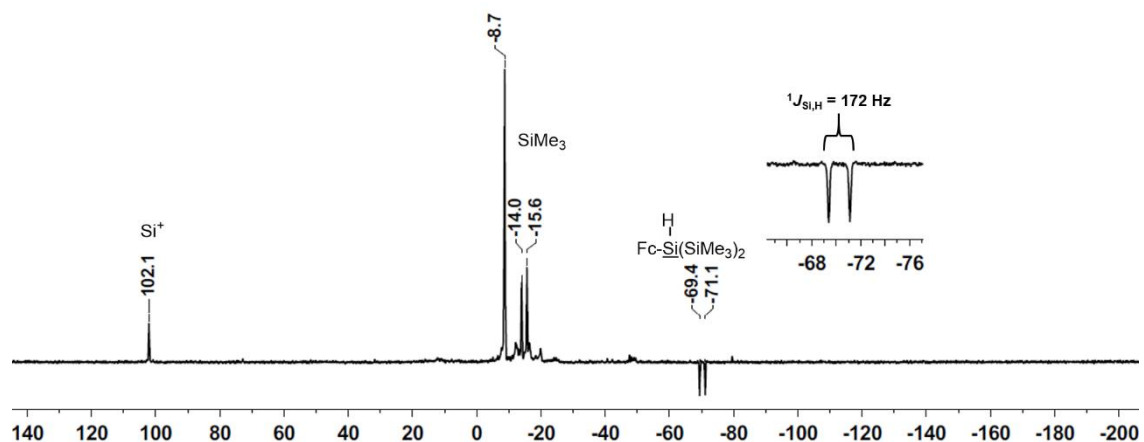


Figure 75. 99 MHz  $^{29}\text{Si}$  INEPT NMR spectrum ( $\text{C}_6\text{D}_5\text{Cl}$ ,  $T = -40\text{ }^\circ\text{C}$ ) after hydride abstraction from 1,1'-bissilylferrocene **134**.

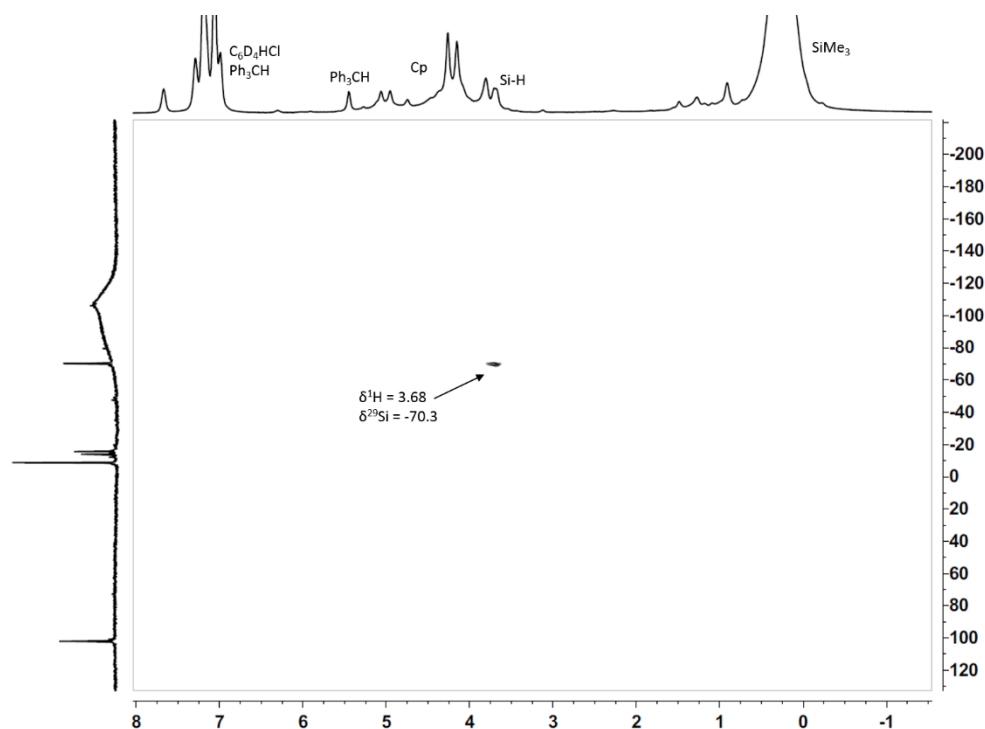


Figure 76. 500 MHz/99 MHz  $^1\text{H}/^{29}\text{Si}$  HMQC NMR spectrum ( $\text{C}_6\text{D}_5\text{Cl}$ ,  $T = -40\text{ }^\circ\text{C}$ ) after hydride abstraction from 1,1'-bissilylferrocene **134**.

A chemical shift of  $\delta^{29}\text{Si} = -70.3$  is typical of silicon atoms which are substituted by at least two other silyl groups and the signal is a doublet with a coupling constant of  $^1J_{\text{Si,H}} = 172\text{ Hz}$ , which allows the assignment of this signal to a  $(\text{Me}_3\text{Si})_2\text{Si-H}$  group. In the  $^1\text{H}/^{29}\text{Si}$  HMQC NMR spectrum, this signal correlates with a broad singlet in the  $^1\text{H}$  NMR spectrum at  $\delta^1\text{H} = 3.68$  which is in the characteristic

chemical shift range for Si-H groups. The cross peak of this signal in the  $^1\text{H}^{29}\text{Si}$  HMBC NMR spectrum is a doublet, with a coupling constant of  $^1J = 172$  Hz, which further proves the existence of the Si-H group. Moreover this Si-H hydrogen couples with two neighbouring  $\text{SiMe}_3$  groups at  $\delta^{29}\text{Si} = -15.6$  and  $-14.0$  as indicated by the cross peak in the  $^1\text{H}^{29}\text{Si}$  HMBC NMR spectrum.

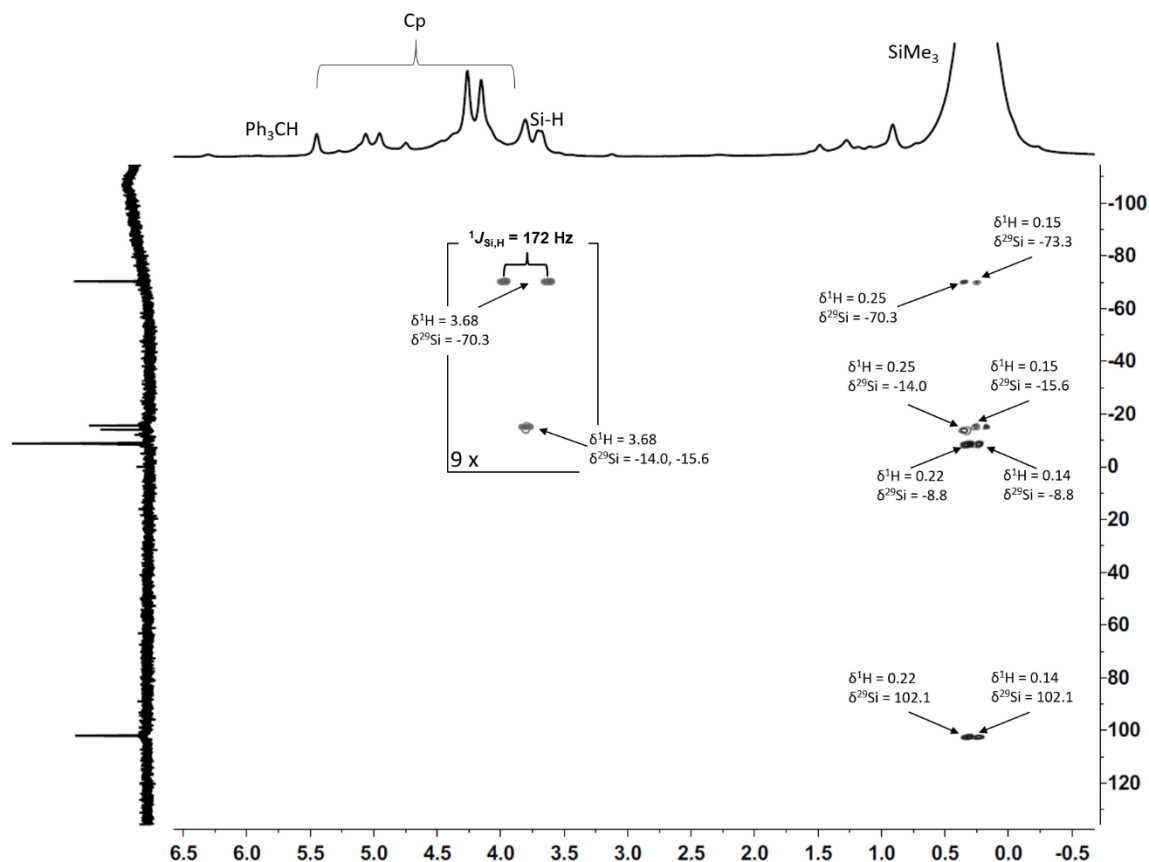
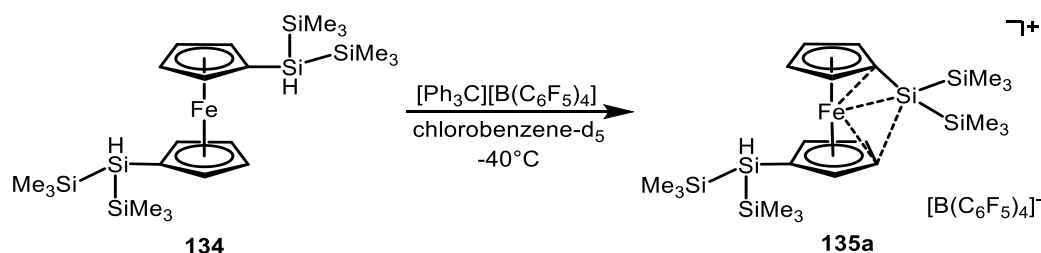


Figure 77. 500 MHz/99 MHz  $^1\text{H}^{29}\text{Si}$  HMBC NMR spectrum ( $\text{C}_6\text{D}_5\text{Cl}$ ,  $T = -40^\circ\text{C}$ ) after hydride abstraction from 1,1'-bissilylferrocene **134**.

The same resonance at  $\delta^{29}\text{Si} = -70.3$  exhibits a cross peak in the  $^1\text{H}^{29}\text{Si}$  HMBC NMR spectrum with two  $^1\text{H}$  resonances of methyl groups at  $\delta^1\text{H} = 0.15$  and  $0.25$ , which themselves correlate with two signals of  $\text{SiMe}_3$  groups at  $\delta^{29}\text{Si} = -15.6$  and  $-14.0$ . These three signals show no interaction with the remaining two signals at  $\delta^{29}\text{Si} = -8.8$  and  $102.1$ , which can be explained by the existence of two independent silyl groups, not being connected. The signal with a chemical shift of  $\delta^{29}\text{Si} = -8.8$  can again be assigned to a  $\text{SiMe}_3$  group and correlates in the  $^1\text{H}^{29}\text{Si}$  HMBC NMR spectrum with two signals in the  $^1\text{H}$  NMR spectrum at  $\delta^1\text{H} = 0.14$  and  $0.22$ . The highly deshielded resonance at  $\delta^{29}\text{Si} = 102.1$  indicates a cationic silyl unit, which also shows a cross peak to the methyl groups at  $\delta^1\text{H} = 0.14$  and  $0.22$  in the  $^1\text{H}^{29}\text{Si}$

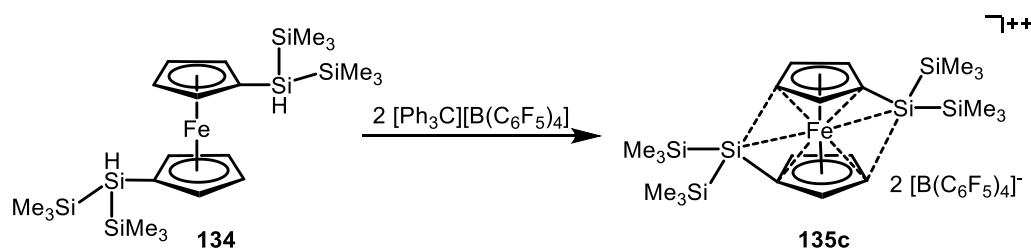
HMBC NMR spectrum. These data together with the integration of the resonances in the  $^{29}\text{Si}\{^1\text{H}\}$  spectrum and the  $^1\text{H}$  spectrum allow the formulation of the reaction product **135a** (Scheme 107).



Scheme 107. Formation of ferrocene-stabilised silylium ion **135a** after hydride abstraction from 1,1'-bissilylferrocene **134**.

This ferrocene-stabilised silylium ion **135a** exhibits a similar  $^{29}\text{Si}$  chemical shift as the alkyl-substituted silylium ion **77** of Oestreich et al. and consequently a similar electronic nature can be assumed for this cation. Interestingly, the two trimethylsilyl groups of the neutral silane moiety show two separated resonances in the  $^{29}\text{Si}$  NMR spectrum but for the trimethylsilyl groups at the cationic silicon atom only one signal in the  $^{29}\text{Si}\{^1\text{H}\}$  spectrum is visible. The  $^1\text{H}^{29}\text{Si}$  HMBC NMR spectrum reveals two times two cross peaks for the trimethylsilyl groups. The inequality of the trimethylsilyl groups of the neutral silyl-unit is rationalised by hindered rotation and the trimethylsilyl groups of the cationic silicon atom have incidentally the same  $^{29}\text{Si}$  NMR chemical shift.

In a second low temperature experiment, the 1,1'-bissilylferrocene was reacted with two equivalents of trityl tetrakis(pentafluorophenyl)borate in order to obtain a dicationic structure by twofold hydride abstraction reaction. (Scheme 108)



Scheme 108. Supposed formation of ferrocene-substituted silyl dication **135c** after twofold hydride abstraction from 1,1'-bissilylferrocene **134**.

The reaction was performed in the same manner as the reaction with only one equivalent of trityl borate. Surprisingly, the  $^{29}\text{Si}\{^1\text{H}\}$  NMR spectrum exhibits the same signals as the spectrum of the

equimolar reaction. It is obvious, that the formation of the monocation was successful, but the abstraction of the other hydrogen atom of the second silyl group did not take place. This was also supported by the presence of a significant amount of unreacted trityl borate as indicated by the presence of the characteristic low field resonance in the  $^{13}\text{C}\{^1\text{H}\}$  NMR spectrum at  $\delta^{13}\text{C}\{^1\text{H}\} = 209.8$ .

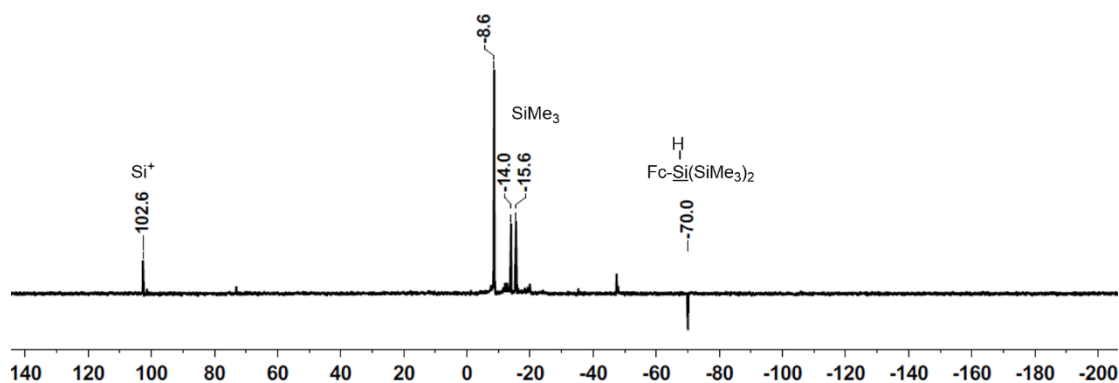
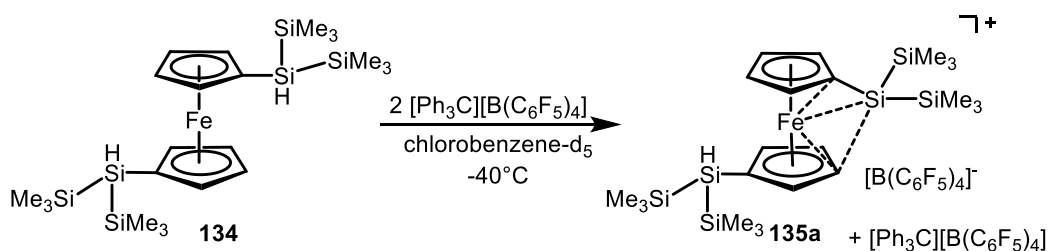


Figure 78. 99 MHz  $^{29}\text{Si}\{^1\text{H}\}$  INEPT NMR spectrum ( $\text{C}_6\text{D}_5\text{Cl}$ ,  $T = -40^\circ\text{C}$ ) of ferrocenylsilylium ion **135a**.



Scheme 109. Reaction of silane **134** with two equivalents of trityl borate.

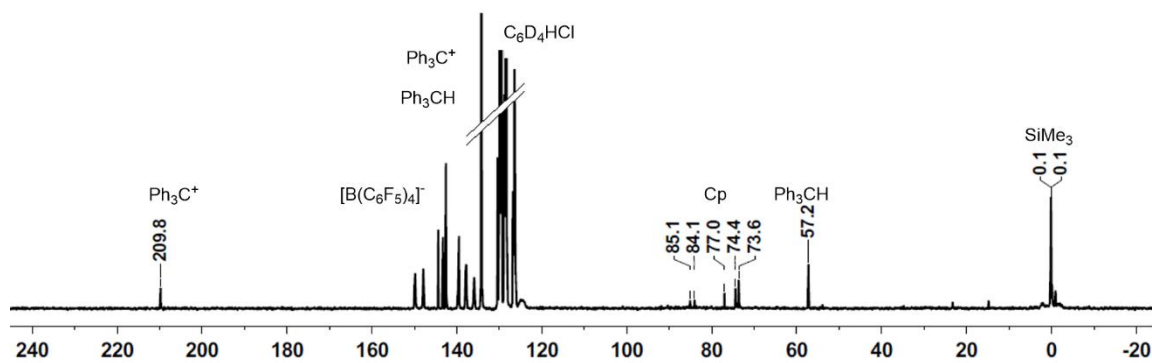


Figure 79. 125 MHz  $^{13}\text{C}\{^1\text{H}\}$  NMR spectrum ( $\text{C}_6\text{D}_5\text{Cl}$ ,  $T = -40^\circ\text{C}$ ) of ferrocene-stabilized silylium ion **135a** and  $[\text{Ph}_3\text{C}][\text{B}(\text{C}_6\text{F}_5)_4]$ .

Complete consumption of trityl borate and the formation of the dication was attempted by warming the sample to room temperature. The larger number of signals in the  $^{29}\text{Si}\{^1\text{H}\}$  spectrum indicated a complex mixture of products or even decomposition and identification of the products was not possible. A twofold hydride abstraction and the formation of a bisilyl dication with the use of naphthylsilanes was reported by Panisch et al.<sup>[107]</sup> The reaction resulted in the exclusive formation of a fluoronium ion with decomposition of the perfluorinated borate anion.

Based on the optimised structure of the ferrocene-stabilised silylium ion **135a** the  $^{29}\text{Si}$  NMR chemical shifts were calculated at the M06-L/6-311G(2d,p)//M06-2X/6-311+G(d,p) level of theory. According to our experience, this combination of method and basis sets represents the  $^{29}\text{Si}$  chemical shift of these polysilanylsilyl cations very well. Figure 80 shows the experimental and calculated  $^{29}\text{Si}$  NMR spectrum, which are in very good accordance with each other.

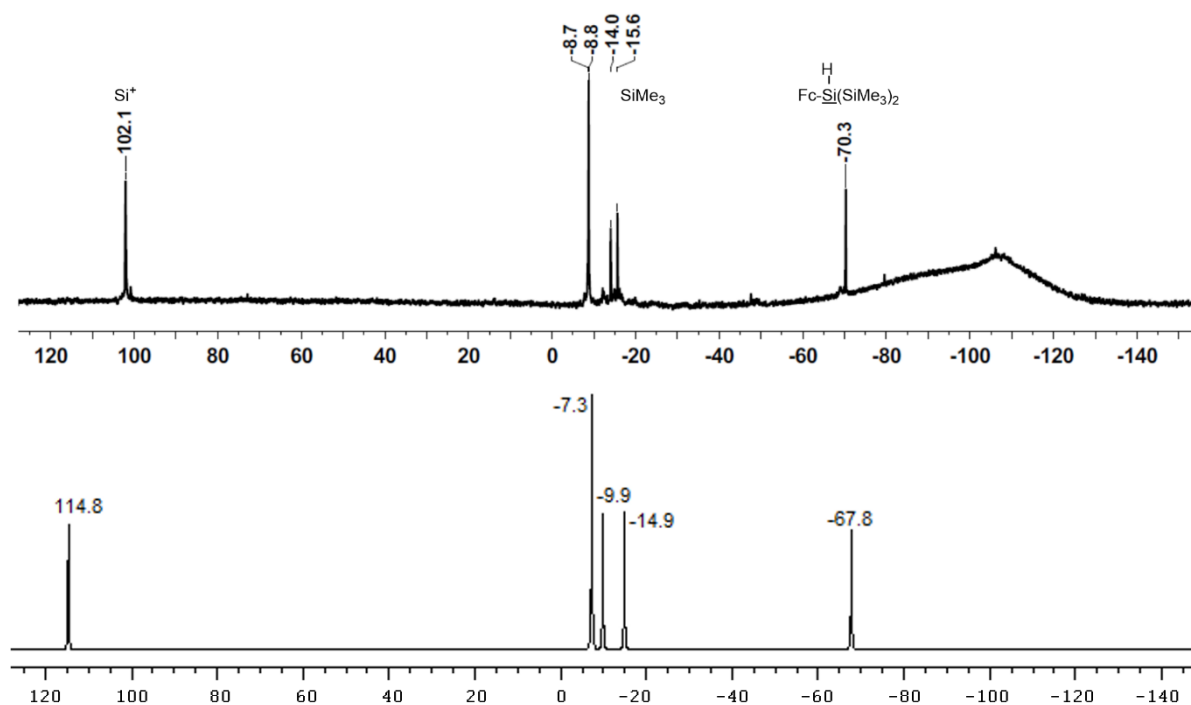
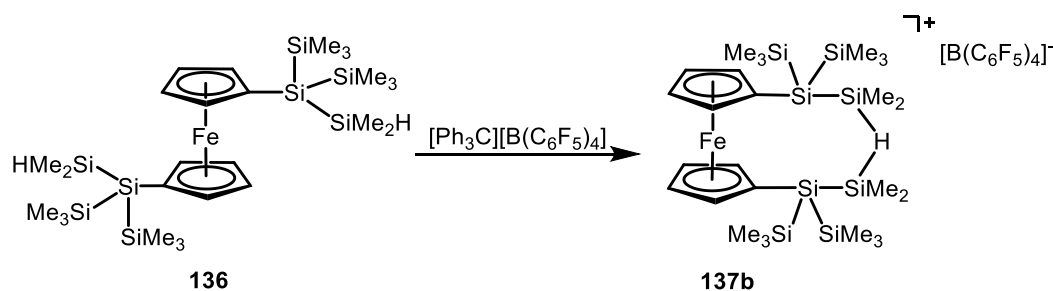


Figure 80. **top:** measured 99 MHz  $^{29}\text{Si}\{^1\text{H}\}$  NMR spectrum ( $\text{C}_6\text{D}_5\text{Cl}$ ,  $T = -40^\circ\text{C}$ , **bottom:** calculated  $^{29}\text{Si}\{^1\text{H}\}$  NMR spectrum of ferrocene-stabilised silylium ion **135a** at the M06-L/6-311G(2d,p)//M06-2X/6-311+G(d,p) level of theory.

### 3.6.2 Stabilisation of a $\beta$ -Ferrocenylsilylium Ion

The second reaction of interest was the hydride abstraction reaction from 1,1'-bissilylferrocene **136** with trityl tetrakis(pentafluorophenyl)borate. In contrast to silylferrocene **134**, the silyl substituent in **136** has an additional  $\text{Me}_2\text{Si}$ -group and the initial cationic charge is produced in a  $\beta$ -position to the Cp-ring. The distance between the initial cationic silicon atom and the ferrocene backbone has increased. This should decrease the interaction between the ferrocene and the silyl cation and the possibility of forming a 2e3c hydrogen bridge should increase.



Scheme 110. Proposed formation of a 2e3c hydrogen bridge by hydride abstraction from 1,1'-bissilylferrocene **136**.

Based on our knowledge of hydrogen-bridged polysilanylsilyl cations and silylferrocene cations, the hydride abstraction reaction from 1,1'-bissilylferrocene **136** was performed at low temperature. The reaction at  $T = -40\text{ }^{\circ}\text{C}$  showed complete decomposition of the starting material. To suppress any subsequent reactions or decomposition, the same reaction was performed at  $T = -60\text{ }^{\circ}\text{C}$  but due to the melting point of chlorobenzene (m.p.:  $-45\text{ }^{\circ}\text{C}$ ), dichloromethane- $\text{d}_2$  was used as the solvent. Several silyl cationic compounds have been shown to be stable in dichloromethane, but only at temperatures lower than  $T = -40\text{ }^{\circ}\text{C}$ . At higher temperatures, activation of the C-Cl bond by the silylium ions occurs and silyl chlorides are formed.<sup>[67, 75, 77, 79]</sup> Therefore, precise control of the temperature is necessary.

The  $^1\text{H}$  NMR spectrum of the reaction at  $T = -60\text{ }^{\circ}\text{C}$  shows the formation of triphenylmethane ( $\delta^1\text{H} = 5.59$ ), which is a sign for a successful hydride abstraction from the silane. Furthermore, a characteristic broad singlet at  $\delta^1\text{H} = 2.01$  appears in the typical region of the bridging hydrogen atom of a Si-H-Si group.

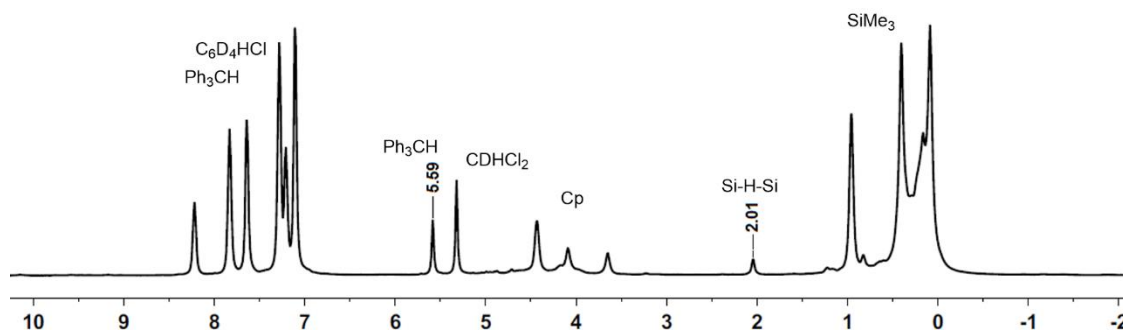


Figure 81. 500 MHz  $^1\text{H}$  NMR spectrum ( $\text{CD}_2\text{Cl}_2$ ,  $T = -60^\circ\text{C}$ ) after hydride abstraction of 1,1'-bissilylferrocene **136** after 5 min.

The  $^{29}\text{Si}\{^1\text{H}\}$  NMR spectrum acquired after five minutes reveals a sharp signal at  $\delta^{29}\text{Si} = 83.5$  in the typical chemical shift range for cationic silicon atoms and a second signal at  $\delta^{29}\text{Si} = -72.1$ , specific for silicon atoms substituted with at least two silyl groups. In the hydrogen-coupled  $^{29}\text{Si}$  INEPT NMR spectrum the low field shifted signal is a doublet of multiplets with a coupling constant of approx.  $^1J \approx 50$  Hz, which is typical for 2e3c Si-H-Si bridges (Figure 82).<sup>[106-107]</sup> Due to the bad signal-to-noise ratio and difficulties associated with phase correction, the coupling constant is not explicitly determinable. In the chemical shift range from  $\delta^{29}\text{Si} = -10$  to -13 several signals can be found, which are assigned to trimethylsilyl groups.

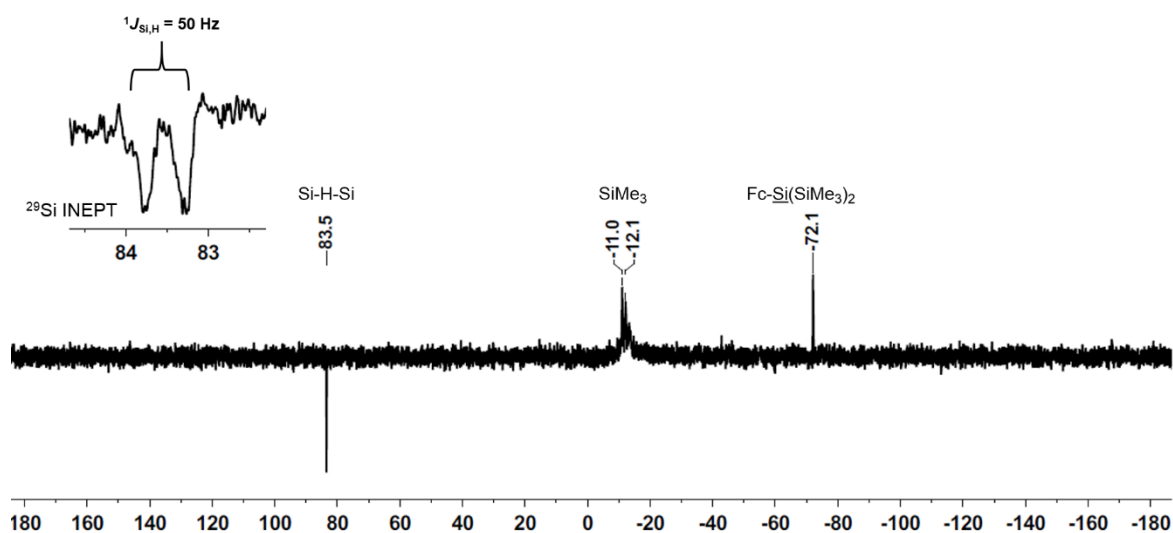


Figure 82. 99 MHz  $^{29}\text{Si}\{^1\text{H}\}$  INEPT NMR spectrum ( $\text{CD}_2\text{Cl}_2$ ,  $T = -60^\circ\text{C}$ ) and an excerpt of the  $^{29}\text{Si}$  INEPT NMR spectrum after hydride abstraction of 1,1'-bissilylferrocene **136** after 5 min.

After three hours at  $T = -60\text{ }^{\circ}\text{C}$ , the signals of the initially formed cation decrease (marked with an asterisk in Figure 83) and new signals appeared. Some of these signals can be related to C-Cl bond cleavage of the solvent, and therefore, the formation of chlorinated silyl ferrocenes (Figure 83).

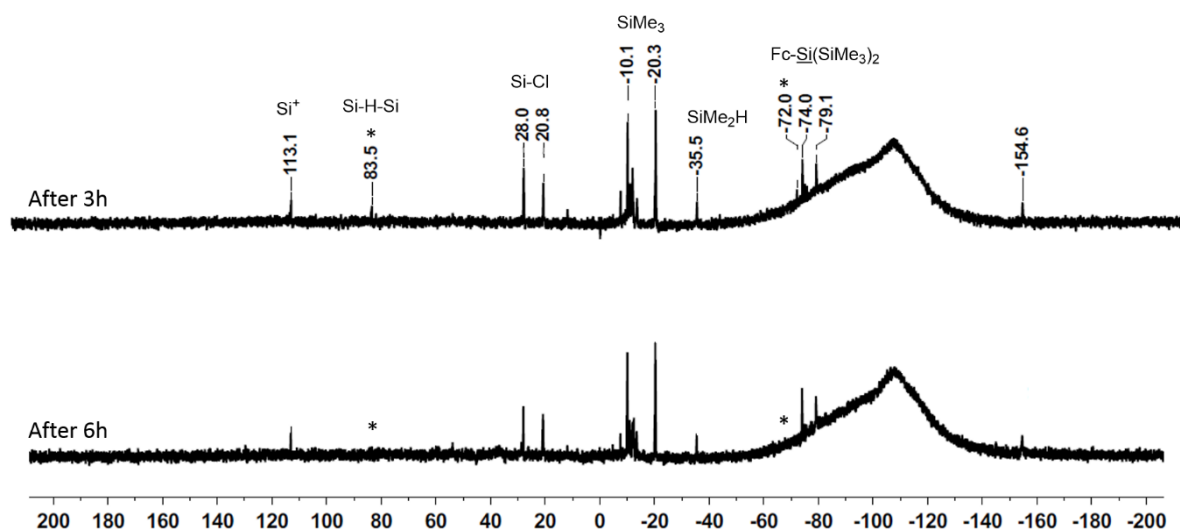


Figure 83. 99 MHz  $^{29}\text{Si}\{^1\text{H}\}$  NMR spectrum ( $\text{CD}_2\text{Cl}_2$ ,  $T = -60\text{ }^{\circ}\text{C}$ ) after hydride abstraction of 1,1'-bissilylferrocene **136** after 2 h (**top**) and 6 h (**bottom**).

After the acquisition of the low temperature NMR spectra, the sample was allowed to warm to room temperature to see if the thermodynamic most stable product will be formed. After two days, the mixture was examined by NMR spectroscopy again. Figure 84 shows the  $^{29}\text{Si}$  NMR spectrum which is dominated by five signals. Resonances in the chemical shift range of  $\delta^{29}\text{Si} = 20 - 30$  are characteristic for silylated chlorosilanes.<sup>[138, 149]</sup> Thus, the signal at  $\delta^{29}\text{Si} = 29.3$  represents a chlorinated silicon atom and, together with the  $^1\text{H}^{29}\text{Si}$  HMBC NMR spectrum, the signals at  $\delta^{29}\text{Si} = -12.6$  and  $-12.7$  are assigned to trimethylsilyl groups and the two high field signals can be assigned to tetrasilyl-substituted silicon atoms connected to the ferrocene.

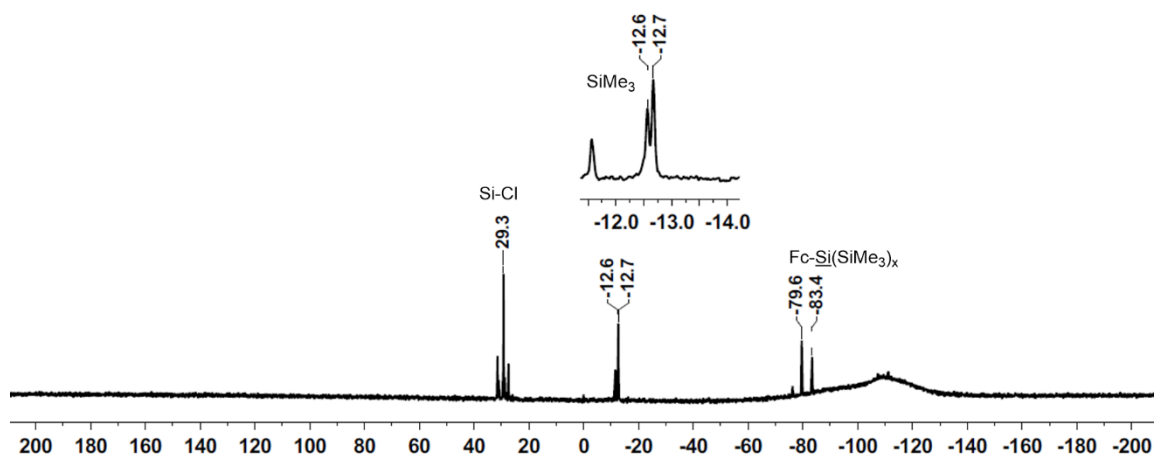
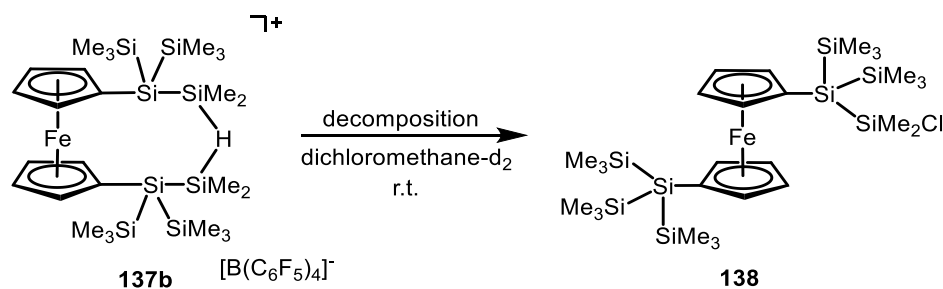


Figure 84. 99 MHz  $^{29}\text{Si}\{^1\text{H}\}$  NMR spectrum ( $\text{CD}_2\text{Cl}_2$ , r.t.) after hydride abstraction of 1,1'-bissilylferrocene **136**.

Consequently, a reasonable structure can be formulated, which is the product of a reaction with the solvent.



Scheme 111. Formation of a chlorosilane **138** from hydrogen-bridged silylium ion **137b** at room temperature.

This structure can also be justified by comparison of the  $^{29}\text{Si}$  NMR chemical shifts with known compounds. For example, in 1,1'-bis(tris(trimethylsilyl)silyl)ferrocene **139**<sup>[116]</sup> the threefold silyl-substituted silicon atoms at the ferrocene show  $^{29}\text{Si}$  NMR chemical shifts of  $\delta^{29}\text{Si} = -82.3$  and the trimethylsilyl groups resonate at  $\delta^{29}\text{Si} = -13.5$ . The chloro-substituted dimethylsilyl group in tris(trimethylsilyl)chlorodimethylsilane **140**<sup>[31]</sup> shows a resonance at  $\delta^{29}\text{Si} = 32.7$ , which matches with the chemical shift found for the decomposition product **138**.

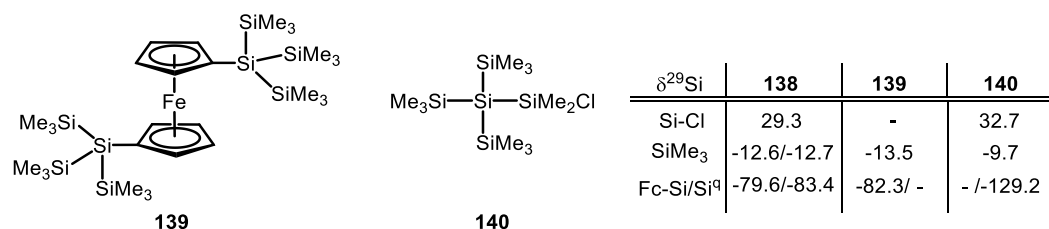


Figure 85. Comparison of the  $^{29}\text{Si}$  NMR chemical shifts of chlorosilane **138** and literature known silanes **139**<sup>[116]</sup> and **140**<sup>[31]</sup>.

The fact that the pure cation was only detected during the first minutes indicates the possibility of the generation of the Me<sub>2</sub>Si-H-SiMe<sub>2</sub> bridge but also shows the high temperature lability of this silylium ion in dichloromethane. Hence, the same experiment was conducted at even lower temperatures. The NMR tube containing trityl tetrakis(pentafluorophenyl)borate and 1,1'-bissilyl-ferrocene was cooled to T = -80 °C and pre-cooled dichloromethane-d<sub>2</sub> was added. After a very slow addition of the solvent, the mixture was stirred for a short period of time but effectively using a vortex mixer and then frozen with liquid nitrogen until the NMR tube was transferred into the pre-cooled NMR spectrometer at T = -80 °C. As the  $^{29}\text{Si}$  NMR spectrum (Figure 86) shows, this temperature allows for the clean formation of the Me<sub>2</sub>Si-H-SiMe<sub>2</sub> bridged, ferrocene-substituted silylium ion in dichloromethane-d<sub>2</sub>.

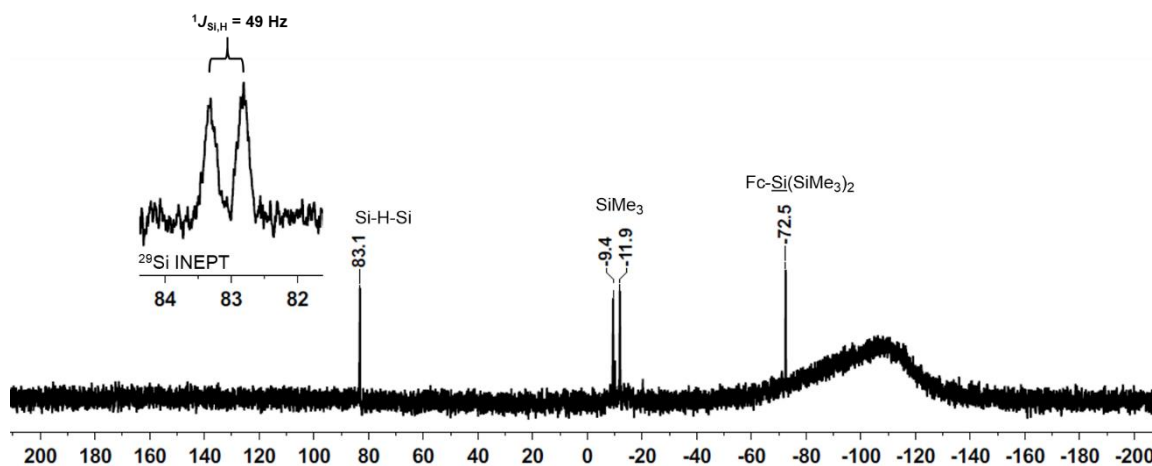
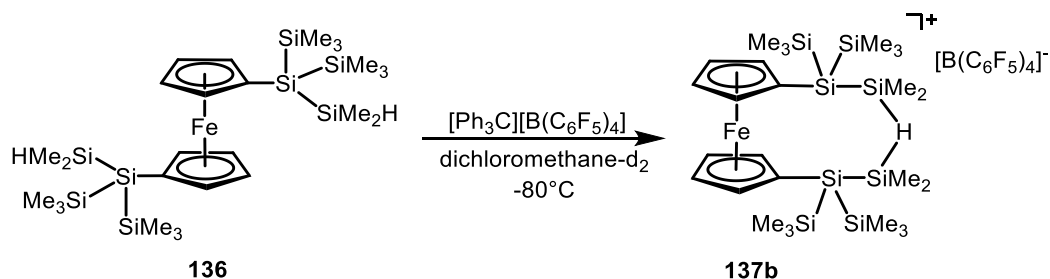


Figure 86. 99 MHz  $^{29}\text{Si}\{^1\text{H}\}$  NMR spectrum (CD<sub>2</sub>Cl<sub>2</sub>, T = -80 °C) of ferrocenylsilylium ion **137b** after 40 min.

The chemical shifts, together with the  $^1\text{H}^{29}\text{Si}$  HMBC and HMQC NMR spectra, reveal several structural motifs. Tetrasilyl-substituted silicon atoms show a resonance at  $\delta^{29}\text{Si} = -72.5$  and two signals of SiMe<sub>3</sub> groups appear at  $\delta^{29}\text{Si} = -11.9$  and -9.4. The singlet in the  $^1\text{H}$  NMR spectrum at  $\delta^1\text{H} = 2.01$  correlates

in the  $^1\text{H}^{29}\text{Si}$  HMQC NMR spectrum with the low field Si resonance at  $\delta^{29}\text{Si} = 83.1$ . This signal is a doublet of septets in the hydrogen-coupled  $^{29}\text{Si}$  INEPT NMR spectrum. This multiplicity can only be produced if a  $\text{Me}_2\text{Si-H}$  group is present. All  $^{29}\text{Si}$  signals have relative integral intensities of 1:1:1:1 and when the starting material is considered, the integrals should be assigned to two each, to account for the eight silicon atoms in the molecule. These data clearly indicate the formation of the hydrogen-bridged ferrocenylbissilyl cation **137b** (Scheme 112).



Scheme 112. Formation of a 2e3c hydrogen bridge by hydride abstraction from 1,1'-bissilylferrocene **136**.

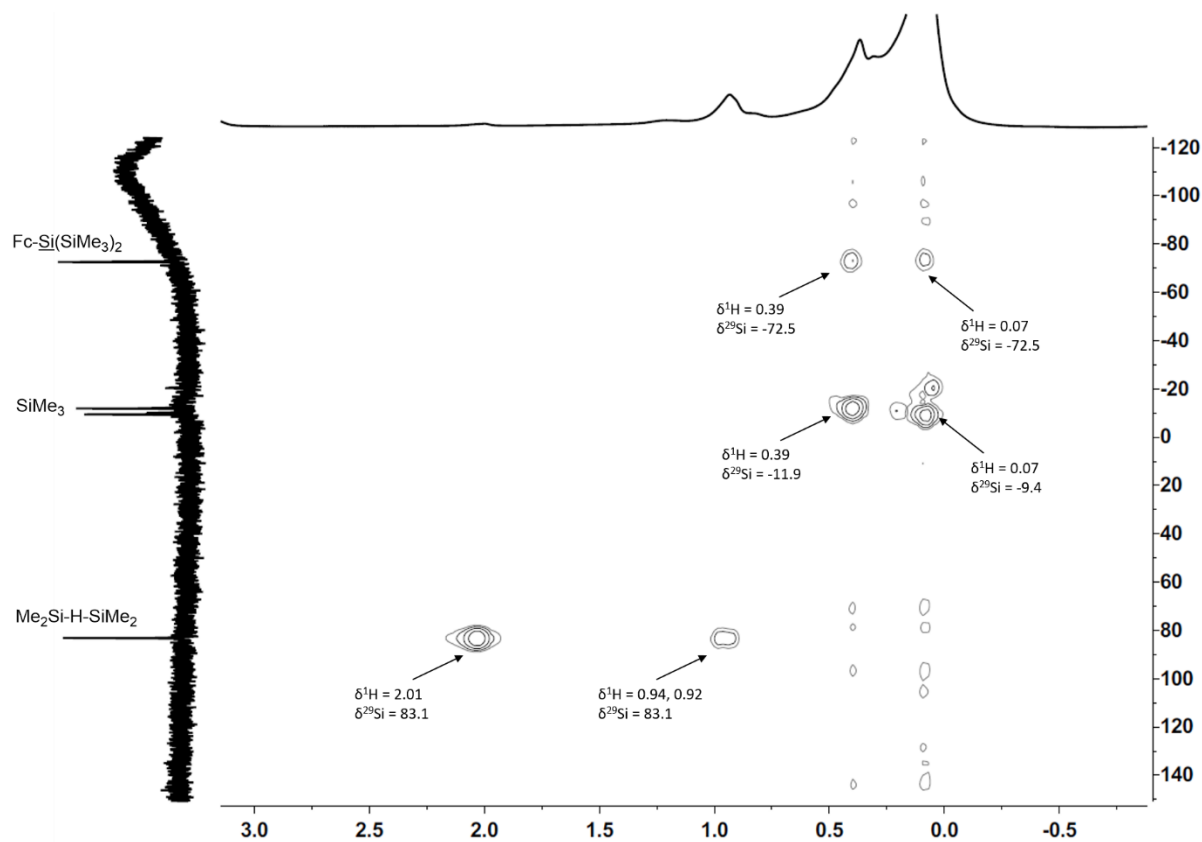


Figure 87. 500 MHz/99 MHz  $^1\text{H}^{29}\text{Si}$  HMQC NMR spectrum ( $\text{CD}_2\text{Cl}_2$ ,  $T = -80^\circ\text{C}$ ) of hydrogen-bridged ferrocenylbissilyl cation **137b**.

Even after four hours, only the ferrocenylbissilyl cation **137b** was observed in the NMR spectra, as evidenced by a comparison of the  $^{29}\text{Si}$  and  $^1\text{H}$  NMR spectra. (Figure 88 and Figure 89).

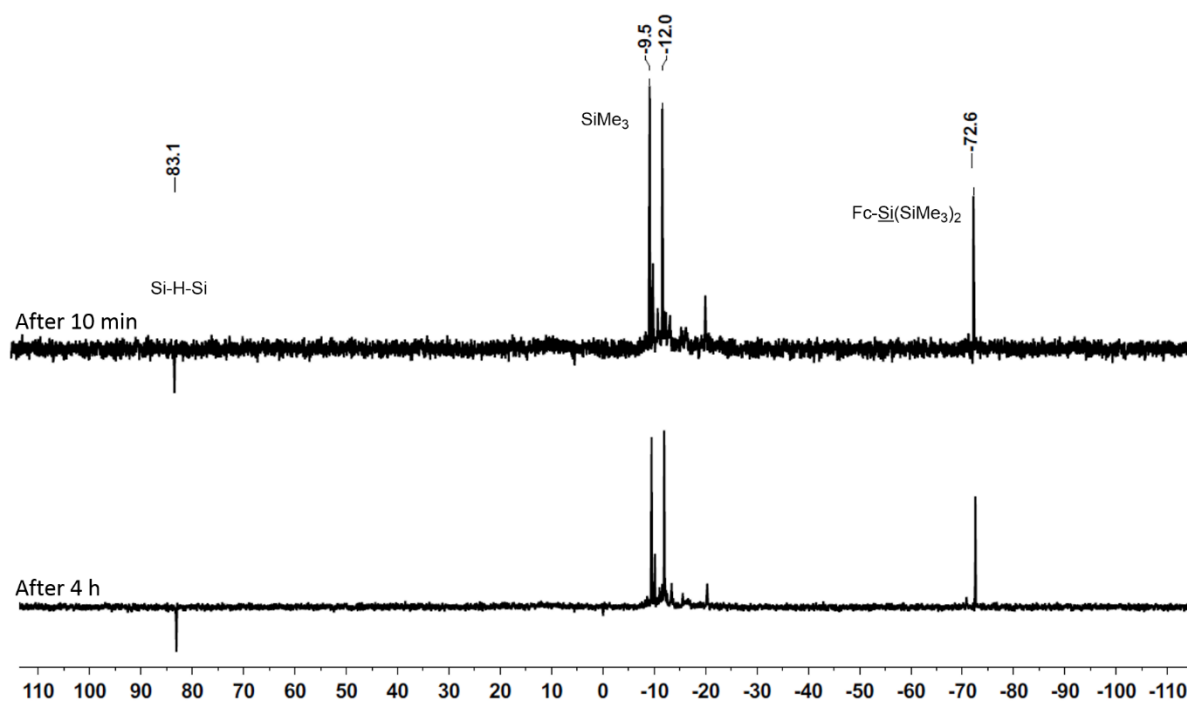


Figure 88. 99 MHz  $^{29}\text{Si}\{^1\text{H}\}$  INEPT NMR spectrum ( $\text{CD}_2\text{Cl}_2$ ,  $T = -80^\circ\text{C}$ ) of ferrocenylbissilyl cation **137b** after 10 min (**top**) and 4 h (**bottom**).

The  $^{29}\text{Si}$  NMR chemical shifts were calculated for the hydrogen-bridged bissilyl cation **137b** at the M06-L/6-311+G(2d,p)//M06-2X/6-311+G(d,p)(Si,C,H),def2tzvpd(Fe) level of theory. Figure 90 shows the experimental and calculated  $^{29}\text{Si}$  NMR spectrum, which are in very good agreement with each other. The calculated Si-H coupling constant of  $^1J_{\text{Si,H}} = 52$  Hz agrees well with the experimental coupling constant of  $^1J_{\text{Si,H}} = 49$  Hz.

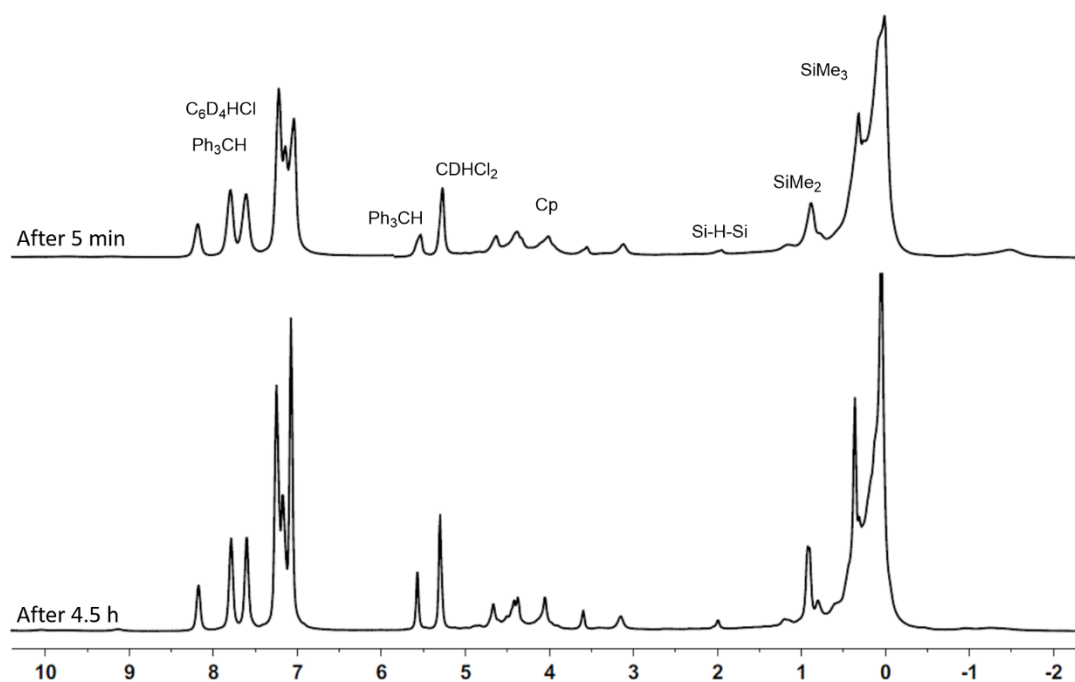


Figure 89. 500 MHz  $^1\text{H}$  NMR spectrum ( $\text{CD}_2\text{Cl}_2$ ,  $T = -80^\circ\text{C}$ ) of ferrocenylbissilyl cation **137b** after 5 min (**top**) and 4.5 h (**bottom**).

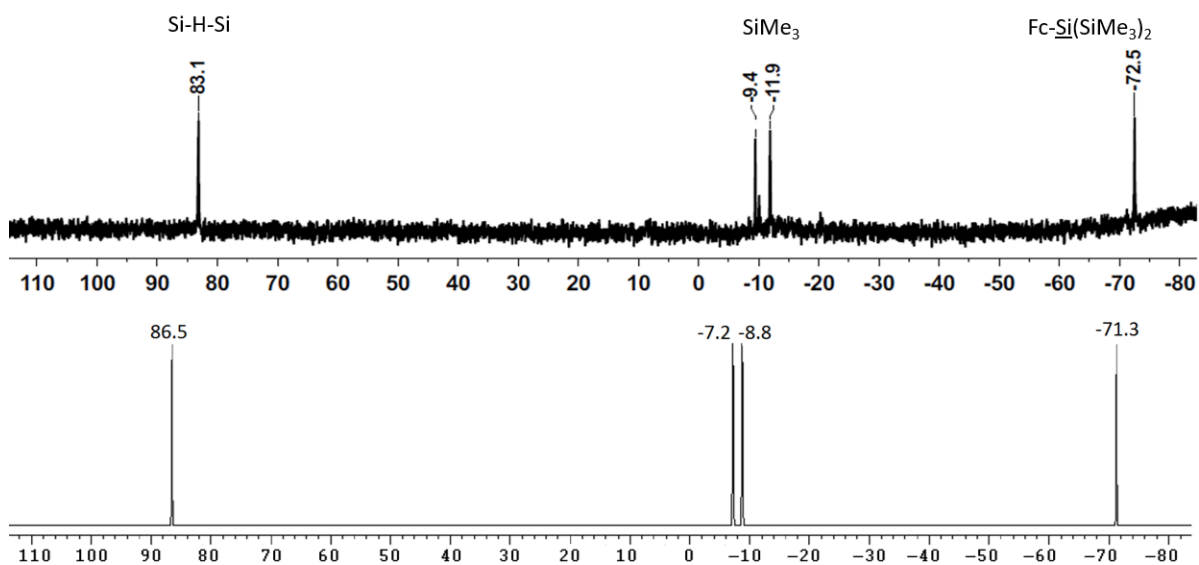


Figure 90. **top**: measured 99 MHz  $^{29}\text{Si}\{^1\text{H}\}$  NMR spectrum ( $\text{CD}_2\text{Cl}_2$ ,  $T = -40^\circ\text{C}$ ), **bottom**: calculated  $^{29}\text{Si}\{^1\text{H}\}$  NMR spectrum of 2e3c hydrogen-bridged bisilyl cation **137b** at M06-L/6-311G(2d,p)//M06-2X/6-311+G(d,p)(Si,C,H),def2tzvpd(Fe) level of theory.

### 3.6.3 Computational Investigations on the 1,1-Oligosilylferrocene Cations

Computational investigations at the M06-2X level of theory for the two proposed silylium ions **135a** and **137b** are contradictory compared to experimental results. Using this model chemistry (M06-2X/6-311+G(d,p)), the hydrogen-bridged structure **135b** is predicted to be stabilised by 44.4 kJ mol<sup>-1</sup> compared to the ferrocene-stabilised silylium ion **135a** (Figure 91).

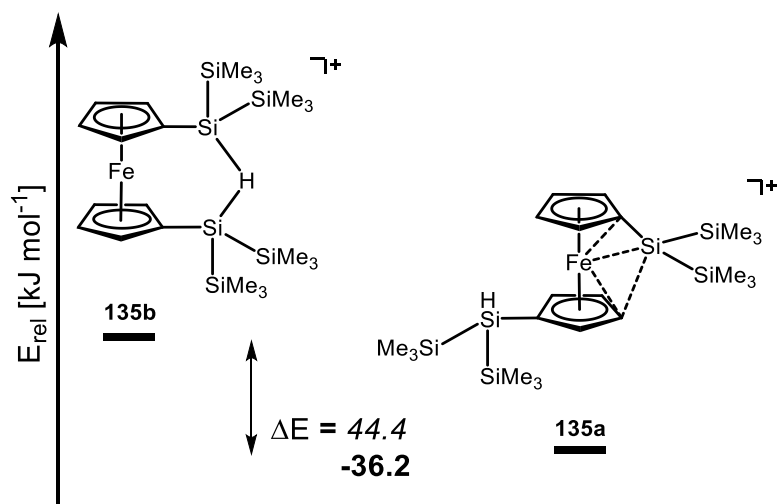


Figure 91. Plot of the relative energy of **135a** vs **135b**.  $E_{\text{rel}} = E_{\text{absolute}}(\mathbf{135a}) - E_{\text{absolute}}(\mathbf{135b})$ . M06-2X/6-311+G(d,p)(Si,C,H),def2tzvpd(Fe) (*italic*), MP2/6-31G(d,p)// M06-2X/6-311+G(d,p)(Si,C,H),def2tzvpd(Fe) (**bold**). Negative values correspond to an energetic preference of the ferrocene stabilised silylium ion **135a**.

A similar phenomenon was described previously for stability calculations of hydrogen-bridged silylium ions.<sup>[150]</sup> It was found that the relative energies of hydrogen-bridged structures calculated at the B3LYP level of theory are always predicted to be the most stable ones. When comparing the relative stabilities of the hydrogen-bridged naphthylsilyl cation **141** versus its phenyl bridged isomer **142**, Panisch et al. noted the inability of the B3LYP method to predict the correct relative energies (Figure 92).<sup>[150]</sup> Only when a correlated *ab initio* method which takes dynamic electron correlation explicitly into account (Møller-Plesset second-order perturbation theory, MP2) was applied, the energetic order reversed and was in agreement with the experimental results (Figure 92). The outcomes of computations with the widely used B3LYP hybrid density functional predict the incorrect isomer to be the most stable one. Single-point calculations at the MP2 level of theory are required to correct this failure and to propose an energy diagram that is in agreement with the experimental results.<sup>[150]</sup> Indeed, in our investigations, single point calculations of the two ferrocenylsilylium ions

at the MP2 level of theory predict the ferrocene-stabilised structure **135b** to be more stable by 36.2 kJ mol<sup>-1</sup> compared to the 2e3c hydrogen-bridged one (Figure 91).

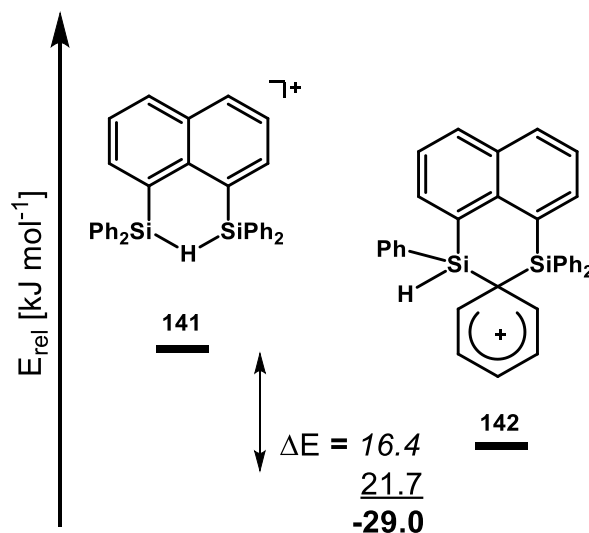
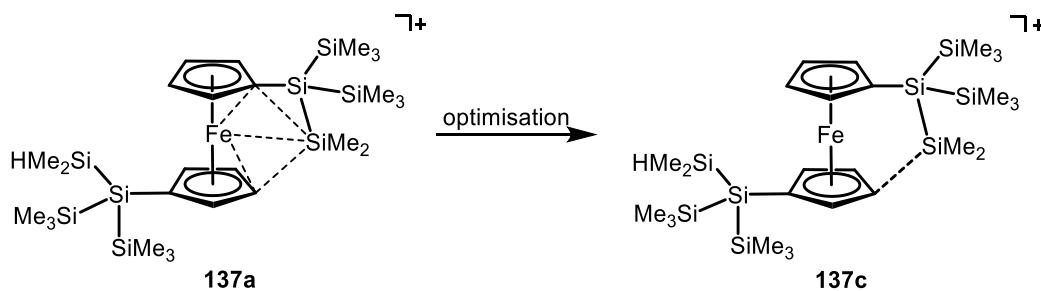


Figure 92. Plot of the relative energy of **141** vs **142**.  $E_{\text{rel}} = E_{\text{absolute}}(\mathbf{142}) - E_{\text{absolute}}(\mathbf{141})$ . B3LYP/6-31G(d,p) (*italic*), B3LYP/6-311G(d,p)//B3LYP/6-31G(d,p) (underlined), MP2/6-31G(d,p)//B3LYP/6-31G(d,p) (**bold**). Negative values correspond to an energetic preference of the arenium ion **142**.<sup>[150]</sup>

The ferrocenylsilyl cation **137a** reveals an interesting behaviour during quantum mechanical optimisation of the structure. The iron-coordinated silylium ion **137a** is not a minimum on the energy surface. During the optimisation, cation **137a** rearranges to give the Cp-coordinated structure **137c**. A detailed computational study of this structure can be found in the bachelor thesis of Hanna Cramer.<sup>[151]</sup>



Scheme 113. Rearrangement of the silylium ion **137a** during the quantum mechanical optimisation at M06-2X/6-311+G(d,p)(Si,C,H),def2tzvpd(Fe).

Computational investigations at the M06-2X level of theory for the two proposed silylium ions, **137a** and **137b**, were in agreement with the experimental results. Using this model chemistry (M06-2X/6-311+G(d,p)) the hydrogen-bridged structure **137b** was predicted to be more stable by 39.8 kJ mol<sup>-1</sup> compared to the ferrocene-stabilised silylium ion **137c**. To determine whether this is a consequence of the inaccurate M06-2X method or not, single point calculations at the MP2 level of theory were performed on the optimised structures. These calculations also predict the 2e3c hydrogen-bridged structure **137b** to be more stable by 45.7 kJ mol<sup>-1</sup> compared to **137c** (Figure 93).

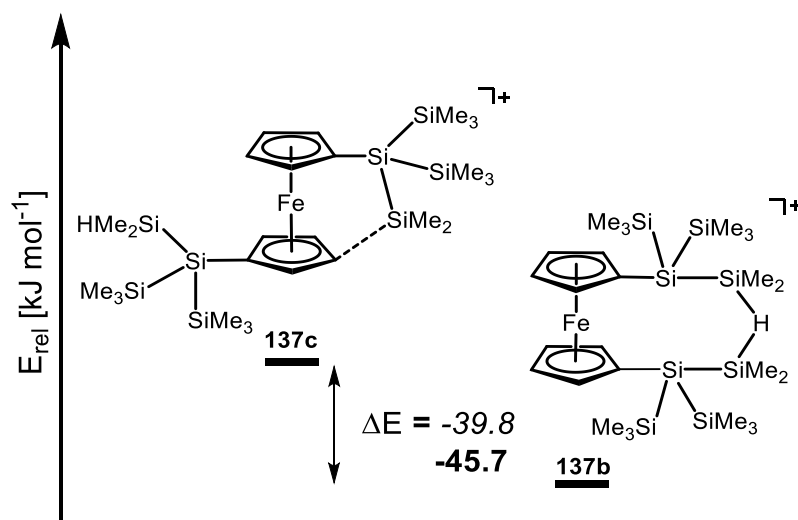


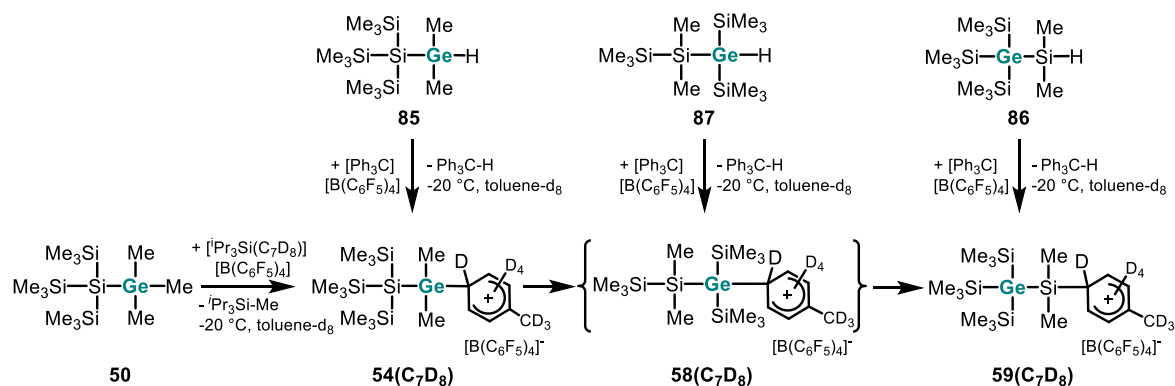
Figure 93. Plot of the relative energy of **137c** vs **137b**.  $E_{\text{rel}} = E_{\text{absolute}}(\mathbf{137b}) - E_{\text{absolute}}(\mathbf{137c})$ . M06-2X/6-311+G(d,p)(Si,C,H),def2tzvpd(Fe) (*italic*), MP2/6-31G(d,p)// M06-2X/6-311+G(d,p)(Si,C,H),def2tzvpd(Fe) (**bold**). Negative values correspond to an energetic preference of the 2e3c hydrogen bridged silylium ion **137b**.

These results clearly indicate the differences in the stabilisation properties in ferrocene-stabilised silyl cations. The two different ferrocenylsilanes **134** and **136** allowed for the preparation of silyl cations in the  $\alpha$ - or  $\beta$ -position to the ferrocene backbone. Very low temperatures are required because of the extremely high reactivity of these species. The relative energies of the silyl cations, which correctly reflect the experimental results, can only be calculated with very expensive *ab initio* methods such as MP2.

## 4 Summary and Outlook

This work elucidated several rearrangement reactions in polysilanes and germapolysilanes, which are predicted to proceed via cationic intermediates. These fleeting intermediates were detected in low temperature  $^{29}\text{Si}$  NMR spectroscopic studies and mechanisms for these rearrangements were established. In addition, the interpretations of the  $^{29}\text{Si}$  NMR spectra and mechanistic ideas were supported by quantum mechanical calculations of  $^{29}\text{Si}$  NMR chemical shifts and ground state energies of the cationic intermediates.

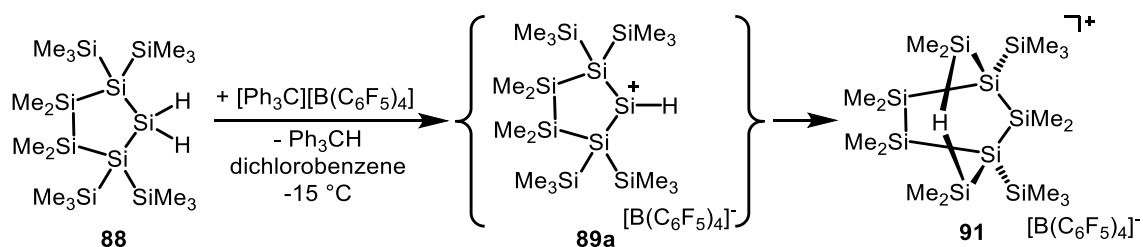
In the first part of this work, the synthesis and NMR spectroscopic characterisation of polysilanylgermyl cation **54** and germapolysilanylsilyl cation **59** were presented (Scheme 114). These cations were obtained in the form of their arene complexes at low temperatures using the weakly coordinating  $[\text{B}(\text{C}_6\text{F}_5)_4]^-$  anion. The cation synthesis was performed using either the stoichiometric reaction of germapolysilanes with a cationic Lewis acid such as tri-*iso*-propylsilyl toluenium ion **65b**, or, in a more regio-controlled way, by the standard hydride transfer reaction between hydridosilanes and -germanes with the trityl cation. The cationic species were identified by low-temperature NMR spectroscopy supported by the results of quantum mechanical NMR chemical shift calculations. By applying these techniques it was possible to unambiguously identify several silyl- and germyl cations and their solvent complexes as intermediates in the sila-Wagner–Meerwein rearrangement of germylsilane **50** and to provide strong evidence for their clean interconversion at low temperatures.



Scheme 114. Formation of silyl toluenium ion **59(C<sub>7</sub>D<sub>8</sub>)** from different precursor compounds.

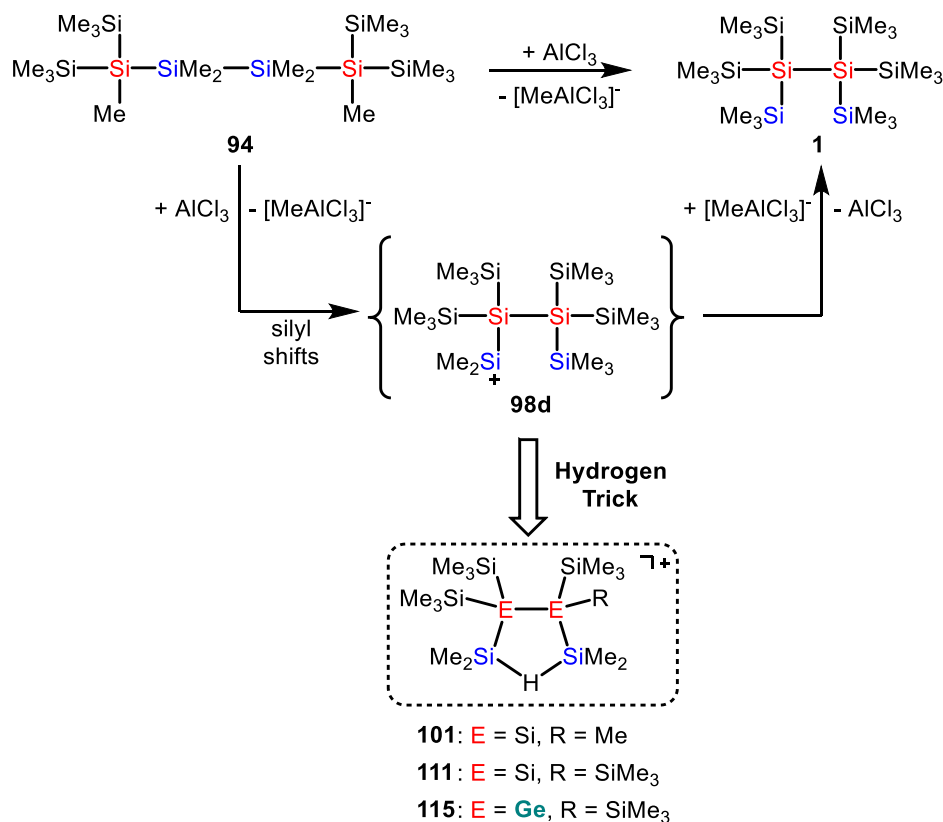
This reaction is expected to be archetypical for many synthetic useful Lewis acid-catalysed skeletal rearrangements of polysilanes and germapolysilanes.

Investigations on the synthesis of hydridosilylium ions revealed a surprising tendency for these cations to rearrange the silicon skeletal framework and undergo several 1,2-methyl shifts in order to isomerise to their thermodynamically most stable isomer (Scheme 115). Hydride abstraction from dihydridosilane **88** did not yield the hydridosilylium ion **89a** but rather the 2e3c hydrogen-bridged bissilyl cation **91**. Quantum mechanical predictions of the  $^{29}\text{Si}$  NMR chemical shifts clearly support the assignment of the  $^{29}\text{Si}$  resonances and energy calculations substantiate the proposed mechanistic pathway.



Scheme 115. Rearrangement of the hydridosilylium ion **89a** towards 2e3c Si-H-Si bridged bissilyl cation **91** after hydride abstraction from dihydrosilane **88**.

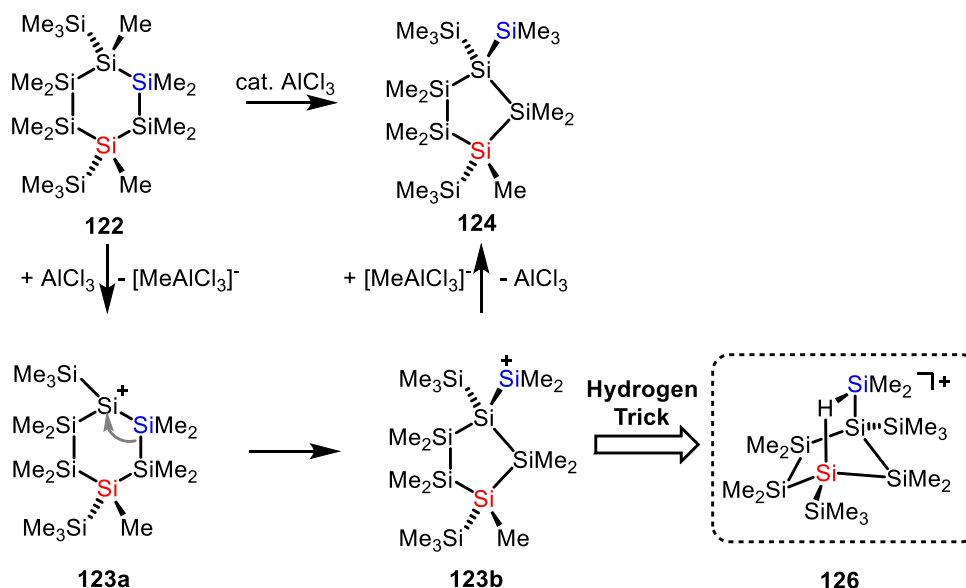
These findings laid the groundwork for further investigations on the rearrangements of polysilanes and germapolysilanes. The clean and selective formation of cation **91** after a complex series of skeletal rearrangements indicates that the formation of a 2e3c Si-H-Si bond can be used to extend the lifetime of highly reactive intermediates and allows their unequivocal spectroscopic detection. The hydrogen trick was extended to other polysilanylsilyl cations and was found to be a useful tool to trap highly reactive silyl cationic species, which could not be isolated or even detected by other means. For example, prior to this work, no evidence was provided for the proposed cationic rearrangement of linear polysilanes. The transformation of tetrasilane **94** into its branched isomer **1** was explored in this work (Scheme 116). Well-designed modification of the starting materials resulted in the successful synthesis and identification of the preliminary proposed, fleeting and highly reactive intermediate **98d** during this rearrangement in the form of three 2e3c hydrogen-bridged analogues, the bissilyl cations **101**, **111** and **115**.



Scheme 116. Abbreviated mechanism of the rearrangement of tetrasilane **94** to give isomer **1**. Cationic intermediate **98d** was identified in the form of its Si-H-Si bridged analogues **101**, **111** and **115**.

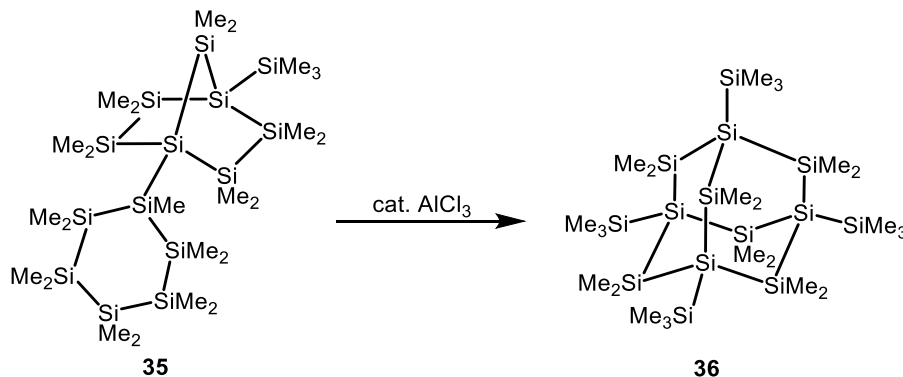
Complementary density functional calculations suggest that the formation of these highly branched isomers is promoted by attractive dispersion interactions between the flanking trimethylsilyl groups. An augmented functional, which includes dispersion contributions, clearly indicates that attractive dispersion energies are the thermodynamic driving force for these unexpected rearrangements.<sup>[140, 144]</sup>

These results encouraged the use of the hydrogen trick to elucidate other, even more complex rearrangements of polysilanes. The rearrangement of six-membered ring polysilanes to five-membered ring polysilanes was already a well-known reaction but mechanistic details were not available. The application of the subtle hydrogen trick facilitated the detection of a cationic intermediate during the rearrangement of cyclohexasilane **122** to cyclopentasilane **124** in the form of its 2e3c hydrogen-bridged analogue, the bisilyl cation **126** (Scheme 117). Consequently, the proposed initial cation, the six-membered ring **123a**, is either not an intermediate or its lifetime is very short and it immediately rearranges to the five-membered ring **123b**.

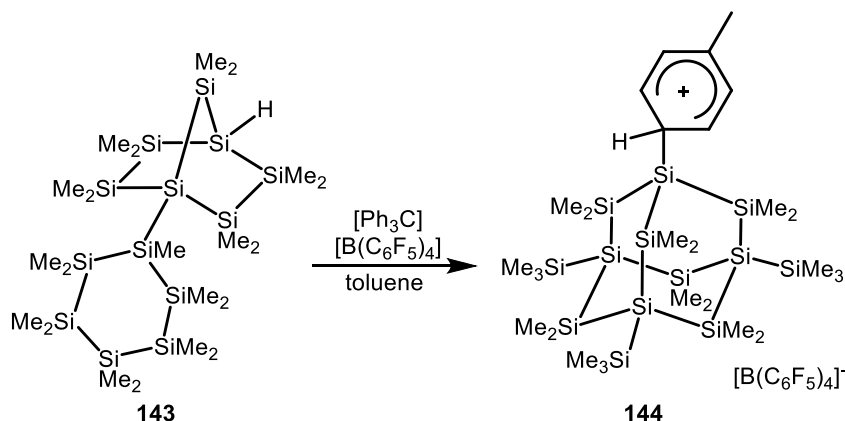


Scheme 117. Mechanism of the rearrangement of cyclohexasilane **122** to give cyclopentasilane **124**. Cationic intermediate **123b** was identified in the form of its Si-H-Si bridged analogue **126**.

The intriguing rearrangement of a tricyclic silane **35** into sila-adamantane **36** found by the Marschner group<sup>[46]</sup> is not yet clarified mechanistically (Scheme 118). This reaction was examined in a few experiments in this work but the design of the precursor has to be improved. Based on the knowledge of arene stabilisation of silyl cations, a modified, hydrogen-substituted precursor might offer a chance to synthesise appropriate silyl cationic intermediates by hydride abstraction reactions. This might clarify the structure of the rearrangement intermediate (Scheme 119). Additionally, the introduction of a second hydrogen atom into the precursor molecule and the application of the elaborated hydrogen trick might facilitate the stabilisation of a cationic intermediate in the form of its 2e3c hydrogen-bridged bis-silyl cation to illuminate the mechanism of this striking rearrangement.



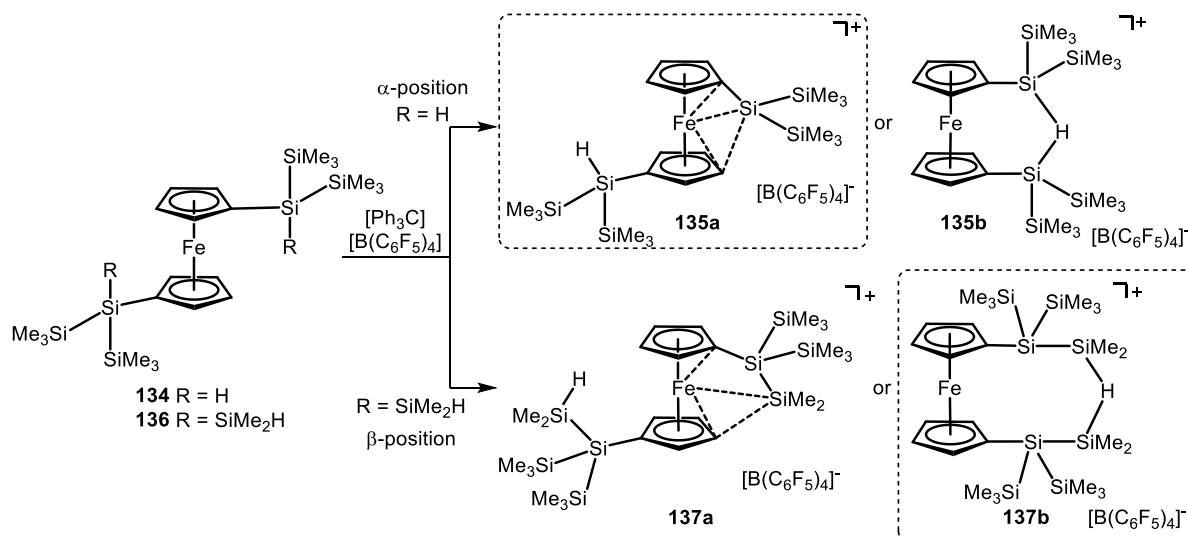
Scheme 118 Rearrangement of bicyclo[2.2.1]heptasilane **35** to give sila-adamantane **36**.<sup>[46]</sup>



Scheme 119. Possible reaction to detect cationic intermediate **144** as a cationic intermediate during the rearrangement towards sila-adamantane **36**.

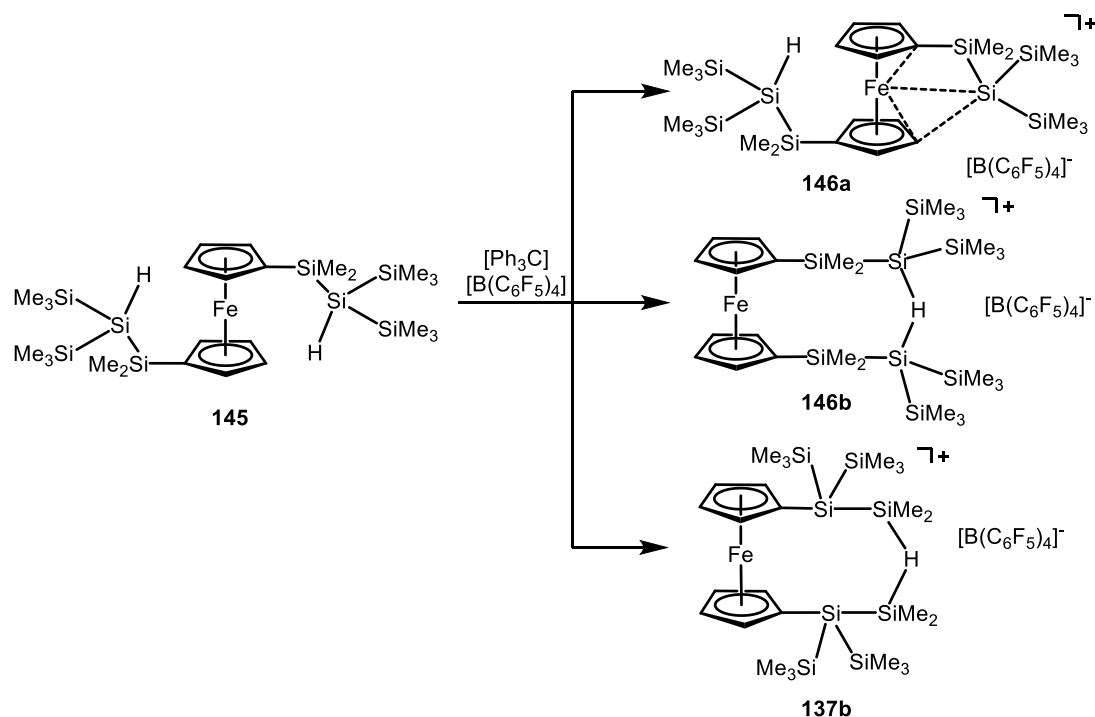
The ability of different substituents to stabilise polysilanylsilyl cations and their competition was tested for two groups, which are widely used for the stabilisation of silylium ions, the ferrocenyl substituent<sup>[77-78]</sup> and the Si-H-Si unit<sup>[106-110, 136]</sup>. Two different ferrocenylsilanes were synthesised which provide both options: either by coordination of the silyl cationic centre by the ferrocene backbone or the formation of a 2e3c Si-H-Si bridge.

It was found that a silyl cation in an  $\alpha$ -position to the Cp-moiety forms the ferrocene-stabilised silylium ion **135a**, whereas a silyl cation in a  $\beta$ -position to the ferrocene backbone gives the 2e3c Si-H-Si bridged compound **137b**. Both ferrocenylsilyl cations **135a** and **137b** were successfully characterised by NMR spectroscopy at very low temperatures.



Scheme 120. Summary of the possible reaction products after hydride abstraction from 1,1'-bissilylferrocenes **134** and **136**.

Together with the knowledge that polysilanylsilyl cations always rearrange to the most highly branched and thermodynamically most stable isomer, this field offers a variety of possibilities. For example, the question arises whether or not the silyl substituent at the ferrocene in compound **145** (Scheme 121) will undergo skeletal rearrangement after hydride abstraction. The cation may form a 2e3c Si-H-Si bridge with or without skeletal rearrangement or it may be stabilised by the ferrocene backbone. The answer to this question should facilitate the use of the ferrocenyl moiety as a preparative tool for the selective formation of cationic intermediates, which should also lead to a control over the formation of rearrangement products.



Scheme 121. Possible reaction products after hydride abstraction from 1,1'-bissilylferrocene **145**.

This work established new preparative methods for the synthesis and detection of polysilanylsilyl and -germyl cations, namely low temperature NMR spectroscopic experiments. A new synthetic approach was established to trap highly reactive and short-lived cationic intermediates. Well-designed hydrogen-substituted polysilanes and germapolysilanes were used to define the position of the initial positively charged atom by a hydride transfer reaction, which allowed the investigation of the rearrangement mechanisms. The subtle choice of substituents and by this means the formation of Si-H-Si bridges and quantum mechanical considerations provided insight into the reaction mechanisms of several Lewis acid-catalysed rearrangements. This research lays the groundwork for mechanistic investigations of Lewis acid-catalysed rearrangements in polysilanes and germapolysilanes. New synthetic and analytical methods provide the possibility to detect cationic intermediates, which have previously only been proposed.

## 5 Experimental

### 5.1 General Experimental Procedures

All manipulations of air- and moisture-sensitive compounds were carried out under an argon or nitrogen atmosphere using Schlenk techniques or a standard glove box (Braun Unilab). Glassware was dried in an oven at  $T = 120\text{ }^{\circ}\text{C}$  and evacuated prior to use. The solvents tetrahydrofuran (THF), dimethoxyethane (DME), *n*-pentane, benzene and toluene were dried over sodium and distilled under a nitrogen atmosphere. Chlorobenzene, *o*-dichlorobenzene and dichloromethane were dried over  $\text{CaCl}_2$  and stored over molecular sieves (4 Å). Benzene- $\text{d}_6$  and toluene- $\text{d}_8$  were stored over molecular sieves (4 Å) after drying over sodium. Chlorobenzene- $\text{d}_5$  and dichloromethane- $\text{d}_2$  were dried over molecular sieves (4 Å).

NMR spectra were recorded on a Bruker Avance 500, a Bruker Avance III 500 or a Varian Inova 300 spectrometer.  $^1\text{H}$  NMR spectra were calibrated against the residual proton signal of the solvent as an internal reference and the  $^{13}\text{C}$  NMR spectra by using the central line of the solvent signal (Table 4).

Table 4. References for the  $^1\text{H}$  and  $^{13}\text{C}$  NMR spectra.

Solvent	Reference	
Acetone	$\delta^1\text{H}((\text{CD}_3)(\text{CD}_2\text{H})\text{CO}) = 2.05$	$\delta^{13}\text{C}((\text{CD}_3)_2\text{CO}) = 29.8$
Benzene	$\delta^1\text{H}(\text{C}_6\text{D}_5\text{H}) = 7.20$	$\delta^{13}\text{C}(\text{C}_6\text{D}_6) = 128.0$
Chlorobenzene	$\delta^1\text{H}(\text{C}_6\text{D}_4\text{HCl}) = 7.14$	$\delta^{13}\text{C}(\text{C}_6\text{D}_5\text{Cl}) = 134.2$
Chloroform	$\delta^1\text{H}(\text{CHCl}_3) = 7.24$	$\delta^{13}\text{C}(\text{CDCl}_3) = 77.0$
Dichloromethane	$\delta^1\text{H}(\text{CDHCl}_2) = 5.32$	$\delta^{13}\text{C}(\text{CD}_2\text{Cl}_2) = 53.8$
Toluene	$\delta^1\text{H}(\text{C}_6\text{D}_5\text{CD}_2\text{H}) = 2.08$	$\delta^{13}\text{C}(\text{C}_6\text{D}_5\text{CD}_3) = 20.4$
Water	$\delta^1\text{H}(\text{DHO}) = 4.79$	- / -

$^{11}\text{B}$  NMR,  $^{19}\text{F}$  NMR and  $^{29}\text{Si}$  NMR spectra were calibrated against external standards (Table 5). The  $^{29}\text{Si}\{^1\text{H}\}$  NMR inverse gated spectra were recorded with a relaxation delay  $\text{D1} = 10\text{ s}$ . Based on experience, in most cases this delay is long enough to allow reliable integration of the peaks. The  $^{29}\text{Si}\{^1\text{H}\}$  INEPT NMR spectra were recorded with delays  $\text{D3} = 0.0084\text{ s}$  and  $\text{D4} = 0.0313\text{ s}$ .

Table 5. References for the  $^{11}\text{B}$ ,  $^{19}\text{F}$  and  $^{29}\text{Si}$  spectra.

NMR Active Nucleus	External Standard	Reference
$^{11}\text{B}$	$\text{BF}_3 \cdot \text{OEt}_2$	$\delta^{11}\text{B}(\text{BF}_3 \cdot \text{OEt}_2) = 0.0$
$^{19}\text{F}$	$\text{CFCl}_3$	$\delta^{19}\text{F}(\text{CFCl}_3) = 0.0$
$^{29}\text{Si}$	$\text{Me}_2\text{HSiCl}$	$\delta^1\text{H}(\text{Me}_2\text{HSiCl}) = 11.1$

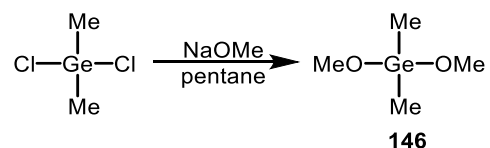
The corresponding spectrometer frequencies and temperatures are indicated individually for every spectrum in the experimental procedures. A clear assignment of the signals was carried out by two-dimensional experiments, such as  $^1\text{H}^{13}\text{C}$  HMQC,  $^1\text{H}^{13}\text{C}$  HMBC,  $^1\text{H}^{29}\text{Si}$  HMQC or  $^1\text{H}^{29}\text{Si}$  HMBC.

IR spectra were recorded on a Bruker Tensor 27 instrument. GC-MS spectra were performed on a Thermo Focus DSQ spectrometer and high resolution mass spectra on a DFS Thermo scientific mass spectrometer. Combustion analyses (C, H, N, S) were obtained with an EuroVector equipment and a Euro EA Element Analyzer. Analysis values for carbon are often too low, which we attribute to the formation and incomplete combustion of silicon carbide, although vanadium pentoxide was used as combustion aid.

## 5.2 Synthesis of Starting Materials

Potassium *tert*-butoxide, lithium tri-*tert*-butoxyaluminium hydride, sodium triethylborohydride solution in toluene, dichlorodimethylgermane, chlorodimethylsilane, chlorotrimethylsilane triethylsilane, tri-*iso*-propylsilane and 18-crown-6 ether were obtained from commercial suppliers and the silanes were dried over molecular sieves. Sodium methanolate was prepared by addition of sodium to an excess of methanol. After all sodium was consumed, the solvent was removed *in vacuo*. Triphenylmethyl tetrakis(pentafluorophenyl) borate ([Ph<sub>3</sub>C][B(C<sub>6</sub>F<sub>5</sub>)<sub>4</sub>]) was prepared according to a modified literature procedure.<sup>[152-153]</sup> Trimethylsilane<sup>[143]</sup>, tetrakis(trimethylsilyl)silane<sup>[154]</sup>, tris(trimethylsilyl)silyltrimethylgermane **50**<sup>[155]</sup>, tetrakis(trimethylsilyl)germane **51**<sup>[156]</sup>, tris(trimethylsilyl)silylpotassium<sup>[118]</sup>, tris(trimethylsilyl)germylpotassium<sup>[69]</sup>, chloropentamethyldisilane<sup>[157]</sup>, 1,1-tris(trimethylsilyl)dimethylphenyldisilane<sup>[118]</sup>, 1,4-bis(trimethylgermyl)-1,1,4,4-tetrakis(trimethylsilyl)tetramethyltetrasilane **45**<sup>[68]</sup>, 1,1,1,4,4,4-hexakis(trimethylsilyl)tetramethyl-1,4-digermatetrasilane **46**<sup>[69]</sup>, 1-trimethylsilyl-4-undecamethylcyclohexasilyldecamethylbicyclo-[2.2.1]heptasilane **35**<sup>[46]</sup>, 1,1'-bis(tris(trimethylsilyl)silyl)ferrocene **139**<sup>[116]</sup>, 1,1'-bis(bis(trimethylsilyl)silyl)ferrocenyldipotassium **155**<sup>[116]</sup> and 1,1'-bis(bis(trimethylsilyl)silyl)ferrocene **134**<sup>[116]</sup> were synthesised according to reported procedures. 1,1,1,4,4-Pentakis(trimethylsilyl)pentamethyltetrasilane **92**<sup>[129]</sup>, 1,1-dihydrido-2,2,5,5-tetrakis(trimethylsilyl)tetramethylcyclopentasilane **88**, dodecamethylcyclohexasilane **3**<sup>[158-159]</sup>, 1,4-dihydrido-1,4-bis(trimethylsilyl)octamethylcyclohexasilane **24**<sup>[10]</sup> were thankfully received from the group of Prof. Marschner.

### Dimethoxydimethylgermane **146**<sup>[160-161]</sup>

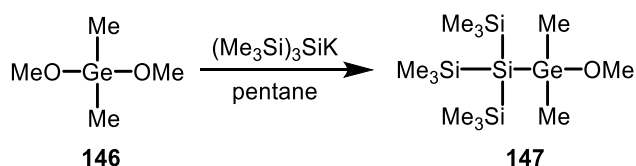


2.84 g (3.5 equiv., 52.57 mmol) of NaOMe was suspended in pentane (40 mL) and 1.74 mL (1 equiv., 15.00 mmol) of dichlorodimethylgermane was slowly added with a syringe. The mixture was stirred overnight at room temperature. Excess NaOMe and formed NaCl were separated from the solution by using a centrifuge (20 min, 2000 rpm) and then the product-containing pentane solution was decanted using a Teflon tube. The salts were washed with 10 mL pentane and again centrifuged and

decanted. The pentane solutions were combined and the product was separated from the solvent by fractional distillation (b.p.: 118°C at ambient pressure (1.45 g, 58 %).

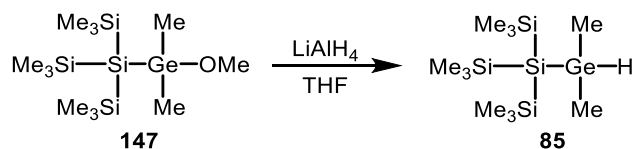
$^1\text{H}$  NMR (500.13 MHz, 297.9 K,  $\text{C}_6\text{D}_6$ ,  $\delta$  ppm): 0.30 (s, 6 H,  $(\text{CH}_3)_2\text{Ge}$ ), 3.54 (s, 6 H,  $\text{Ge}(\text{OCH}_3)_2$ ).  $^{13}\text{C}\{^1\text{H}\}$  NMR (125.77 MHz, 298.1K,  $\text{C}_6\text{D}_6$ ,  $\delta$  ppm): -2.9 ( $(\text{CH}_3)_2\text{Ge}$ ), 51.6 ( $\text{Ge}(\text{OCH}_3)_2$ ). Mass required for  $\text{C}_4\text{H}_{12}\text{GeO}_2$ : 166.0. Mass found GC/MS: 164.9 (0.5) [ $\text{M}^+-\text{H}$ ], 150.8 (100) [ $\text{M}^+-\text{Me}$ ], 135.9 (72) [ $\text{M}^+-\text{OMe}$ ], 120.9 (88) [ $\text{M}^+-\text{OMe-Me}$ ], 104.9 (84) [ $\text{M}^+-\text{OMe-2Me}$ ].

Tris(trimethylsilyl)silyldimethylmethoxygermane **147**



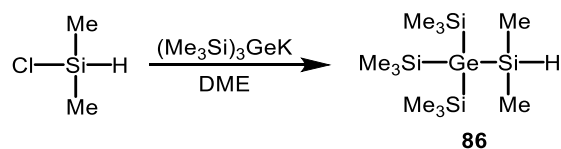
A solution of 4.50 mmol (1 equiv.) of tris(trimethylsilyl)silylpotassium in pentane (40 mL) and a solution of 0.75 g (1 equiv., 4.50 mmol) of dimethoxydimethylgermane **146** in pentane (40 mL) were cooled to  $T = 0^\circ\text{C}$ . The silylpotassium compound was added drop wise to the germane solution. The ice bath was allowed to warm to room temperature overnight. The reaction mixture was then hydrolysed with 1 M hydrochloric acid. The organic layer was separated and dried over sodium sulfate. The solvent was removed under reduced pressure and the product was purified by Kugelrohr distillation (0.62 g, 36 %). Due to the use of hydrochloric acid about 14% of the corresponding germly chloride was formed as a by-product, which was observed in the GC chromatograms and the NMR spectra.

$^1\text{H}$  NMR (499.87 MHz, 305.0 K,  $\text{C}_6\text{D}_6$ ,  $\delta$  ppm): 0.34 (s, 27 H,  $(\text{CH}_3)_3\text{Si}$ ), 0.60 (s, 6 H,  $(\text{CH}_3)_2\text{Ge}$ ), 3.54 (s, 3H,  $\text{CH}_3\text{OGe}$ ).  $^{13}\text{C}\{^1\text{H}\}$  NMR (125.69 MHz, 305.0 K,  $\text{C}_6\text{D}_6$ ,  $\delta$  ppm): 2.6 ( $(\text{CH}_3)_3\text{Si}$ ), 4.1 ( $(\text{CH}_3)_2\text{Ge}$ ), 52.6 ( $\text{CH}_3\text{OGe}$ ).  $^{29}\text{Si}\{^1\text{H}\}$  INEPT NMR (99.31 MHz, 305.0 K,  $\text{C}_6\text{D}_6$ ,  $\delta$  ppm): -124.6 ( $((\text{CH}_3)_3\text{Si})_3\text{Si}$ ), -9.9 ( $((\text{CH}_3)_3\text{Si})_3\text{Si}$ ). Mass required for  $\text{C}_{12}\text{H}_{36}\text{GeOSi}_4$ : 382.1. Mass found GC/MS: 367.2 (1) [ $\text{M}^+-\text{Me}$ ], 351.2 (0.5) [ $\text{M}^+-\text{OMe}$ ], 278.0 (8) [ $\text{M}^+-\text{SiMe}_3-\text{OMe}$ ], 205.1 (13) [ $\text{M}^+-2\text{SiMe}_3-\text{OMe}$ ], 73.0 (100) [ $\text{Me}_3\text{Si}^+$ ]. No satisfactory combustion analysis was obtained due to contamination with the chloride side-product.

Tris(trimethylsilyl)silyldimethylgermane **85**

A solution of 0.62 g (1 equiv., 1.62 mmol) of tris(trimethylsilyl)silyldimethylmethoxygermane **147** in THF (30 mL) and a suspension of 0.062 g (1 equiv., 1.62 mmol) of LiAlH<sub>4</sub> in THF (50 mL) were cooled to T = 0 °C with an ice bath. The solution of silagermane **85** was added to the LiAlH<sub>4</sub> suspension and the reaction mixture was stirred for 20 min at T = 0 °C before it was allowed to warm to room temperature and stirred for another 20 min. The mixture was slowly added to ice cold 2 M sulfuric acid. The phases were separated and the aqueous phase was extracted two times with 50 mL diethyl ether. The combined organic phases were dried over sodium sulfate, filtered and the solvent was removed under reduced pressure. The product was crystallised from ethanol as a waxy, colourless solid (0.38 g, 1.09 mmol, 67 %).

<sup>1</sup>H NMR (499.87 MHz, 305.0 K, C<sub>6</sub>D<sub>6</sub>, δ ppm): 0.30 (s, 27 H, (CH<sub>3</sub>)<sub>3</sub>Si), 0.50 (d, <sup>3</sup>J<sub>H,H</sub> = 4.2 Hz, 6 H, (CH<sub>3</sub>)<sub>2</sub>Ge), 4.04 (sept, <sup>3</sup>J<sub>H,H</sub> = 4.2 Hz, 1 H, GeH). <sup>13</sup>C{<sup>1</sup>H} NMR (125.69 MHz, 305.0 K, C<sub>6</sub>D<sub>6</sub>, δ ppm): -2.3 ((CH<sub>3</sub>)<sub>2</sub>Ge), 2.5 ((CH<sub>3</sub>)<sub>3</sub>Si). <sup>29</sup>Si{<sup>1</sup>H} NMR (99.31 MHz, 305.0 K, C<sub>6</sub>D<sub>6</sub>, δ ppm): -128.3 (((CH<sub>3</sub>)<sub>3</sub>Si)<sub>3</sub>Si), -9.4 (((CH<sub>3</sub>)<sub>3</sub>Si)<sub>2</sub>Si). Mass required for C<sub>11</sub>H<sub>34</sub>GeSi<sub>4</sub>: 352.1. Mass found GC/MS: 351.1 (0.1) [M<sup>+</sup>-H], 337.1 (0.6) [M<sup>+</sup>-Me-H], 278.0 (30) [M<sup>+</sup>-SiMe<sub>3</sub>-H], 189.1 (13) [M<sup>+</sup>-2SiMe<sub>3</sub>-Me-H], 174.0 (4) [M<sup>+</sup>-SiMe<sub>3</sub>-GeMe<sub>2</sub>H], 73.1 (100) [Me<sub>3</sub>Si<sup>+</sup>]. IR (ATR, neat):  $\tilde{\nu}_{\text{Ge-H}}$  1982 cm<sup>-1</sup>, Anal. found/calcd. for C<sub>11</sub>H<sub>34</sub>GeSi<sub>4</sub>: C 37.63/37.60, H 10.67/9.75.

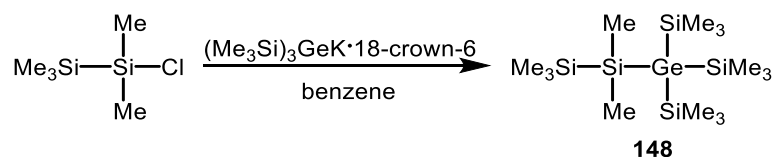
Tris(trimethylsilyl)germyldimethylsilane **86**<sup>[162]</sup>

Solutions of 2.99 mmol (1 equiv.) of tris(trimethylsilyl)germylpotassium in DME (30 mL) and of 0.6 mL (1.85 equiv., 5.52 mmol) of chlorodimethylsilane in DME (30 mL) were cooled to T = 0 °C with an ice bath. The germylpotassium compound was slowly added to the chlorosilane solution during 1 h. The ice bath was allowed to warm to room temperature overnight. The reaction mixture was then

hydrolysed with 1 M sulfuric acid. The organic layer was separated and the aqueous phase was extracted with diethyl ether (10 mL). The combined organic phases were dried over sodium sulfate and the filtrate was concentrated to 5 mL under reduced pressure. The product **86** crystallised by adding acetonitrile (2 mL) as a colourless, waxy solid (0.847 g, 80.6 %).

$^1\text{H}$  NMR (499.87 MHz, 305.0 K,  $\text{CDCl}_3$ ,  $\delta$  ppm)<sup>[162]</sup>: 0.22 (s, 27 H,  $(\text{CH}_3)_3\text{Si}$ ), 0.27 (d,  $^3J_{\text{H,H}} = 4.2$  Hz, 6 H,  $(\text{CH}_3)_2\text{Si}$ ), 4.12 (sept,  $^3J_{\text{H,H}} = 4.2$  Hz, 1 H, SiH).  $^{13}\text{C}\{^1\text{H}\}$  NMR (125.71 MHz, 305.0 K,  $\text{CDCl}_3$ ,  $\delta$  ppm): -1.4 ( $(\text{CH}_3)_2\text{Si}$ ), 3.1 ( $(\text{CH}_3)_3\text{Si}$ ).  $^{29}\text{Si}$  INEPT NMR (99.31 MHz, 305.0 K,  $\text{CDCl}_3$ ,  $\delta$  ppm): -29.8 (dsept,  $^1J_{\text{Si,H}} = 180.5$  Hz,  $^2J_{\text{Si,H}} = 7.0$  Hz, SiH), -4.7 ( $(\text{CH}_3)_3\text{Si}$ ). Mass required for  $\text{C}_{11}\text{H}_{34}\text{GeSi}_4$ : 352.1. Mass found GC/MS:  $m/z$  (%) = 351.1 (0.3) [ $\text{M}^+ - \text{H}$ ], 337.1 (2.5) [ $\text{M}^+ - \text{Me} - \text{H}$ ], 278.1 (64) [ $\text{M}^+ - \text{SiMe}_3 - \text{H}$ ], 189.9 (22) [ $\text{M}^+ - 2\text{SiMe}_3 - \text{Me} - \text{H}$ ], 174.0 (2) [ $\text{M}^+ - \text{SiMe}_3 - \text{GeMe}_2\text{H}$ ], 73.0 (100) [ $\text{Me}_3\text{Si}^+$ ]. IR (ATR, neat):  $\tilde{\nu}_{\text{Si-H}}$  2085  $\text{cm}^{-1}$ . Anal. found/calcd. for  $\text{C}_{11}\text{H}_{34}\text{GeSi}_4$ : C 36.31/37.60, H 9.98/9.75.

#### 1,1,1-Tris(trimethylsilyl)pentamethyl-1-germatrisilane **148**

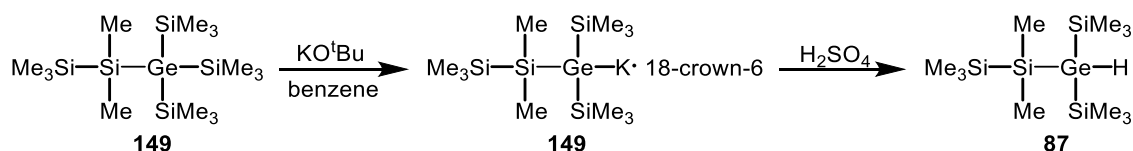


A solution of 1.37 mmol (1 equiv.) of tris(trimethylsilyl)germylpotassium-18-crown-6 in benzene (3 mL) was added drop wise to a solution of 0.25 g (1.1 equiv., 1.51 mmol) of chloropentamethylsilane in benzene (3 mL). After 5 h, the solution mixture was quenched with 1 M sulfuric acid and the phases were separated. The aqueous phase was extracted with pentane and the combined organic phases were dried over sodium sulfate, filtered and the solvent was removed under reduced pressure. The product **148** was obtained as colourless crystals by crystallisation from methanol/diethyl ether 1:2 (0.42 g, 73 %).

$^1\text{H}$  NMR (299.94 MHz, 298.0 K,  $\text{C}_6\text{D}_6$ ,  $\delta$  ppm): 0.22 (s, 9 H,  $\text{Si}(\text{CH}_3)_2\text{Si}(\text{CH}_3)_3$ ), 0.36 (s, 27 H,  $(\text{CH}_3)_3\text{Si}$ ), 0.40 (s, 6 H,  $\text{Si}(\text{CH}_3)_2\text{Si}(\text{CH}_3)_3$ ).  $^{13}\text{C}\{^1\text{H}\}$  NMR (75.43 MHz, 298.0 K,  $\text{C}_6\text{D}_6$ ,  $\delta$  ppm): -0.8 ( $\text{Si}(\text{CH}_3)_2\text{Si}(\text{CH}_3)_3$ ), -0.4 ( $\text{Si}(\text{CH}_3)_2\text{Si}(\text{CH}_3)_3$ ), 4.0 ( $(\text{CH}_3)_3\text{Si}$ ).  $^{29}\text{Si}\{^1\text{H}\}$  INEPT NMR (59.59 MHz, 295.0 K,  $\text{C}_6\text{D}_6$ ,  $\delta$  ppm): -34.0 ( $\text{Si}(\text{CH}_3)_2\text{Si}(\text{CH}_3)_3$ ), -15.5 ( $\text{Si}(\text{CH}_3)_2\text{Si}(\text{CH}_3)_3$ ), -5.2 ( $(\text{CH}_3)_3\text{Si}$ ). Mass required for  $\text{C}_{14}\text{H}_{42}\text{GeSi}_5$ : 424.1. Mass found GC/MS:  $m/z$  (%) = 424 (1) [ $\text{M}^+$ ], 408 (1) [ $\text{M}^+ - \text{Me} - \text{H}$ ], 351 (3) [ $\text{M}^+ - \text{SiMe}_3$ ], 278 (10) [ $\text{M}^+ - 2\text{SiMe}_3$ ], 259 (1) [ $\text{GeSi}_3\text{C}_7\text{H}_{17}^+$ ], 243 (1) [ $\text{GeSi}_3\text{C}_6\text{H}_{13}^+$ ], 219 (3) [ $\text{GeSi}_2\text{C}_6\text{H}_{17}^+$ ], 203 (11) [ $\text{M}^+ - 3\text{SiMe}_3 - 2\text{H}$ ];

187(8)[M<sup>+</sup>-3SiMe<sub>3</sub>-Me-4H]; 147 (7) [GeSiMe<sub>3</sub><sup>+</sup>]; 131 (35) [SiMe<sub>3</sub>SiMe<sub>2</sub><sup>+</sup>]; 73 (100) [SiMe<sub>3</sub><sup>+</sup>]. Anal. found/calcd. for C<sub>14</sub>H<sub>42</sub>GeSi<sub>5</sub> C 39.33/39.70, H 9.50/9.99.

1,1-bis(trimethylsilyl)pentamethyl-1-germatrisilane **87**



A mixture of 0.21 g (1 equiv., 0.49 mmol) of germatrisilane **148**, 0.062 g (1.04 equiv., 0.51 mmol) of potassium *tert*-butoxide and 0.134 g (1.04 equiv., 0.51 mmol) of 18-crown-6 ether was dissolved in benzene (2 mL). After the complete formation of the germylpotassium compound **149** was confirmed by NMR spectroscopy, the solution was added to a stirred mixture of degassed diethyl ether (10 mL) and degassed 2M sulfuric acid (20 mL) cooled with an ice bath. The phases were separated, the aqueous phase was extracted with degassed diethyl ether and the combined organic phases dried over sodium sulfate. The solvents were removed under reduced pressure and the product **87** was obtained as a colourless oil (0.15 g, 91 %) The germane is sensitive to oxygen and should be stored under argon at T = -20 °C.

1-Potassium-1,1-bis(trimethylsilyl)pentamethyl-1-germatrisilane **149**

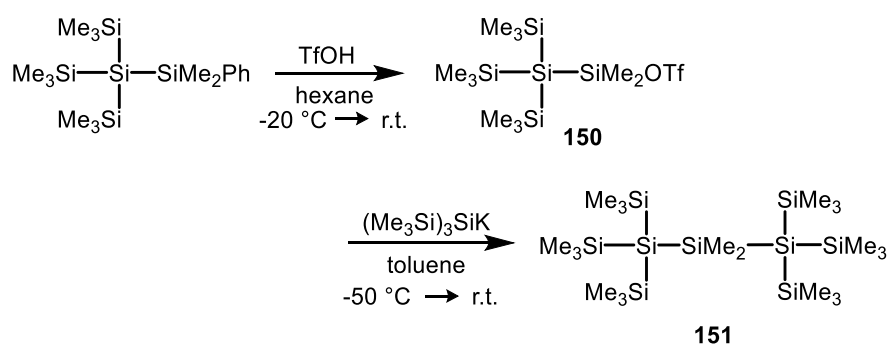
<sup>1</sup>H NMR (299.94 MHz, 298.0 K, C<sub>6</sub>D<sub>6</sub>, δ ppm): 0.39 (s, 9 H (Si(CH<sub>3</sub>)<sub>2</sub>Si(CH<sub>3</sub>)<sub>3</sub>), 0.59 (s, 18 H ((CH<sub>3</sub>)<sub>3</sub>Si)<sub>2</sub>GeK), 0.64 (s, 6 H, Si(CH<sub>3</sub>)<sub>2</sub>Si(CH<sub>3</sub>)<sub>3</sub>), 3.25 (s, 24 H, CH<sub>2</sub>O). <sup>13</sup>C{<sup>1</sup>H} NMR (75.43 MHz, 295.0 K, C<sub>6</sub>D<sub>6</sub>, δ ppm): 0.0 (Si(CH<sub>3</sub>)<sub>2</sub>Si(CH<sub>3</sub>)<sub>3</sub>), 3.5 (Si(CH<sub>3</sub>)<sub>2</sub>Si(CH<sub>3</sub>)<sub>3</sub>), 8.5 ((CH<sub>3</sub>)<sub>3</sub>Si)<sub>2</sub>GeK, 70.0 (CH<sub>2</sub>O). <sup>29</sup>Si{<sup>1</sup>H} INEPT NMR (59.59 MHz, 295.0 K, C<sub>6</sub>D<sub>6</sub>, δ ppm): -33.0 (Si(CH<sub>3</sub>)<sub>2</sub>Si(CH<sub>3</sub>)<sub>3</sub>), -16.6 (Si(CH<sub>3</sub>)<sub>2</sub>Si(CH<sub>3</sub>)<sub>3</sub>), -3.4 (((CH<sub>3</sub>)<sub>3</sub>Si)<sub>2</sub>GeK). Mass required for C<sub>13</sub>H<sub>38</sub>GeSi<sub>4</sub> after ethylbromide derivatization: 380.1. Mass found after ethylbromide derivatisation GC/MS: m/z (%) = 380 (1) [M<sup>+</sup>]; 365 (1) [M<sup>+</sup>-Me]; 350 (3) [M<sup>+</sup>-Et-H]; 307 (1) [M<sup>+</sup>-SiMe<sub>3</sub>]; 292 (1) [M<sup>+</sup>-SiMe<sub>3</sub>-Me]; 277 (3) [M<sup>+</sup>-SiMe<sub>3</sub>-2Me]; 262 (1) [M<sup>+</sup>-SiMe<sub>3</sub>-3Me]; 234 (3) [M<sup>+</sup>-2SiMe<sub>3</sub>]; 219 (8) [M<sup>+</sup>-2SiMe<sub>3</sub>-Me]; 203 (17) [M<sup>+</sup>-2SiMe<sub>3</sub>-2Me-H]; 187 (6) [M<sup>+</sup>-2SiMe<sub>3</sub>-3Me-2H]; 159 (4) [M<sup>+</sup>-3SiMe<sub>3</sub>-H]; 145 (10) [M<sup>+</sup>-3SiMe<sub>3</sub>-Me]; 131 (33) [GeSiC<sub>2</sub>H<sub>5</sub><sup>+</sup>]; 115 (9) [GeSiCH<sup>+</sup>]; 73 (100) [SiMe<sub>3</sub><sup>+</sup>].

1,1-Bis(trimethylsilyl)pentamethyl-1-germatrisilane **87**

<sup>1</sup>H NMR (499.87 MHz, 305.1 K, C<sub>6</sub>D<sub>6</sub>, δ ppm): 0.22 (s, 9 H, Si(CH<sub>3</sub>)<sub>2</sub>Si(CH<sub>3</sub>)<sub>3</sub>), 0.35 (s, 18 H, ((CH<sub>3</sub>)<sub>3</sub>Si)<sub>2</sub>Ge), 0.40 (s, 6 H, Si(CH<sub>3</sub>)<sub>2</sub>Si(CH<sub>3</sub>)<sub>3</sub>), 2.25 (s, 1 H, GeH). <sup>13</sup>C{<sup>1</sup>H} NMR (125.71 MHz, 305.0 K, CDCl<sub>3</sub>, δ ppm): -1.7

(Si(CH<sub>3</sub>)<sub>2</sub>Si(CH<sub>3</sub>)<sub>2</sub>), -1.6 (Si(CH<sub>3</sub>)<sub>3</sub>Si(CH<sub>3</sub>)<sub>2</sub>), 3.1 (((CH<sub>3</sub>)<sub>3</sub>Si)<sub>2</sub>Ge). <sup>29</sup>Si{<sup>1</sup>H} NMR (99.31 MHz, 305.0 K, C<sub>6</sub>D<sub>6</sub>, δ ppm): -34.3 (Si(CH<sub>3</sub>)<sub>2</sub>Si(CH<sub>3</sub>)<sub>3</sub>), -16.2 (Si(CH<sub>3</sub>)<sub>2</sub>Si(CH<sub>3</sub>)<sub>3</sub>), -5.7 (((CH<sub>3</sub>)<sub>3</sub>Si)<sub>2</sub>Ge). Mass required for C<sub>11</sub>H<sub>34</sub>GeSi<sub>4</sub>: 352.1. Mass found GC/MS: 335 (2) [M<sup>+</sup>-Me-2H]; 278 (27) [M<sup>+</sup>-SiMe<sub>3</sub>-H]; 263 (2) [M<sup>+</sup>-SiMe<sub>3</sub>-Me-H]; 203 (13) [M<sup>+</sup>-2SiMe<sub>3</sub>-2H]; 189 (10) [M<sup>+</sup>-2SiMe<sub>3</sub>-Me-2H]; 173 (2) [M<sup>+</sup>-2SiMe<sub>3</sub>-2Me-2H]; 131 (24) [SiMe<sub>3</sub>SiMe<sub>2</sub><sup>+</sup>]; 115 (14) [Si<sub>2</sub>C<sub>4</sub>H<sub>11</sub><sup>+</sup>]; 73 (100) [SiMe<sub>3</sub><sup>+</sup>]. IR (ATR, neat)  $\tilde{\nu}_{\text{Ge-H}}$  1951 cm<sup>-1</sup>. Anal. found/calcd. for C<sub>11</sub>H<sub>34</sub>GeSi<sub>4</sub> C 38.85/37.60, H 9.41/9.75.

### 1,1,1,3,3,3-Hexakis(trimethylsilyl)dimethyltrisilane **151**



The trisilane was synthesised according to a modified literature procedure, instead of the bromosilane the silyl triflate was prepared.<sup>[118]</sup> A solution of 1.37 g (1 equiv., 3.60 mmol) of 1,1-tris(trimethylsilyl)dimethylphenyldisilane in hexane (20 mL) was cooled to T = -20 °C and 0.32 mL (1 equiv., 0.54 g, 3.60 mmol) of trifluoromethanesulfonic acid was added dropwise with a syringe. The complete formation of the silyl triflate **150** was confirmed by <sup>29</sup>Si NMR spectroscopy. The solvent was removed under reduced pressure and the remaining residue was dissolved in toluene (10 mL). A solution of 3.60 mmol (1 equiv.) of tris(trimethylsilyl)silylpotassium in toluene (5 mL) was slowly added at T = -50 °C to the solution of silyl triflate. The reaction mixture was allowed to warm to room temperature overnight. The solution was added to an aqueous H<sub>2</sub>SO<sub>4</sub>/ice mixture, the phases were separated, the aqueous layer was extracted with diethyl ether and the combined organic phases were dried over Na<sub>2</sub>SO<sub>4</sub>. After removal of the solvent under reduced pressure and crystallisation from ethanol/ethyl acetate a colourless, waxy solid was obtained (1.79 g, 90 %).

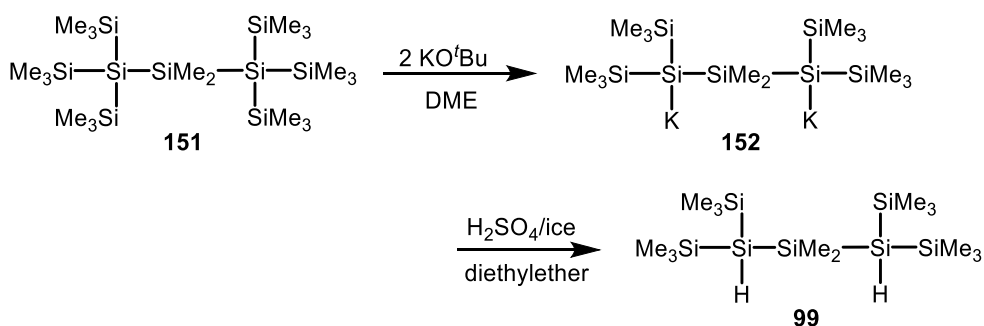
### 1,1-Tris(trimethylsilyl)dimethyltrifluoromethansulfonyldisilane **150**

$^1\text{H}$  NMR (499.87 MHz, 305.1 K, hexane/ $\text{D}_2\text{O}$ -lock,  $\delta$  ppm): 0.77 (s, 27 H,  $\text{Si}(\text{CH}_3)_3$ ), 1.19 (s, 6 H,  $\text{Si}(\text{CH}_3)_2\text{OTf}$ ).  $^{29}\text{Si}\{^1\text{H}\}$  NMR (99.31 MHz, 305.0 K, hexane/ $\text{D}_2\text{O}$ -lock,  $\delta$  ppm): -132.5 ( $\text{Si}_4\text{Si}$ ), -9.7 ( $\text{Si}(\text{CH}_3)_3$ ), 53.7 ( $\text{Si}(\text{CH}_3)_2\text{OTf}$ ).

### 1,1,1,3,3,3-Hexakis(trimethylsilyl)dimethyltrisilane **151**<sup>[118]</sup>

$^1\text{H}$  NMR (499.87 MHz, 305.1 K,  $\text{C}_6\text{D}_6$ ,  $\delta$  ppm): 0.40 (s, 54 H,  $\text{Si}(\text{CH}_3)_3$ ), 0.67 (s, 6 H,  $\text{Si}(\text{CH}_3)_2$ ).  $^{29}\text{Si}\{^1\text{H}\}$  NMR (99.31 MHz, 305.0 K,  $\text{C}_6\text{D}_6$ ,  $\delta$  ppm): -118.5 ( $\text{Si}_4\text{Si}$ ), -26.1 ( $\text{Si}(\text{CH}_3)_2$ ), -9.6 ( $\text{Si}(\text{CH}_3)_3$ ).

### 1,3-Dihydrido-1,1,3,3-tetrakis(trimethylsilyl)dimethyltrisilane **99**



A solution of 0.36 g (2.2 equiv., 3.25 mmol) of potassium *tert*-butoxide in DME (10 mL) was added to a solution of 0.82 g (1 equiv., 1.48 mmol) of trisilane **151**<sup>[118]</sup> in DME (10 mL) at room temperature. The reaction mixture immediately turned yellow and was stirred overnight. The formation of the dianion **152** was followed by  $^{29}\text{Si}\{^1\text{H}\}$  NMR spectroscopy. The solution of 1,3-dipotassiumtrisilane **152** was slowly dropped into a mixture of ice, 10 mL 1 M sulfuric acid and 20 mL diethyl ether. The two phases were separated and the aqueous phase was washed two times with 20 mL diethyl ether. The combined organic phases were dried over  $\text{Na}_2\text{SO}_4$ . The  $\text{Na}_2\text{SO}_4$  was removed by filtration and the solvent was evacuated under reduced pressure. The crude colourless oil was purified by Kugelrohr distillation ( $T = 100\text{ }^\circ\text{C}$ ,  $p = 1.3 \cdot 10^{-1}$  mbar) to give a colourless oil (0.26 g, 0.64 mmol, 44%).

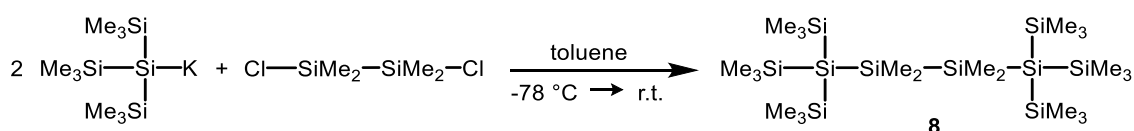
### 1,3-Dipotassium-1,1,3,3-tetrakis(trimethylsilyl)dimethyltrisilane **152**<sup>[34]</sup>

$^{29}\text{Si}\{^1\text{H}\}$  INEPT NMR (99.31 MHz, 305.0 K, DME/ $\text{D}_2\text{O}$ -lock,  $\delta$  ppm): -171.6 ( $\text{SiK}$ ), -16.6 ( $\text{Si}(\text{CH}_3)_2$ ), -4.7 ( $\text{Si}(\text{CH}_3)_3$ ).

### 1,3-Dihydrido-1,1,3,3-tetrakis(trimethylsilyl)dimethyltrisilane **99**

$^1\text{H}$  NMR (499.87 MHz, 305.0 K,  $\text{C}_6\text{D}_6$ ,  $\delta$  ppm): 0.34 (s, 36 H,  $\text{Si}(\text{CH}_3)_3$ ), 0.54 (s, 6 H,  $\text{Si}(\text{CH}_3)_2$ ), 2.78 (s, 2 H, Si-H,  $^1J_{\text{Si,H}} = 190$  Hz).  $^{13}\text{C}\{^1\text{H}\}$  NMR (125.71 MHz, 305.0 K,  $\text{C}_6\text{D}_6$ ,  $\delta$  ppm): 1.2 ( $\text{Si}(\text{CH}_3)_2$ ), 2.3 ( $\text{Si}(\text{CH}_3)_3$ ).  $^{29}\text{Si}\{^1\text{H}\}$  NMR (99.31 MHz, 305.0 K,  $\text{C}_6\text{D}_6$ ,  $\delta$  ppm): -109.1 (SiH), -35.9 ( $\text{Si}(\text{CH}_3)_2$ ), -11.2 ( $\text{Si}(\text{CH}_3)_3$ ). HR/MS found/calcd. for  $\text{C}_{14}\text{H}_{44}\text{Si}_7$ : 409.1892/409.1906. IR:  $\tilde{\nu}_{\text{Si-H}} = 2061\text{ cm}^{-1}$  (ATR, neat); Anal. found/calcd. for  $\text{C}_{14}\text{H}_{44}\text{Si}_7$ : C 37.62/41.10, H 10.95/10.84.

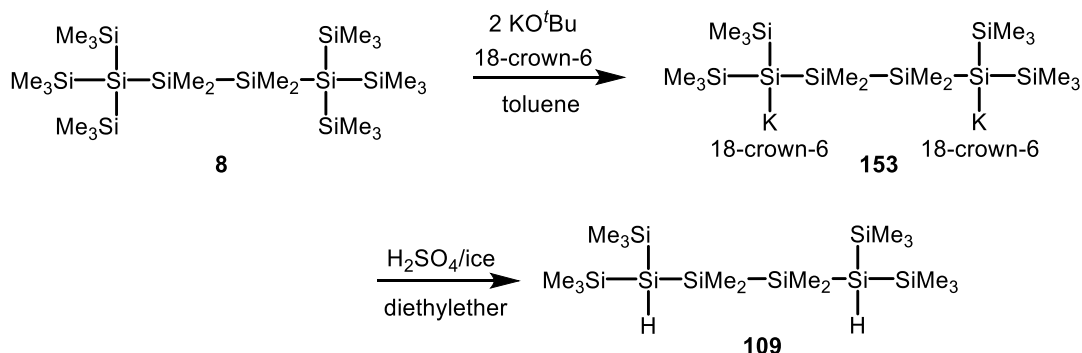
### 1,1,1,4,4,4-Hexakis(trimethylsilyl)tetramethyltetrasilane **8**<sup>[9, 31, 45]</sup>



A solution of 1.03 g (1 equiv., 5.50 mmol) of 1,2-dichlorotetramethyltrisilane in toluene (10 mL) at  $T = -78\text{ }^\circ\text{C}$  was added to a solution of 11.00 mmol (2 equiv.) of tris(trimethylsilyl)silylpotassium in toluene (20 mL) within 30 min. After stirring overnight at room temperature, the mixture was subjected to aqueous workup (dilute sulfuric acid, extraction with ether, drying over sodium sulfate). After removal of the solvent the product **8** was obtained as colourless wax (3.18 g, 5.20 mmol, 95 %).

$^1\text{H}$  NMR (499.87 MHz, 305.0 K,  $\text{CDCl}_3$ ,  $\delta$  ppm): 0.22 (s, 54 H,  $\text{Si}(\text{CH}_3)_3$ ), 0.36 (s, 12 H,  $\text{Si}(\text{CH}_3)_2$ ).  $^{13}\text{C}\{^1\text{H}\}$  NMR (125.71 MHz, 305.0 K,  $\text{CDCl}_3$ ,  $\delta$  ppm): 1.2 ( $\text{Si}(\text{CH}_3)_2$ ), 3.5 ( $\text{Si}(\text{CH}_3)_3$ ).  $^{29}\text{Si}\{^1\text{H}\}$  NMR (99.31 MHz, 305.0 K,  $\text{CDCl}_3$ ,  $\delta$  ppm): -127.7 ( $\text{Si}_4\text{Si}$ ), -29.8 ( $\text{Si}(\text{CH}_3)_2$ ), -9.5 ( $\text{Si}(\text{CH}_3)_3$ ).

### 1,4-Dihydrido-1,1,4,4-tetrakis(trimethylsilyl)tetramethyltetrasilane **109**<sup>[34]</sup>



A solution of 0.27 g (2.2 equiv., 2.20 mmol) of potassium *tert*-butoxide and 0.53 g (2 equiv., 2.00 mmol) of 18-crown-6 ether in benzene (10 mL) was added to a solution of 0.61 g (1 equiv., 1.00 mmol) of tetrasilane **8** in benzene (10 mL) at room temperature. The reaction mixture immediately turned yellow and was stirred overnight. The formation of the dianion **153** was confirmed by  $^{29}\text{Si}\{^1\text{H}\}$  NMR spectroscopy. Then the solution of 1,4-dipotassiumtetrasilane · 2 18-crown-6 **153** was hydrolysed by adding it to a mixture of ice, 1M sulfuric acid (25 mL) and diethyl ether (15 mL). The two phases were separated and the aqueous phase washed two times with pentane (10 mL). The combined organic phases were dried over  $\text{Na}_2\text{SO}_4$ . The  $\text{Na}_2\text{SO}_4$  was removed by filtration and the solvent was evacuated under reduced pressure. After recrystallisation from acetone, the product was obtained as colourless solid (0.39 g, 0.84 mmol, 84 %).

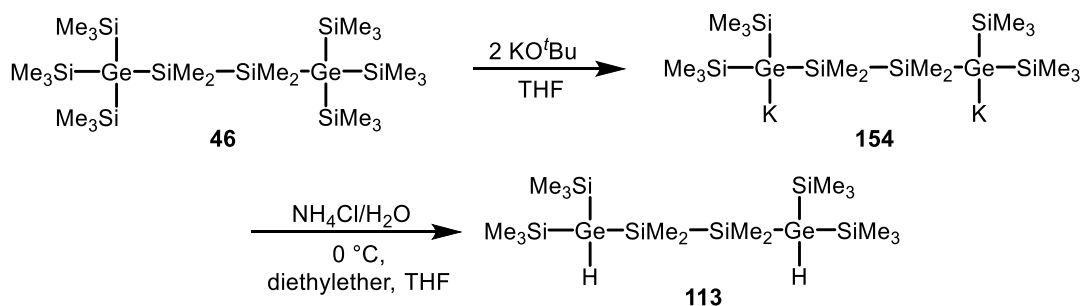
1,4-Dipotassium-1,1,4,4-tetrakis(trimethylsilyl)tetramethyltetrasilane · 2 18-crown-6 **153**<sup>[9]</sup>

$^1\text{H}$  NMR (499.87 MHz, 305.1 K,  $\text{C}_6\text{H}_6$ ,  $\text{D}_2\text{O}$ -lock  $\delta$  ppm): 0.81 (s, 36 H,  $\text{Si}(\text{CH}_3)_3$ ), 0.92 (s, 12 H  $\text{Si}(\text{CH}_3)_2$ ), 3.43 (s, 48 H,  $\text{CH}_2\text{O}$ ).  $^{13}\text{C}\{^1\text{H}\}$  NMR (125.71 MHz, 305.0 K,  $\text{C}_6\text{H}_6$ ,  $\text{D}_2\text{O}$ -lock,  $\delta$  ppm): 5.0 ( $\text{Si}(\text{CH}_3)_2$ ), 8.4 ( $\text{Si}(\text{CH}_3)_3$ ), 69.7 ( $\text{CH}_2\text{O}$ ).  $^{29}\text{Si}\{^1\text{H}\}$  NMR (99.31 MHz, 305.0 K,  $\text{C}_6\text{H}_6$ ,  $\text{D}_2\text{O}$ -lock,  $\delta$  ppm): -3.8 ( $\text{Si}(\text{CH}_3)_3$ ), -24.5 ( $\text{Si}(\text{CH}_3)(\text{CH}_3)_2$ ), -189.6 ( $\text{SiK}$ ).

1,4-Dihydrido-1,1,4,4-tetrakis(trimethylsilyl)tetramethyltetrasilane **109**<sup>[34]</sup>

$^1\text{H}$  NMR (499.87 MHz, 305.1 K,  $\text{C}_6\text{D}_6$ ,  $\delta$  ppm): 0.34 (s, 36 H,  $\text{Si}(\text{CH}_3)_3$ ), 0.49 (s, 12 H,  $\text{Si}(\text{CH}_3)_2$ ), 2.74 (s, 2 H,  $\text{SiH}$ ).  $^{13}\text{C}\{^1\text{H}\}$  NMR (125.71 MHz, 305.0 K,  $\text{C}_6\text{D}_6$ ,  $\delta$  ppm): -1.3 ( $\text{Si}(\text{CH}_3)_2$ ), 2.4 ( $\text{Si}(\text{CH}_3)_3$ ).  $^{29}\text{Si}\{^1\text{H}\}$  NMR (99.31 MHz, 305.0 K,  $\text{C}_6\text{D}_6$ ,  $\delta$  ppm): -116.2 ( $\text{SiH}$ ), -36.4 ( $\text{Si}(\text{CH}_3)_2$ ), -11.2 ( $\text{Si}(\text{CH}_3)_3$ ). IR:  $\tilde{\nu}_{\text{Si-H}}$  2085  $\text{cm}^{-1}$  (ATR, neat). Anal. found/calcd. for  $\text{C}_{16}\text{H}_{50}\text{Si}_8$ : C 38.58/41.13, H 11.21/10.79.

1,4-Dihydrido-1,1,4,4-tetrakis(trimethylsilyl)tetramethyl-1,4-digermatetrasilane **113**



A solution of 0.35 g (2.2 equiv., 3.14 mmol) of potassium *tert*-butoxide in degassed THF (10 mL) was added to a solution of 1.00 g (1 equiv., 1.43 mmol) of 1,4-digermatetrasilane **46** in degassed THF

(10 mL) at room temperature. The reaction mixture immediately turned yellow and was stirred overnight. The completeness of the reaction was confirmed by  $^{29}\text{Si}\{^1\text{H}\}$  NMR spectroscopy. Then the solution of **154** was hydrolysed by adding it to a cooled ( $T = 0\text{ }^\circ\text{C}$ ) mixture of degassed aqueous  $\text{NH}_4\text{Cl}$ -solution (1 M, 30 mL) and degassed diethyl ether (30 mL). The organic phases was decanted and the aqueous phase was extracted three times with degassed diethyl ether (5 mL). The combined organic phases were dried over  $\text{Na}_2\text{SO}_4$ . After filtration, the solvent was removed under reduced pressure and the product **113** was obtained as colourless wax (0.48 g, 0.86 mmol, 61 %). The product is sensitive to temperature and oxygen and was stored under argon atmosphere at  $T = -20\text{ }^\circ\text{C}$ .

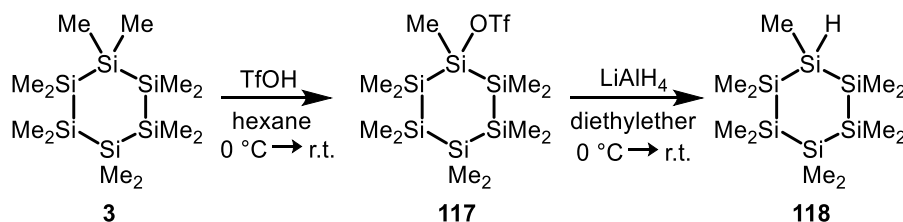
1,4-Dipotassium-1,1,4,4-tetrakis(trimethylsilyl)tetramethyl-1,4-digermatetrasilane **154**

$^1\text{H}$  NMR (499.87 MHz, 305.1 K, THF,  $\text{D}_2\text{O}$ -lock,  $\delta$  ppm): 0.46 (s, 36 H,  $\text{Si}(\text{CH}_3)_3$ ), 0.58 (s, 12 H  $\text{Si}(\text{CH}_3)_2$ ).  $^{13}\text{C}\{^1\text{H}\}$  NMR (125.71 MHz, 305.0 K, THF,  $\text{D}_2\text{O}$ -lock,  $\delta$  ppm): 3.2 ( $\text{Si}(\text{CH}_3)_3$ ), 4.5 ( $\text{Si}(\text{CH}_3)_2$ ).  $^{29}\text{Si}\{^1\text{H}\}$  NMR (99.31 MHz, 305.0 K, THF,  $\text{D}_2\text{O}$ -lock,  $\delta$  ppm): -24.6 ( $\text{Si}(\text{CH}_3)_2$ ), -3.2 ( $\text{Si}(\text{CH}_3)_3$ ).

1,4-Dihydrido-1,1,4,4-tetrakis(trimethylsilyl)tetramethyl-1,4-digermatetrasilane **113**

$^1\text{H}$  NMR (499.87 MHz, 305.1 K,  $\text{C}_6\text{D}_6$ ,  $\delta$  ppm): 0.38 (s, 36 H,  $\text{Si}(\text{CH}_3)_3$ ), 0.54 (s, 12 H  $\text{Si}(\text{CH}_3)_2$ ), 2.36 (s, 2 H, GeH).  $^{13}\text{C}\{^1\text{H}\}$  NMR (125.71 MHz, 305.0 K,  $\text{C}_6\text{D}_6$ ,  $\delta$  ppm): -0.5 ( $\text{Si}(\text{CH}_3)_2$ ), 3.1 ( $\text{Si}(\text{CH}_3)_3$ ).  $^{29}\text{Si}\{^1\text{H}\}$  NMR (99.31 MHz, 305.0 K,  $\text{C}_6\text{D}_6$ ,  $\delta$  ppm): -29.2 ( $\text{Si}(\text{CH}_3)_2$ ), -5.5 ( $\text{Si}(\text{CH}_3)_3$ ). HR/MS ( $m/z$ ) found/calcd. for  $\text{C}_{16}\text{H}_{50}\text{Ge}_2\text{Si}_6$ : 558.0965/558.0946. IR  $\tilde{\nu}_{\text{Si-H}}$  1945  $\text{cm}^{-1}$  (ATR, neat). No satisfactory combustion analysis was obtained due to small amounts of by-products, which are visible in the  $^1\text{H}$  NMR spectrum. Anal. found/calcd. for  $\text{C}_{16}\text{H}_{50}\text{Ge}_2\text{Si}_6$ : C 37.12/34.54, H 8.99/9.06.

Hydridoundecamethylcyclohexasilane **118**



A solution of 3.00 g (1 equiv., 8.60 mmol) of dodecamethylcyclohexasilane **3** in hexane (20 mL) was cooled to  $T = 0\text{ }^\circ\text{C}$  in an ice bath and 0.91 mL (1.2 equiv., 1.55 g, 10.32 mmol) of trifluoromethanesulfuric acid was added dropwise. The mixture was stirred for several days at room temperature and the completeness of the reaction was confirmed by  $^{29}\text{Si}\{^1\text{H}\}$  NMR spectroscopy.

Complete consumption of the starting material was confirmed by the absence of a signal at  $\delta^{29}\text{Si} = -42.0$ .

To a suspension of 0.33 g (1 equiv., 8.60 mmol) of  $\text{LiAlH}_4$  in  $\text{Et}_2\text{O}$  (10 mL) was added the solution of 8.60 mmol (1 equiv.) of silyl triflate **117** in hexane (10 mL) at  $T = 0^\circ\text{C}$  and the mixture was stirred at room temperature overnight. The progress of the reaction was followed by GC/MS. After aqueous workup ( $\text{H}_2\text{SO}_4$ , ice,  $\text{Et}_2\text{O}$ ), the combined organic phases were dried over  $\text{Na}_2\text{SO}_4$ . After filtration, the solvent was removed under reduced pressure and the crude product **118** was purified by Kugelrohr distillation ( $T = 150^\circ\text{C}$ ,  $p = 7 \cdot 10^{-3}$  mbar). The product **118** was obtained as a colourless wax (2.30 g, 6.90 mmol, 80 %).

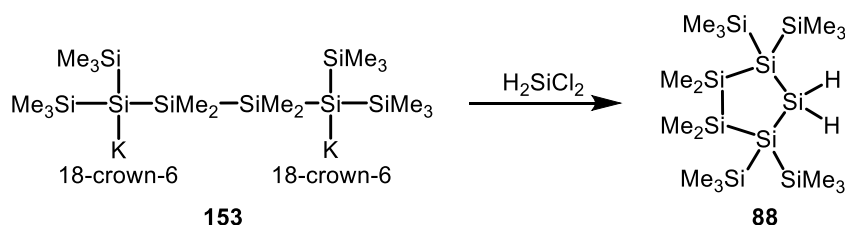
#### Trifluoromethanesulfonylundecamethylcyclohexasilane **117**

$^{29}\text{Si}\{^1\text{H}\}$  INEPT NMR (99.31 MHz, 305.0 K, hexane/ $\text{D}_2\text{O}$ -lock,  $\delta$  ppm): -42.6, -42.2, -39.2 ( $\text{Si}(\text{CH}_3)_2$ ), 50.2 ( $\text{SiOTf}$ ).

#### Hydridoundecamethylcyclohexasilane **118**

$^1\text{H}$  NMR (499.87 MHz, 305.1 K,  $\text{C}_6\text{D}_6$ ,  $\delta$  ppm): 0.25 (s, 3 H,  $\text{Si}(\text{CH}_3)$ ), 0.26 (s, 6 H, 2 x  $\text{Si}(\text{CH}_3)$ ), 0.26 (s, 3 H,  $\text{Si}(\text{CH}_3)$ ), 0.27 (s, 6 H, 2 x  $\text{Si}(\text{CH}_3)$ ), 0.30 (s, 6 H, 2 x  $\text{Si}(\text{CH}_3)$ ), 0.34 (s, 6 H, 2 x  $\text{Si}(\text{CH}_3)$ ), 3.68 (q, 1 H, Si-H,  $^3J_{\text{H,H}} = 5$  Hz,  $^1J_{\text{Si,H}} = 166$  Hz).  $^{13}\text{C}\{^1\text{H}\}$  NMR (125.71 MHz, 305.0 K,  $\text{C}_6\text{D}_6$ ,  $\delta$  ppm): -6.2 (2 x  $\text{Si}(\text{CH}_3)$ ), -6.0 ( $\text{Si}(\text{CH}_3)$ ), -6.0 (2 x  $\text{Si}(\text{CH}_3)$ ), -5.9 ( $\text{Si}(\text{CH}_3)$ ), -5.1 (2 x  $\text{Si}(\text{CH}_3)$ ), -4.4 (2 x  $\text{Si}(\text{CH}_3)$ ), -12.3 ( $\text{HSi}(\text{CH}_3)$ ).  $^{29}\text{Si}\{^1\text{H}\}$  NMR (99.31 MHz, 305.0 K,  $\text{C}_6\text{D}_6$ ,  $\delta$  ppm): -68.2 (Si-H), -42.2 (*p*- $\text{Si}(\text{CH}_3)_2$ ), -42.0 (*o*-, *m*- $\text{Si}(\text{CH}_3)_2$ ), -41.3 (*o*-, *m*- $\text{Si}(\text{CH}_3)_2$ ). HR/MS ( $m/z$ ) found/calcd. for  $\text{C}_{11}\text{H}_{34}\text{Si}_6$ : 334.1266/334.1271. IR  $\tilde{\nu}_{\text{Si-H}} = 2063\text{ cm}^{-1}$  (ATR, neat). Anal. found/calcd. for  $\text{C}_{11}\text{H}_{34}\text{Si}_6$ : C 37.27/39.45, H 11.04/10.23.

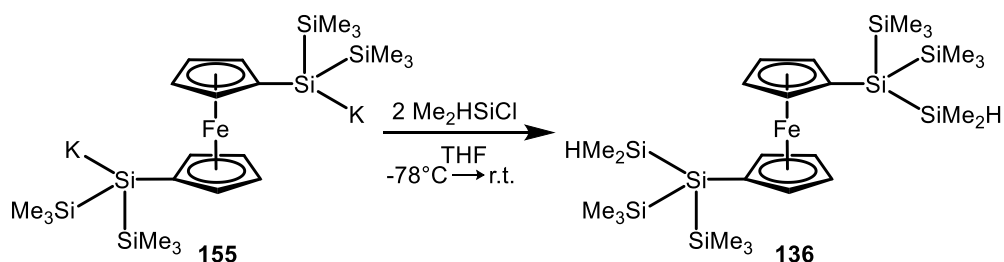
#### 1,1-Dihydrido-2,2,4,4-tetrakis(trimethylsilyl)tetramethylcyclopentasilane **88**



This compound was prepared by the Marschner group. The NMR data are given here, because no experimental data are available in literature.

$^1\text{H}$  NMR (499.87 MHz, 305.1 K,  $\text{C}_6\text{D}_6$ ,  $\delta$  ppm): 0.35 (s, 36 H,  $\text{Si}(\text{CH}_3)_3$ ), 0.42 (s, 12 H,  $\text{Si}(\text{CH}_2)_2$ ), 3.63 (s, 2 H,  $\text{SiH}_2$ ,  $^1J_{\text{Si,H}} = 178$  Hz).  $^{13}\text{C}\{^1\text{H}\}$  NMR (125.71 MHz, 305.0 K,  $\text{CDCl}_3$ ,  $\delta$  ppm): -2.1 ( $\text{Si}(\text{CH}_3)_2$ ), 2.4 ( $\text{Si}(\text{CH}_3)_3$ ).  $^{29}\text{Si}\{^1\text{H}\}$  NMR (99.31 MHz, 305.0 K,  $\text{C}_6\text{D}_6$ ,  $\delta$  ppm): -136.5 ( $\text{Si}_4\text{Si}$ ), -97.6 ( $\text{SiH}_2$ ), -23.2 ( $\text{Si}(\text{CH}_3)_2$ ), -7.8 ( $\text{Si}(\text{CH}_3)_3$ ).

### 1,1'-Bis(bis(trimethylsilyl)dimethylsilyl)silyl)ferrocene **136**



0.24 g (2.1 equiv., 2.48 mmol) of chlorodimethylsilane was added to a solution of 0.72 g (1 equiv., 1.18 mmol) of 1,1'-bis(bis(trimethylsilyl)silyl)ferrocenyldipotassium **155** in THF at  $T = -78^\circ\text{C}$ . The mixture was stirred overnight and was allowed to warm to room temperature. The solution was then slowly dropped into a mixture of ice, 1 M sulfuric acid (10 mL) and pentane (20 mL). The two phases were separated and the aqueous phase was washed three times with pentane (5 mL). The aqueous phase was neutralised with  $\text{NaHCO}_3$  and extracted two times with pentane (5 mL). The combined organic phases were dried over  $\text{Na}_2\text{SO}_4$ , which was then removed by filtration, and the solvent was removed under reduced pressure. The crude residue was crystallised from degassed *iso*-propanol and the pure product **136** was obtained as orange, waxy solid (0.32 g, 41%).

$^1\text{H}$  NMR (499.87 MHz, 305.0 K,  $\text{C}_6\text{D}_6$ ,  $\delta$  ppm): 0.30 (s, 36 H,  $\text{Si}(\text{CH}_3)_3$ ), 0.39 (d, 12 H,  $^3J_{\text{H,H}} = 4$  Hz,  $\text{HSi}(\text{CH}_3)_2$ ), 4.10 (s, 4 H, CpH), 4.39 (sept, 2 H,  $^3J_{\text{H,H}} = 4$  Hz,  $\text{HSi}(\text{CH}_3)_2$ ), 4.44 (s, 4 H, CpH).  $^{13}\text{C}\{^1\text{H}\}$  NMR (125.71 MHz, 305.1 K,  $\text{C}_6\text{D}_6$ ,  $\delta$  ppm): -2.7 ( $\text{HSi}(\text{CH}_3)_2$ ), 1.7 ( $\text{Si}(\text{CH}_3)_3$ ), 67.0 ( $\text{Cp}^{\text{ipso}}$ ), 72.4 ( $\text{Cp}^\alpha$ ), 75.4 ( $\text{Cp}^\beta$ ).  $^{29}\text{Si}\{^1\text{H}\}$  NMR (99.31 MHz, 305.0 K,  $\text{C}_6\text{D}_6$ ,  $\delta$  ppm): -81.9 (2 Si, ( $\text{Si}_4\text{Si}$ ), -36.0 (2 x  $\text{HSi}(\text{CH}_3)_2$ ), -13.1 (2 x  $\text{Si}(\text{CH}_3)_3$ ).  $^{29}\text{Si}$  INEPT NMR (99.31 MHz, 305.0 K,  $\text{C}_6\text{D}_6$ ,  $\delta$  ppm): 36.0 (dsept,  $^2J_{\text{Si,H}} = 7$  Hz,  $^1J_{\text{Si,H}} = 177$  Hz). IR:  $\tilde{\nu}_{\text{Si,H}} = 1242\text{ cm}^{-1}$  (ATR, neat). HR/MS ( $m/z$ ) found/calcd. for  $\text{C}_{27}\text{H}_{62}\text{FeSi}_8$ : 650.2042/650.2042. Anal. found/calcd. for  $\text{C}_{27}\text{H}_{62}\text{FeSi}_8$ : C 49.75/47.95, H 9.48/8.98.

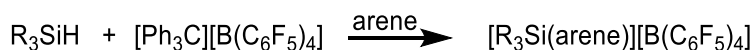
### 5.3 Cation Preparation

In the preparation reactions for the cations, the tetrakis(pentafluorophenyl)borate salt of the Lewis acid was used. The NMR characterisation data for the anion are given below and not repeated for each preparation reaction. Negligible differences compared to these data were found for the NMR chemical shifts or coupling constants of the anion depending on the solvent or temperature.

[B(C<sub>6</sub>F<sub>5</sub>)<sub>4</sub>]<sup>-</sup>:

<sup>13</sup>C{<sup>1</sup>H} NMR (125.71 MHz, 243.1 K, C<sub>6</sub>D<sub>5</sub>Cl) δ: 148.9 (d, <sup>1</sup>J<sub>C,F</sub> = 238.9 Hz, CF<sub>para</sub>, [B(C<sub>6</sub>F<sub>5</sub>)<sub>4</sub>]<sup>-</sup>), 138.8 (d, <sup>1</sup>J<sub>C,F</sub> = 235.4 Hz, CF<sub>para</sub>, [B(C<sub>6</sub>F<sub>5</sub>)<sub>4</sub>]<sup>-</sup>), 136.9 (d, <sup>1</sup>J<sub>C,F</sub> = 232.7 Hz, CF<sub>meta</sub>, [B(C<sub>6</sub>F<sub>5</sub>)<sub>4</sub>]<sup>-</sup>), 123.7-125.6 (m, C<sub>ipso</sub>, [B(C<sub>6</sub>F<sub>5</sub>)<sub>4</sub>]<sup>-</sup>). <sup>19</sup>F{<sup>1</sup>H} NMR (470.28 MHz, 243.1 K, C<sub>6</sub>D<sub>5</sub>Cl) δ: -131.9 (brs, 2 F, CF<sub>ortho</sub>, [B(C<sub>6</sub>F<sub>5</sub>)<sub>4</sub>]<sup>-</sup>), -161.9 (brs, 1 F, CF<sub>para</sub>, [B(C<sub>6</sub>F<sub>5</sub>)<sub>4</sub>]<sup>-</sup>), -165.8 (brs, 2 F, CF<sub>meta</sub>, [B(C<sub>6</sub>F<sub>5</sub>)<sub>4</sub>]<sup>-</sup>); <sup>11</sup>B{<sup>1</sup>H} (160.38 MHz, 243.1 K, C<sub>6</sub>D<sub>5</sub>Cl) δ: -16.8 ([B(C<sub>6</sub>F<sub>5</sub>)<sub>4</sub>]<sup>-</sup>).

General preparation of trialkylsilyl arenium borates [65a-c][B(C<sub>6</sub>F<sub>5</sub>)<sub>4</sub>]<sup>[163]</sup>



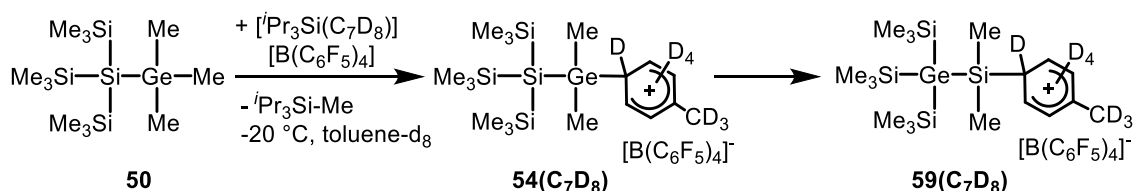
Trityl tetrakis(pentafluorophenyl)borate was dissolved in 3 mL of the indicated solvent and the silane was added. The formation of two phases could be observed and the biphasic reaction mixture was vigorously stirred for 30 min. The upper, non-polar phase was removed and the lower, polar phase was washed with 2 mL of the used solvent and again the non-polar phase was removed. The polar phase was dried under reduced pressure for 30 min and then dissolved in the respective deuterated solvent.

Triethylsilyl benzenium borate [65a][B(C<sub>6</sub>F<sub>5</sub>)<sub>4</sub>]: 0.50 g (1 equiv., 0.54 mmol) of trityl tetrakis(pentafluorophenyl)borate was dissolved in benzene and 0.14 mL (1.6 equiv., 0.87 mmol) of triethylsilane was added.

Tri-*iso*-propylsilyl toluenium borate [65b][B(C<sub>6</sub>F<sub>5</sub>)<sub>4</sub>]: 0.46 g (1 equiv., 0.50 mmol) of trityl tetrakis(pentafluorophenyl)borate was dissolved in toluene and 0.11 mL (1.1 equiv., 0.55 mmol) of tri-*iso*-propylsilane was added.

Trimethylsilyl toluenium borate [65c][B(C<sub>6</sub>F<sub>5</sub>)<sub>4</sub>]: 0.46 g (1 equiv., 0.50 mmol) of trityl tetrakis(pentafluorophenyl)borate was dissolved in toluene and 0.06 mL (1.1 equiv., 1 equiv., 0.55 mmol) of trimethylsilane was added.

Rearrangement of tris(trimethylsilyl)silyldimethylgermyl toluenium borate [3(C<sub>7</sub>D<sub>8</sub>)][B(C<sub>6</sub>F<sub>5</sub>)<sub>4</sub>] to tris(trimethylsilyl)germyldimethylsilyl toluenium borate [59(C<sub>7</sub>D<sub>8</sub>)][B(C<sub>6</sub>F<sub>5</sub>)<sub>4</sub>] starting from silagermane 50



To a solution of 0.18 g (1 equiv., 0.50 mmol) of tris(trimethylsilyl)silyldimethylgermane **50** in toluene-d<sub>8</sub> (1 mL) cooled to T = -20 °C, 1 equiv. of tri-*iso*-propylsilyl toluenium borate **65b** was slowly added via a Teflon tube. The mixture was stirred for 1 h at -20 °C. The brown polar phase and the light yellow non-polar phase were each transferred to separate NMR tubes at T = -20 °C and stored at T = -60 °C overnight until the NMR spectra were recorded the next morning. The polar phase contained borates **[54(C<sub>7</sub>D<sub>8</sub>)][B(C<sub>6</sub>F<sub>5</sub>)<sub>4</sub>]** and **[59(C<sub>7</sub>D<sub>8</sub>)][B(C<sub>6</sub>F<sub>5</sub>)<sub>4</sub>]**. The non-polar phase contained the rearrangement product **51** and methyl-tri-*iso*-propylsilane.

#### Polar phase

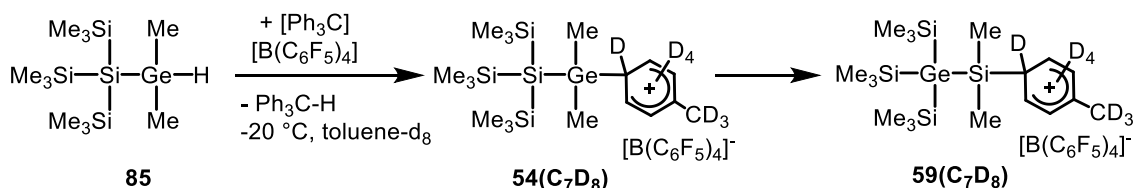
<sup>1</sup>H NMR (499.87 MHz, 253.0 K, C<sub>7</sub>D<sub>8</sub>, δ ppm): -0.15 (((CH<sub>3</sub>)<sub>3</sub>Si)<sub>3</sub>GeSi(CH<sub>3</sub>)<sub>2</sub><sup>+</sup>), 0.07 (((CH<sub>3</sub>)<sub>3</sub>Si)<sub>3</sub>GeSi(CH<sub>3</sub>)<sub>2</sub><sup>+</sup>), 0.12 (((CH<sub>3</sub>)<sub>3</sub>Si)<sub>3</sub>SiGe(CH<sub>3</sub>)<sub>2</sub><sup>+</sup>), 0.28 (((CH<sub>3</sub>)<sub>3</sub>Si)<sub>3</sub>SiGe(CH<sub>3</sub>)<sub>2</sub><sup>+</sup>). <sup>13</sup>C{<sup>1</sup>H} NMR (125.71 MHz, 253.0 K, C<sub>7</sub>D<sub>8</sub>, δ ppm): 1.6 (((CH<sub>3</sub>)<sub>3</sub>Si)<sub>3</sub>SiGe(CH<sub>3</sub>)<sub>2</sub><sup>+</sup>), 2.5 (((CH<sub>3</sub>)<sub>3</sub>Si)<sub>3</sub>GeSi(CH<sub>3</sub>)<sub>2</sub><sup>+</sup>), 5.5 (((CH<sub>3</sub>)<sub>3</sub>Si)<sub>3</sub>GeSi(CH<sub>3</sub>)<sub>2</sub><sup>+</sup>), 12.1 (((CH<sub>3</sub>)<sub>3</sub>Si)<sub>3</sub>SiGe(CH<sub>3</sub>)<sub>2</sub><sup>+</sup>). <sup>29</sup>Si{<sup>1</sup>H} NMR (99.31 MHz, 253.0 K, C<sub>7</sub>D<sub>8</sub>, δ ppm): -87.9 (((CH<sub>3</sub>)<sub>3</sub>Si)<sub>3</sub>SiGe(CH<sub>3</sub>)<sub>2</sub><sup>+</sup>), -7.9 (((CH<sub>3</sub>)<sub>3</sub>Si)<sub>3</sub>SiGe(CH<sub>3</sub>)<sub>2</sub><sup>+</sup>), -2.4 (((CH<sub>3</sub>)<sub>3</sub>Si)<sub>3</sub>GeSi(CH<sub>3</sub>)<sub>2</sub><sup>+</sup>), 98.1 (((CH<sub>3</sub>)<sub>3</sub>Si)<sub>3</sub>GeSi(CH<sub>3</sub>)<sub>2</sub><sup>+</sup>).

#### Non-polar phase

<sup>1</sup>H NMR (499.87 MHz, 305.0 K, C<sub>7</sub>D<sub>8</sub>, δ ppm): -0.17 (s, ((CH<sub>3</sub>)<sub>2</sub>CH)<sub>3</sub>SiCH<sub>3</sub>), 0.26 (s, ((CH<sub>3</sub>)<sub>3</sub>Si)<sub>4</sub>Ge), 0.86 (sept, <sup>3</sup>J<sub>H,H</sub> = 7.3 Hz, ((CH<sub>3</sub>)<sub>2</sub>CH)<sub>3</sub>SiCH<sub>3</sub>), 0.97 (d, <sup>3</sup>J<sub>H,H</sub> = 7.3 Hz, ((CH<sub>3</sub>)<sub>2</sub>CH)<sub>3</sub>SiCH<sub>3</sub>). <sup>13</sup>C{<sup>1</sup>H} NMR (127.71 MHz, 305.0 K, C<sub>7</sub>D<sub>8</sub>, δ ppm): -10.1 (((CH<sub>3</sub>)<sub>2</sub>CH)<sub>3</sub>SiCH<sub>3</sub>), 3.5 (((CH<sub>3</sub>)<sub>3</sub>Si)<sub>4</sub>Ge), 11.8

(((CH<sub>3</sub>)<sub>2</sub>CH)<sub>3</sub>SiCH<sub>3</sub>), 18.8 (((CH<sub>3</sub>)<sub>2</sub>CH)<sub>3</sub>SiCH<sub>3</sub>). <sup>29</sup>Si{<sup>1</sup>H} NMR (99.31 MHz, 305.0 K, C<sub>7</sub>D<sub>8</sub>, δ ppm): -5.1 (((CH<sub>3</sub>)<sub>3</sub>Si)<sub>4</sub>Ge), 9.0 (((CH<sub>3</sub>)<sub>2</sub>CH)<sub>3</sub>SiCH<sub>3</sub>).

Rearrangement of tris(trimethylsilyl)silyldimethylgermyl toluenium borate [54(C<sub>7</sub>D<sub>8</sub>)] [B(C<sub>6</sub>F<sub>5</sub>)<sub>4</sub>] to tris(trimethylsilyl)germyldimethylsilyl toluenium borate [59(C<sub>7</sub>D<sub>8</sub>)] [B(C<sub>6</sub>F<sub>5</sub>)<sub>4</sub>] starting from hydrogen-substituted silylgermane **85**



0.14 g (1 equiv., 0.40 mmol) of tris(trimethylsilyl)silyldimethylgermane **85** and 0.37 g (1 equiv., 0.40 mmol) of trityl tetrakis(pentafluorophenyl)borate were each dissolved in toluene-d<sub>8</sub> (1 mL) and cooled to T = -20 °C. Silylgermane **85** was slowly added to the borate salt via a Teflon tube and the mixture was stirred at T = -20 °C for 1.5 h. The brown polar phase and the light yellow non-polar phase were each transferred to NMR tubes at T = -20 °C. The NMR spectra were recorded at T = -20 °C. The polar phase contained borates [54(C<sub>7</sub>D<sub>8</sub>)] [B(C<sub>6</sub>F<sub>5</sub>)<sub>4</sub>] and [59(C<sub>7</sub>D<sub>8</sub>)] [B(C<sub>6</sub>F<sub>5</sub>)<sub>4</sub>]. The non-polar phase contained the rearrangement product **51** and triphenylmethane.

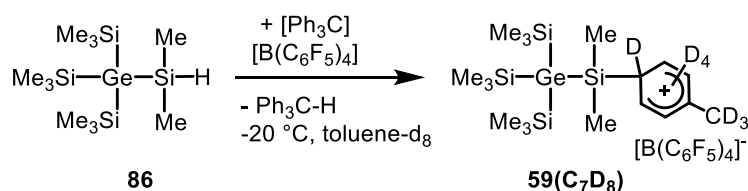
#### Polar phase

<sup>1</sup>H NMR (499.87 MHz, 253.0 K, C<sub>7</sub>D<sub>8</sub>, δ ppm): -0.15 (((CH<sub>3</sub>)<sub>3</sub>Si)<sub>3</sub>GeSi(CH<sub>3</sub>)<sub>2</sub><sup>+</sup>), 0.07 (((CH<sub>3</sub>)<sub>3</sub>Si)<sub>3</sub>Si-Ge(CH<sub>3</sub>)<sub>2</sub><sup>+</sup>), 0.12 (((CH<sub>3</sub>)<sub>3</sub>Si)<sub>3</sub>GeSi(CH<sub>3</sub>)<sub>2</sub><sup>+</sup>), 0.28 (((CH<sub>3</sub>)<sub>3</sub>Si)<sub>3</sub>SiGe(CH<sub>3</sub>)<sub>2</sub><sup>+</sup>). <sup>13</sup>C{<sup>1</sup>H} NMR (125.71 MHz, 253.0 K, C<sub>7</sub>D<sub>8</sub>, δ ppm): 1.6 (((CH<sub>3</sub>)<sub>3</sub>Si)<sub>3</sub>SiGe(CH<sub>3</sub>)<sub>2</sub><sup>+</sup>), 2.4 (((CH<sub>3</sub>)<sub>3</sub>Si)<sub>3</sub>GeSi(CH<sub>3</sub>)<sub>2</sub><sup>+</sup>), 5.5 (((CH<sub>3</sub>)<sub>3</sub>Si)<sub>3</sub>Ge-Si(CH<sub>3</sub>)<sub>2</sub><sup>+</sup>), 12.1 (((CH<sub>3</sub>)<sub>3</sub>Si)<sub>3</sub>SiGe(CH<sub>3</sub>)<sub>2</sub><sup>+</sup>). <sup>29</sup>Si{<sup>1</sup>H} NMR (99.31 MHz, 253.0 K, C<sub>7</sub>D<sub>8</sub>, δ ppm): -87.9 (((CH<sub>3</sub>)<sub>3</sub>Si)<sub>3</sub>SiGe(CH<sub>3</sub>)<sub>2</sub><sup>+</sup>), -7.9 (((CH<sub>3</sub>)<sub>3</sub>Si)<sub>3</sub>SiGe(CH<sub>3</sub>)<sub>2</sub><sup>+</sup>), -2.4 (((CH<sub>3</sub>)<sub>3</sub>Si)<sub>3</sub>GeSi(CH<sub>3</sub>)<sub>2</sub><sup>+</sup>), 98.1 (((CH<sub>3</sub>)<sub>3</sub>Si)<sub>3</sub>Ge-Si(CH<sub>3</sub>)<sub>2</sub><sup>+</sup>).

#### Non-polar phase

<sup>1</sup>H NMR (499.87 MHz, 305.0 K, C<sub>7</sub>D<sub>8</sub>, δ ppm): 0.30 (s, ((CH<sub>3</sub>)<sub>3</sub>Si)<sub>4</sub>Ge), 5.38 (s, Ph<sub>3</sub>CH), 6.98-7.09 (m, Ph<sub>3</sub>CH). <sup>13</sup>C{<sup>1</sup>H} NMR (127.71 MHz, 305.0 K, C<sub>7</sub>D<sub>8</sub>, δ ppm): 3.5 ((CH<sub>3</sub>)<sub>3</sub>Si)<sub>4</sub>Ge), 57.1 (Ph<sub>3</sub>CH), 125.4 (Ph<sub>3</sub>CH), 128.3 (Ph<sub>3</sub>CH), 129.2 (Ph<sub>3</sub>CH), 144.3 (Ph<sub>3</sub>CH). <sup>29</sup>Si{<sup>1</sup>H} NMR (99.31 MHz, 305.0 K, C<sub>7</sub>D<sub>8</sub>, δ ppm): -5.1 ((CH<sub>3</sub>)<sub>3</sub>Si)<sub>4</sub>Ge).

Synthesis of tris(trimethylsilyl)germyldimethylsilyl toluenium borate [59(C<sub>7</sub>H<sub>8</sub>)] [B(C<sub>6</sub>F<sub>5</sub>)<sub>4</sub>] from hydrogen-substituted germysilane **86**



0.18 g (1 equiv., 0.50 mmol) of germysilane **86** and 0.46 g (1 equiv., 0.50 mmol) of trityl tetrakis(pentafluorophenyl)borate were both dissolved in toluene-d<sub>8</sub> (1 mL) and cooled to T = -20 °C. Germysilane **86** was slowly added to the borate salt via a Teflon tube and the mixture was stirred at T = -20 °C for 1.5 h. The brown polar phase and the light yellow non-polar phase were each transferred to separate NMR tubes at T = -20 °C and stored at T = -60 °C overnight until the NMR spectra were recorded the next morning. The polar phase contained borate [59(C<sub>7</sub>D<sub>8</sub>)] [B(C<sub>6</sub>F<sub>5</sub>)<sub>4</sub>]. The non-polar phase contained the rearrangement product **51** and triphenylmethane.

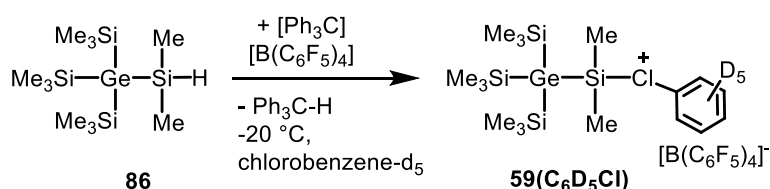
Polar phase

<sup>1</sup>H NMR (499.87 MHz, 253.0 K, C<sub>7</sub>D<sub>8</sub>, δ ppm): -0.15 (((CH<sub>3</sub>)<sub>3</sub>Si)<sub>3</sub>GeSi(CH<sub>3</sub>)<sub>2</sub><sup>+</sup>), 0.12 (((CH<sub>3</sub>)<sub>3</sub>Si)<sub>3</sub>GeSi(CH<sub>3</sub>)<sub>2</sub><sup>+</sup>). <sup>13</sup>C{<sup>1</sup>H} NMR (125.71 MHz, 253.0 K, C<sub>7</sub>D<sub>8</sub>, δ ppm): 2.5 (((CH<sub>3</sub>)<sub>3</sub>Si)<sub>3</sub>GeSi(CH<sub>3</sub>)<sub>2</sub><sup>+</sup>), 5.5 (((CH<sub>3</sub>)<sub>3</sub>Si)<sub>3</sub>GeSi(CH<sub>3</sub>)<sub>2</sub><sup>+</sup>). <sup>29</sup>Si{<sup>1</sup>H} NMR (99.31 MHz, 253.0 K, C<sub>7</sub>D<sub>8</sub>, δ ppm): -2.4 (((CH<sub>3</sub>)<sub>3</sub>Si)<sub>3</sub>GeSi(CH<sub>3</sub>)<sub>2</sub><sup>+</sup>), 98.1 (((CH<sub>3</sub>)<sub>3</sub>Si)<sub>3</sub>GeSi(CH<sub>3</sub>)<sub>2</sub><sup>+</sup>).

Non-polar phase

<sup>1</sup>H NMR (499.87 MHz, 305.0 K, C<sub>7</sub>D<sub>8</sub>, δ ppm): 0.29 (s, ((CH<sub>3</sub>)<sub>3</sub>Si)<sub>4</sub>Ge), 5.38 (s, Ph<sub>3</sub>CH), 6.98-7.10 (m, Ph<sub>3</sub>CH). <sup>13</sup>C{<sup>1</sup>H} NMR (125.69 MHz, 305.0 K, C<sub>7</sub>D<sub>8</sub>, δ ppm): 3.5 (((CH<sub>3</sub>)<sub>3</sub>Si)<sub>4</sub>Ge), 57.2 (Ph<sub>3</sub>CH), 125.4 (Ph<sub>3</sub>CH), 128.3 (Ph<sub>3</sub>CH), 129.2 (Ph<sub>3</sub>CH), 144.3 (Ph<sub>3</sub>CH). <sup>29</sup>Si{<sup>1</sup>H} NMR (99.31 MHz, 305.0 K, C<sub>7</sub>D<sub>8</sub>, δ ppm): -5.1 (((CH<sub>3</sub>)<sub>3</sub>Si)<sub>4</sub>Ge).

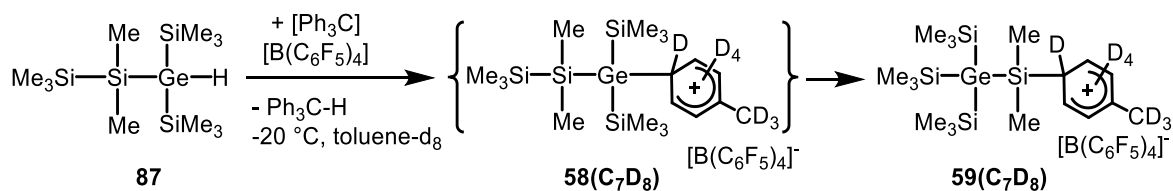
Synthesis of tris(trimethylsilyl)germyldimethylsilyl phenylchloronium borate [59(C<sub>6</sub>D<sub>5</sub>Cl)] [B(C<sub>6</sub>F<sub>5</sub>)<sub>4</sub>] from germysilane **86**



0.09 g (1 equiv., 0.25 mmol) of germysilane **86** and 0.23 g (1 equiv., 0.25 mmol) of trityl tetrakis-(pentafluorophenyl)borate were both dissolved in chlorobenzene- $d_5$  (0.5 mL) and cooled to  $T = -20\text{ }^{\circ}\text{C}$ . Germysilane **86** was slowly added to the borate salt via a Teflon tube and the mixture was stirred at  $T = -20\text{ }^{\circ}\text{C}$  for 1.5 h. The brown solution was transferred into an NMR tube at  $T = -20\text{ }^{\circ}\text{C}$  and stored at  $T = -60\text{ }^{\circ}\text{C}$  overnight until the NMR spectra were recorded the next morning. The mixture contained silyl phenylchloronium borate [**59**( $\text{C}_6\text{D}_5\text{Cl}$ )] $[\text{B}(\text{C}_6\text{F}_5)_4]$ , the rearrangement product **51** and triphenylmethane.

$^{29}\text{Si}\{^1\text{H}\}$  NMR (99.31 MHz, 253.0 K,  $\text{C}_6\text{D}_6\text{Cl}$ ,  $\delta$  ppm): -5.1 ( $((\text{CH}_3)_3\text{Si})_4\text{Ge}$ ), -1.4 ( $((\text{CH}_3)_3\text{Si})_3\text{GeSi}(\text{CH}_3)_2^+$ ), 154.3 ( $((\text{CH}_3)_3\text{Si})_3\text{GeSi}(\text{CH}_3)_2^+$ ).

#### Synthesis of tris(trimethylsilyl)germyldimethylsilyl toluenium borate [**59**( $\text{C}_7\text{D}_8$ )] $[\text{B}(\text{C}_6\text{F}_5)_4]$ from germatrisilane **87**



0.11 g (1 equiv., 0.32 mmol) of germatrisilane **87** and 0.29 g (1 equiv., 0.32 mmol) of trityl tetrakis-(pentafluorophenyl)borate were both dissolved in toluene- $d_8$  (1 mL) and cooled to  $T = -20\text{ }^{\circ}\text{C}$ . Germatrisilane **87** was slowly added to the borate salt via a Teflon tube and the mixture was stirred at  $T = -20\text{ }^{\circ}\text{C}$  for 5 min. The brown polar phase and the light yellow non-polar phase were each transferred to separate NMR tubes at  $T = -20\text{ }^{\circ}\text{C}$  and stored at  $T = -60\text{ }^{\circ}\text{C}$  for 5 h until the NMR spectra were recorded. At  $T = -60\text{ }^{\circ}\text{C}$  the polar phase solidifies and no further reaction is expected. The NMR spectra of the polar phase recorded at  $T = -20\text{ }^{\circ}\text{C}$  contained nearly exclusively borate [**59**( $\text{C}_7\text{D}_8$ )] $[\text{B}(\text{C}_6\text{F}_5)_4]$ . The non-polar phase contained the rearrangement product **51** and triphenylmethane.

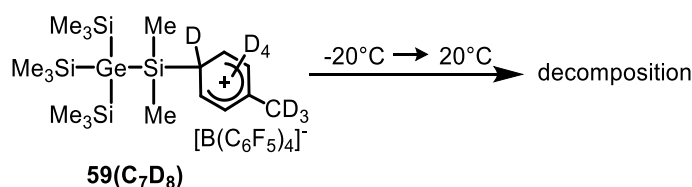
#### Polar phase

$^1\text{H}$  NMR (499.87 MHz, 253.0 K,  $\text{C}_7\text{D}_8$ ,  $\delta$  ppm): -0.16 ( $((\text{CH}_3)_3\text{Si})_3\text{GeSi}(\text{CH}_3)_2^+$ ), 0.12 ( $((\text{CH}_3)_3\text{Si})_3\text{GeSi}(\text{CH}_3)_2^+$ ).  $^{13}\text{C}\{^1\text{H}\}$  NMR (125.71 MHz, 253.0 K,  $\text{C}_7\text{D}_8$ ,  $\delta$  ppm): 2.5 ( $((\text{CH}_3)_3\text{Si})_3\text{GeSi}(\text{CH}_3)_2^+$ ), 5.5 ( $((\text{CH}_3)_3\text{Si})_3\text{GeSi}(\text{CH}_3)_2^+$ ).  $^{29}\text{Si}\{^1\text{H}\}$  NMR (99.31 MHz, 253.0 K,  $\text{C}_7\text{D}_8$ ,  $\delta$  ppm): -2.4 ( $((\text{CH}_3)_3\text{Si})_3\text{GeSi}(\text{CH}_3)_2^+$ ), 98.2 ( $((\text{CH}_3)_3\text{Si})_3\text{GeSi}(\text{CH}_3)_2^+$ ).

### Non-polar phase

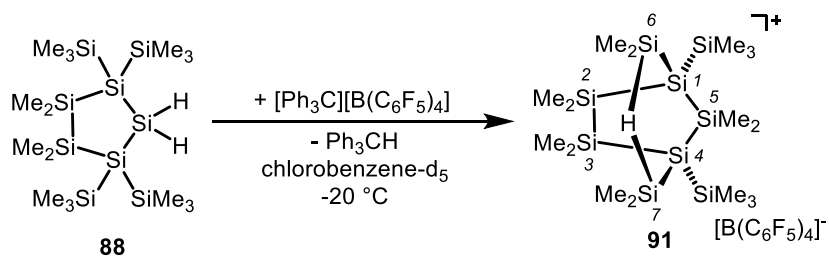
$^1\text{H}$  NMR (499.87 MHz, 305.0 K,  $\text{C}_7\text{D}_8$ ,  $\delta$  ppm): 0.30 (s,  $((\text{CH}_3)_3\text{Si})_4\text{Ge}$ ), 5.38 (s,  $\text{Ph}_3\text{CH}$ ), 6.98-7.10 (m,  $\text{Ph}_3\text{CH}$ ).  $^{13}\text{C}\{^1\text{H}\}$  NMR (125.69 MHz, 305.0 K,  $\text{C}_7\text{D}_8$ ,  $\delta$  ppm): 3.5 ( $((\text{CH}_3)_3\text{Si})_4\text{Ge}$ ), 57.1 ( $\text{Ph}_3\text{CH}$ ), 125.4 ( $\text{Ph}_3\text{CH}$ ), 128.2 ( $\text{Ph}_3\text{CH}$ ), 129.1 ( $\text{Ph}_3\text{CH}$ ), 144.3 ( $\text{Ph}_3\text{CH}$ ).  $^{29}\text{Si}\{^1\text{H}\}$  NMR (99.31 MHz, 305.0 K,  $\text{C}_7\text{D}_8$ ,  $\delta$  ppm): -5.1 ( $((\text{CH}_3)_3\text{Si})_4\text{Ge}$ ).

### Decomposition of silyl toluenium borate **59**( $\text{C}_7\text{D}_8$ )[ $\text{B}(\text{C}_6\text{F}_5)_4$ ] at higher temperatures



The thermolability of silyl toluenium ion **59**( $\text{C}_7\text{D}_8$ ) was shown by  $^{29}\text{Si}\{^1\text{H}\}$  NMR spectroscopy at different temperatures. The amount of decomposition products increases with higher temperatures and the intensity of **59**( $\text{C}_7\text{D}_8$ ) decreases. In the independent synthesis of **59**( $\text{C}_7\text{D}_8$ ), the same decomposition products appear at  $T = -20^\circ\text{C}$  (Figure 18).

### Synthesis of hydrogen-bridged bissilyl borate **91**[ $\text{B}(\text{C}_6\text{F}_5)_4$ ] from dihydridocyclopentasilane **88**

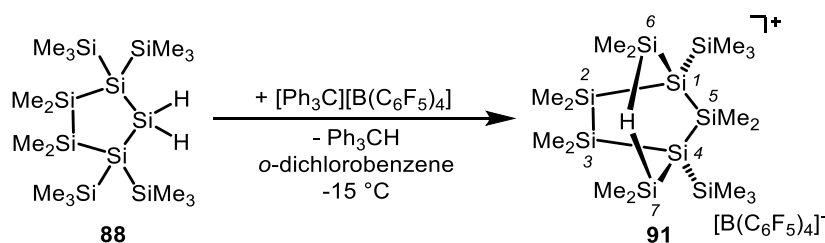


87 mg (1 equiv., 0.18 mmol) of dihydridocyclopentasilane **88** and 0.162 g (1 equiv., 0.18 mmol) of trityl tetrakis(pentafluorophenyl)borate were evacuated in different Schlenk tubes for 1 h and then each dissolved in chlorobenzene- $\text{d}_5$  (0.5 mL). The solution of trityl tetrakis(pentafluoro)phenyl borate was cooled to  $T = -20^\circ\text{C}$  with an  $\text{EtOH}/\text{N}_2$  bath. The silane was added via a Teflon tube and the reaction mixture was stirred at  $T = -20^\circ\text{C}$  for 1.5 h. The solution was then transferred into an NMR tube and stored at  $T = -60^\circ\text{C}$  overnight. The NMR spectra were recorded at  $T = -20^\circ\text{C}$ .

### Cation **91**

$^1\text{H}$  NMR (499.87 MHz, 253.0 K,  $\text{C}_6\text{H}_5\text{Cl}$ ,  $\delta$  ppm): 0.18 (s, 18 H,  $\text{Si}(\text{CH}_3)_3$ ), 0.19 (s, 6 H,  $\text{Si}^{2,3}(\text{CH}_3)_2$ ), 0.20 (s, 6 H,  $\text{Si}^{2,3}(\text{CH}_3)_2$ ), 0.32 (2s,  $2 \times 3$  H,  $\text{Si}^5(\text{CH}_3)_2$ ), 0.48 (d, 6 H,  $^3J_{\text{H,H}} = 2.3$  Hz,  $\text{Si}^{6,7}(\text{CH}_3)_2$ ), 0.56 (d, 6 H,  $^3J_{\text{H,H}} = 2.3$  Hz,  $\text{Si}^{6,7}(\text{CH}_3)_2$ ), 1.10 (m, 1 H,  $^1J_{\text{Si,H}} = 46$  Hz,  $^3J_{\text{H,H}} = 2.3$  Hz, Si-H-Si).  $^{13}\text{C}\{^1\text{H}\}$  NMR (125.71 MHz, 253.0 K,  $\text{C}_6\text{H}_5\text{Cl}$ )  $\delta$ : -2.5 ( $\text{Si}^{2,3}(\text{CH}_3)_2$ ), -1.6 ( $\text{Si}^{2,3}(\text{CH}_3)_2$ ), 0.0 ( $\text{Si}^5(\text{CH}_3)_2$ ), 0.2 ( $\text{Si}^5(\text{CH}_3)_2$ ), 2.0 ( $\text{Si}^{6,7}(\text{CH}_3)_2$ ), 2.8 ( $\text{Si}^{6,7}(\text{CH}_3)_2$ ), 2.9 ( $\text{Si}(\text{CH}_3)_3$ ).  $^{29}\text{Si}\{^1\text{H}\}$  NMR (99.31 MHz, 253 K,  $\text{C}_6\text{H}_5\text{Cl}$ ,  $\delta$  ppm): -128.8 ( $\text{Si}^{1,4}$ ), -32.8 ( $\text{Si}^{2,3}$ ), -16.3 ( $\text{Si}^5$ ), -5.7 ( $2 \times \text{Si}(\text{CH}_3)_3$ ), 94.2 ( $\text{Si}^{6,7}$ ).  $^{29}\text{Si}$  INEPT NMR (99.31 MHz, 253 K,  $\text{C}_6\text{H}_5\text{Cl}$ ,  $\delta$  pm): -128.8 (s,  $\text{Si}^{1,4}$ ), -32.8 (m,  $\text{Si}^{2,3}$ ), -16.3 (sept,  $^2J_{\text{Si,H}} = 6$  Hz,  $\text{Si}^5$ ), -5.7 (m,  $2 \times \text{Si}(\text{CH}_3)_3$ ), 94.2 (dsept,  $^1J_{\text{Si,H}} = 46$  Hz,  $^2J_{\text{Si,H}} = 6$  Hz,  $\text{Si}^{6,7}$ ),

### Synthesis of hydrogen-bridged bissilyl borate **91** $[\text{B}(\text{C}_6\text{F}_5)_4]$ from dihydridocyclopentasilane **88**

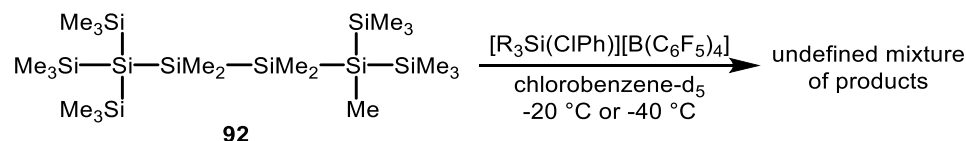


50 mg (1 equiv., 0.10 mmol) of dihydridocyclopentasilane **88** and 0.92 g (1 equiv., 0.10 mmol) of trityl tetrakis(pentafluorophenyl)borate were evacuated in different Schlenk tubes for 1 h and then dissolved each in *o*-dichlorobenzene (1 mL). The solution of trityl tetrakis(pentafluoro)phenyl borate was cooled to  $T = -15$  °C with an EtOH/ $\text{N}_2$  bath. The silane was added via a Teflon tube and the reaction mixture was stirred at  $T = -15$  °C for 2 h. The solution was then transferred into an NMR tube and stored at  $T = -25$  °C overnight. The NMR spectra were recorded at  $T = -15$  °C with an external acetone- $\text{d}_6$  lock.

### Cation **91**

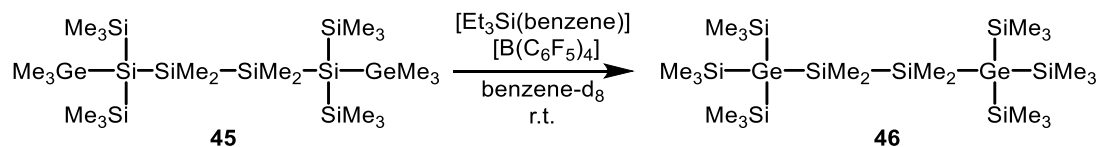
$^{29}\text{Si}\{^1\text{H}\}$  NMR (99.31 MHz, 253 K,  $\text{C}_6\text{D}_4\text{Cl}_2$ ,  $\delta$  ppm): -128.8 ( $\text{Si}^{1,4}$ ), -32.9 ( $\text{Si}^{2,3}$ ), -16.4 ( $\text{Si}^5$ ), -5.9 ( $2 \times \text{Si}(\text{CH}_3)_3$ ), 94.1 ( $\text{Si}^{6,7}$ ).  $^{29}\text{Si}$  INEPT NMR (99.31 MHz, 253 K,  $\text{C}_6\text{D}_4\text{Cl}_2$ ,  $\delta$  ppm): -128.8 (s,  $\text{Si}^{1,4}$ ), -32.9 (m,  $\text{Si}^{2,3}$ ), -16.4 (m,  $\text{Si}^5$ ), -5.9 (m,  $2 \times \text{Si}(\text{CH}_3)_3$ ), 94.1 (dsept,  $^1J_{\text{Si,H}} = 46$  Hz,  $^2J_{\text{Si,H}} = 6$  Hz,  $\text{Si}^{6,7}$ ).

### Methyl group abstraction of tetrasilane **92**



0.11 mg (1.2 equiv., 0.12 mmol) of trityl tetrakis(pentafluorophenyl)borate and 0.12 mmol (1.2 equiv.) of trialkylsilane were dissolved in chlorobenzene- $\text{d}_5$  (0.5 mL) and stirred for 10 min and to give trialkylsilyl chloronium tetrakis(pentafluorophenyl)borate. This solution was cooled to  $T = -20\text{ }^\circ\text{C}$  (for alkyl = *iso*-propyl) or  $T = -40\text{ }^\circ\text{C}$  (alkyl = ethyl). A solution of 55 mg (1 equiv., 0.10 mmol) of tetrasilane **92**<sup>[129]</sup> in chlorobenzene- $\text{d}_5$  was slowly added to the cold silyl chloronium ion. The mixture was stirred for 5 minutes, transferred into the precooled NMR tube and the NMR spectra were acquired immediately at  $T = -20\text{ }^\circ\text{C}$  or  $T = -40\text{ }^\circ\text{C}$ . An assignment of the signals was not possible.

### Rearrangement of 1,4-digermyltetrasilane **45** to 1,4-digermatetrasilane **46**



0.4 mmol (1 equiv.) of triethylsilyl benzenium tetrakis(pentafluorophenyl)borate **65a** $[\text{B}(\text{C}_6\text{F}_5)_4]$  was synthesised according to the general procedure and dissolved in benzene- $\text{d}_6$  (2 mL). A solution of 0.283 g (1 equiv., 0.40 mmol) of 1,4-digermyltetrasilane **45**<sup>[68]</sup> in benzene- $\text{d}_6$  (1 mL) was slowly added. The mixture was stirred at room temperature for 2 h and the polar and non-polar were analysed by NMR spectroscopy separately.

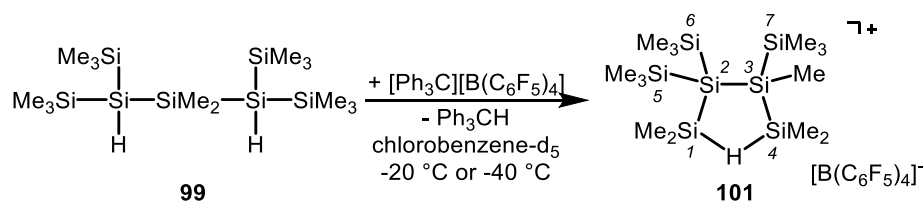
#### Polar phase

The polar phase contained too many signals in the  $^1\text{H}$ ,  $^{13}\text{C}\{^1\text{H}\}$  and  $^{29}\text{Si}\{^1\text{H}\}$  spectra to make a clear assignment.

#### Non-polar phase

$^1\text{H}$  NMR (499.87 MHz, 305.0 K,  $\text{C}_6\text{D}_6$ ,  $\delta$  ppm): 0.41 (s, 54 H,  $\text{Si}(\text{CH}_3)_3$ ), 0.61 (s, 12 H,  $\text{Si}(\text{CH}_3)_2$ ).  $^{13}\text{C}\{^1\text{H}\}$  NMR (125.69 MHz, 305.0 K,  $\text{C}_6\text{D}_6$ ,  $\delta$  ppm): 2.0 ( $\text{Si}(\text{CH}_3)_2$ ), 4.1 ( $\text{Si}(\text{CH}_3)_3$ ).  $^{29}\text{Si}\{^1\text{H}\}$  INEPT NMR (99.31 MHz, 305.0 K,  $\text{C}_6\text{D}_6$ ,  $\delta$  ppm): -24.3 ( $\text{Si}(\text{CH}_3)_2$ ), -5.0 ( $\text{Si}(\text{CH}_3)_3$ ).

Synthesis of hydrogen-bridged bissilyl borate **101**[B(C<sub>6</sub>F<sub>5</sub>)<sub>4</sub>] from 1,3-dihydridotrisilane **99**



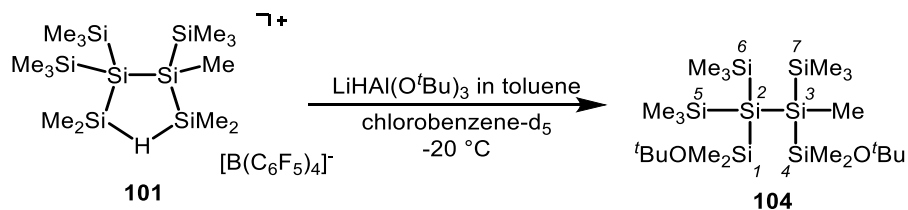
92 mg (1 equiv., 0.10 mmol) of trityl tetrakis(pentafluorophenyl)borate was evacuated in the NMR tube and cooled to  $T = -80\text{ }^{\circ}\text{C}$ . A solution of 41 mg (1 equiv., 0.10 mmol) of 1,3-dihydridotrisilane **99** in chlorobenzene- $d_5$  (0.7 mL) was added to the cold trityl borate via a syringe. The addition was performed so slowly that the solution froze before it reached the trityl borate. The NMR tube was slowly allowed to warm up until the solvent melted and the silane slowly reached the trityl borate. At that point, the NMR tube, which was wrapped in a gauze bandage soaked by  $T = -70\text{ }^{\circ}\text{C}$  cold ethanol, was quickly shaken with a vortex mixer and then instantly transferred to the NMR spectrometer pre-cooled to  $T = -20\text{ }^{\circ}\text{C}$  or  $T = -40\text{ }^{\circ}\text{C}$ .

Cation **101**

$^1\text{H}$  NMR (499.87 MHz, 233.1 K,  $\text{C}_6\text{D}_5\text{Cl}$ ,  $\delta$  ppm): 0.12 (s, 9 H,  $\text{Si}^7(\text{CH}_3)_3$ ), 0.14 (s, 9 H,  $\text{Si}^{5/6}(\text{CH}_3)_3$ ), 0.18 (s, 9 H,  $\text{Si}^{5/6}(\text{CH}_3)_3$ ), 0.27 (s, 3 H,  $\text{Si}^3\text{CH}_3$ ), 0.57 (s, 3 H,  $\text{Si}^4(\text{CH}_3)_2$ ), 0.59 (s, 3 H,  $\text{Si}^1(\text{CH}_3)_2$ ), 0.62 (s, 3 H,  $\text{Si}^4(\text{CH}_3)_2$ ), 0.63 (s, 3 H,  $\text{Si}^1(\text{CH}_3)_2$ ), 2.05 (brs, 1 H,  $^1J_{\text{Si,H}} = 45\text{ Hz Si-H-Si}$ ).  $^{13}\text{C}\{^1\text{H}\}$  NMR (125.71 MHz, 233.1 K,  $\text{C}_6\text{D}_5\text{Cl}$ ,  $\delta$  ppm): -8.4 ( $\text{Si}^3\text{CH}_3$ ), -0.3 ( $\text{Si}^{5/6}(\text{CH}_3)_3$ ), 2.3 ( $\text{Si}^7(\text{CH}_3)_3$ ), 2.6 ( $\text{Si}^{5/6}(\text{CH}_3)_3$ ), ( $\text{Si}^1(\text{CH}_3)_2$  and  $\text{Si}^4(\text{CH}_3)_2$  cannot be assigned).  $^{29}\text{Si}\{^1\text{H}\}$  NMR (99.31 MHz, 233.1 K,  $\text{C}_6\text{D}_5\text{Cl}$ ,  $\delta$  ppm): -120.0 ( $\text{Si}^2$ ), -73.0 ( $\text{Si}^3$ ), -9.3 ( $\text{Si}^7$ ), -8.1 ( $\text{Si}^{5/6}$ ), -5.2 ( $\text{Si}^{5/6}$ ), 105.2 ( $\text{Si}^1$ ), 110.2 ( $\text{Si}^4$ ).  $^{29}\text{Si}$  INEPT NMR (99.31 MHz, 233.1 K,  $\text{C}_6\text{D}_5\text{Cl}$ ,  $\delta$  ppm): -120.0 (s,  $\text{Si}^2$ ), -73.0 (s,  $\text{Si}^3$ ), -9.3 (m,  $\text{Si}^7$ ), -8.1 (m,  $\text{Si}^{5/6}$ ), -5.2 (m,  $\text{Si}^{5/6}$ ), 105.2 (dsept,  $^1J_{\text{Si,H}} = 43\text{ Hz}$ ,  $^2J_{\text{Si,H}} = 5\text{ Hz}$ ,  $\text{Si}^1$ ), 110.2 (dm,  $^1J_{\text{Si,H}} = 43\text{ Hz}$ ,  $\text{Si}^4$ ).

Intermediate **105**

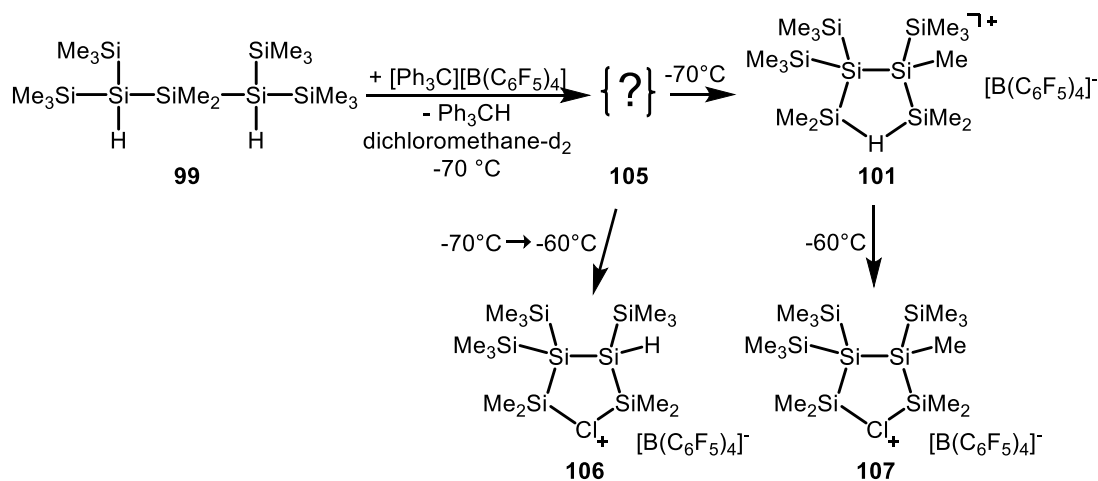
The reaction at  $T = -40\text{ }^{\circ}\text{C}$  revealed a second set of signals which were assigned to a cationic intermediate. A detailed discussion of the signals of this intermediate can be found in chapter 3.4.3.  $^{29}\text{Si}\{^1\text{H}\}$  NMR (99.31 MHz, 233.1 K,  $\text{C}_6\text{D}_5\text{Cl}$ ,  $\delta$  ppm): -138.0 ( $\text{Si}_4\text{Si}$ ), -124.4 ( $\text{Si}_4\text{Si}$ ), -118.5 ( $\text{SiH}$ ), -111.1 ( $\text{SiH}$ ), -11.5 ( $\text{Si}(\text{CH}_3)_3$ ), -9.9 ( $\text{Si}(\text{CH}_3)_3$ ), -9.3 ( $\text{Si}(\text{CH}_3)_3$ ), -7.8 ( $\text{Si}(\text{CH}_3)_3$ ), -7.8 ( $\text{Si}(\text{CH}_3)_3$ ), -6.1 ( $\text{Si}(\text{CH}_3)_3$ ), 107.8 ( $(\text{CH}_3)_2\text{Si-H-Si}(\text{CH}_3)_2$ ), 109.4 ( $(\text{CH}_3)_2\text{Si-H-Si}(\text{CH}_3)_2$ ).

Trapping reaction of hydrogen-bridged bissilyl cation **101**

A suspension of 0.127 g (0.50 mmol) of  $\text{LiHAl(O}^t\text{Bu)}_3$  in toluene- $\text{d}_8$  (2 mL) was added to the NMR sample containing silyl borate **101** $[\text{B(C}_6\text{F}_5)_4]^-$  at  $T = -20^\circ\text{C}$  and the mixture was stirred with the vortex mixer. The sample was allowed to warm to room temperature and the NMR spectra were recorded. Due to many signals in the  $^1\text{H}$  and  $^{13}\text{C}\{^1\text{H}\}$  spectra and lack of 2D NMR spectra, a detailed assignment of the signals and their integrals was not possible.

$^{29}\text{Si}\{^1\text{H}\}$  INEPT NMR (99.31 MHz, 305.1 K,  $\text{C}_6\text{D}_5\text{Cl}$ ,  $\delta$  ppm): -130.1 ( $\text{Si}^2$ ), -76.5 ( $\text{Si}^3$ ), -7.2 ( $\text{Si}^7$ ), -5.1 ( $\text{Si}^{5/6}$ ), -3.5 ( $\text{Si}^{5/6}$ ), 24.1 ( $\text{Si}^{1/4}$ ), 26.9 ( $\text{Si}^{1/4}$ ).

Synthesis of hydrogen-bridged bissilyl borate **101** $[\text{B(C}_6\text{F}_5)_4]^-$  and formation of chloronium borates **106** $[\text{B(C}_6\text{F}_5)_4]^-$  and **107** $[\text{B(C}_6\text{F}_5)_4]^-$  from 1,3-dihydridotrisilane **99**



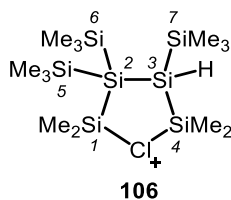
92 mg (1 equiv., 0.10 mmol) of trityl tetrakis(pentafluorophenyl)borate was evacuated in the NMR tube and then cooled to  $T = -80^\circ\text{C}$ . 41 mg (1 equiv., 0.10 mmol) of oily 1,3-dihydridotrisilane **99** was added to the cold trityl borate without solvent and the mixture was frozen with liquid nitrogen. Pre-cooled dichloromethane- $\text{d}_2$  (0.7 mL) was slowly added in such a way to keep it frozen and suspended above the starting materials. The NMR tube was slowly allowed to warm until the

dichloromethane- $d_2$  melted. At that point, the NMR tube was quickly shaken with a vortex mixer and quickly transferred to the NMR spectrometer pre-cooled to  $T = -70\text{ }^{\circ}\text{C}$ . The acquired NMR spectra are discussed in detail in chapter 3.4.3.

### Intermediate **105**

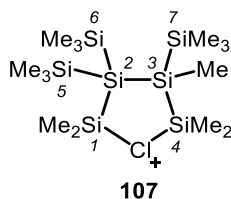
$^1\text{H}$  NMR (499.87 MHz, 203.1 K,  $\text{CD}_2\text{Cl}_2$ ,  $\delta$  ppm): 0.13 (s,  $\text{Si}_4\text{Si}(\text{CH}_3)_3$ ), 0.15 (s,  $\text{Si}_4\text{Si}(\text{CH}_3)_3$ ), 0.25 (s,  $\text{Si}(\text{CH}_3)_3$ ), 0.28 (s,  $\text{Si}(\text{CH}_3)_2$ ), 0.33 (s,  $\text{Si}(\text{CH}_3)_2$ ), 0.94 (s,  $(\text{CH}_3)_2\text{Si-H-Si}(\text{CH}_3)_2$ ), 0.97 (s,  $(\text{CH}_3)_2\text{Si-H-Si}(\text{CH}_3)_2$ ), 2.30 (brs,  $^1J_{\text{Si,H}} = 43\text{ Hz}$ ,  $(\text{CH}_3)_2\text{Si-H-Si}(\text{CH}_3)_2$ ), 2.36 (s,  $^1J_{\text{Si,H}} = 154\text{ Hz}$ , SiH), 3.14 (s,  $^1J_{\text{Si,H}} = 171\text{ Hz}$ , SiH).  $^{29}\text{Si}\{^1\text{H}\}$  NMR (99.31 MHz, 203.1 K,  $\text{CD}_2\text{Cl}_2$ ,  $\delta$  ppm): -137.3 ( $\text{Si}_4\text{Si}$ ), -124.7 ( $\text{Si}_4\text{Si}$ ), -119.0 (SiH), -111.1 (SiH), -11.1 ( $\text{Si}(\text{CH}_3)_3$ ), -9.5 ( $\text{Si}(\text{CH}_3)_3$ ), -5.6 ( $\text{Si}(\text{CH}_3)_3$ ), -7.3 ( $\text{Si}(\text{CH}_3)_3$ ), -7.1 ( $\text{Si}(\text{CH}_3)_3$ ), -5.6 ( $\text{Si}(\text{CH}_3)_3$ ), 107.4 ( $(\text{CH}_3)_2\text{Si-H-Si}(\text{CH}_3)_2$ ), 110.5 ( $(\text{CH}_3)_2\text{Si-H-Si}(\text{CH}_3)_2$ ).  $^{29}\text{Si}$  INEPT NMR (99.31 MHz, 203.1 K,  $\text{CD}_2\text{Cl}_2$ ,  $\delta$  ppm): -137.3 (s,  $\text{Si}_4\text{Si}$ ), -124.7 (s,  $\text{Si}_4\text{Si}$ ), -119.0 (d,  $^1J_{\text{Si,H}} = 154\text{ Hz}$ , SiH), -111.1 (d,  $^1J_{\text{Si,H}} = 171\text{ Hz}$ , SiH), -11.1 (m,  $\text{Si}(\text{CH}_3)_3$ ), -9.5 (m,  $\text{Si}(\text{CH}_3)_3$ ), -5.6 (m,  $\text{Si}(\text{CH}_3)_3$ ), -7.3 (m,  $\text{Si}(\text{CH}_3)_3$ ), -7.1 (m,  $\text{Si}(\text{CH}_3)_3$ ), -5.6 (m,  $\text{Si}(\text{CH}_3)_3$ ), 107.4 (dm,  $^1J_{\text{Si,H}} = 44\text{ Hz}$ ,  $(\text{CH}_3)_2\text{Si-H-Si}(\text{CH}_3)_2$ ), 110.5 (dm,  $^1J_{\text{Si,H}} = 42\text{ Hz}$ ,  $(\text{CH}_3)_2\text{Si-H-Si}(\text{CH}_3)_2$ ).

### Chloronium ion **106**



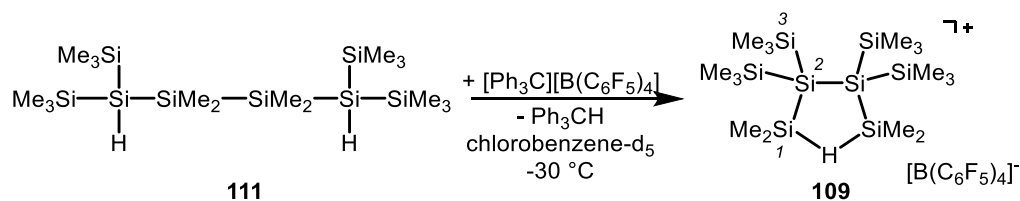
$^1\text{H}$  NMR (499.87 MHz, 213.1 K,  $\text{CD}_2\text{Cl}_2$ ,  $\delta$  ppm): 0.27, 0.28 (s,  $2 \times 9\text{ H}$ ,  $\text{Si}^{5/6}(\text{CH}_3)_3$ ), 0.32 (s,  $9\text{ H}$ ,  $\text{Si}^7(\text{CH}_3)_3$ ), 0.88 (s,  $3\text{ H}$ ,  $\text{Si}^1(\text{CH}_3)_2$ ), 0.93 (s,  $3\text{ H}$ ,  $\text{Si}^4(\text{CH}_3)_2$ ), 0.97 (s,  $3\text{ H}$ ,  $\text{Si}^4(\text{CH}_3)_2$ ), 1.02 (s,  $3\text{ H}$ ,  $\text{Si}^1(\text{CH}_3)_2$ ), 2.94 (s,  $1\text{ H}$ , SiH,  $^1J_{\text{Si,H}} = 107\text{ Hz}$ ).  $^{29}\text{Si}\{^1\text{H}\}$  NMR (99.31 MHz, 213.1 K,  $\text{CD}_2\text{Cl}_2$ ,  $\delta$  ppm): -125.3 ( $\text{Si}^2$ ), -109.0 ( $\text{Si}^3$ ), -8.0 ( $\text{Si}^{5/6/7}(\text{CH}_3)_3$ ), -7.8 ( $\text{Si}^{5/6/7}(\text{CH}_3)_3$ ), -7.4 ( $\text{Si}^{5/6/7}(\text{CH}_3)_3$ ), 101.7 ( $\text{Si}^4$ ), 109.6 ( $\text{Si}^1$ ).  $^{29}\text{Si}$  INEPT NMR (99.31 MHz, 213.1 K,  $\text{CD}_2\text{Cl}_2$ ,  $\delta$  ppm): -125.3 (s,  $\text{Si}^2$ ), -109.0 (d,  $^1J_{\text{Si,H}} = 107\text{ Hz}$ ,  $\text{Si}^3$ ), -8.0 (m,  $\text{Si}^{5/6/7}(\text{CH}_3)_3$ ), -7.8 (m,  $\text{Si}^{5/6/7}(\text{CH}_3)_3$ ), -7.4 (m,  $\text{Si}^{5/6/7}(\text{CH}_3)_3$ ), 101.7 (m,  $\text{Si}^4$ ), 109.6 (m,  $\text{Si}^1$ ).

### Chloronium ion **107**



$^1\text{H}$  NMR (499.87 MHz, 213.1 K,  $\text{CD}_2\text{Cl}_2$ ,  $\delta$  ppm): 0.25 - 0.28 (s, 3 x 9H,  $\text{Si}^{5/6/7}(\text{CH}_3)_3$ ), 0.89, 0.91, 0.92, 1.01 (s, 4 x 3 H,  $\text{Si}^{1/4}(\text{CH}_3)_2$ ).  $^{29}\text{Si}\{^1\text{H}\}$  NMR (99.31 MHz, 213.1 K,  $\text{CD}_2\text{Cl}_2$ ,  $\delta$  ppm): -122.7 ( $\text{Si}^2$ ), -73.1 ( $\text{Si}^3$ ), 103.3 ( $\text{Si}^1$ ), 108.7 ( $\text{Si}^4$ ),  $\text{Si}(\text{CH}_3)_3$ -groups could not be assigned clearly.

Synthesis of hydrogen-bridged bissilyl borate **111** $[\text{B}(\text{C}_6\text{F}_5)_4]$  from 1,4-dihydridotetrasilane **109**

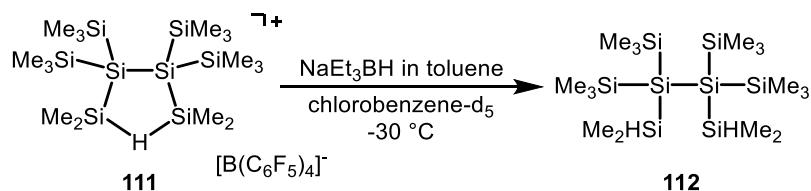


92 mg (1 equiv., 0.10 mmol) of trityl tetrakis(pentafluorophenyl)borate was evacuated in the NMR tube and then cooled to  $T = -80$  °C. A solution of 47 mg (1 equiv., 0.10 mmol) of 1,4-dihydridotetrasilane **111**<sup>[34]</sup> in chlorobenzene- $\text{d}_5$  (0.7 mL) was added to the cold trityl borate via a syringe. The addition was performed so slowly that the solution froze before it reached the trityl borate. The NMR tube was slowly allowed to warm until the solvent melted and the silane slowly reached the trityl borate. At that point, the NMR tube, which was wrapped in a gauze bandage soaked by  $T = -70$  °C cold ethanol, was quickly shaken with a vortex mixer and then quickly transferred to the NMR spectrometer pre-cooled to  $T = -30$  °C.

Cation **109**

$^1\text{H}$  NMR (499.87 MHz, 243.1 K,  $\text{C}_6\text{D}_5\text{Cl}$ ,  $\delta$  ppm): 0.21 (s, 36 H,  $\text{Si}^3(\text{CH}_3)_3$ ), 0.67 (s, 12 H,  $\text{Si}^1(\text{CH}_3)_2$ ), 2.15 (brs, 1H,  $^1J_{\text{Si,H}} = 43$  Hz, Si-H-Si).  $^{13}\text{C}\{^1\text{H}\}$  NMR (125.71 MHz, 243.1 K,  $\text{C}_6\text{D}_5\text{Cl}$ ,  $\delta$  ppm): 3.3 ( $\text{Si}^1(\text{CH}_3)_2$ ), 2.9 ( $\text{Si}^3(\text{CH}_3)_3$ ).  $^{29}\text{Si}\{^1\text{H}\}$  NMR (99.31 MHz, 243.1 K,  $\text{C}_6\text{D}_5\text{Cl}$ ,  $\delta$  ppm): -120.9 ( $\text{Si}^2$ ), -6.4 ( $\text{Si}^3$ ), 108.9 ( $\text{Si}^1$ ).  $^{29}\text{Si}$  INEPT NMR (99.31 MHz, 243.1 K,  $\text{C}_6\text{D}_5\text{Cl}$ ,  $\delta$  ppm): -120.9 (brs,  $\text{Si}^2$ ), -6.4 (decet,  $^2J_{\text{Si,H}} = 6$  Hz,  $\text{Si}^3$ ), 108.9 (dsept,  $^1J_{\text{Si,H}} = 43$  Hz,  $^2J_{\text{Si,H}} = 5$  Hz,  $\text{Si}^1$ ).

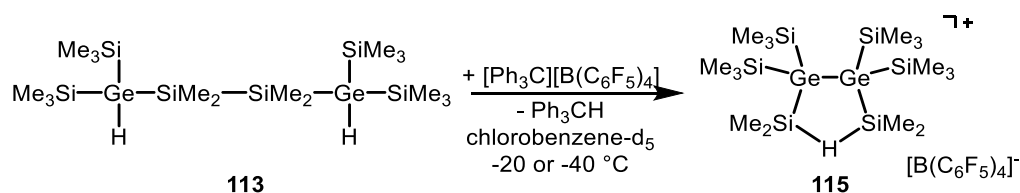
Trapping reaction of hydrogen-bridged bissilyl cation **111**



0.1 mL (0.10 mmol, 1 M in toluene) of sodium triethylborohydride was added to the NMR sample of bisilyl borate **111**[B(C<sub>6</sub>F<sub>5</sub>)<sub>4</sub>] at T = -30 °C. The mixture was allowed to warm to room temperature and the NMR spectra were recorded.

<sup>29</sup>Si INEPT NMR (99.31 MHz, 305.1 K, C<sub>6</sub>D<sub>5</sub>Cl, δ ppm): -132.9 (Si<sub>4</sub>Si), -30.2 (HSi(CH<sub>3</sub>)<sub>2</sub>), -8.8 (Si(CH<sub>3</sub>)<sub>3</sub>).

Synthesis of hydrogen-bridged bisilyl borate **115**[B(C<sub>6</sub>F<sub>5</sub>)<sub>4</sub>] from 1,4-dihydrido-1,4-digermatetrasilane **113**

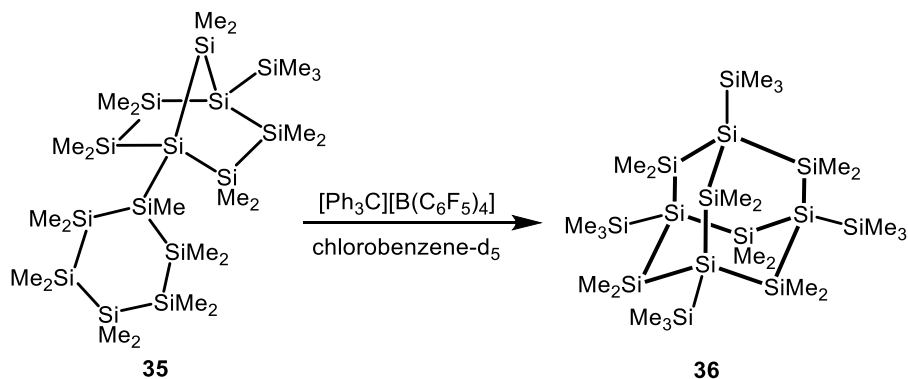


92 mg (1 equiv., 0.10 mmol) of trityl tetrakis(pentafluorophenyl)borate was evacuated in the NMR tube and then cooled to T = -80 °C. A solution of 56 mg (1 equiv., 0.10 mmol) of 1,4-dihydrido-1,4-digermatetrasilane **113** in chlorobenzene-d<sub>5</sub> (0.7 mL) was added to the cold trityl borate via syringe. The addition was performed so slowly that the solution froze before it reached the trityl borate. The NMR tube was slowly allowed to warm until the solvent melted and the silane slowly reached the trityl borate. At that point, the NMR tube, which was wrapped in a gauze bandage soaked by T = -70 °C cold ethanol, was quickly shaken with a vortex mixer and then quickly transferred to the NMR spectrometer pre-cooled at T = -20 °C or T = -40 °C.

Cation **115**

<sup>1</sup>H NMR (499.87 MHz, 232.9 K, C<sub>6</sub>D<sub>5</sub>Cl, δ ppm): 0.25 (s, 36 H, Si(CH<sub>3</sub>)<sub>3</sub>), 0.71 (s, 12 H, Si(CH<sub>3</sub>)<sub>2</sub>), 2.47 (brs, 1 H, <sup>1</sup>J<sub>Si,H</sub> = 45 Hz, (CH<sub>3</sub>)<sub>2</sub>Si-H-Si(CH<sub>3</sub>)<sub>2</sub>). <sup>13</sup>C{<sup>1</sup>H} NMR (125.71 MHz, 233.3 K, C<sub>6</sub>D<sub>5</sub>Cl, δ ppm): 4.1 ((CH<sub>3</sub>)<sub>2</sub>Si-H-Si(CH<sub>3</sub>)<sub>2</sub>), 3.4 (Si(CH<sub>3</sub>)<sub>3</sub>). <sup>29</sup>Si{<sup>1</sup>H} NMR (99.31 MHz, 233.0 K, C<sub>6</sub>D<sub>5</sub>Cl, δ ppm): 0.5 (Si(CH<sub>3</sub>)<sub>3</sub>), 117.5 (Si(CH<sub>3</sub>)<sub>2</sub>). <sup>29</sup>Si INEPT NMR (99.31 MHz, 233.0 K, C<sub>6</sub>D<sub>5</sub>Cl, δ ppm): -0.5 (m, Si(CH<sub>3</sub>)<sub>3</sub>), 117.5 (dsept, <sup>1</sup>J<sub>Si,H</sub> = 45 Hz, <sup>2</sup>J<sub>Si,H</sub> = 6 Hz, (CH<sub>3</sub>)<sub>2</sub>Si-H-Si(CH<sub>3</sub>)<sub>2</sub>).

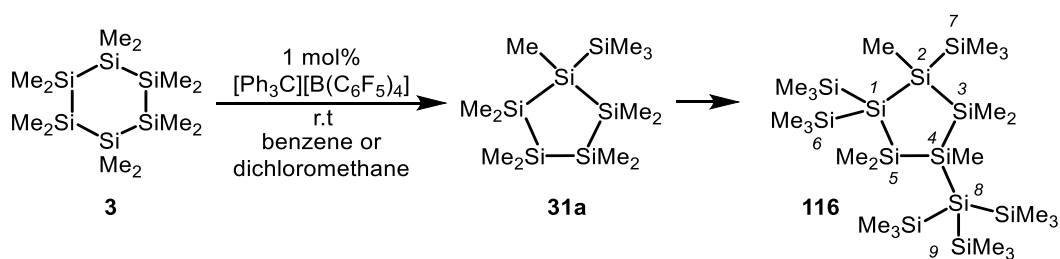
### Rearrangement of bicyclo[2.2.1]heptasilane **35** to sila-adamantane **36**



92 mg (1 equiv., 0.10 mmol) of trityl tetrakis(pentafluorophenyl)borate and 76 mg (1 equiv., 0.10 mmol) of bicyclo[2.2.1]heptasilane **35**<sup>[46]</sup> were evacuated in an Schlenk tube for 1 h and chlorobenzene- $\text{d}_5$  (0.7 mL) was added. The mixture was stirred overnight at room temperature and the progress of the reaction was monitored by  $^{29}\text{Si}$  NMR spectroscopy. The presence of sila-adamantane **36** and the starting material was confirmed by  $^{29}\text{Si}$  INEPT spectroscopy. The NMR sample was stored at room temperature for an additional 35 days. The  $^{29}\text{Si}\{^1\text{H}\}$  NMR spectrum indicates the complete consumption of the starting material and the formation of sila-adamantane **36**.

$^{29}\text{Si}\{^1\text{H}\}$  NMR (99.31 MHz, 305.0 K,  $\text{C}_6\text{D}_5\text{Cl}$ ,  $\delta$  ppm): -118.5 ( $\text{Si}_4\text{Si}$ ), -25.9 ( $\text{Si}(\text{CH}_3)_2$ ), -4.7 ( $\text{Si}(\text{CH}_3)_3$ ).

### Catalytic rearrangement of cyclohexasilane **3** to cyclopentasilanes **31a** and **116**



Two preparations were performed simultaneously which contained of 5 mg (0.01 equiv., 5  $\mu\text{mol}$ ) of trityl tetrakis(pentafluorophenyl)borate and 0.175 g (1 equiv., 0.50 mmol) of cyclohexasilane **3**. Both starting materials were evacuated together in a Schlenk tube for 1 h and dichloromethane- $\text{d}_2$  (2 mL) was added into one tube and benzene- $\text{d}_6$  (2 mL) into the second tube. The mixtures were stirred

overnight at room temperature and the progress of the reactions was monitored by  $^{29}\text{Si}$  NMR spectroscopy.

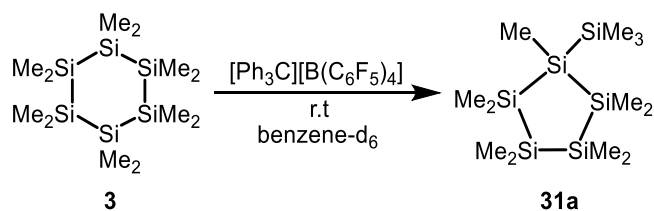
Cyclopentasilane **31a**<sup>[44]</sup>

$^{29}\text{Si}\{^1\text{H}\}$  NMR (99.31 MHz, 305.0 K,  $\text{C}_6\text{D}_6$ ,  $\delta$  ppm): -83.5 ( $\text{Si}_4\text{Si}$ ), -41.2 ( $\text{Si}(\text{CH}_3)_2$ ), -36.4 ( $\text{Si}(\text{CH}_3)_2$ ), -10.5 ( $\text{Si}(\text{CH}_3)_3$ ).

Cyclopentasilane **116**<sup>[119]</sup>

$^{29}\text{Si}\{^1\text{H}\}$  NMR (99.31 MHz, 305.0 K,  $\text{C}_6\text{D}_6$ ,  $\delta$  ppm): -128.5 ( $\text{Si}^8$ ), -127.3 ( $\text{Si}^1$ ), -74.7 ( $\text{Si}^4$ ), -72.0 ( $\text{Si}^1$ ) ( $\text{Si}^2$ ), -24.0 ( $\text{Si}^3$ ), -22.0 ( $\text{Si}^5$ ), -9.6 ( $\text{Si}^{6/7/9}$ ), -8.7 ( $\text{Si}^{6/7/9}$ ), -8.0 ( $\text{Si}^{6/7/9}$ ).

Rearrangement of cyclohexasilane **3** to cyclopentasilane **31a**



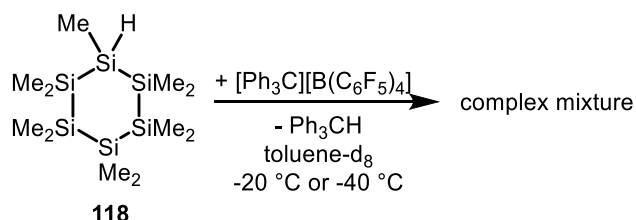
37 mg (1 equiv., 0.4 mmol) of trityl tetrakis(pentafluorophenyl)borate and 0.139 g (1 equiv., 0.40 mmol) of cyclohexasilane **3** were evacuated together in a Schlenk tube for 1 h and benzene- $\text{d}_6$  (2 mL) was added. The mixture was stirred for 1 h at room temperature and the progress of the reaction was monitored by  $^{29}\text{Si}$  NMR spectroscopy. The non-polar phase contained the rearrangement product **31a** and starting material **3**.

Cyclopentasilane **31a**<sup>[44]</sup>

$^{29}\text{Si}\{^1\text{H}\}$  NMR (99.31 MHz, 305.0 K,  $\text{C}_6\text{D}_6$ ,  $\delta$  ppm): -83.3 ( $\text{Si}_4\text{Si}$ ), -41.1 ( $\text{Si}(\text{CH}_3)_2$ ), -36.3 ( $\text{Si}(\text{CH}_3)_2$ ), -10.4 ( $\text{Si}(\text{CH}_3)_3$ ).

Dodecamethylcyclohexasilane **3**<sup>[44]</sup>

$^{29}\text{Si}\{^1\text{H}\}$  NMR (99.31 MHz, 305.0 K,  $\text{C}_6\text{D}_6$ ,  $\delta$  ppm): -42.2 ( $\text{Si}(\text{CH}_3)_2$ ).

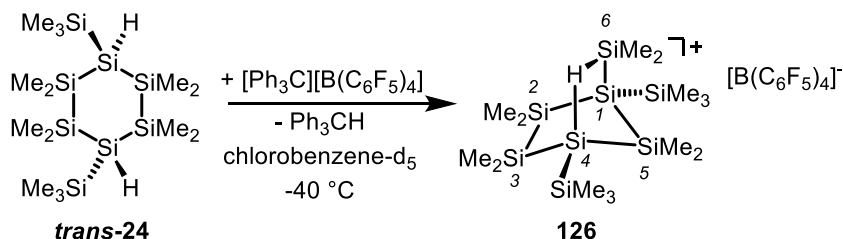
Hydride abstraction from hydridocyclohexasilane **118**

For the reaction at  $T = -20\text{ }^\circ\text{C}$ , 0.369 g (1 equiv., 0.40 mmol) of trityl tetrakis(pentafluorophenyl)-borate and 0.134 g (1 equiv., 0.40 mmol) of hydridocyclohexasilane **118** were both dissolved in toluene- $\text{d}_8$  (0.5 mL) and cooled to  $T = -20\text{ }^\circ\text{C}$ . Hydridocyclohexasilane **118** was slowly added to the borate salt via a Teflon tube and the mixture was stirred at  $T = -20\text{ }^\circ\text{C}$  for 2 h. The polar and non-polar phase were each transferred to separate NMR tubes at  $T = -20\text{ }^\circ\text{C}$  and the NMR spectra were recorded.

For the reaction at  $T = -40\text{ }^\circ\text{C}$ , 0.369 g (1 equiv., 0.40 mmol) of trityl tetrakis(pentafluorophenyl)-borate was evacuated in the NMR tube and dissolved in toluene- $\text{d}_8$  (0.5 mL). The hydridocyclohexasilane **118** was evacuated in a Schlenk tube and also dissolved in toluene- $\text{d}_8$  (0.5 mL). The trityl borate containing NMR tube was cooled to  $T = -40\text{ }^\circ\text{C}$  and the silane was added slowly. The sample was quickly shaken with a vortex mixer and the NMR spectra were acquired immediately at  $T = -40\text{ }^\circ\text{C}$ .

Main signals and possible assignments

$^{29}\text{Si}\{^1\text{H}\}$  NMR (99.31 MHz, 233.0 K,  $\text{C}_7\text{D}_8$ ,  $\delta$  ppm): -88.6 ( $\text{Si}_4\text{Si}$ ), -42.9 ( $\text{Si}(\text{CH}_3)_2$ ), -35.2, -24.7 ( $\text{Si}(\text{CH}_3)_2$ ), -7.4 ( $\text{Si}(\text{CH}_3)_3$ ), 68.3 ( $\text{Si}(\text{C}_7\text{D}_8)^+$ ).

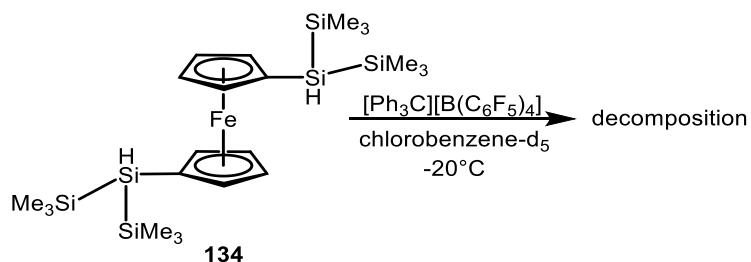
Synthesis of hydrogen-bridged bisilyl borate **126** $[\text{B}(\text{C}_6\text{F}_5)_4]$  from 1,4-dihydridocyclohexasilane *trans*-**24**

92 mg (1 equiv., 0.10 mmol) of trityl tetrakis(pentafluorophenyl)borate was evacuated in the NMR tube and cooled to  $T = -80\text{ }^{\circ}\text{C}$ . A solution of 44 mg (1 equiv., 0.10 mmol) of 1,4-dihydridocyclohexasilane **trans-24**<sup>[10]</sup> in chlorobenzene- $d_5$  (0.7 mL) was added to the cold trityl borate via a syringe. The addition was performed so slowly that the solution froze before it reached the trityl borate. The NMR tube was slowly allowed to warm until the solvent melted and the silane slowly reached the trityl borate. At that point, the NMR tube, which was wrapped in a gauze bandage soaked by  $T = -70\text{ }^{\circ}\text{C}$  cold ethanol, was quickly shaken with a vortex mixer and then quickly transferred to the NMR spectrometer pre-cooled to  $T = -40\text{ }^{\circ}\text{C}$ .

### Cation **126**

$^1\text{H}$  NMR (499.87 MHz, 233.0 K,  $\text{C}_6\text{D}_5\text{Cl}$ ,  $\delta$  ppm): -1.07 (br, Si-H-Si,  $^1J_{\text{Si,H}} = 40\text{ Hz}$ ), 0.17 ( $\text{Si}^1\text{-Si}(\text{CH}_3)_3$ ), 0.20 ( $\text{Si}^4\text{-Si}(\text{CH}_3)_3$ ), 0.23 ( $\text{Si}^2(\text{CH}_3)_2$ ), 0.32 ( $\text{Si}^5(\text{CH}_3)_2$ ), 0.50 ( $\text{Si}^3(\text{CH}_3)_2$ ), 0.62 ( $\text{Si}^6(\text{CH}_3)_2$ ).  $^{13}\text{C}\{^1\text{H}\}$  NMR (125.71 MHz, 233.0 K,  $\text{C}_6\text{D}_5\text{Cl}$ ,  $\delta$  ppm): -5.0 ( $\text{Si}(\text{CH}_3)_2$ ), -3.4 ( $\text{Si}(\text{CH}_3)_2$ ), -2.7 ( $\text{Si}(\text{CH}_3)_2$ ), -2.5 ( $\text{Si}(\text{CH}_3)_2$ ), -2.4 ( $\text{Si}(\text{CH}_3)_2$ ), -1.6 ( $\text{Si}(\text{CH}_3)_2$ ), -0.9 ( $\text{Si}(\text{CH}_3)_2$ ), 0.2 ( $\text{Si}(\text{CH}_3)_3$ ), 1.8 ( $\text{Si}(\text{CH}_3)_3$ ).  $^{29}\text{Si}\{^1\text{H}\}$  NMR (99.31 MHz, 233 K,  $\text{C}_6\text{D}_5\text{Cl}$ ,  $\delta$  ppm): -107.5 ( $\text{Si}^1$ ), -35.3 ( $\text{Si}^2$ ), -33.4 ( $\text{Si}^5$ ), -33.0 ( $\text{Si}^3$ ), -4.2 ( $\text{Si}^1\text{-Si}(\text{CH}_3)_3$ ), -0.7 ( $\text{Si}^4\text{-Si}(\text{CH}_3)_3$ ), 64.1 ( $\text{Si}^4$ ), 78.1 ( $\text{Si}^6$ ).  $^{29}\text{Si}$  INEPT NMR (99.31 MHz, 233 K,  $\text{C}_6\text{D}_5\text{Cl}$ ,  $\delta$  ppm): -107.5 (m,  $\text{Si}^1$ ), -35.3 (m,  $\text{Si}^2$ ), -33.4 (m,  $\text{Si}^5$ ), -33.0 (m,  $\text{Si}^3$ ), -4.2 (m,  $\text{Si}^1\text{-Si}(\text{CH}_3)_3$ ), -0.7 (oct,  $^2J_{\text{Si,H}} = 7\text{ Hz}$ , ( $\text{Si}^4\text{-Si}(\text{CH}_3)_3$ )), 64.1 (d,  $^1J_{\text{Si,H}} = 43\text{ Hz}$ ,  $\text{Si}^4$ ), 78.1 (dsept,  $^1J_{\text{Si,H}} = 39\text{ Hz}$ ,  $^2J_{\text{Si,H}} = 5\text{ Hz}$ ,  $\text{Si}^6$ ).

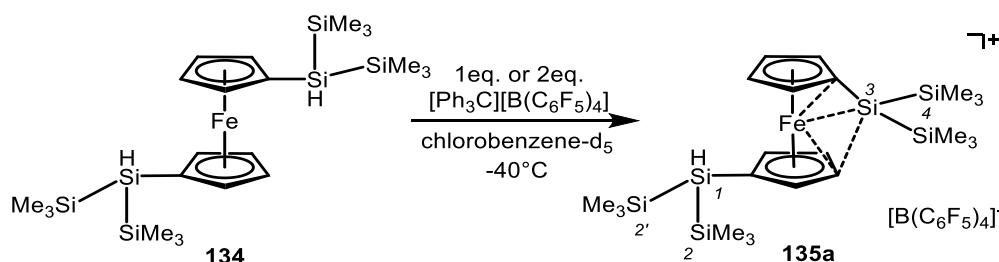
### Hydride abstraction from 1,1'-bissilylferrocene **134**



0.185 g (1 equiv., 0.20 mmol) of trityl tetrakis(pentafluorophenyl)borate and 0.107 g (1 equiv., 0.20 mmol) of 1,1'-bissilylferrocene **134**<sup>[116]</sup> were each dissolved in chlorobenzene- $d_5$  (0.5 mL) in separate Schlenk tubes and cooled to  $T = -20\text{ }^{\circ}\text{C}$ . Silylferrocene was slowly added to the borate salt via a Teflon tube and the mixture was stirred at  $T = -20\text{ }^{\circ}\text{C}$  for 1 h. The solution was transferred into the NMR tube at  $T = -20\text{ }^{\circ}\text{C}$ , stored at  $T = -60\text{ }^{\circ}\text{C}$  overnight until the NMR spectra were recorded the

next morning. The NMR spectra recorded at  $T = -20\text{ }^{\circ}\text{C}$  revealed complete decomposition of the starting material.

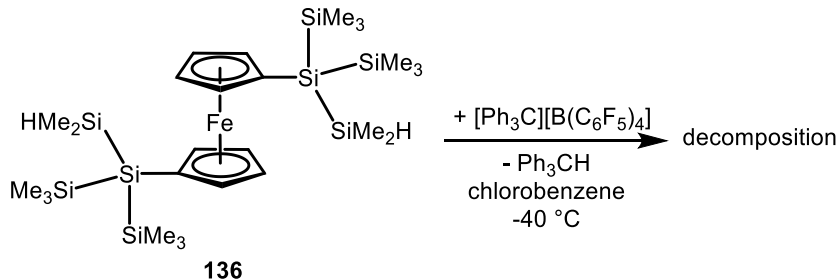
**Synthesis of ferrocene-stabilised silyl borate **135a**[B(C<sub>6</sub>F<sub>5</sub>)<sub>4</sub>] from 1,1'-bissilylferrocene **134****



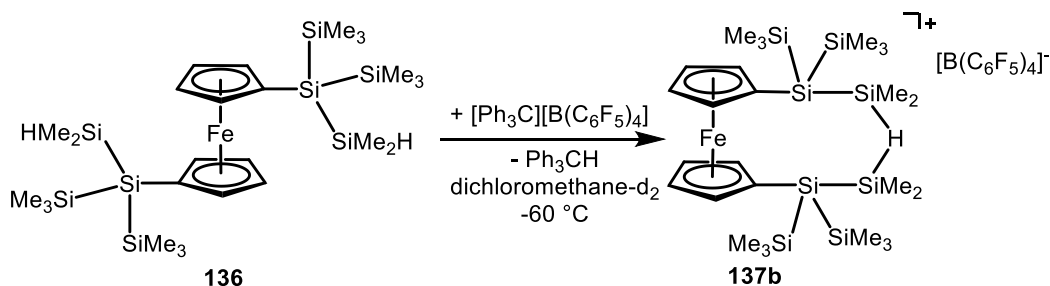
0.185 g (1 equiv. 0.20 mmol) of trityl tetrakis(pentafluorophenyl)borate was evacuated in the NMR tube and cooled to  $T = -80\text{ }^{\circ}\text{C}$ . 0.107 g (1 equiv., 0.20 mmol, or 0.5 equiv. 54 mg, 0.10 mmol) of 1,1'-bissilylferrocene **134**<sup>[116]</sup> was evacuated in a Schlenk tube and dissolved in chlorobenzene- $d_5$  (0.7 mL). The 1,1'-bissilylferrocene **134** was added to the cold trityl borate via syringe. The addition was performed so slowly that the solution froze before it reached the trityl borate. The NMR tube was slowly allowed to warm until the solvent melted and the silane slowly reached the trityl borate. At that point, the NMR tube, which was wrapped in a gauze bandage soaked by  $T = -70\text{ }^{\circ}\text{C}$  cold ethanol, was quickly shaken with a vortex mixer and then quickly transferred to the NMR spectrometer pre-cooled to  $T = -40\text{ }^{\circ}\text{C}$ .

**Cation **135a****

$^1\text{H}$  NMR (499.87 MHz, 233.0 K, C<sub>6</sub>D<sub>5</sub>Cl,  $\delta$  ppm): 0.19 (s, 2 x 9 H, Si<sup>2+2'</sup>(CH<sub>3</sub>)<sub>3</sub>), 0.24 (s, 18 H, Si<sup>4</sup>(CH<sub>3</sub>)<sub>3</sub>), 3.68 (brs, 1 H,  $^1J_{\text{Si,H}} = 172\text{ Hz}$ , Si<sup>1</sup>-H), 3.71 – 5.07 (m, 8 H, Cp-H).  $^{13}\text{C}\{^1\text{H}\}$  NMR (125.71 MHz, 233.0 K, C<sub>6</sub>D<sub>5</sub>Cl,  $\delta$  ppm): 0.2 (s, 2 x Si(CH<sub>3</sub>)<sub>3</sub>), 0.3 (s, 2 x Si(CH<sub>3</sub>)<sub>3</sub>), 56.2 (Cp-C), 73.7 (Cp-C), 74.05 (Cp-C), 77.1 (Cp-C), 84.1 (Cp-C), 85.1 (Cp-C), 89.6 (Cp-C), 90.5 (Cp-C), 91.9 (Cp-C).  $^{29}\text{Si}\{^1\text{H}\}$  NMR (99.31 MHz, 233 K, C<sub>6</sub>D<sub>5</sub>Cl,  $\delta$  ppm): -70.3 (Si<sup>1</sup>), -15.6 (Si<sup>2/2'</sup>), -14.0 (Si<sup>2/2'</sup>), -8.0 (Si<sup>4</sup>), 102.1 (Si<sup>3</sup>).  $^{29}\text{Si}$  INEPT NMR (99.31 MHz, 233 K, C<sub>6</sub>D<sub>5</sub>Cl,  $\delta$  ppm): -70.3 (d,  $^1J_{\text{Si,H}} = 172\text{ Hz}$ , Si<sup>1</sup>), -15.6 (m, Si<sup>2/2'</sup>), -14.0 (m, Si<sup>2/2'</sup>), -8.0 (m, Si<sup>4</sup>), 102.1 (brs, Si<sup>3</sup>).

Hydride abstraction from 1,1'-bissilylferrocene **136**

92 mg (1 equiv. 0.10 mmol) of trityl tetrakis(pentafluorophenyl)borate was evacuated in the NMR tube and cooled to  $T = -80\text{ }^{\circ}\text{C}$ . 67 mg (1 equiv., 0.10 mmol) of 1,1'-bissilylferrocene **136** was evacuated in a Schlenk tube and dissolved in chlorobenzene- $d_5$  (0.7 mL). The silylferrocene was added to the cold trityl borate via syringe. The addition was performed so slowly that the solution froze before it reached the trityl borate. The NMR tube was slowly allowed to warm until the solvent melted and the silane slowly reached the trityl borate. At that point, the NMR tube, which was wrapped in a gauze bandage soaked by  $T = -70\text{ }^{\circ}\text{C}$  cold ethanol, was quickly shaken with a vortex mixer and then quickly transferred to the NMR spectrometer pre-cooled to  $T = -40\text{ }^{\circ}\text{C}$ . The NMR spectra recorded at  $T = -40\text{ }^{\circ}\text{C}$  revealed complete decomposition of the starting material.

Synthesis of hydrogen-bridged ferrocenylbissilyl borate **137b**[B(C<sub>6</sub>F<sub>5</sub>)<sub>4</sub>] from 1,1'-bissilylferrocene **136**

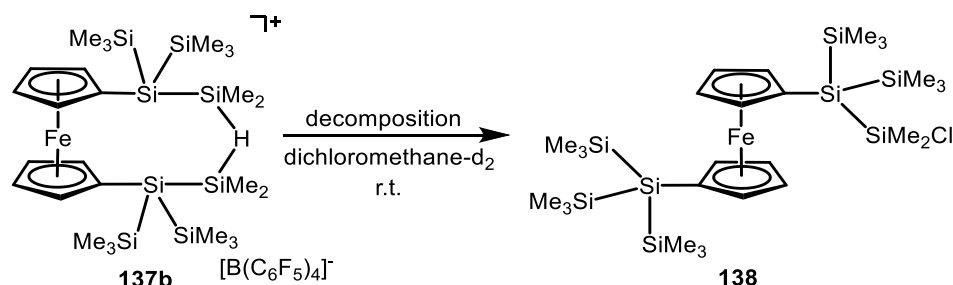
92 mg (1 equiv. 0.10 mmol) of trityl tetrakis(pentafluorophenyl)borate was evacuated in the NMR tube and cooled to  $T = -80\text{ }^{\circ}\text{C}$ . 67 mg (1 equiv., 0.10 mmol) of 1,1'-bissilylferrocene **136** was evacuated in a Schlenk tube and dissolved in dichloromethane- $d_2$  (0.7 mL). The silylferrocene **136** was added to the cold trityl borate via a syringe. The addition was performed so slowly that the solution froze before it reached the trityl borate. The NMR tube was slowly allowed to warm until the solvent melted and the silane slowly reached the trityl borate. At that point, the NMR tube, which was

wrapped in a gauze bandage soaked by  $T = -80\text{ }^{\circ}\text{C}$  cold ethanol, was quickly shaken with a vortex mixer and then quickly transferred to the NMR spectrometer pre-cooled at  $T = -60\text{ }^{\circ}\text{C}$ . The first  $^{29}\text{Si}$  NMR spectrum recorded at  $T = -60\text{ }^{\circ}\text{C}$  revealed signals assigned to the hydrogen-bridged bissilyl cation **137b** but the cation reacted with the solvent very quickly and probably formed the chlorosilane **138** which was stable at room temperature. Due to the short lifetime of the cation, only  $^{29}\text{Si}$  spectra were recorded.

Main signals and possible assignments:

$^{29}\text{Si}\{^1\text{H}\}$  NMR (99.31 MHz, 213 K,  $\text{CD}_2\text{Cl}_2$ ,  $\delta$  ppm): -72.1 ( $\text{Si}_3\text{Si}$ ), -12.1 ( $\text{Si}(\text{CH}_3)_3$ ), -11.0 ( $\text{Si}(\text{CH}_3)_3$ ), 83.5 ( $\text{Si-H-Si}$ ).  $^{29}\text{Si}$  INEPT NMR (99.31 MHz, 213 K,  $\text{CD}_2\text{Cl}_2$ ,  $\delta$  ppm): -72.1 ( $\text{Si}_3\text{Si}$ ), -12.1 (m,  $\text{Si}(\text{CH}_3)_3$ ), -11.0 (m,  $\text{Si}(\text{CH}_3)_3$ ), 83.5 (dm,  $^1J_{\text{Si,H}} \approx 50\text{ Hz}$ ,  $(\text{CH}_3)_2\text{Si-H-Si}(\text{CH}_3)_2$ ).

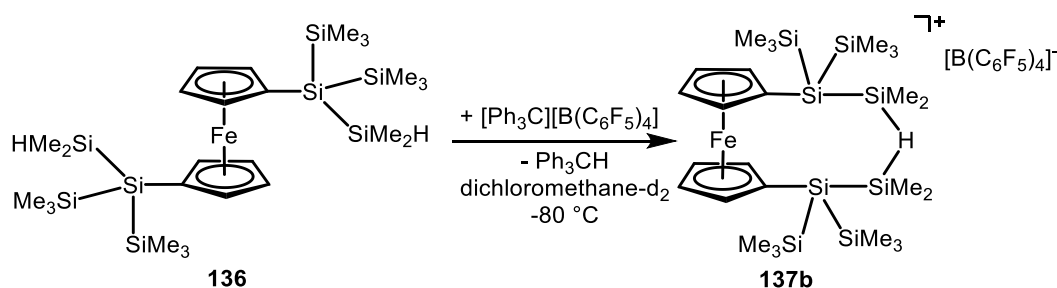
Reaction of hydrogen-bridged ferrocenylbissilyl borate **137b** $[\text{B}(\text{C}_6\text{F}_5)_4]$  with dichloromethane



The NMR sample containing ferrocenylbissilyl borate **137b** $[\text{B}(\text{C}_6\text{F}_5)_4]$  was warmed to room temperature and the  $^{29}\text{Si}\{^1\text{H}\}$  spectrum was recorded.

$^{29}\text{Si}\{^1\text{H}\}$  NMR (99.31 MHz, 305.1 K,  $\text{CD}_2\text{Cl}_2$ ,  $\delta$  ppm): -83.4 ( $((\text{CH}_3)_3\text{Si})_3\text{Si}$ ), -79.6 ( $((\text{CH}_3)_3\text{Si})_2\text{Si-Si}(\text{CH}_3)_2\text{Cl}$ ), -12.7 (3 x  $\text{Si}(\text{CH}_3)_3$ ), -12.6 (2 x  $\text{Si}(\text{CH}_3)_3$ ), 29.3 ( $\text{Si-Cl}$ ).

Synthesis of hydrogen-bridged ferrocenylbissilyl borate **137b**[B(C<sub>6</sub>F<sub>5</sub>)<sub>4</sub>] from 1,1'-bissilylferrocene **136**



92 mg (1 equiv. 0.10 mmol) of trityl tetrakis(pentafluorophenyl)borate was evacuated in the NMR tube and cooled to  $T = -80\text{ }^{\circ}\text{C}$ . 67 mg (1 equiv., 0.10 mmol) of 1,1'-bissilylferrocene **136** was evacuated in a Schlenk tube and dissolved in dichloromethane- $d_2$  (0.7 mL). The silylferrocene **136** was added to the cold trityl borate via syringe. The addition was performed so slowly that the solution froze before it reached the trityl borate. The NMR tube was slowly allowed to warm until the solvent melted and the silane slowly reached the trityl borate. At that point, the NMR tube, which was wrapped in a gauze bandage soaked by  $T = -80\text{ }^{\circ}\text{C}$  cold ethanol, was quickly shaken with a vortex mixer. The NMR tube was frozen in liquid nitrogen and then quickly transferred to the NMR spectrometer pre-cooled to  $T = -80\text{ }^{\circ}\text{C}$ . Due to the broad line width in the  $^1\text{H}$  and  $^{13}\text{C}\{^1\text{H}\}$  spectra, a detailed assignment of the signals and their integrals was not possible.

Cation **137b**

$^1\text{H}$  NMR (499.87 MHz, 193.0,  $\text{CD}_2\text{Cl}_2$ ,  $\delta$  ppm): 0.07 (brs,  $\text{Si}(\text{CH}_3)_3$ ), 0.39 (brs,  $\text{Si}(\text{CH}_3)_3$ ), 0.92 (brs,  $\text{Si}(\text{CH}_3)_2$ ), 0.94 (brs,  $\text{Si}(\text{CH}_3)_2$ ), 2.01 (brs, 1 H,  $((\text{CH}_3)_2\text{Si}-\underline{\text{H}}-\text{Si}(\text{CH}_3)_2)$ ), 3.62 – 4.69 (m, Cp-H).  $^{13}\text{C}\{^1\text{H}\}$  NMR (125.71 MHz, 193.0 K,  $\text{CD}_2\text{Cl}_2$ ,  $\delta$  ppm): -0.9 ( $\text{Si}(\text{CH}_3)_3$ ), -0.4 ( $\text{Si}(\text{CH}_3)_2$ ), 0.9 ( $\text{Si}(\text{CH}_3)_3$ ), 61.4, 70.4 (Cp-C), 71.9 (Cp-C), 74.3 (Cp-C), 74.3 (Cp-C), 74.6 (Cp-C), 75.9 (Cp-C).  $^{29}\text{Si}\{^1\text{H}\}$  NMR (99.31 MHz, 193.0 K,  $\text{CD}_2\text{Cl}_2$ ,  $\delta$  ppm): -72.5 ( $\text{Si}_3\text{Si}$ ), -11.9 ( $\text{Si}(\text{CH}_3)_3$ ), -9.4 ( $\text{Si}(\text{CH}_3)_3$ ), 83.1 ( $((\text{CH}_3)_2\text{Si}-\text{H}-\text{Si}(\text{CH}_3)_2)$ ).  $^{29}\text{Si}$  INEPT NMR (99.31 MHz, 193 K,  $\text{CD}_2\text{Cl}_2$ ,  $\delta$  ppm): -72.5 (m,  $\text{Si}_3\text{Si}$ ), -11.9 (m,  $\text{Si}(\text{CH}_3)_3$ ), -9.4 (m,  $\text{Si}(\text{CH}_3)_3$ ), 83.1 (dm,  $^1J_{\text{Si,H}} = 49\text{ Hz}$ ,  $(\text{CH}_3)_2\text{Si}-\text{H}-\text{Si}(\text{CH}_3)_2$ ).

## 6 Literature

- [1] P. Trefonas, J. R. Damewood, R. West, R. D. Miller, *Organometallics* **1985**, *4*, 1318.
- [2] S. S. Bukalov, L. A. Leites, R. West, *Macromolecules* **2001**, *34*, 6003.
- [3] K. Song, R. D. Miller, G. M. Wallraff, J. F. Rabolt, *Macromolecules* **1992**, *25*, 3629.
- [4] K. Oka, N. Fujiue, T. Dohmaru, C.-H. Yuan, R. West, *J. Am. Chem. Soc.* **1997**, *119*, 4074.
- [5] R. G. Jones, S. J. Holder, *Polym. Int.* **2006**, *55*, 711.
- [6] C. Marschner, in *Struct. Bond.*, Ed.: Scheschkewitz, Springer, Stuttgart, **2014**, Vol. 155, pp. 163.
- [7] M. Ishifune, S. Kashimura, Y. Kogai, Y. Fukuhara, T. Kato, H.-B. Bu, N. Yamashita, Y. Murai, H. Murase, R. Nishida, *J. Organomet. Chem.* **2000**, *611*, 26.
- [8] J. Y. Corey, *Adv. Organomet. Chem.* **2004**, *51*, 1.
- [9] R. Fischer, D. Frank, W. Gaderbauer, C. Kayser, C. Mechtler, J. Baumgartner, C. Marschner, *Organometallics* **2003**, *22*, 3723.
- [10] R. Fischer, T. Konopa, S. Ully, J. Baumgartner, C. Marschner, *J. Organomet. Chem.* **2003**, *685*, 79.
- [11] R. Fischer, J. Baumgartner, G. Kickelbick, K. Hassler, C. Marschner, *Chem. Eur. J.* **2004**, *10*, 1021.
- [12] C. Marschner, J. Baumgartner, A. Wallner, *Dalton Trans.* **2006**, 5667.
- [13] J. Hlina, C. Mechtler, H. Wagner, J. Baumgartner, C. Marschner, *Organometallics* **2009**, *28*, 4065.
- [14] R. Fischer, J. Baumgartner, G. Kickelbick, K. Hassler, C. Marschner, *Monatsh. Chem.* **2006**, *137*, 613.
- [15] J. Baumgartner, R. Fischer, J. Fischer, A. Wallner, C. Marschner, U. Flörke, *Organometallics* **2005**, *24*, 6450.
- [16] A. Sekiguchi, V. Y. Lee, M. Nanjo, *Coord. Chem. Rev.* **2000**, *210*, 11.
- [17] P. D. Lickiss, C. M. Smith, *Coord. Chem. Rev.* **1995**, *145*, 75.
- [18] K. Tamao, A. Kawachi, *Adv. Organomet. Chem.* **1995**, *38*, 1.
- [19] J. Belzner, U. Dehnert, in *The Chemistry of Organic Silicon Compounds*, Eds.: Z. Rappoport, Apeloig, Wiley, Chichester, **2003**, Vol. 2, pp. 779.
- [20] W. C. Still, *J. Org. Chem.* **1976**, *41*, 3063.
- [21] H. Gilman, J. M. Holmes, C. L. Smith, *Chem. Ind. (London)* **1965**, 848.
- [22] H. Gilman, C. L. Smith, *J. Organomet. Chem.* **1968**, *14*, 91.
- [23] G. Gutekunst, A. G. Brook, *J. Organomet. Chem.* **1982**, *225*, 1.
- [24] H. Gilman, R. L. Harrell Jr., *J. Organomet. Chem.* **1967**, *9*, 67.
- [25] H. Sakurai, A. Okada, M. Kira, K. Yonezawa, *Tetrahedron Lett.* **1971**, *12*, 1511.
- [26] Y. Apeloig, G. Korogodsky, D. Bravo-Zhivotovskii, D. Bläser, R. Boese, *Eur. J. Inorg. Chem.* **2000**, *2000*, 1091.
- [27] H. Sakurai, F. Kondo, *J. Organomet. Chem.* **1975**, *92*, C46.
- [28] E. Buncel, T. K. Venkatachalam U. Edlund, *J. Organomet. Chem.* **1992**, *437*, 85.
- [29] F. Uhlig, P. Gspaltl, M. Trabi, E. Hengge, *J. Organomet. Chem.* **1995**, *493*, 33.
- [30] C. Marschner, *Organometallics* **2006**, *25*, 2110.
- [31] S. M. Whittaker, M.-C. Brun, F. Cervantes-Lee, K. H. Pannell, *J. Organomet. Chem.* **1995**, *499*, 247.
- [32] J. R. Blanton, J. B. Diminnie, T. Chen, A. M. Wiltz, Z. Xue, *Organometallics* **2001**, *20*, 5542.
- [33] C. Mechtler, C. Marschner, *Tetrahedron Lett.* **1999**, *40*, 7777.
- [34] C. Kayser, G. Kickelbick, C. Marschner, *Angew. Chem. Int. Ed.* **2002**, *41*, 989.

- [35] R. Fischer, C. Marschner, in *Organosilicon Chemistry V: From Molecules to Materials*, Eds.: Auner, Weis, Wiley-VCH Verlag GmbH, **2008**, pp. 190.
- [36] E. Colomer, R. Corriu, *J. Chem. Soc., Chem. Commun.* **1976**, 176.
- [37] C. D. Nenitzescu, A. Drăgan, *Ber. Dtsch. Chem. Ges.* **1933**, 66, 1892.
- [38] G. Calingaert, H. A. Beatty, *J. Am. Chem. Soc.* **1936**, 58, 51.
- [39] A. L. Glasebrook, N. E. Phillips, W. G. Lovell, *J. Am. Chem. Soc.* **1936**, 58, 1944.
- [40] C. W. Montgomery, J. H. McAteer, N. W. Franke, *J. Am. Chem. Soc.* **1937**, 59, 1768.
- [41] P. von R. Schleyer, *J. Am. Chem. Soc.* **1957**, 79, 3292.
- [42] M. Ishikawa, M. Kumada, *J. Chem. Soc., Chem. Commun.* **1969**, 567.
- [43] M. Ishikawa, M. Kumada, *J. Chem. Soc., Chem. Commun.* **1970**, 157.
- [44] M. Ishikawa, M. Watanabe, J. Iyoda, H. Ikeda, M. Kumada, *Organometallics* **1982**, 1, 317.
- [45] M. Ishikawa, J. Iyoda, H. Ikeda, K. Kotake, T. Hashimoto, M. Kumada, *J. Am. Chem. Soc.* **1981**, 103, 4845.
- [46] J. Fischer, J. Baumgartner, C. Marschner, *Science* **2005**, 310, 825.
- [47] T. A. Blinka, R. West, *Organometallics* **1986**, 5, 128.
- [48] G. Märkl, R. Wagner, *Tetrahedron Lett.* **1986**, 27, 4015.
- [49] S. Sharma, N. Caballero, H. Li, K. H. Pannell, *Organometallics* **1999**, 18, 2855.
- [50] M. Kumada, M. Ishikawa, S. Maeda, *J. Organomet. Chem.* **1966**, 5, 120.
- [51] C. Eaborn, D. A. R. Happer, K. D. Safa, D. R. M. Walton, *J. Organomet. Chem.* **1978**, 157, C50.
- [52] C. Eaborn, D. A. R. Happer, S. P. Hopper, K. D. Safa, *J. Organomet. Chem.* **1980**, 188, 179.
- [53] C. Eaborn, P. D. Lickiss, S. T. Najim, W. A. Stanczyk, *J. Chem. Soc., Chem. Commun.* **1987**, 1461.
- [54] C. Eaborn, *J. Chem. Soc., Dalton Trans.* **2001**, 3397.
- [55] A. Schäfer, M. Reißmann, A. Schäfer, M. Schmidtman, T. Müller, *Chem. Eur. J.* **2014**, 20, 9381.
- [56] T. Müller, in *Struct. Bond.*, Ed.: Scheschkewitz, Springer, Berlin, **2014**, Vol. 155, pp. 107.
- [57] T. Müller, in *Science of Synthesis Knowledge Updates*, Ed.: Oestreich, Thieme Verlag, Stuttgart, **2013**, Vol. 3, pp. 1.
- [58] T. Müller, *Adv. Organomet. Chem.* **2005**, 53, 155.
- [59] J. B. Lambert, S. Zhang, *J. Chem. Soc., Chem. Commun.* **1993**, 383.
- [60] J. B. Lambert, S. Zhang, S. M. Ciro, *Organometallics* **1994**, 13, 2430.
- [61] C.-H. Ottosson, D. Cremer, *Organometallics* **1996**, 15, 5495.
- [62] C.-H. Ottosson, K. J. Szabó, D. Cremer, *Organometallics* **1997**, 16, 2377.
- [63] M. Ichinohe, M. Igarashi, K. Sanuki, A. Sekiguchi, *J. Am. Chem. Soc.* **2005**, 127, 9978.
- [64] A. Sekiguchi, T. Matsuno, M. Ichinohe, *J. Am. Chem. Soc.* **2000**, 122, 11250.
- [65] S. Inoue, M. Ichinohe, T. Yamaguchi, A. Sekiguchi, *Organometallics* **2008**, 27, 6056.
- [66] M. Igarashi, M. Ichinohe, A. Sekiguchi, *J. Am. Chem. Soc.* **2007**, 129, 12660.
- [67] M. Nakamoto, T. Fukawa, A. Sekiguchi, *Chem. Lett.* **2004**, 33, 38.
- [68] H. Wagner, J. Baumgartner, T. Müller, C. Marschner, *J. Am. Chem. Soc.* **2009**, 131, 5022.
- [69] J. Fischer, J. Baumgartner, C. Marschner, *Organometallics* **2005**, 24, 1263.
- [70] A. Schäfer, W. Saak, D. Haase, T. Müller, *Angew. Chem. Int. Ed.* **2012**, 51, 2981.
- [71] S. P. Hoffmann, T. Kato, F. S. Tham, C. A. Reed, *Chem. Commun.* **2006**, 767.
- [72] M. Nava, C. A. Reed, *Organometallics* **2011**, 30, 4798.
- [73] Z. Xie, R. Bau, C. A. Reed, *J. Chem. Soc., Chem. Commun.* **1994**, 2519.
- [74] S. R. Bahr, P. Boudjouk, *J. Am. Chem. Soc.* **1993**, 115, 4514.
- [75] T. Nishinaga, Y. Izukawa, K. Komatsu, *J. Am. Chem. Soc.* **2000**, 122, 9312.
- [76] T. Nishinaga, Y. Izukawa, K. Komatsu, *Tetrahedron* **2001**, 57, 3645.
- [77] H. F. T. Klare, K. Bergander, M. Oestreich, *Angew. Chem. Int. Ed.* **2009**, 48, 9077.

- [78] K. Müther, R. Fröhlich, C. Mück-Lichtenfeld, S. Grimme, M. Oestreich, *J. Am. Chem. Soc.* **2011**, *133*, 12442.
- [79] C. A. Reed, Z. Xie, R. Bau, A. Benesi, *Science* **1993**, *262*, 402.
- [80] C. A. Reed, *Acc. Chem. Res.* **1998**, *31*, 325.
- [81] Z. Xie, J. Manning, R. W. Reed, R. Mathur, P. D. W. Boyd, A. Benesi, C. A. Reed, *J. Am. Chem. Soc.* **1996**, *118*, 2922.
- [82] A. Avelar, F. S. Tham, C. A. Reed, *Angew. Chem. Int. Ed.* **2009**, *48*, 3491.
- [83] T. Küppers, E. Bernhardt, R. Eujen, H. Willner, C. W. Lehmann, *Angew. Chem. Int. Ed.* **2007**, *46*, 6346.
- [84] Z. Xie, C.-W. Tsang, E. T.-P. Sze, Q. Yang, D. T. W. Chan, T. C. W. Mak, *Inorg. Chem.* **1998**, *37*, 6444.
- [85] C.-W. Tsang, Q. Yang, E. T.-P. Sze, T. C. W. Mak, D. T. W. Chan, Z. Xie, *Inorg. Chem.* **2000**, *39*, 5851.
- [86] C. A. Reed, *Acc. Chem. Res.* **1998**, *31*, 133.
- [87] B. T. King, Z. Janoušek, B. Grüner, M. Trammell, B. C. Noll, J. Michl, *J. Am. Chem. Soc.* **1996**, *118*, 3313.
- [88] M. Kessler, C. Knapp, V. Sagawe, H. Scherer, R. Uzun, *Inorg. Chem.* **2010**, *49*, 5223.
- [89] C. Bolli, J. Derendorf, C. Jenne, H. Scherer, C. P. Sindlinger, B. Wegener, *Chem. Eur. J.* **2014**, *20*, 13783.
- [90] I. Krossing, *Chem. Eur. J.* **2001**, *7*, 490.
- [91] J. B. Lambert, S. Zhang, C. L. Stern, J. C. Huffman, *Science* **1993**, *260*, 1917.
- [92] J. B. Lambert, Y. Zhao, *Angew. Chem. Int. Ed.* **1997**, *36*, 400.
- [93] T. Müller, Y. Zhao, J. B. Lambert, *Organometallics* **1998**, *17*, 278.
- [94] J. B. Lambert, Y. Zhao, H. Wu, W. C. Tse, B. Kuhlmann, *J. Am. Chem. Soc.* **1999**, *121*, 5001.
- [95] K.-C. Kim, C. A. Reed, D. W. Elliott, L. J. Mueller, F. Tham, L. Lin, J. B. Lambert, *Science* **2002**, *297*, 825.
- [96] P. D. Bartlett, F. E. Condon, A. Schneider, *J. Am. Chem. Soc.* **1944**, *66*, 1531.
- [97] J. Y. Corey, *J. Am. Chem. Soc.* **1975**, *97*, 3237.
- [98] J. B. Lambert, J. A. McConnell, W. J. Schulz, *J. Am. Chem. Soc.* **1986**, *108*, 2482.
- [99] H. Mayr, N. Basso, G. Hagen, *J. Am. Chem. Soc.* **1992**, *114*, 3060.
- [100] J. Chojnowski, W. Fortuniak, W. Stanczyk, *J. Am. Chem. Soc.* **1987**, *109*, 7776.
- [101] Y. Apeloig, O. Merin-Aharoni, D. Danovich, A. Ioffe, S. Shaik, *Isr. J. Chem.* **1993**, *33*, 387.
- [102] I. Krossing, H. Brands, R. Feuerhake, S. Koenig, *J. Fluorine Chem.* **2001**, *112*, 83.
- [103] M. Reissmann, Dissertation thesis, Carl von Ossietzky University (Oldenburg), **2014**.
- [104] S. J. Connelly, W. Kaminsky, D. M. Heinekey, *Organometallics* **2013**, *32*, 7478.
- [105] M. F. Ibad, P. Langer, A. Schulz, A. Villinger, *J. Am. Chem. Soc.* **2011**, *133*, 21016.
- [106] T. Müller, *Angew. Chem. Int. Ed.* **2001**, *40*, 3033.
- [107] R. Panisch, M. Bolte, T. Müller, *J. Am. Chem. Soc.* **2006**, *128*, 9676.
- [108] A. Y. Khalimon, Z. H. Lin, R. Simionescu, S. F. Vyboishchikov, G. I. Nikonov, *Angew. Chem. Int. Ed.* **2007**, *46*, 4530.
- [109] A. Sekiguchi, Y. Murakami, N. Fukaya, Y. Kabe, *Chem. Lett.* **2004**, *33*, 530.
- [110] N. Kordts, C. Borner, R. Panisch, W. Saak, T. Müller, *Organometallics* **2014**, *33*, 1492.
- [111] M. A. R. George, M. Savoca, O. Dopfer, *Chem. Eur. J.* **2013**, *19*, 15315.
- [112] M. Savoca, J. Langer, O. Dopfer, *Angew. Chem. Int. Ed.* **2013**, *52*, 1568.
- [113] A. Schäfer, M. Reißmann, A. Schäfer, W. Saak, D. Haase, T. Müller, *Angew. Chem. Int. Ed.* **2011**, *50*, 12636.
- [114] A. Schäfer, M. Reißmann, S. Jung, A. Schäfer, W. Saak, E. Brendler, T. Müller, *Organometallics* **2013**, *32*, 4713.

- [115] U. Baumeister, K. Schenzel, R. Zink, K. Hassler, *J. Organomet. Chem.* **1997**, *543*, 117.
- [116] H. Wagner, J. Baumgartner, C. Marschner, *Organometallics* **2007**, *26*, 1762.
- [117] C. Krempner, *Polymers* **2002**, *4*, 408.
- [118] C. Marschner, *Eur. J. Inorg. Chem.* **1998**, *1998*, 221.
- [119] H. Wagner, A. Wallner, J. Fischer, M. Flock, J. Baumgartner, C. Marschner, *Organometallics* **2007**, *26*, 6704.
- [120] D. A. Stanislawski, R. West, *J. Organomet. Chem.* **1981**, *204*, 307.
- [121] G. Kollegger, K. Hassler, *J. Organomet. Chem.* **1995**, *485*, 233.
- [122] H. Schuster, E. Hengge, *Monatsh. Chem.* **1983**, *114*, 1305.
- [123] K. Schenzel, K. Hassler, *Spectrochim. Acta, Part A* **1994**, *50*, 127.
- [124] U. Herzog, G. Roewer, *J. Organomet. Chem.* **1997**, *527*, 117.
- [125] W. Uhlig, *Chem. Ber.* **1992**, *125*, 47.
- [126] W. Uhlig, *J. Organomet. Chem.* **1991**, *409*, 377.
- [127] W. Uhlig, *J. Organomet. Chem.* **1993**, *463*, 73.
- [128] A. Wallner, J. Hlina, H. Wagner, J. Baumgartner, C. Marschner, *Organometallics* **2011**, *30*, 3930.
- [129] H. Wagner, J. Baumgartner, C. Marschner, P. Poelt, *Organometallics* **2011**, *30*, 3939.
- [130] E. V. Anslyn, D. A. Dougherty, *Modern Physical Organic Chemistry*, University Science Books, Sausalito, California, **2006**.
- [131] C. Hansch, A. Leo, R. W. Taft, *Chem. Rev.* **1991**, *91*, 165.
- [132] H. C. Brown, Y. Okamoto, *J. Am. Chem. Soc.* **1958**, *80*, 4979.
- [133] L. M. Stock, H. C. Brown, *Adv. Phys. Org. Chem.* **1963**, *1*, 35.
- [134] L. Albers, M. A. Meshgi, J. Baumgartner, C. Marschner, T. Müller, *Organometallics* **2015**, *34*, 3756.
- [135] H. F. T. Klare, M. Oestreich, *Dalton Trans.* **2010**, *39*, 9176.
- [136] P. D. Lickiss, P. C. Masangane, W. Sohal, G. L. Veneziani, in *Organosilicon Chemistry V*, Wiley-VCH Verlag GmbH, **2008**, pp. 45.
- [137] A. F. Holleman, E. Wiberg, N. Wiberg, *Lehrbuch der Anorganischen Chemie*, Vol. 102, Walter de Gruyter-VCH Verlag GmbH, Berlin, **2007**.
- [138] U. Herzog, N. Schulze, K. Trommer, G. Roewer, *J. Organomet. Chem.* **1997**, *547*, 133.
- [139] S. Grimme, J. Antony, S. Ehrlich, H. Krieg, *J. Chem. Phys.* **2010**, *132*, 154104.
- [140] J. P. Wagner, P. R. Schreiner, *Angew. Chem. Int. Ed.* **2015**, *54*, 12274.
- [141] S. Grimme, *Wiley Interdisciplinary Reviews: Computational Molecular Science* **2011**, *1*, 211.
- [142] H. Arp, M. Zirngast, C. Marschner, J. Baumgartner, K. Rasmussen, P. Zark, T. Müller, *Organometallics* **2012**, *31*, 4309.
- [143] M. Lehmann, A. Schulz, A. Villinger, *Angew. Chem. Int. Ed.* **2009**, *48*, 7444.
- [144] J. P. Wagner, P. R. Schreiner, *Angew. Chem. Int. Ed.* **2015**, n/a.
- [145] J. Y. Corey, D. Gust, K. Mislow, *J. Organomet. Chem.* **1975**, *101*, C7.
- [146] M. J. MacLachlan, S. C. Bourke, A. J. Lough, I. Manners, *J. Am. Chem. Soc.* **2000**, *122*, 2126.
- [147] S. C. Bourke, M. J. MacLachlan, A. J. Lough, I. Manners, *Chem. Eur. J.* **2005**, *11*, 1989.
- [148] M. Kira, T. Hino, H. Sakurai, *J. Am. Chem. Soc.* **1992**, *114*, 6697.
- [149] K. Trommer, U. Herzog, G. Roewer, *J. Prakt. Chem.* **1997**, *339*, 637.
- [150] R. Panisch, M. Bolte, T. Müller, *Organometallics* **2007**, *26*, 3524.
- [151] H. H. Cramer, Bachelor thesis, Carl von Ossietzky University (Oldenburg), **2015**.
- [152] A. G. Massey, A. J. Park, *J. Organomet. Chem.* **1964**, *2*, 245.
- [153] J. C. W. Chien, W. M. Tsai, M. D. Rausch, *J. Am. Chem. Soc.* **1991**, *113*, 8570.
- [154] H. Gilman, C. L. Smith, *J. Organomet. Chem.* **1967**, *8*, 245.
- [155] S. P. Mallela, M. A. Ghuman, R. A. Geanangel, *Inorg. Chim. Acta* **1992**, *202*, 211.

- [156] A. G. Brook, F. Abdesaken, H. Söllradl, *J. Organomet. Chem.* **1986**, 299, 9.
- [157] J. B. G. Gluyas, C. Burschka, P. Kraft, R. Tacke, *Organometallics* **2010**, 29, 5897.
- [158] L. F. Brough, K. Matsumura, R. West, *Angew. Chem. Int. Ed.* **1979**, 18, 955.
- [159] D. A. Stanislawski, R. West, *J. Organomet. Chem.* **1980**, 204, 295.
- [160] R. West, H. R. Hunt, R. O. Whipple, *J. Am. Chem. Soc.* **1954**, 76, 310.
- [161] K. Moedritzer, J. R. Van Wazer, *Inorg. Chem.* **1965**, 4, 1753.
- [162] S. Sharma, K. H. Pannell, *Organometallics* **2000**, 19, 1225.
- [163] A. Schäfer, A. Schäfer, T. Müller, *Dalton Trans.* **2010**, 39, 9296.
- [164] M. J. T. Frisch, G. W.; Cheeseman, J. R.; Scalmani, G.; Caricato, M.; Hratchian, H. P.; Li, X.; Barone, V.; Bloino, J.; Zheng, G.; Vreven, T.; Montgomery, J. A.; Petersson, G., G. E. S. A.; Scuseria, H. B.; Nakatsuji, H.; Izmaylov, A. F.; Martin, R. L.; J. L. P. Sonnenberg, J. E.; Heyd, J. J.; Brothers, E.; Ogliaro, F.; Bearpark, M.; Robb,, B. K. M. A.; Mennucci, K. N.; Staroverov, V. N.; Kobayashi, R.; Normand, J.;, A. G. Rendell, R.; Zakrzewski, V. G.; Hada, M.; Ehara, M.; Toyota, K.; Fukuda,, J. I. R.; Hasegawa, M.; Nakajima, T.; Honda, Y.; Kitao, O.; Nakai, H., *Gaussian 09*.
- [165] D. Rappoport, F. Furche, *J. Chem. Phys.* **2010**, 133, 134105.
- [166] Y. Zhao, D. Truhlar, *Theor. Chem. Acc.* **2008**, 120, 215.
- [167] J. Tomasi, B. Mennucci, R. Cammi, *Chem. Rev.* **2005**, 105, 2999.
- [168] W. Kutzelnigg, U. Fleischer, M. Schindler, *The IGLO-Method: Ab Initio Calculation and Interpretation of NMR Chemical Shifts and Magnetic Susceptibilities*, Springer-Verlag, Heidelberg, **1990**.

## 7 Appendix

### 7.1 Computational Details

All quantum chemical calculations were carried out using the Gaussian09 package.<sup>[164]</sup> If not noted otherwise, structure optimisations were performed using the M06-2X functional along with the 6-311+G(d,p) basis set as implemented in Gaussian 09. Structure optimisations of iron containing structures were performed using the M06-2X functional together with a generated basis set using 6-311+g(d,p) for Si, C and H and def2tzvpd<sup>[165]</sup> for Fe. In order to be consistent with previously reported data<sup>[68]</sup>, the molecular structures of toluene complexes  $[54(\text{C}_7\text{H}_8)]^+$  -  $[59(\text{C}_7\text{H}_8)]^+$  were optimised at the density functional B3LYP level of theory<sup>[166]</sup> using the 6-311+G(d,p) basis. Every stationary point was identified by a subsequent frequency calculation as minimum (Number of imaginary frequencies (NIMAG): 0). NMR chemical shift computations were performed using the GIAO method as implemented in Gaussian 09 and the M06-L functional along with the 6-311G(2d,p) basis set for molecular structures obtained at the M06-2X/6-311+G(d,p) level of theory.<sup>[167]</sup> Si-H coupling constants were calculated at B3LYP level of theory along with the IGLOIII basis set<sup>[168]</sup>.

All optimised structures and their ground state energies can be found in the form of their xyz-files on the attached CD-ROM.

Simulated  $^{29}\text{Si}$  NMR spectra were obtained by plotting the calculated  $^{29}\text{Si}$  NMR calculated shifts with the NMR simulation program gNMR, at revision level 5.1, marketed by Adept Scientific until May 2005.

### 7.2 Index of Abbreviations

Ar	aryl
b.p.	boiling point
br (NMR)	broad signal
Cp	cyclopentadienyl
d (NMR)	doublet
DME	dimethoxyethane

DMI	1,3-dimethyl-2-imidazolidinone
DMPU	1,3-dimethyltetrahydropyrimidin-2-one
E	energy
Et	ethyl
Fc	ferrocenyl
G	Gibbs free energy
GC	gas chromatography
h	hour
HMBC	heteronuclear multiple bond coherence
HMPA	hexamethylphosphoramide
HMQC	heteronuclear multiple quantum coherence
HR/MS	high-resolution mass spectrometry
INEPT	insensitive nuclei enhanced by polarisation transfer
IR	infrared spectroscopy
<i>J</i>	coupling constant
m (NMR)	multiplet
<i>m</i>	<i>meta</i>
Me	methyl
Mes	mesityl (2,4,6-trimethylphenyl)
min	minute
m.p.	melting point
NMR	nuclear spin magnetic resonance
<i>o</i>	<i>ortho</i>

OTf	triflate (trifluoromethanesulfonyl)
<i>p</i>	<i>para</i>
p	pressure
Ph	phenyl
ppm	parts per million
<i>i</i> Pr	<i>iso</i> -propyl
r.t.	room temperature
s (NMR)	singlet
sept (NMR)	septet
T	temperature
thexyl	<i>tert</i> -hexyl
Tol	tolyl
<i>t</i> Bu	<i>tert</i> -butyl
THF	tetrahydrofuran
Tipp	2,4,6-tri- <i>iso</i> -propylphenyl
trityl	triphenylmethyl
$\tilde{\nu}$	wavenumber
Xyl	xylyl (2,6-dimethylphenyl)

## 8 Curriculum Vitae

### Lena Albers

Artillerieweg 8 • 26129 Oldenburg • Tel.: +49 176 / 831 20 446

Lena.albers@uni-oldenburg.de

Date of birth: 4<sup>th</sup> Nov. 1986 in Emden

Nationality: German

---

#### • Education

- 01/2012 - 10/2015    **Postgraduate studies** in the workgroup of Prof. Müller at the Institute of Chemistry at the Carl von Ossietzky University Oldenburg, Germany.
- 10/2009 - 11/2011    **Master studies** at the Institute of Chemistry at the Carl von Ossietzky University Oldenburg, Germany. (Grade 1.20)
- 10/2006 - 09/2009    **Bachelor studies**, at the Institute of Chemistry at the Carl von Ossietzky University Oldenburg, Germany. (Grade 1.64)
- 08/1999 - 06/2006    **A-levels**, grammar school, Johannes–Althusius Gymnasium in Emden, Germany. (Grade 2.30)

#### • Work Experience

- Since 01/2012        **Dissertation** in Prof. Müller's group at the Institute of Chemistry at the Carl von Ossietzky University Oldenburg, Germany.  
Title: *"Mechanistic investigations on Lewis acid-catalysed skeletal rearrangement reactions of polysilanes and germapolysilanes - Subtle capture of intermediates"*
- 11/2013 - 12/2013    **Research stay** at international corporation-partner to learn new methodical expertise; Prof. Marschner, TU Graz, Austria.
- 04/2011 - 11/2011    **Master Thesis** in Prof. Müller's group at the Institute of Chemistry at the Carl von Ossietzky University Oldenburg, Germany.  
Title: *"Lewis acid catalysed rearrangements reactions of germapolysilanes."*
- 09/2010 - 12/2010    **Internship** in Prof. Wirth's group at Cardiff University, UK.  
Title: *"Rearrangement of chalcones using hypervalent iodine reagents."*

- 04/2010 - 10.2015    **Supervising** Master and Bachelor students during research projects and theses.  
                         **Tutoring** first year students in their first inorganic and organic lab courses.
- 04/2009 - 09/2009    **Bachelor Thesis** in Prof. Martens' group at the Institute of Chemistry at the Carl von Ossietzky University Oldenburg, Germany.  
  
                         Title: "*Investigations on the synthesis of linear or cyclic dipeptides using the Ugi-reaction and metathesis.*"

• **Conference Contributions**

- 07/2015                **Poster:** Internat. Symposium on Inorganic Ring Systems, Regensburg, Germany
- 06/2015                **Poster:** Gordon Research Conference, New Hampshire, USA
- 09/2014                **Poster:** Wöhler-Conference, Saarbrücken, Germany
- 09/2014                **Poster:** North-German PhD Colloquium, Rostock, Germany
- 08/2014                **Poster:** Internat. Symposium on Silicon Chemistry, Berlin, Germany
- 09/2013                **Oral Presentation + Poster:** North-German PhD Colloquium, Bremen, Germany
- 09/2013                **Poster:** GDCh Science Forum Chemistry, Darmstadt, Germany
- 09/2012                **Poster:** North-German PhD Colloquium, Walsrode, Germany
- 09/2012                **Poster:** Wöhler-Conference, Göttingen, Germany
- 09/2012                **Poster:** European Silicon Days, Lyon, France

• **Publications**

- 2015                    *Recent Advances in the Chemistry of Silylium Ions*, L. Albers, H. Klare, T. Müller, M. Oestreich, *Chem. Rev.* **2015**, invited to submit in autumn.
- 04/2015                *Wagner Meerwein-Type Rearrangements in Germapolysilanes - A Stable Ion Study*, Albers, L.; Meshgi, M. A.; Baumgartner, J.; Marschner, C.; Müller, T.; *Organometallics* **2015**, 34, 3756.
- 06/2014                *Formation and Properties of a Bicyclic Silylated Digermene*, Hlina, J.; Baumgartner, J.; Marschner, C.; Albers, L.; Müller, T.; Jouikov, V. V. *Chem. Eur. J.* **2014**, 20, 9357.

- 05/2013      *Cyclic Disilylated and Digermylated Germylenes*, Hlina, J.; Baumgartner, J.; Marschner, C.; Albers, L.; Müller, T.; *Organometallics* **2013**, 32, 3404.
- 05/2013      *Stereoselective Rearrangements with Chiral Hypervalent Iodine Reagents*, Farid, U.; Malmedy, F.; Claveau, R.; Albers, L.; Wirth, T.; *Angew. Chem. Int. Ed.* **2013**, 52, 7018.

• **Achievements**

- 04/2015      **Liebig-Scholarship (GDCh)**, Travel-Scholarship for young researcher for the participation at the “*Gordon Research Seminar and Conference*” at the New Holderness School, New Hampshire, USA, in June 2015.
- 08/2014      **Poster Prize** at the “*International Symposium on Silicon Chemistry*” in Berlin.  
Title: “*Cationic Rearrangements in Polysilanes - The Surprising Preference for Hydrogen-Bridged Silyl Cations*”
- Since 01/2012      **Funding of the Dissertation** by the DFG (Germany) and the FWF (Austria) within the ERA-chemistry program.
- 09/2010 – 12/2010      **DAAD Scholarship**, Funding of the internship in Cardiff by a scholarship of the project MIX IT 2010.
- 06/2006      **GDCh-Abiturientenpreis 2006**, Price for the best high-school graduate in chemistry.

• **Other**

- Scientific Software      NMR Software *TopSpin*, *Gaussian09*, *GaussView*
- Languages      **German**: native, **English**: fluent in spoken and written,  
**French**: basic, **Dutch**: basic
- Interests      **Marathon, Triathlon**, successfully completed several marathons. Member of the triathlon club in Oldenburg. Participate regular training and several team and league challenges.